HYBRID MENSURATIONAL-PHYSIOLOGICAL MODELS FOR *Pinus taeda* AND *Eucalyptus grandis* IN URUGUAY

A thesis
submitted in partial fulfilment of
the requirements for the degree of

Doctor of Philosophy in Forestry

by
Ana Cecilia Rachid Casnati

New Zealand School of Forestry
University of Canterbury

2016

ABSTRACT

There is a consensus that prediction systems should be complex enough to predict yield, and the effect of various combinations of forest management practices on the functioning of interactive natural systems, but at the same time maintain a low level of detail in order to have low implementation costs and facilitate their use. For this reason hybrid mensurational-physiological models have gained importance and attention, and it is expected that their adoption will increase in the near future. This study aimed to explore the potential advantages of a hybrid mensurational–physiological model compared to models currently used in forest plantation management, and provide a better understanding of their capability to improve precision and explanation maintaining a certain level of simplicity as required for forest management. This work also aimed to provide updated tools for managing *Pinus taeda* and *Eucalyptus grandis* in Uruguay.

In Chapter 2, taper and volume equations were adjusted as those are essential to estimate individual volume and wood products. Emphasis was on testing compatible taper equations, since no models of this type have been developed to date for any species in Uruguay. However, variable exponent equations gave the best performance for predicting diameter at any height with the lowest prediction errors.

In Chapters 3 to 5, three systems of stand level equations comprising dominant height, basal area, maximum diameter, standard deviation of diameters, and mortality were developed using differential equations through three approaches:

i. Traditional time-based models using sigmoidal difference equations that restricted independent variables to age and parameters as functions of variables for region (base approach).
ii. Augmented time-based models that had parameters as linear functions of water holding capacity and physiographical variables such as elevation, aspect and slope.
iii. Hybrid physiological-mensurational models based on cumulative light sums since time of planting, with potential radiation-use calculated by modifiers accounting for influences of temperature, vapour pressure deficit (VPD), and water balance. These modified light sums replaced time in sigmoidal growth and yield difference equations.

Water holding capacity was the most significant among the surrogate variables tested in the mensurational models for both species (Chapter 3), whereas elevation was seldom significant. Sine

and cosine of aspect weighted by the slope, and slope were usually included but to a greater extent to one species than the other. Gains in accuracy of the augmented approach were small compared to the base equations.

When adjusting hybrid growth models (Chapter 4), combinations of radiation modifiers were selected that yielded accurate results. It was important to determine whether or not the gains in accuracy were sufficiently high to justify dropping the least representative modifiers and lose flexibility. Differences in global radiation across terrain corresponding to a variety of slopes orientations were tested to see whether or not they significantly affected growth. Radiation-use modifiers related to water balance and vapour pressure deficit (VPD) produced the highest gains in precision; however the complete formulation (including also temperature) was preferred in order to maximize the model utility. Accounting for aspect and slope when computing radiation flux did not improve precision in any of the state variables for either species.

For fitting hybrid mortality models (Chapter 5), it was hypothesised that the light-use efficiency approach could better explain the process leading to mortality because it accounts for predisposing site characteristics, recurring perturbations, and aggregation of stress. Extended periods of low water stress and short periods of high water stress were specifically tested as predictors of the probability of mortality. Results suggested that increase in stress did not influence the probability of mortality for *Pinus taeda*. However, stress helped explain the probability of mortality for *Eucalyptus grandis* with a negative effect: the accumulation of mild water stress tended to decrease the probability of mortality.

For *P. taeda*, resource availability increased growth and decreased the probability of mortality and mortality rate, but for *E. grandis,* higher levels of resources increased growth, probability of mortality, and mortality rate. It was hypothesized that the eucalypt species is more sensitive to factors other than water, given a potentially higher tolerance to drought episodes and resilience compared to the pine species.

A comparison of the three contrasting systems in terms of precision and bias as well as their capacity to reflect growth rates changes when site conditions vary was conducted. The comparison was extended to explore possible gains in diameter structure estimates. Results showed that precision tended to increase with higher levels of information; however explanatory variables included in the components of each approach and precision gains varied with species. Any of the three systems of equations can be applied for managing forests in Uruguay, especially for projecting diameter distributions, since the three approaches provided diameter distributions of

similar accuracy. Nonetheless models based on the hybrid approach were more precise, especially for *E. grandis* (with precision gains between 9 and 14% among state variables). Biases of the predicted variables were similar between approaches, but consistently less for estimating mortality in long intervals in the hybrid formulation. Along with precision, this approach offered higher utility.

ACKNOWLEDGEMENTS

This work is the result of the support and effort of many people and organizations.

First and foremost, I would like to thank my supervisory team, with whom it was a real pleasure and a privilege to work. I am grateful to Dr. Euan Mason, for his enthusiasm, advice and teachings in all modelling matters, and invaluable assistance with R coding and programming. I deeply appreciate his encouragement in the most difficult stages of this process. I also owe my gratitude to Dr Richard Woollons, for his enormous help in modelling procedures, and for sharing with me his experience in this fascinating field of knowledge. I am indebted also with Dr Joe Landsberg for his support right from the beginning, for his teachings in forest eco-physiology, and all the constructive criticism that helped to greatly improve this work.

I am grateful to the National Institute of Agricultural Research (INIA Uruguay) for boosting the opportunity of studying abroad and all the people there that helped me in one way or another. Specially, I thank Dr Roberto Scoz, for all his assistance from the planning stages of this PhD; his support made a real difference in its completion. I also would like to thank the support of all my colleagues in the Forestry Research Program, especially Andrés Hirigoyen, Fernando Resquin, and Gustavo Balmelli for backing me up and helping me to make the most of my PhD studies. I was lucky to count on the kind help of Javier Alonso in all the administrative tasks.

I owe my deepest gratitude to the New Zealand Aid Programme of the Ministry of Foreign Affairs and Trade for the financial support which was crucial for completing my studies. Special thanks go to Craig Forman, for all his help and patience through the most challenging times, and Idoia Gonzalez who also provided invaluable aid in the first stages.

This study would not have been possible without the generosity of Forestal Oriental, Global Forest Partners, Bosques del Sur, Cloverly, Cambium, the Unit of Climate and Information Systems (GRAS, INIA Uruguay), General Direction of Renewable Natural Resources of the Ministry of Cattle, Agriculture and Fisheries of Uruguay (RENARE, MGAP), Uruguayan Institute of Meteorology (INUMET). I sincerely appreciate the contribution of all the people in those companies and organizations that offered their valuable time and responded to numerous queries: Ricardo Methol, Diego Cárdenas, Pablo Tarigo, Daniel Ramirez, Juan Pablo Burgos, Agustín Giménez, Mario Pereira, Mariana Hill, and Rodolfo Pedocchi.

At the School of Forestry I'm indebted with Dr Luis Apiolaza, for his aid with R programming. To all my colleague postgraduates for their friendship and teachings, and to Jeanette Allen for her assistance and support: thank you.

Special thanks go to my family in Uruguay, for their love and encouragement throughout the course of this study. I want to particularly thank Robert, Ana, Bea, Luis, and Loreley for their priceless help in all the housekeeping tasks and paperwork while we were away from home.

I thank my parents, Ana and Robert for their faith and inspirational dedication to mine as well as others' education and wellbeing.

Finally, I would like to express my love and gratitude to Alejandro, whose love, sense of adventure, and contagious optimism supported me throughout; and to Rafaela, who arrived to our lives in the middle of this journey and became my greatest teacher.

PUBLICATIONS AND PRESENTATIONS

Journal articles

Material covered in Chapter 2 has been published as:

Rachid Casnati, C.; Mason, E. G.; Woollons, R.; Resquin, F. 2014.Volume and taper equations for *P. taeda* (L.), and *E. grandis* (Hill ex. Maiden). Agrociencia Uruguay 18(2): 47-60. Available through: http://www.fagro.edu.uy/~agrociencia/index.php/directorio/article/view/956

Presentations

2012 August, How good are your predictive skills? *Thesis in 3*, Engeneering Department Round. University of Canterbury.

2013 November, Precision and flexibility of hybrid physiological-mensurational models predicting growth in *Pinus taeda* and *Eucalyptus grandis*. Course *Concepts and tools for managing sustainable forest production*, SLU (Sweden)-Universidad de Concepción (Chile). Concepción, Chile.

2015 October, Comparisons between time-based mensurational models, augmented mensurational models, and modified radiation-sum hybrid models in Uruguay. Guest speaker at the meeting *Research proposal for precision forestry*. School of Forestry, University of Canterbury.

2016 February, Forest growth and yield models in Uruguay. Guest speaker at *Mini workshop on precision forestry*. School of Forestry, University of Canterbury.

TABLE OF CONTENTS

LIST OF FIGURES

Figure Short title Page

Figure Short title Page

Figure Short title Page

LIST OF TABLES

LIST OF SYMBOLS AND ACRONYMS

Symbol/Acronym	Description	Units
AIC	Akaike information criterion	related to variable
AUC	Area under the *ROC* curve	-
APAR	Absorbed photosynthetically active radiation	$MJ.m^{-2}.day^{-1}$
ASW	Available soil water	mm
c_θ	Coefficient of soil water modifier	-
d	Diameter breast-height	cm
d_i	Diameter at any height	cm
d_{max}	Maximum diameter breast height	cm
d_r	Inverse relative distance Earth-Sun	-
D	Drainage	mm
DT_{max}	Saturated vapour pressure when temperature = T_{max}	kPa
DT_{min}	Saturated vapour pressure when temperature = T_{min}	kPa
E	Evapotranspiration	mm
EF	Model efficiency	-
EI	Error Index	$stems.ha^{-1}$
Elev	Elevation	m
f_b	Slope reduction factor	-
f_D	Vapour pressure deficit modifier	-
f_T	Temperature modifier	-
f_F	Fertility modifier	-
f_{Fr}	Frost modifier	-
f_θ	Soil water modifier	-
f_S	Senescence modifier	-
f_{Cl}	Light competition modifier	-
g_b	Leave and boundary canopy layer conductance	$m.s^{-1}$
g_c	Canopy conductance	$m.s^{-1}$
g_{c_x}	Maximum canopy conductance	$m.s^{-1}$
G	Basal area	m^2
G_{sc}	Solar constant	Wm^{-2}
h	Total height	m
h_i	Height at a reference diameter	m
h_d	Day length	hours
h_{dom}	Mean top height	m
h_1	Sunrise hour angle on an arbitrary slope	rad
h_0	Sunset hour angle on an arbitrary slope	rad
H_s	Global horizontal radiation	$MJ.m^{-2}.day^{-1}$
H_s^*	Global radiation of a tilted surface	$MJ.m^{-2}.day^{-1}$
H_o	Extraterrestrial radiation	$MJ.m^{-2}.day^{-1}$
I	Interception	mm
Int	Interval	years or $MJ.m^{-2}$
J	Julian day	-
k_g	Coefficient of the relationship between stomatal conductance and VPD	$mbar^{-1}$
K_r	Proportion of diffuse radiation to the global horizontal radiation	-
K_t	Proportion of global horizontal radiation to extraterrestrial radiation	-

Symbol/Acronym	Description	Units
L	Leaf area index	-
L_{gC}	Leaf area index at maximum conductance	-
LUE	Light use efficiency	-
$L_{25}, L_{30}, L_{35}, L_{40}$	Number of consecutive months since planting where *waterMod*≤ 0.25, 0.30, 0.35, or 0.40	months
MR	Mean residual	related to variable
n	Actual sunshine duration	hours
n_θ	Power of soil water modifier	-
n_{ve}	Number of days since vernal equinox	days
N	Stocking	stems.ha^{-1}
N_o	Maximum sunshine duration	hours
N_2	Mortality rate	stems.ha^{-1}
N_{2adj}	Adjusted stocking calculated using the probability of mortality and mortality rate	stems.ha^{-1}
P	Probability of mortality occurrence	-
P_n	Net primary productivity	mol.m^{-2}
PSP	Permanent sample plot	-
PULS	Potentially useable light sum	-
PULSE	Potentially useable light sum equations	-
r_θ	Moisture ratio	-
R	Rainfall	mm
R_d	Direct radiation proportion of that on a flat surface given aspect and slope	-
RMSE	Root of mean square error	related to variable
ROC	Receiver operating characteristic	-
R_n	Net radiation	MJ.m^{-2}.month^{-1}
R_T	Radiation in month t	MJ.m^{-2}
Resp	Respiration	mol.s^{-1}
$R_{\theta DT}$	Accumulated radiation modified by water, VPD, and temperature modifiers	MJ.m^{-2}
$R_{\theta D}$	Accumulated radiation modified by water, and VPD modifiers	MJ.m^{-2}
$R_{\theta T}$	Accumulated radiation modified by water, and temperature modifiers	MJ.m^{-2}
R_{DT}	Accumulated radiation modified by water, VPD, and temperature modifiers	MJ.m^{-2}
R_θ	Accumulated radiation modified by the water modifier	MJ.m^{-2}
R_D	Accumulated radiation modified by the VPD modifier	MJ.m^{-2}
R_T	Accumulated radiation modified by the temperature modifier	MJ.m^{-2}
$\bar{R}_{\theta D}$	30-year average of radiation modified by *waterMod*	MJ.m^{-2}.month^{-1}
S	Slope of the saturation vapour pressure curve for water	KPa.^{o}C^{-1}
SD_d	Standard deviation of the diameters at breast height	cm
SDI	Stand density index	-
SE	Standrd error of the estimate	-
SI	Site Index	m
SWPA	Soil water potentially available	mm
$S_{05}, S_{10}, S_{15}, S_{20}, S_{25}$	Number of months since planting where *waterMod* 0.5, 0.10, 0.15, 0.20, or 0.25	months
t	Time or age	years
Ta	Mean temp for each month	^{o}C

Symbol/Acronym	Description	Units
T_{min}	Minimum temperature required for growth	^oC
T_{opt}	Optimum temperature for growth	^oC
v	Under-bark total stem volume	m^3
v_m	Under-bark merchantable stem volume	m^3
waterMod	Minimum value between water and VPD modifiers	-
Y	Yield	related to variable
α_s	$\sin(\alpha)\beta$	-
α_c	$\cos(\alpha)\beta$	-
β	Slope	% or degrees
γ	Psychrometric parameter	$kPa.^oC^{-1}$
δ	Solar declination	rad
ε	Maximum quantum efficiency	-
θ_T	Root zone water balance	mm
λ	Latent heat of water vaporization	J.Kg
ρ_a	Air density	$Kg.m^{-3}$
φ	Latitude	rad
φ^*	Modified latitude relative to slope and aspect	rad
ω_s	Sunrise hour angle	rad
$\omega_s{}^*$	Sunrise hour angle relative to slope and aspect	rad

CHAPTER 1

INTRODUCTION

BACKGROUND

Sustainable management of long-cycle resources such as forests poses a challenge in a world where a major constant is change. Variations in climate and market requirements associated with an increasing world population, increasing consumption per capita (Kimmins, 2008), and diminishing resources demand a constant update of qualitative and quantitative methods for efficient forest management. Forest models are essential tools in the decision making process. (Von Teuffel *et al.*, 2006) enumerate three basic functions of forest models: i) to enhance the analysis of alternatives in the short and medium-term decisions; ii) to develop and assess silvicultural strategies in the long term; and iii) to instruct diverse public figures about the consequences of silvicultural decisions.

Forest managers have largely used statistical models with no physiological inputs (traditional mensurational models). These are based on periodic tree measurements taken from growing stands and analysed statistically to establish logical mathematical relationships. They provide valuable information about volumes of wood, log sizes and diameter distributions in the stands. Because they are designed to describe growth and yield of stems as a function of time, they are relatively simple formulations and generally renowned for being robust and precise.

Mensurational models can be sub-divided into the following categories (Munro, 1974; Weiskittel *et al.*, 2011):

i. Whole stand models: use population variables to estimate future characteristics of the stand
ii. Single tree models: the modelling unit is a tree
iii. Size class models: the stand is divided in classes of diameter breast height (*d*), representing an intermediate case between the other approaches

Whole stand models have a simpler model configuration, usually relying on easily available stand variables as mean top height (h_{dom}), basal area per hectare (G) and stocking (N), for which they are suitable to single-species plantations. Two procedures must be differentiated here: i) fitting the main state variables independently as a function of time as proposed by Clutter *et al.* (1983); and ii) fitting the main state variables simultaneously as introduced by García (1994, 1984) where the state variables are fitted through a transition function that models increments. Whereas the latter has the advantage of considering the relationship of dependence between state variables, the former methodology has the advantage of flexibility to choose the functional form that best fit each state variable, and for that reason it has been broadly applied and chosen for this study.

Sigmoidal equations, which express growth as a function of time, suppose a phase of multiplicative reproduction and a phase of growth control common to all living organism (Zeide, 2002; Zeide, 1993). An example of this relationship is given by the Von Bertalanffy-Richards equation:

$$Y = \alpha\left(1 - e^{-\beta t}\right)^{\gamma} \tag{1.1}$$

where Y represent yield in any time (t), α is an asymptotic parameter, and β and γ are shape parameters.

Desirable properties of growth functions aiming to be consistent with the principles of biological growth are (Burkhart and Tomé, 2012):

i. The curve should show an inflection point separating an initial phase of increasing growth rate from a second phase of decreasing growth rate.
ii. There is a maximum y_2 value achieved at an older age.

Those types of equations can be transformed into projection equations of two types: anamorphic (curves with similar shapes but variable asymptotes) or polymorphic (curves with variable shapes and similar asymptotes) through the algebraic difference method (Bailey and Clutter, 1974). Examples can be found in Amaro *et al.* (1998), Clutter *et al.* (1983), Diéguez-Aranda *et al.* (2005), McDill and Amateis (1992), Palahí *et al.* (2004).

Non-sigmoid equations are also used in forest modelling, also available in differential forms, however they do not satisfy all of the properties cited above (Burkhart and Tomé, 2012), and that is why this study is focused on sigmoid formulations.

Traditional mensurational models have been criticised for their poor explanatory capacity leading to inflexibility under climate changing scenarios (Korzukhin *et al.*, 1996; Porté and Bartelink, 2002; Landsberg, 2003; Kimmins, 2008). In order to improve precision and make outputs more dependable on site conditions, different strategies have been explored to use causative information such as: directly adding climate or soil information as covariates (Woollons *et al*., 1997; Temps, 2005), using eco-physiological information such as water balance or evapotranspiration (Maestri, 2003; Pinjuv, *et al.*, 2006), and using climatic indices derived from physiological models (Snowdon *et al.*, 1999; Henning and Burk, 2004).

Models specifically designed to explain physiological processes driving tree growth, condense the understanding of the dynamics of forest growth through process descriptions based on hypotheses about the relationships of variables involved in photosynthate production, respiration, reserve dynamics and allocation of assimilates. Those relationships describe the rate of change of state variables expressed in difference equations (Roux *et al.*, 2001). The information is organized in several levels from biochemical processes to relations between organs to conform the different components, with increasing uncertainty from lower levels to aggregated systems (Landsberg and Sands, 2011). Unfortunately, these models are science-oriented and hardly used by forest managers mainly due to complexity of the information required for their parameterization and application (Fontes *et al.*, 2010), but also because of the poor or non-existent characterization of wood products that they usually offer.

There is a need for prediction systems that are complex enough to predict yield, and the effect of various combinations of forest management practices on the functioning of interactive natural systems (Kimmins, 1985), but at the same time maintain the level of detail at its minimum in order to have low implementation costs and an increase in the adoption (Kimmins *et al.*, 2008). For this reason hybrid mensurational-physiological models have gained importance and attention. Although the majority of models hybridize to some degree (Weiskittel *et al.*, 2011), this type of model is defined as a formulation comprising causal and descriptive elements at the same hierarchical level (Mäkelä *et al.*, 2000). A series of hybridizing strategies include: linking a physiological model with a mensurational model (Baldwin *et al*., 2001; Pinkard and Battaglia,

2001; Almeida *et al.*, 2003), linking more than two models (Peng *et al.*, 2002; Robinson and Ek, 2003), or modelling mensurational variables directly based on eco-physiological principles (Mason *et al*., 2007, 2011; Montes, 2012). All those strategies emphasize to different extent the advantages of mensurational and eco-physiological approaches: robustness, ease of use, capability to assess wood product mix, environment-dependence, and capability to predict growth in non-afforested areas. Therefore each strategy finds different balance points between simplicity and flexibility.

There is a consensus that hybrid physiological-mensurational models are the most appropriate approach for facing the new challenges posed by forest management (Bartelink and Mohren, 2004; Bugmann *et al.*, 2010; Fontes *et al.*, 2010; Landsberg, 2003; Mäkelä *et al.*, 2000). Therefore, it is expected that adoption of this class of model will increase in the near future.

OBJECTIVES

The work described here aimed to explore the potential advantages of hybrid physiological – mensurational models compared to models currently used in forest plantation management, and provide a better understanding of their capability to improve precision whilst maintaining a certain level of simplicity as required for forest management. The analysis was based on comparisons of three approaches using increasing levels of information to account for different growth and mortality rates. The comparison was based on precision and explanatory capacity of growth, potential wood products, and mortality.

Specific objectives were:

i. To develop compatible taper and volume equations for *Pinus taeda* and *Eucalyptus grandis* in Uruguay to be used in association with growth and yield models.
ii. To understand the gains in prediction quality of mensurational models using variables that represent surrogates of factors influencing growth.
iii. To adjust a hybrid model based on light-use efficiency for modelling all components representing growth on forecasting systems.
iv. To assess whether the method based on light-use efficiency can be used to represent the decline process that leads to mortality.

v. To determine if the hybrid approach is more suitable than its mensurational counterparts for predicting stand dynamics and structure and whether results are consistent for contrasting species.

STUDY AREA AND SPECIES

The study was developed using permanent sample plots of plantations located in the northern half of Uruguay, between 30°50' and 32°49'N and 53°43' and 58°21'W (Figure 1). The species selected were *Eucalyptus grandis*, which is managed for sawmills in the North and part of the Central regions, and managed in short rotations for pulp mills in the West; and *Pinus taeda*, which is mostly planted and managed for sawmilling in the North and also smaller portions of Central and Western regions. Forest plantations in Uruguay are mostly distributed in areas prioritized for this purpose, according to law 15939. Those areas are defined based on production characteristics and limitations of the soils mainly oriented to agriculture. Soils with similar production characteristics are grouped in broad categories defined by a number, and plantations occur mainly in groups 7, 8, 9, and 2 (see Figure 1).

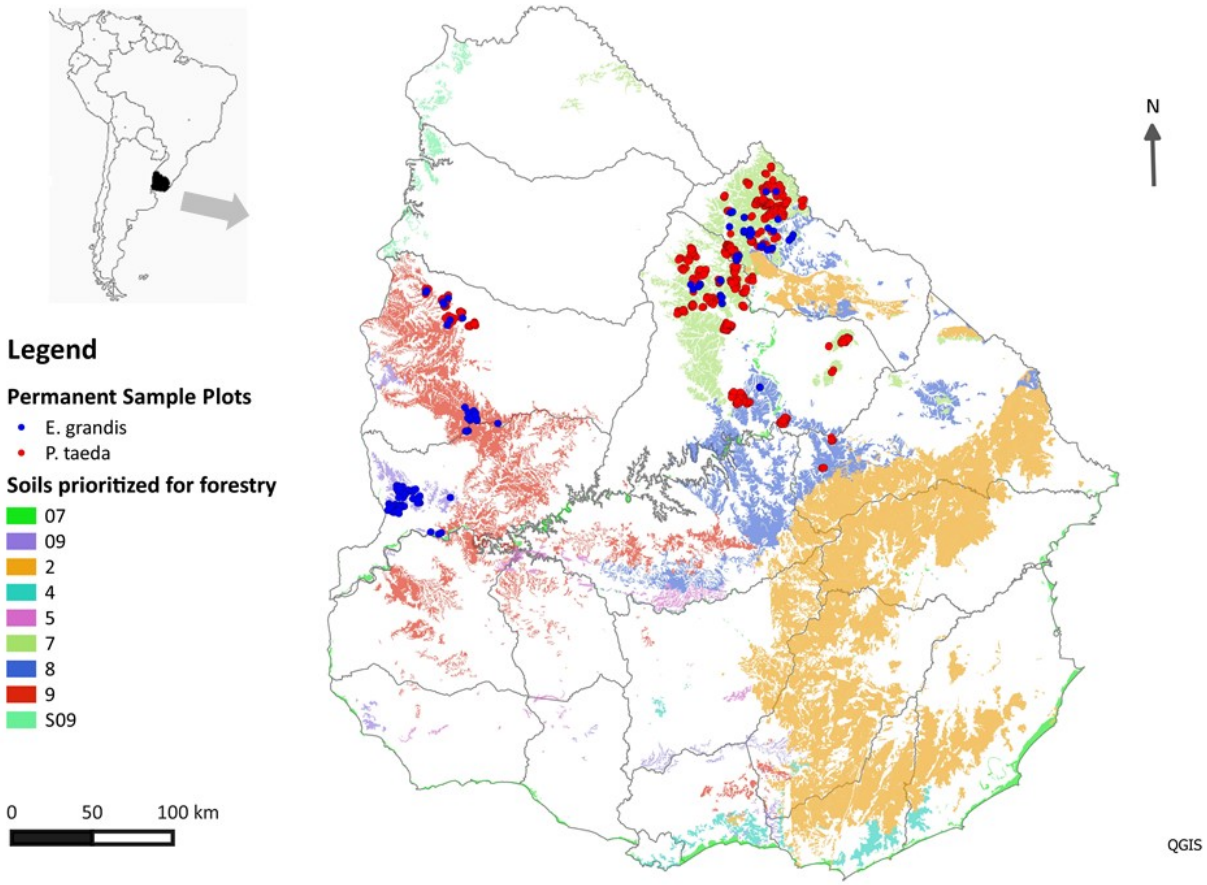

Figure 1.1 Prioritized soils for forestry and plots localization. Produced with spatial information of soils prioritized for forestry (2010) available through the Ministry of Cattle, Agriculture and Fisheries (MGAP/RENARE) in http://www.cebra.com.uy/renare/mapa/cartas-tematicas/.

Climate

According to the Koppen-Geigen classification system the climate in Uruguay is tropical-sub humid, without marked variations in the country. This is caused by its position respect to both the Pacific and Atlantic Oceans, and the absence of prominent mountain ranges (Castaño *et al.*, 2011). Despite the fact that rainfall is well distributed during the year, it has a highly irregular pattern. The main climate features are presented in Table 1.

Table 1.1 Climate characteristics.

Descriptor	Climate variable (values corresponding to the period 1980-2009, (Castaño *et al.*, 2011)					
	Rainfall (mm)	Temperature (°C)	Accumulated days with frosts	Radiation hours.day^{-1}	Annual air relative humidity (%)	Penman-Monteith ETP (mm.month^{-1})
Mean	1400	17.7	30	7	74	1100
Maximum	1600	22.6	40	-	78	1200
Minimum	1200	12.9	20	-	70	1000

Geology, soils and topography

Uruguay presents relative homogeneity in climate, vegetation (mostly herbaceous), and elevation (up to 514 meters over the sea level), but soils are highly diverse due the heterogeneity in geological parent material, plus local topography and variations in natural drainage (Durán and García-Préchac, 2007).

In the North area, parent soil materials of the group 7 (see Figure 1.1) comprise sandstones formed during the Mesozoic era (Triassic, Jurassic and Cretaceous). With some exceptions, soils of this region are deep, reaching 1.5 to 3m, and poor with high levels of aluminium (MGAP/RENARE, 1994). In a smaller portion, soils corresponding to the Precambrian supereon can be found, but are less explored for forestry purposes.

The high variability of parent geological material of the West area corresponding to group 9 and 09 is reflected in the variability of soil characteristics, nonetheless they are mostly sandy stones formed in the Cretaceous period. The slopes range from 1 to 6%, occasionally 12%, and with some variability in soil depth (MGAP/RENARE, 1994)

The Central area corresponding to group 8 comprises sandstones from the Devonian, Permic and Carboniferous periods, as well as sandy materials deposited over those formations. Soils of this zone are generally sandy with low fertility but comparatively more fertile than the North area, and shallower. The topography varies from smooth hills with 2% slopes to steeper slopes of 12-15% (MGAP/RENARE, 1994).

THESIS STRUCTURE

This thesis analyses and compares systems of equations predicting stand dynamics and structure at a regional scale with an increasing level of resolution. Accordingly, the study is organized in six chapters following the logic sequence of developing and testing the simplest approach to the most complex one, with a final comparison. Chapter 2 describes the development of taper and volume equations which are essential to estimate individual volume and possible wood products, and are often used jointly with growth and yield models. Several formulations were adjusted and offered for its use, but emphasis was on testing compatible taper equations, since no models of this type have been developed to date for any species in Uruguay.

In Chapter 3, the inclusion of soil-based and physiographic variables (i. e. water holding capacity, altitude, slope, and aspect) representing surrogates of growth modifier factors (such as water available, temperature, and radiation), were tested to augment traditional-mensurational models. Base models (using minimal information required to obtain acceptable estimations) were compared to "augmented" models (using soil-based and physiographic information) through precision and bias of estimations using an independent dataset. Very few studies analyse the use of physiographic variables in a system of equations (including mortality and components related to diameters' variability). However, this kind of study leads to a better understanding of the global scope of improvements achieved when explanatory information is incorporated.

Chapter 4 describes results of using a hybrid approach to model all the variables comprising the same system of equations as those described in in Chapter 3. The approach was based on the substitution of time by the accumulation of light restricted by modifiers that account for principal physiological limitations on growth rate. It was tested which combinations of modifiers yield more accurate results and whether the gains in accuracy were sufficiently high to justify dropping the least representative modifiers and lose flexibility. It was also assessed whether there were differences in net radiation across terrain corresponding to a variety of slopes orientations that translated into growth differences. This accumulation of light method has not been used for predicting variables related to diameter variability, nor has it been applied to broadleaf species yet.

Chapter 5 reports the use of both aggregated continued low stress and short high stress as predictors of the probability of mortality, and number of dead trees. Mortality is an essential process and yet very difficult to quantify due to the diversity of factors that interact along the life of stands. It was

hypothesized that the hybrid approach based on light-use efficiency could help to better understand the process and improve estimates.

Based on the results obtained in Chapters 3, 4, and 5. Chapter 6 offers a comparison of the three methodologies in terms of precision and bias as well as their capacity to reflect growth rates changes when site conditions vary. In this way, the gains achieved when the specificity of information regarding growth factors increase across the different approaches can be better understood. The comparison is extended to understanding possible gains in diameter structure estimates.

Finally, the key findings of the study are presented along with their implications for forest management and future research directions in Chapter 7.

Chapters 2 to 6 have been structured to be published as individual papers. Chapter 2 was published in Agrociencia Uruguay as Rachid Casnati, C.; Mason, E. G.; Woollons, R.; Resquin, F. 2014.Volume and taper equations for *P. taeda* (L.), and *E. grandis* (Hill ex. Maiden). Agrociencia Uruguay 18(2): 47-60.

CHAPTER 2

ADJUSTING VOLUME AND TAPER EQUATIONS[1]

INTRODUCTION

Accurate taper and volume functions are essential tools for forest management. They complement inventory information intended to quantify volume stand production and evaluate profitability. They are often associated with growth and yield models and used for developing stand level volume equations.

Individual volume functions estimate wood volume using tree variables that are easy to measure such as diameter breast height (*d*) and total height (*h*). Volume functions have been mostly formulated as linear or logarithmic combinations of *d* and *h* (Clutter *et al.*, 1983). Taper functions describe changes in diameter under or over bark along the stem, and hence they facilitate estimation of log assortments from either inventories or model projections of inventories. Several classes of equations have been used to describe taper: simple polynomial functions (Bruce *et al.*, 1968; Kozak *et al*., 1969; Gordon, 1983), variable exponent functions (Kozak, 1988; Muhairwe, 1999; Valentine and Gregoire, 2001; Westfall and Scott, 2010), trigonometric approaches (Thomas and Parresol, 1991; Bi and Long, 2001) and spline functions (Max and Burkhart, 1976; Liu, 1980; Koskela *et al.*, 2006). Compatible taper and volume equations have the big advantage that both taper and volume models compute identical estimates of tree volume. The first formulation was presented by (Demaerschalk, 1971,1972) and since then several authors have reformulated taper

[1] This chapter have been published as Rachid Casnati, C.; Mason, E. G.; Woollons, R.; Resquin, F. 2014.Volume and taper equations for *P. taeda* (L.), and *E. grandis* (Hill ex. Maiden). Agrociencia Uruguay 18(2): 47-60.

equations to be combined with volume functions (Cao *et al.*, 1980; Fang *et al.*, 1999; Jiang *et al.*, 2005; Jordan *et al.*, 2005).

In Uruguay there are only a few publicly available volume and taper models, especially for the Pinus genus, and compatible taper and volume equations are not available. Leites and Robinson (2004) fitted a segmented taper equation developed by Max and Burkhart (1976) augmented with crown variables such as crown length and crown ratio (calculated as the proportion of crown length with respect to total tree height) for Northern *P. taeda* plantations. For *Eucalyptus grandis*, Methol (2001) fitted a modified segmented equation by Max and Burkhart (1976) to represent the stem profile for this species, while Moras (2010) adjusted volume equations for *Eucalyptus globulus* ssp *globulus* for the South of the country.

The objective of this study is to fit taper and volume equations for *Pinus taeda* and *Eucalyptus grandis*, with special emphasis in testing the suitability of compatible taper equations for plantations of the Northern and Western regions of Uruguay.

METHODS

Data from 863 and 932 trees from *P.taeda* and *E.grandis* respectively, collected by private companies and the National Institute of Agricultural Research (INIA) from the Departments of Rivera, Tacuarembó, Paysandú, and Rio Negro for inventory and research purposes were used. They included measurements of total height (h) and diameter breast height (d) for each tree, as well as diameters under bark (d_i) for every one metre from the stump height to the tip. Part of the *E.grandis* dataset also included measures of diameters between 0.6 and 0.7m of height. Total volume under bark (v) was calculated for each section using Smalian's formula and summating all sections to the tip.

The large dataset available enabled cross-validation for fitting taper and volume equations; hence datasets for taper and volume were randomly split in half for both species. A summary of both datasets (modelling and validation) for each species is given in Tables 2.1 and 2.2.

Work included the following stages: screening, fitting and comparison of equations using the modelling datasets, and testing of equations using the validation dataset. Within the first stage, five linear and non-linear equations were evaluated for volume (Table 2.3), whereas six equations were tested for taper (Table 2.4). For the latter group, equations were selected in order to explore

a range of approaches including simple taper models such as the model proposed by (Ormerod, 1973), a sigmoidal approach based in the von Bertalanffy-Richards model proposed by Biging (1984), the segmented polynomial equation developed by Max and Burkhart (1976), a variable-exponent taper equation proposed by Kozak (2004) and a variation of Muhairwe (1999) equation proposed by Methol (2001), and finally a compatible polynomial taper equation as utilised by Goulding and Murray (1976).

Table 2.1 Characteristics of datasets for modelling and validating taper and volume for *Pinus taeda*.

Variable	Volume dataset		Taper dataset	
	Modelling	Validation	Modelling	Validation
Number of trees	455	408	-	-
Number of total measurements	-	-	4014	4072
Age (years)				
Mean	8.0	8.0	9.6	9.7
Maximum	26.0	27.0	27.0	27.0
Minimum	3.0	3.0	3.0	3.0
d (cm)				
Mean	20.4	20.3	23.2	23.2
Maximum	53.4	57.0	57.0	57.0
Minimum	6.40	6.00	6.40	6.00
Standard deviation	7.63	7.47	8.35	8.54
h (m)				
Mean	11.6	11.5	13.2	13.3
Maximum	26.9	26.8	27.0	27.0
Minimum	4.00	4.20	4.00	4.00
Standard deviation	4.26	4.27	4.63	4.71
Total volume under bark(m3)				
Mean	0.20	0.20	-	-
Maximum	1.79	2.51	-	-
Minimum	0.007	0.007	-	-
Standard deviation	0.26	0.28	-	-

Table 2.2 Characteristics of datasets for modelling and validating taper and volume for *Eucalyptus grandis*.

Variable	Volume dataset		Taper dataset	
	Modelling	Validation	Modelling	Validation
Number of trees	439	493	-	-
Number of total measurements	-	-	10166	10106
Age (years)				
Mean	9.00	9.20	10.0	10.0
Maximum	23.0	23.0	23.0	23.0
Minimum	2.00	2.00	2.00	2.00
d(cm)				
Mean	23.8	23.2	25.3	25.3
Maximum	50.4	52.3	52.3	52.3
Minimum	6.10	6.30	6.10	6.10
Standard deviation	8.34	8.35	8.35	8.35
h (m)				
Mean	25.1	24.7	26.5	26.6
Maximum	47.2	47.2	47.2	47.2
Minimum	6.50	6.70	6.50	6.50
Standard deviation	4.63	4.63	4.63	4.63
Total volume under bark(m3)				
Mean	0.56	0.53	-	-
Maximum	3.42	3.43	-	-
Minimum	0.009	0.01	-	-
Standard deviation	0.56	0.53	-	-

Table 2.3 Volume equations tested.

Equation	Reference	Eq. number
$v = b_0 + b_1 d^2 h$	(Spurr, 1954)	2.1
$v = b_0 + b_1 d^2 h + b_2 h$	-	2.2
$v = b_0 + b_1 d^2 h + b_2 h + b_3 d^2$	(Clutter *et al*., 1983)	2.3
$v = d^2 / (b_0 + b_1 / h)$	(Honer, 1967)	2.4
$v = b_1 d^{b_2} h^{b_3}$	(Schumacher and Hall, 1933)	2.5

The procedure followed to construct the compatible polynomial taper equations was basically the same proposed by Demaerschalk (1972, 1971) and extended by Goulding and Murray (1976):

Notation:

$$z = \frac{h - h_i}{h}, \qquad k = \frac{\pi}{40000}, \qquad y = \frac{k d_i^2 h}{v}$$

Where h_i is height corresponding to any d_i diameter, and v is the volume estimate achieved by using the selected volume function.

Letting

$$y = 2b_1 z + 3b_2 z^2 + \ldots + (i+1) b_i z^i \tag{2.6}$$

Then,

$${d_i}^2 = \frac{v}{kh}\left(2b_1 z + 3b_2 z^2 + \ldots + (i+1) b_i z^i\right) \tag{2.7}$$

Given that:

$$v_i = k \int_0^h {d_i}^2 \, dh_i \tag{2.8}$$

Substituting equation 2.7 into equation 2.8 gives:

$$v_i = k \int_0^h \frac{v}{kh} \left[2b_1 \left(\frac{h - h_i}{h}\right) + 3b_2 \left(\frac{h - h_i}{h}\right)^2 + \ldots + (i+1) b_i \left(\frac{h - h_i}{h}\right)^i \right] dh_i \tag{2.9}$$

Integrating the equation and observing that $h = h_i$ for total volume, then

$$v_i = v\,(b_1 + b_2 + \ldots + b_i) \tag{2.10}$$

Therefore, utilizing the restriction $(b_1 + b_2 + \ldots + b_i) = 1$ achieves compatibility.

Table 2.4 Taper equations tested.

Equation	Reference	Eq. number
$d_i^{\,2} = \frac{v}{kh}\left(\sum (i+1)\, b_i z^i\right)$	(Goulding and Murray, 1976)	2.11
$d_i = b_1 d \left(\frac{h-h_i}{h-1.3}\right)^{b_2}$	(Ormerod, 1973)	2.12
$d_i = d\left[b_1 + b_2 \log\left(1 - X^{\frac{1}{b_3}}\left(1 - e^{\frac{-b_1}{b_2}}\right)\right)\right]$ With $X = \frac{h_i}{h}$	(Biging, 1984)	2.13
$d_i = d\,[b_1(X-1) + b_2(X^2-1) + b_3(a_1 - X)^2 I_1 + b_4(a_2 - X)^2 I_2]^{0.5}$ With $I_i = 1$ if $a_i \geq X$, otherwise $I_i = 0$	(Max and Burkhart, 1976)	2.14
$d_i = a_0 d^{\,a_1}\, a_2^{\,d} \left[1 - \sqrt{X}\right]^C$ With $C = b_1 \log(X + 0.001) + b_2 e^X + b_3 \frac{d}{h} + b_4 \log(d) + b_5 \frac{h}{\sqrt{h_i}} + b_6 \frac{d/h}{h_i}$	(Muhairwe, 1999) modified by Methol (2001)	2.15
$d_i = (a_0 d^{a_1} h^{a_2})\, m^C$ With $C = b_1 X^4 + b_2\left(\frac{1}{e^{d/h}}\right) + b_3 m^{0.1} + b_4 \frac{1}{d} + b_5 h^{\left(1 - X^{1/3}\right)} + b_6 m$ and $m = \frac{1 - X^{1/3}}{1 - \left(\frac{1.3}{h}\right)^{1/3}}$	(Kozak, 2004)	2.16

Equation 2.11 represents the generic form of the compatible taper equation. The final form of the equation was chosen by comparing several forms using up to seven parameters raised from the first to the seventh power (Table 2.5).

Table 2.5 Compatible taper equations tested.

Equation	Number
$d_i{}^2 = \frac{v}{kh}(2\,b_1 z + 3\,b_2 z^2 + 4\,b_3 z^3 + 5\,b_4 z^4 + 6\,b_5 z^5)$	2.17
$d_i{}^2 = \frac{v}{kh}(2\,b_1 z + 3\,b_2 z^2 + 4\,b_3 z^3 + 5\,b_4 z^4 + 6\,b_5 z^5 + 7\,b_6 z^6)$	2.18
$d_i{}^2 = \frac{v}{kh}(3\,b_2 z^2 + 4\,b_3 z^3 + 5\,b_4 z^4 + 6\,b_5 z^5 + 7\,b_6 z^6)$	2.19
$d_i{}^2 = \frac{v}{kh}(4\,b_3 z^3 + 5\,b_4 z^4 + 6\,b_5 z^5)$	2.20
$d_i{}^2 = \frac{v}{kh}(4\,b_3 z^3 + 5\,b_4 z^4 + 6\,b_5 z^5 + 7\,b_6 z^6)$	2.21
$d_i{}^2 = \frac{v}{kh}(4\,b_3 z^3 + 5\,b_4 z^4 + 6\,b_5 z^5 + 7\,b_6 z^6 + 8\,b_7 z^7)$	2.22

All the models (corresponding to taper and volume) were fitted using ordinary least squares (OLS), and compared with the following statistics: the root of mean squared error (*RMSE*) as a measure of precision, mean absolute bias (*MAB*) as a measure of bias (Kozak, 2004), and model efficiency (*EF*) (Pinjuv *et al.*, 2006). These were calculated as it follows:

$$RMSE = \sqrt{\frac{\sum(Y - Y')^2}{N}} \tag{2.23}$$

$$MAB = \frac{\sum(|Y - Y'|)}{N} \tag{2.24}$$

$$EF = 1 - \frac{\sum(Y - Y')^2}{\sum(Y - \bar{Y})^2} \tag{2.25}$$

Where: N = number of observations, Y= observed value, and Y'= expected value, $\bar{Y}$= overall mean

The prediction statistics specify how well the model estimates diameter under bark, as opposed to the fit statistics which indicate how well the models adjust to the data used in its development (Muhairwe, 1999). All four fit statistics were calculated, ranked and an overall rank for each model was calculated by summing up the rank values for all the statistics. Models with the lowest rank were selected. These steps were repeated for the prediction statistics using the validation dataset in order to verify the choice of the best model. Plots of residuals versus predicted values, as well

as versus dependent and independent variables, were examined for bias. In addition, predicted versus observed values were plotted to compare the actual slope with the ideal slope of 1 (Goulding, 1979), and 95% confidence intervals were assessed.

RESULTS

Table 2.6 shows a summary of the fit statistics and their rank as well as overall ranks of volume equations for both species. Although differences between the statistics for all the candidate equations are small, model 2.5 ranked first for both species. Although equation 2.3 ranked second, it gave better residuals' distributions for *P. taeda* and was selected ahead of model 2.5. For *E.grandis* the selected equation was eq. 2.5. Bias indicated by the residual analysis was minimal for both species (not shown).

Table 2.6 Statistics of fit of the volume equations tested for the studied species and their rank position (in brackets).

Species	Equation	RMSE	MAB	EF	Overall rank
P.taeda	2.1	0.0242 (4)	0.0126 (2)	0.991 (4)	3
	2.2	0.0237 (3)	0.0132 (4)	0.991 (4)	4
	2.3	**0.0211 (2)**	**0.0131 (3)**	**0.993 (2)**	**2**
	2.4	0.0237 (3)	0.0134 (5)	0.992 (3)	4
	2.5	0.0198 (1)	0.0125 (1)	0.994 (1)	1
E.grandis	2.1	0.0471 (4)	0.0287 (4)	0.993 (2)	4
	2.2	0.0446 (3)	0.0270 (3)	0.994 (1)	3
	2.3	0.0432 (2)	0.0260 (2)	0.994 (1)	2
	2.4	0.0483 (5)	0.0293 (4)	0.993 (2)	5
	2.5	**0.0422 (1)**	**0.0245 (1)**	**0.994 (1)**	**1**

RMSE: root mean square error; MAB: mean absolute bias; EF: efficiency

For *P.taeda*, plots of predicted versus observed values (Figure 2.1) for the selected equation (eq. 2.3) showed that the slope was slightly different from one. This was confirmed by the confidence interval calculated, which ranged from 1.034 to 1.051. For the volume equation selected for *E.grandis* (eq. 2.5), predicted and observed values were closer; the 95% confidence interval ranged from 0.99 and 1.00.

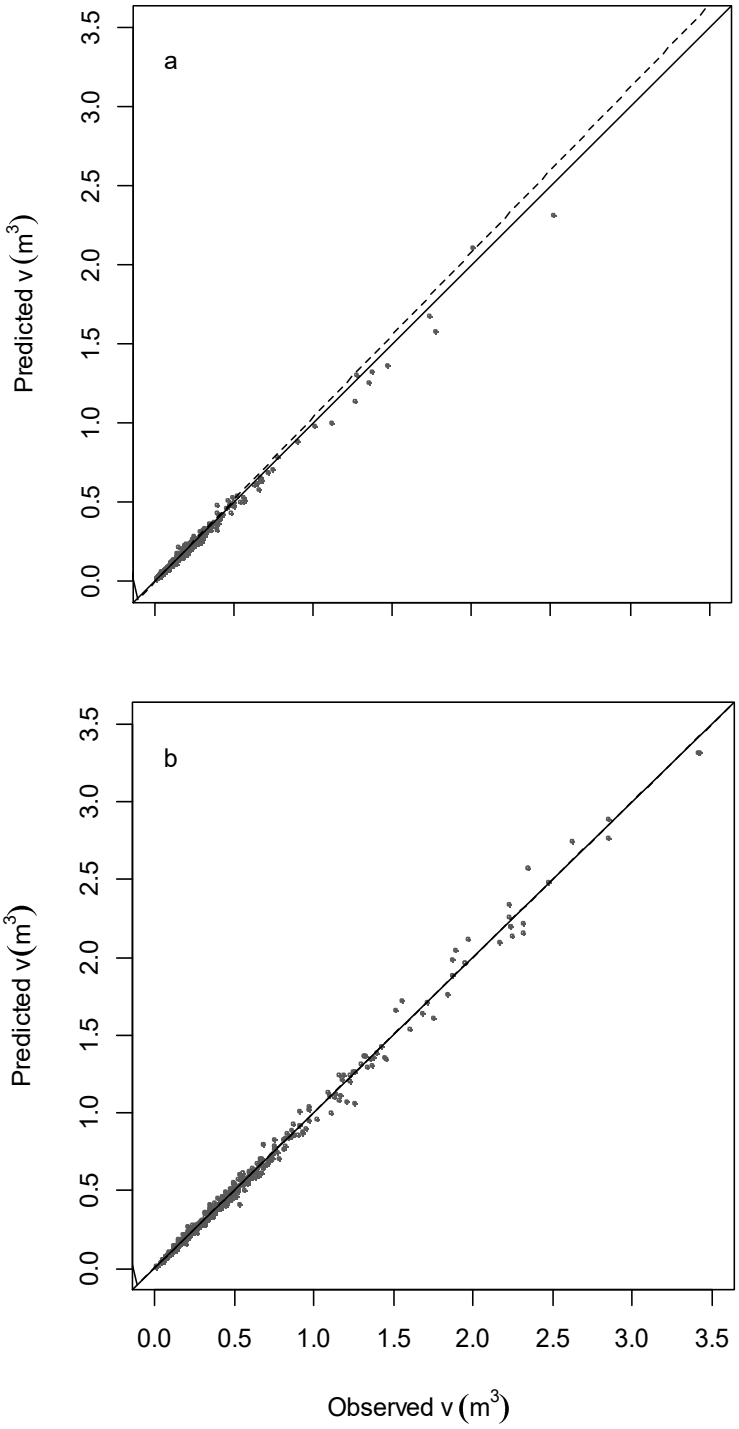

Figure 2.1 Observed independent values versus predicted values with the fitted regression line (dotted) and the (0, 1) line (continued), for volume under bark for (a) *Pinus taeda*, and (b) *Eucalyptus grandis* (overlaid).

The prediction statistics generally showed higher degrees of bias and lower precision than the statistics of fit, which was expected due to the former being calculated with independent data.

However, the ranks were very similar, with small differences between models, and the best equation for each species was confirmed.

The best compatible taper equation for both species comprised a five parameter form with exponents raised from the third to the seventh power (Table 2.7), but with the linear and quadratic terms excluded. Equations 2.19 and 2.22 consistently ranked in the first and second place for both species, whereas the rest of the equations varied in position. Equation 2.18 yielded inconsistent values for *P.taeda* and was excluded from further analysis.

Table 2.7 Statistics of fit of compatible taper equations fitted for *P.taeda* and *E.grandis* and their ranking position (in brackets) for the variable d_i (diameter under bark).

Species	Equation	RMSE	MAB	EF	Overall rank
P.taeda	2.17	1.2396 (5)	0.9141 (5)	0.975 (4)	5
	2.19	**1.1628 (2)**	**0.8734 (2)**	**0.978 (2)**	**2**
	2.20	1.1696 (3)	0.8922 (3)	0.978 (2)	3
	2.21	1.2056 (4)	0.8943 (4)	0.977 (3)	4
	2.22	**1.1323 (1)**	**0.8512 (1)**	**0.980 (1)**	**1**
E.grandis	2.17	1.0064 (3)	0.7581 (3)	0.986 (3)	3
	2.18	1.0262 (4)	0.7641 (4)	0.986 (3)	4
	2.19	0.9251 (2)	0.6984 (2)	0.988 (2)	2
	2.20	1.2805 (6)	0.7581 (3)	0.978 (5)	5
	2.21	1.2304 (5)	0.9274 (5)	0.979 (4)	5
	2.22	**0.8937 (1)**	**0.6747 (1)**	**0.989 (1)**	**1**

RMSE: root mean square error; MAB: mean absolute bias; EF: efficiency

Taper models fitted for *P.taeda* and *E.grandis,* are compared in Table 2.8. The top ranked equations were consistent for both species with the exception of equation 2.16 which ranked second for *P.taeda* but showed an inferior performance for *E.grandis*. Equation 2.15 ranked first, whereas the compatible equation (2.22) ranked slightly worse than the segmented equation (2.14). Equation 2.12 showed the worst performance for both species. Equations 2.14, 2.15, and 2.22 were selected for further analysis while eq. 2.16 was excluded (in spite of its good performance for *P. taeda)* in order to compare different modelling strategies (eq. 2.16 is a variable-exponent taper equation as well as eq. 2.15)

Table 2.8 Statistics of fit of taper equations tested for *P.taeda* and *E.grandis* and their ranking position (in brackets) for the variable d_i (diameter under bark).

Species	Equation	RMSE	MAB	EF	Overall rank
P.taeda	2.22	1.1323 (4)	0.8512 (4)	0.980 (4)	4
	2.12	1.4710 (6)	1.1320 (6)	0.966 (6)	6
	2.13	1.2920 (5)	0.9838 (5)	0.973 (5)	5
	2.14	1.1010 (3)	0.8208 (3)	0.981 (3)	3
	2.15	0.9495 (1)	0.7281 (1)	0.986 (1)	1
	2.16	1.0810 (2)	0.8205 (2)	0.982 (2)	2
E.grandis	2.22	0.8937 (3)	0.6747 (3)	0.989 (2)	3
	2.12	1.0570 (6)	0.7738 (5)	0.985 (4)	6
	2.13	0.9542 (4)	0.7194 (4)	0.988 (3)	4
	2.14	0.8778 (2)	0.6642 (2)	0.989 (2)	2
	2.15	0.7866 (1)	0.5901(1)	0.992 (1)	1
	2.16	0.9927 (5)	0.7526 (5)	0.989 (2)	5

RMSE: root mean square error; MAB: mean absolute bias; EF: efficiency

Residuals of the three selected models plotted against predicted values, and relative height are depicted in figures 2.2 and 2.3. Residuals against *d* were also plotted but are not shown. For *P.taeda*'s sectional diameter (d_i), equations 2.15 and 2.22 showed the smallest bias. However, large trees were scarce in the dataset and small bias was observed for d_i larger than 40 cm. Moreover, equation 2.22 showed some bias across the range of diameter breast height. For relative height, on the other hand, minimal bias was found for both equations,

For *E. grandis*, eq. 2.15 presented minimal bias in general while equation 2.14 showed a tendency to overestimate values of diameter under bark greater than 30 cm as well as trees with large *d* (greater than 40cm). Equation 2.22 tended to underestimate d_i at the tip of the tree, but did not show bias with respect to diameter breast height as presented for *P.taeda*.

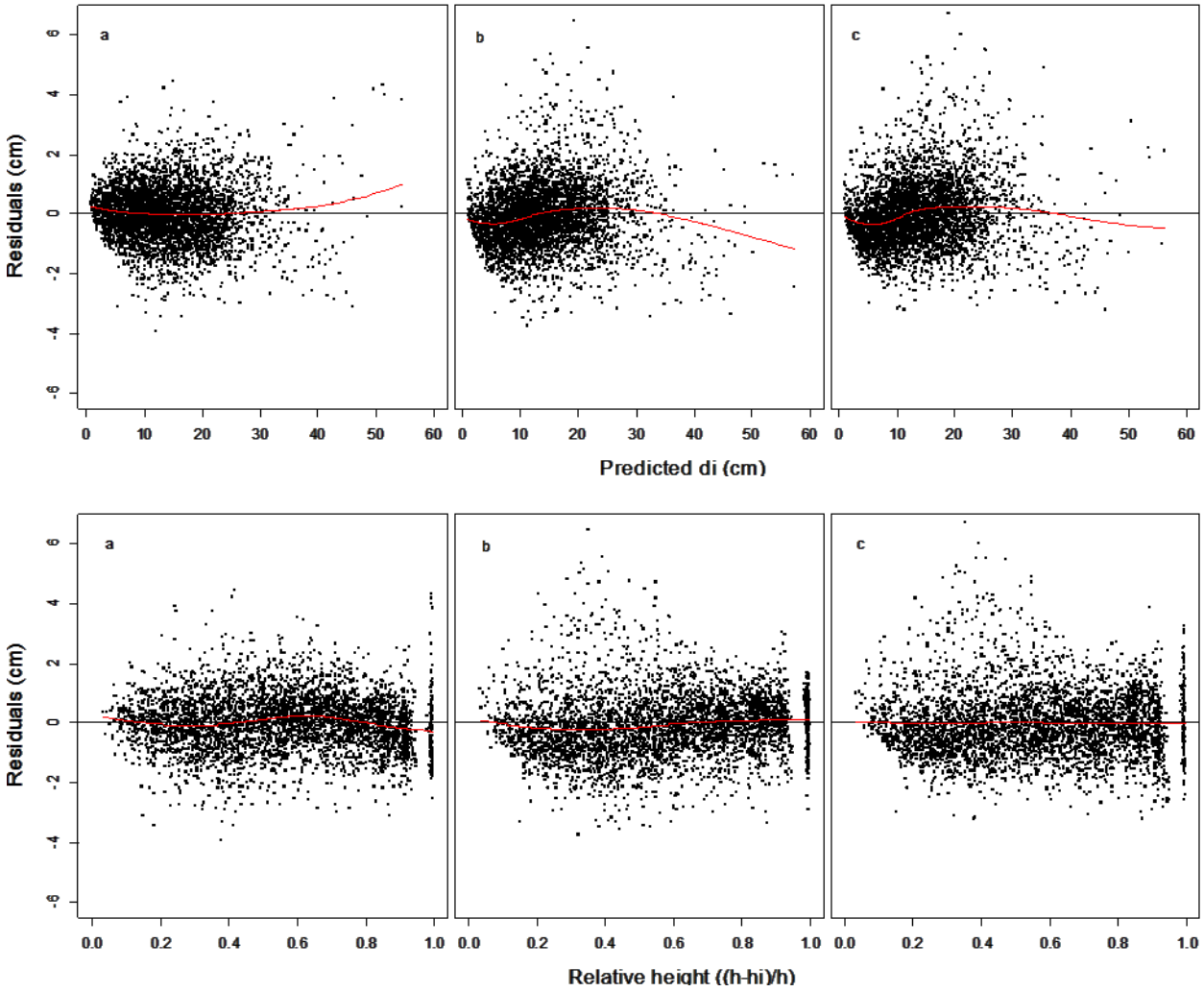

Figure 2.2 Residuals against diameter under bark predicted, and relative height with locally weighted scatterplot smoothing (lowess) for *P.taeda* corresponding to equations: 2.15 (a), 2.14 (b), and 2.22 (c) using the modelling dataset.

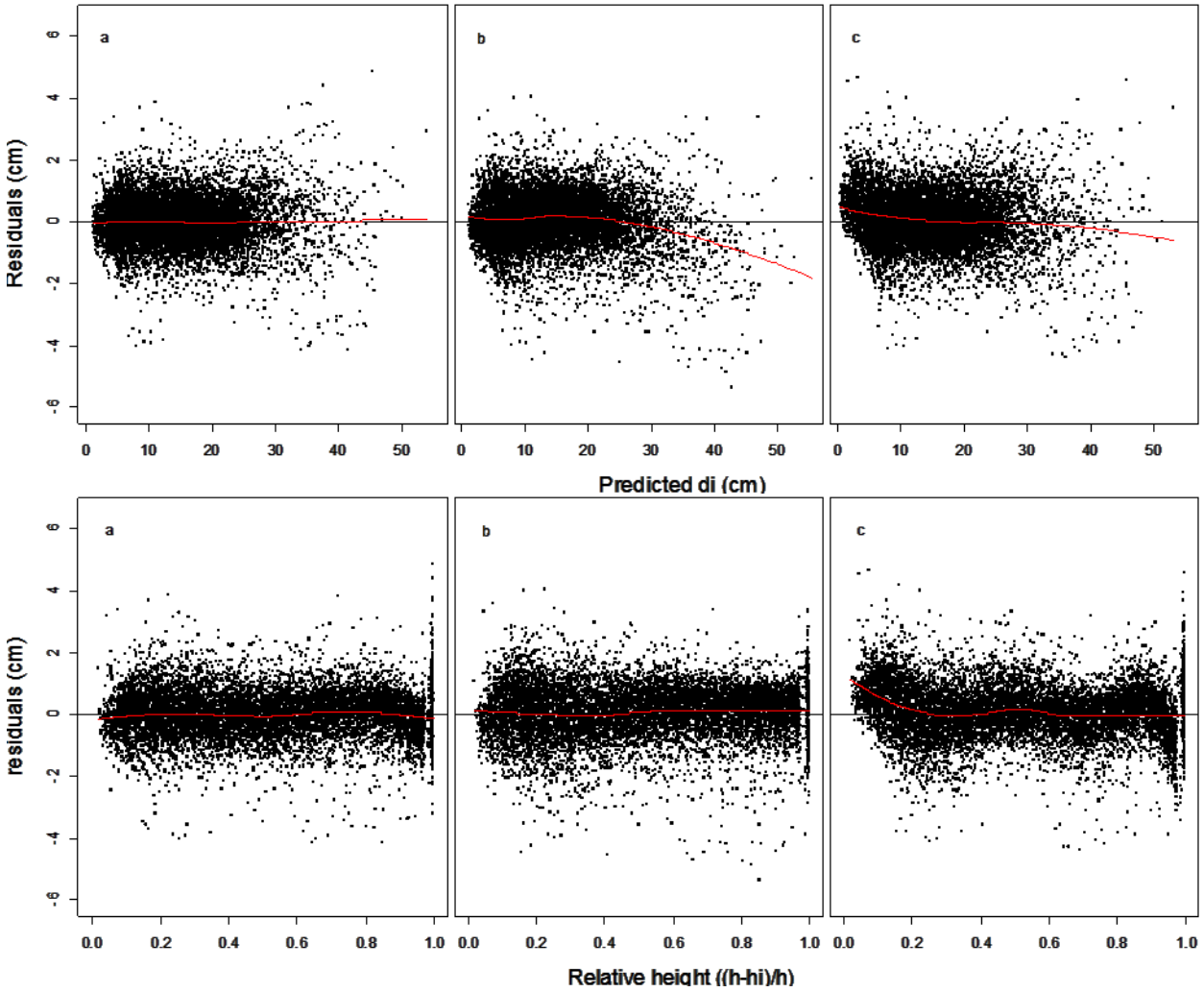

Figure 2.3 Residuals against diameter under bark predicted, and relative height with locally weighted scatterplot smoothing (lowess) for *E.grandis* corresponding to equations: 2.15 (a), 2.14 (b), and 2.22 (c) using the modelling dataset.

The statistics of prediction developed with the validation dataset showed similar ranks to the fit statistics. The residual plots obtained using the validation datasets were examined and presented the same tendencies observed for the fitting residuals.

Analysis of plots of observed versus predicted values for the compatible taper equation (Eq. 2.22) indicated that for *P.taeda* a slope slightly less than 1, with 95% confidence interval ranging from 0.961 and 0.969. For *E.grandis* the range included the value 1 for this equation: from 0.999 to 1.003 thus indicating an excellent fit. Plots of predicted versus observed for the compatible taper equations are depicted in Figure 2.4.

Average tree profiles using independent data and predictions using equations 2.15 and 2.22 suggest reasonable representation of taper for the species studied (Figure 2.6).

Finally, the parameter' estimates for all the fitted volume and taper equations are depicted in Tables 2.9 and 2.10.

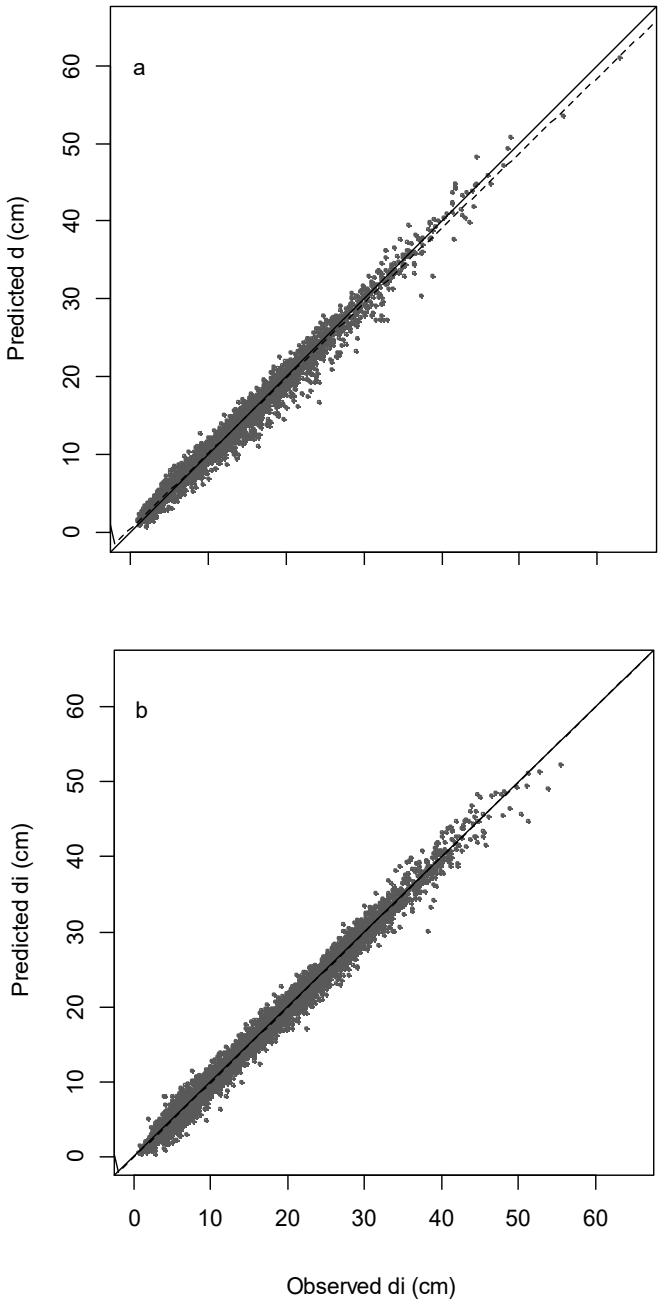

Figure 2.4 Observed independent values of *di* versus predicted values for equation 2.22 with the fitted regression line (dotted) and the (0, 1) line (continued), for diameter under bark for (a) *Pinus taeda*, and (b) *Eucalyptus grandis* (overlaid).

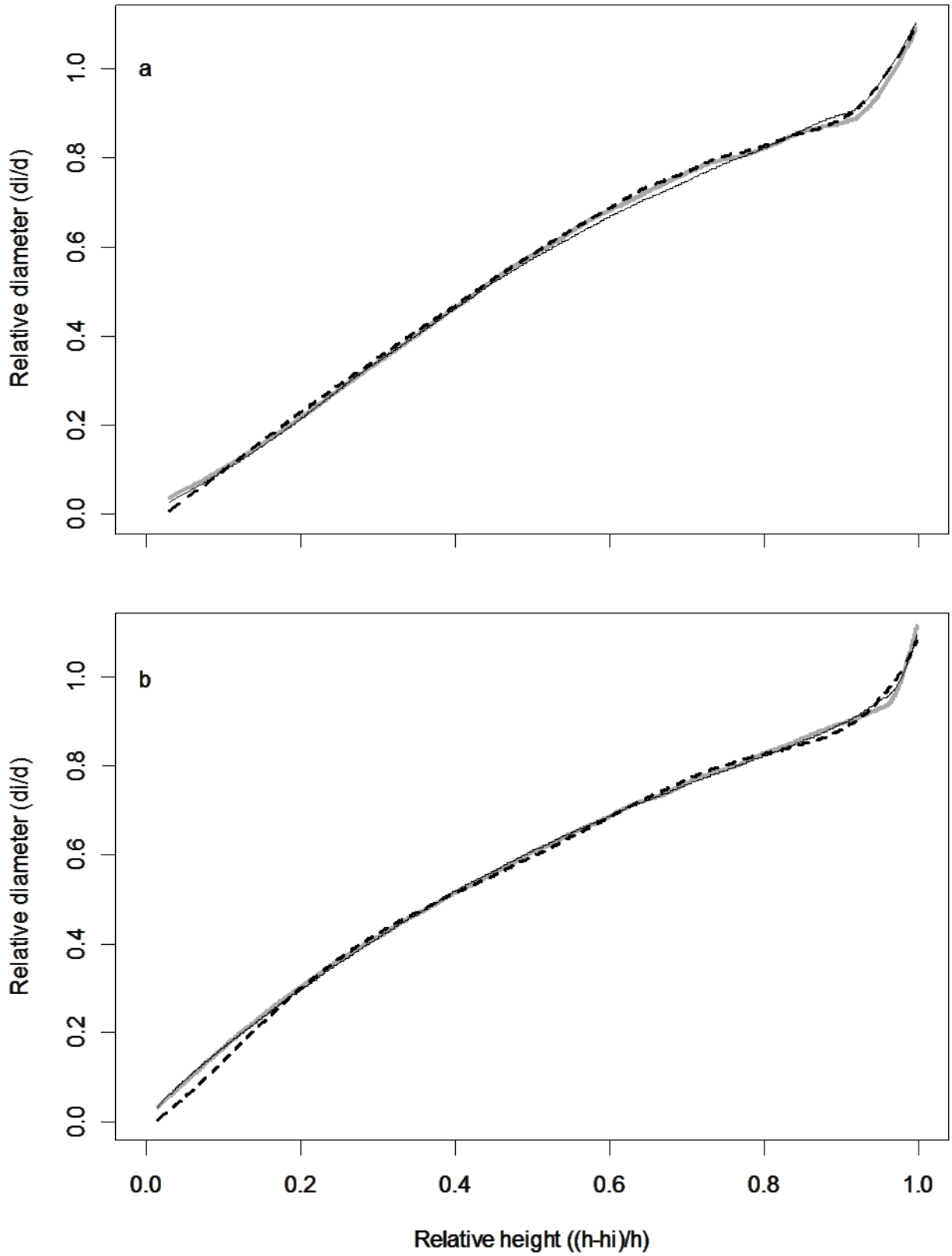

Figure 2.5 Average line (lowess) of independent observed values (grey line), and predicted values using equations 2.15 (continued line), and 2.22 (dashed line) for *P. taeda* (a) and *E. grandis* (b).

Table 2.9 Parameters estimates of the volume equations fitted for *P.taeda* and *E.grandis.*

Species	Equation	b_0	b_1	b_2	b_3
P.taeda	1	0.00328	0.00002912	-	-
	2	-0.0157	0.00002829	0.002058	-
	3	-0.0047	0.00003388	0.003710	-0.0001449
	4	-137.58	36938.21	-	-
	5	-	0.00002837	1.755	1.308
E.grandis	1	0.01482	0.00002974	-	-
	2	-0.05701	0.00002852	0.003766	-
	3	-0.03228	0.00003132	0.003699	-0.0001188
	4	6.054	32967.164	-	-
	5	-	0.00003242	1.804	1.178

Table 2.10 Parameters estimates of the taper equations fitted for *P.taeda* and *E.grandis*.

Species	Eq.	a_0	a_1	a_2	b_1	b_2	b_3	b_4	b_5	b_6	b_7
P.taeda	22	-	-	-	-	-	9.835	-33.258	56.752	-48.262	15.933
	12	-	-	-	0.928027	0.832407	-	-	-	-	-
	13	-	-	-	1.02755	0.93443	1.28321	-	-	-	-
	14	-	0.560245	0.095326	-2.985498	1.511906	-2.052886	41.793622	-	-	-
	15	2.6479678	0.7889123	1.0055376	-0.3664782	0.5185238	0.2192664	-0.3055746	0.0523507	0.0086633	
	16	0.764479	0.989266	0.079908	8.187748	-6.550314	-2.772829	24.505637	0.002694	6.149108	-
E.grandis	22	-	-	-	-	-	19.3731	-73.6115	121.9036	-95.4415	28.7763
	12	-	-	-	0.9525137	0.7400322	-	-	-	-	-
	13	-	-	-	1.061596	0.458419	2.036848	-	-	-	-
	14	-	0.782271	0.046413	-3.656469	1.789581	-1.573512	139.637643	-	-	-
	15	1.3720045	0.9948877	1.0008304	-0.1865372	0.2835609	0.2939950	-0.1521256	0.0382399	-	-
	16	0.950084	0.992462	0.011674	5.505428	-4.093035	-1.334289	16.674367	0.021479	5.068788	-

DISCUSSION

In general, differences between the models' statistics were greater for *P.taeda* than for *E.grandis*. In the case of taper equations, simpler models performed worse than more complex models.

The Clutter *et al.* (1983) and the Schumacher and Hall (1933) equations were the best models for estimating volume for *P.taeda* and *E.grandis* respectively; however the differences between all the volume equations were small. Although the selected equations gave minimal bias, the big majority of the data for *P.taeda* represents volumes smaller than 1 m^3, hence predictions beyond 1.5 m^3 should be treated with caution.

Results for the taper equations fitted for both species indicated that equation 2.15 is the most precise and least biased of the six equations studied for estimating sectional diameter. This modification of the Muhairwe's variable exponent model proposed by Methol (2001), was developed for estimating diameter under and over bark for *Pinus radiata* plantations in New Zealand and diameter over bark for *Eucalyptus grandis* in Uruguay by that author showing comparatively good estimations over 20 models. The original model was developed and fitted for *E. pilularis* and *E. grandis* (Muhairwe, 1999) and showed a marked improvement over other equations, however it was not so effective in studies involving other species (Rojo *et al.*, 2005). In spite of its good performance, this variable exponent equation presents some significant disadvantages: (i) it is a complex model which involves nine parameters, (ii) for calculating volume, predicted diameters under bark the function must be numerically integrated, and (iii) merchantable height for any desired diameter cannot be calculated (Muhairwe, 1999).

Equation 2.14 ranked second and third for *E.grandis* and *P.taeda* respectively and precision and bias values were closer to the values corresponding to the compatible equation than the ones corresponding to the eq. 2.15. This model developed by Max and Burkhart (1976), originally for *P. taeda*, has been fitted to several species (Figueiredo-Filho *et al.*, 1996; Jiang *et al.*, 2005; Rojo *et al.*, 2005; Brooks *et al.*, 2008; Souza *et al.*, 2008; Alegria and Tomé, 2011), and used as a reference to compare new equations (Cao *et al.*, 1980; Muhairwe, 1999). Methol (2001), observed bias for the diameters predicted with respect to *d* for this species and proposed a modification of this equation. This particular problem was studied and small bias was observed for trees larger than 40cm for both species. Moreover, overestimation of large d_i was found for both species but especially pronounced for *E.grandis*.

This equation can be integrated to yield volume to any height (Brooks et al., 2008, 2007), and it can also estimate height to any desired diameter. However, it has a major disadvantage that it is not compatible with estimations obtained through volume equations.

Equation 2.22 based on the polynomial compatible taper equation proposed by Goulding and Murray (1976) remained in intermediate positions in the ranks for both species. It has been suggested that this model does not represent well the basal portion of the stem in species with strong butt swell. Gordon (1983) pointed out that the original five-parameter equation proposed by Goulding and Murray misrepresents the butt log region and also overestimates diameter at the tip in *Pinus radiata*, hence he suggested including an additional term well beyond the fifth degree to improve estimation. Muhairwe (1999) tested two models varying the higher terms but still found some bias for large *d* trees (larger than 60 cm) and for tips of all trees in *Eucalyptus grandis* and *Eucalyptus pilularis*. In this study, inclusion of a term raised up to the sixth and the seventh power, but excluding the first and second lower terms, showed minimal bias of diameter under bark estimates for *P.taeda*, however some bias with respect to diameter breast height was found. Although the slope of predicted versus observed values for this species differed from one, the average profile predicted shows very small variation with respect to the average of observations and with respect to the average of the best equation.

For *E.grandis*, the equation slightly underestimated d_i values on the tip beyond 85% of height. Practically, this problem would have very minor implications for assessing wood products to commercial heights up to 4 to 6 cm of d_i.

Goulding and Murray (1975), show that fitted compatible equations can also be used to estimate merchantable volumes, which is one of the major advantages of this equation. The expressions for *P.taeda* and *E. grandis* based on the equation 2.22 are as follows:

$$v_{mt} =$$

$$v\left[9.835\left(\frac{h-h_i}{h}\right)^4 - 33.258\left(\frac{h-h_i}{h}\right)^5 + 56.752\left(\frac{h-h_i}{h}\right)^6 - 48.262\left(\frac{h-h_i}{h}\right)^7 + 15.933\left(\frac{h-h_i}{h}\right)^8\right] \quad (2.26)$$

$$v_{mg} =$$

$$v\left[19.3731\left(\frac{h-h_i}{h}\right)^4 - 73.6115\left(\frac{h-h_i}{h}\right)^5 + 121.9036\left(\frac{h-h_i}{h}\right)^6 - 95.4415\left(\frac{h-h_i}{h}\right)^7 + 8.7763\left(\frac{h-h_i}{h}\right)^8\right] \quad (2.27)$$

Where v_{mt} and v_{mg} is merchantable volume for *P.taeda* and *E.grandis* respectively to any *h*.

CONCLUSIONS

The equations recommended to estimate total volume for *P.taeda* and *E.grandis* are Clutter *et al*. (1983) (eq. 2.3) and Schumacher and Hall equation (eq. 2.5) respectively. For the former species the prediction error is 12.2 % while for the latter is 7.4%. It is also recommended to use these equations between the ranges of 0.007-1.5 and 0.009-3.4 m^3 for *P.taeda* and *E.grandis* respectively.

The variable- exponent equation (eq. 2.15) is the best equation for estimating diameter at any desired height with the lowest prediction errors of 6.7% and 5.4% for *P.taeda* and *E.grandis* respectively offering comparatively better estimates especially for larger trees (*d* between 35 and 50 cm) in the case of *P.taeda*, and the tip of the tree for *E.grandis*.

Based on prediction statistics the compatible taper equation (eq. 2.22) did not perform quite as well as eq. 2.15 but because of the huge advantages of (a) simplicity, (b) compatibility (c) relatively small differences with respect to bias and precision compared with the equation 2.15, the compatible taper equation is recommended for forecasting systems and use in inventory estimations with prediction errors of 8.00% and 6.18% in diameter under bark for *P.taeda* and

E.grandis respectively. This equation should be used within the *d* ranges of 7 to 40 cm for *P.taeda* and 7 to 50 cm for *E.grandis*, and volume ranges as specified for the volume equations.

Although the fitted models cover a wide range of tree sizes, additional data from trees larger than 45 cm of *d* are required for both species in order to fit models for a wider *d* span, especially for sizes near clear-cut age for sawmilling purposes. A better description of the butt log of *P.taeda* is also needed to improve quality of data and models. In this sense, additional measures at 0.6 to 0.7m of height (Whyte, 1971) are recommended.

CHAPTER 3

USING SOIL-BASED AND PHYSIOGRAPHIC VARIABLES TO IMPROVE GROWTH AND MORTALITY PROJECTIONS

INTRODUCTION

Information provided by traditional mensurational models are essential inputs in the decision making processes for managing planted forests. Age-based sigmoidal equations representing tree growth, fitted using inventory data usually guarantee robustness and simplicity to those models, at the sacrifice of some explanatory ability. In this sense, the introduction of explanatory factors affecting tree development in growth equations attempts not only to improve the quality of predictions, but also to add useful information for underpinning forest management decisions.

A selection of site specific climatic, physiographic and/or soils-based characteristics, are often considered in assessment of productivity (Weiskittel *et al.*, 2011) and also to improve growth predictions. Different strategies have been explored to use this information for augmenting mensurational equations: Temps (2005) included a rainfall variable in the Von Bertalanffy-Richards equation for estimating dominant height and basal area for *Pinus taeda* growing in the southern region of Brazil, which gave modest improvement. Woollons *et al.* (1997) tested the inclusion of solar radiation, rainfall, minimum and maximum temperature at a monthly level, and soil type to improve quality of predictions of mean top height and basal area of *Pinus radiata*. Results led to the conclusions that for dominant height there was no improvement by the integration of climate or soil information, but there was improvement in basal area (*G)* when rainfall and solar radiation were included in equations fitted by soil type.

Other approaches (as opposed to age) used structural indices to make growth more dependable on climatic and soil inputs, Snowdon *et al.* (1999) derived several climatic indices from two physiological models for incorporating annual variations in climatic factors into a Schumacher

projection model for stand basal area of *Pinus radiata*. The indices were annual growth season rainfall, and a growth index obtained from the combination of a light index, a thermal index, and a moisture index (gathering soil information, rainfall and evapotranspiration). A climatic index based on annual photosynthetic carbon fixation was also incorporated. Snowdon *et al.* (1999) compared various forms of generalised Schumacher's equation with these indices, and found results were improved, with the annual growth index derived from a process-based model being the most effective. Based on this work, Henning and Burk (2004) used growth indices derived from physiological models as a factor to improve growth and yield estimates of an empirical model. They found that these external growth indices were effective in reducing bias in basal area estimations, but were less effective in improving precision. Maestri (2003) studied the inclusion of modifiers for Chapman-Richards' parameters for modelling dominant height in *Eucalyptus grandis*, concluding that rainfall, potential evapotranspiration, and maximum and minimum temperature were the most significant explanatory variables of annual increment. However he also found that error reductions using water balance information were not higher than the error reductions obtained by using simpler environmental variables.

Pinjuv *et al.* (2006) included the effects of available soil water in a mensurational model for *Pinus radiata* using the sub-model for water balance of the 3-PG growth model. Comparing the modified model with the original version, they found that the former was slightly more accurate with respect to basal area and dominant height

The advantages of including explanatory variables in mortality functions have also been studied. Authors tested the use of individual or stand variables as well as site information for improving predictions of survival probability at an individual level (Avila and Burkhart, 1992; Monserud and Sterba, 1999; Eid and Tuhus, 2001; Crecente-Campo *et al.*, 2009; Groom *et al.*, 2012) or population level (Bailey *et al*., 1985;Amateis *et al.*, 1989; Uzoh and Mori, 2012). Attempts to augment mortality rate are less frequent; Pinjuv *et al.* (2006) included an index for water balance in the asymptote with modest gains in precision and bias with respect to a counterpart without the water balance index.

At a stand level, it is common to use probability density functions (pdf's) in order to disaggregate the stand and provide information of the forest diameter structure as well as information of products per tree (Bailey and Dell, 1973). How projection of diameter distributions can be improved by using site information has been poorly studied. When choosing the method of

moments for recovering the parameters of probability density functions, outputs of mensurational equations are used. Using the inverse Weibull function, growth functions of basal area, maximum diameter, and standard deviation of diameters (or diameter variances) are needed, hence providing accurate estimates of those variables comprise the basis for sound diameter distribution estimates.

Although the addition of site information in mensurational equations has been assessed, very few studies explore this possibility on a whole set of equations comprising a forecasting system.

The main objective of this chapter is to assess the use of the following soil-based and physiographic attributes: soil water potentially available (*SWPA*), elevation (*Elev*), aspect (α), and slope (β) in a system of mensurational stand equations by comparing models augmented with this information versus base models. The objective was divided into two stages:

(i) fitting and analysis of dominant height, net basal area, maximum diameter, and standard deviation of diameters,

(ii) fitting and assessment of mortality equations,

METHODS

The steps taken for the analyses included: (i) data preparation; (ii) fitting and validation of simple and augmented equations for modelling growth and mortality.

Growth and yield equations were fitted for predicting mean top height or dominant height (h_{dom}), net basal area (G) , maximum diameter at breast height (d_{max}), and standard deviation of diameter at breast height (SD_d) for *Pinus taeda* and *Eucalyptus grandis*. The last two variables are necessary to project diameters distributions by the method of moments using an inverse Weibull function. Stocking (N) was fitted using a two-step procedure proposed by (Woollons, 1998).

Data preparation

Information from 1662 geo-referenced permanent sample plots (PSP) dispersed in areas prioritized for forestry in the Northern half of the country was used to fit the equations (Fig 3.1). Most *P. taeda* plots corresponded to commercial plantations while the *E. grandis* dataset comprised plots

from commercial plantations and trials (pruning, thinning and breeding). Only PSPs with more than two measurements and with locations geo-referenced were included in the dataset.

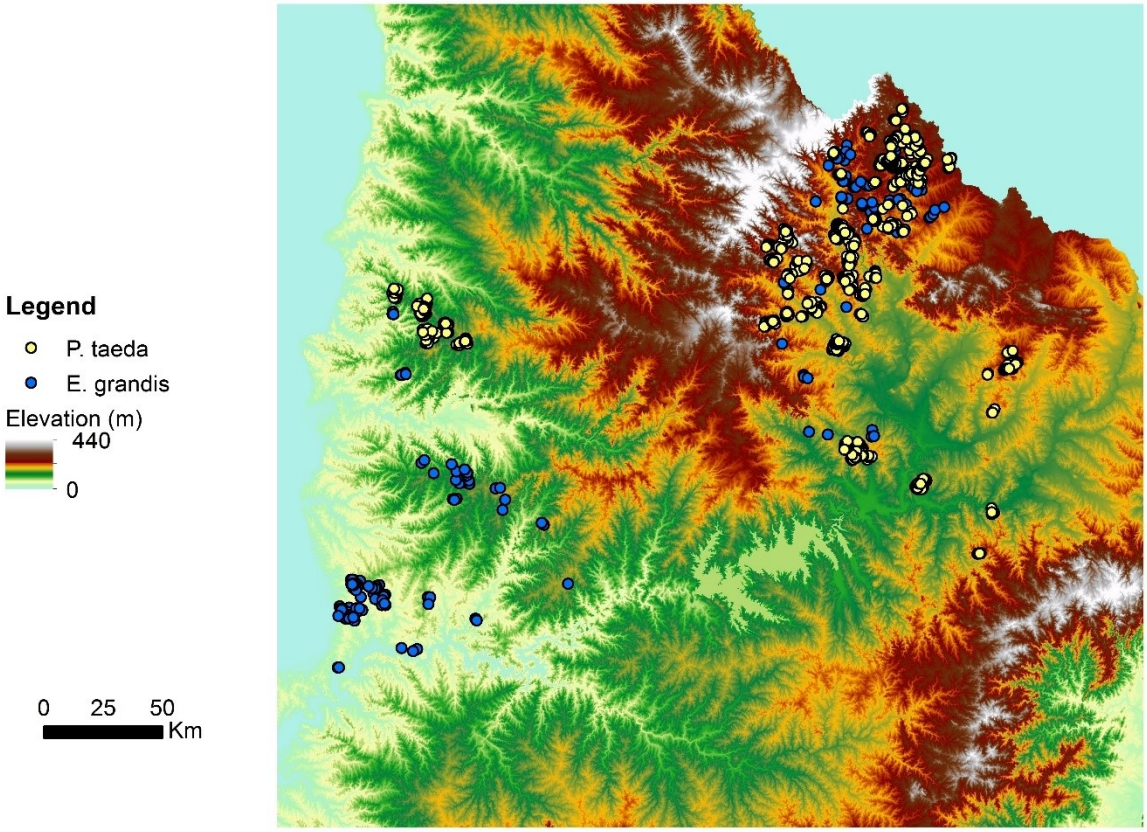

Figure 3.1 PSPs location and topography. Produced with spatial information of the Digital Terrain Model available through the Ministry of Cattle, Agriculture and Fisheries (MGAP/RENARE) in http://www.cebra.com.uy/renare/mapa/modelo-digital-de-terreno/.

PSPs were linked to the following site characteristics: aspect (α), slope (β), elevation (*Elev*), and soil water potentially available (*SWPA*) using information publicly available through the Ministry of Cattle, Agriculture and Fisheries (MGAP/RENARE, n.d.a). For aspect, slope, and elevation, a digital elevation model with a precision of 30 x 30 m was used (MGAP/RENARE, n.d.b). Because slope was classified in categories, the average per category was calculated per plot. Aspect was decomposed to North-South and East-West components by calculating the sine and cosine of the azimuth angle respectively. In this way sine values ranges from 1 to -1 from East to West, and cosine values ranges from 1 to -1 from North to South (Fig 3.2). Both components were weighted by the slope using the method proposed by Stage, (1976), so that the value for flat ground is 0 and it increases along with the slope. Therefore variables obtained were $\alpha_s = \sin(\alpha)\beta$ and $\alpha_c = \cos(\alpha)\beta$ (slope multiplied by sine and cosine of aspect respectively). Soil water potentially available (*SWPA*) was extracted directly from a digital national map developed by Molfino and

Califra (2001) based on the Uruguay Soil Classification Map 1:1.000.000 (MGAP/DS, 1976). The authors calculated *SWPA* for each soil profile type through pedotransfer functions developed for the country to compute water potentially available (between 1/10 to 15 atm). The values were calculated for each sub-horizon's depth per soil type and weighted for the percentage that the soil type occupies on each of the 99 soil classification units. Finally, the authors applied a correction factor that accounts for limiting factors such as erosion, rockiness, stoniness, and salinity to get a value of net *SWPA*. The range of this variables across the plots is depicted in Figure 3.3.

Procedures involving georeferenced information were developed using QuantumGis (QGIS Development Team, 2015), and ArcGis for Desktop (ESRI, 2013).

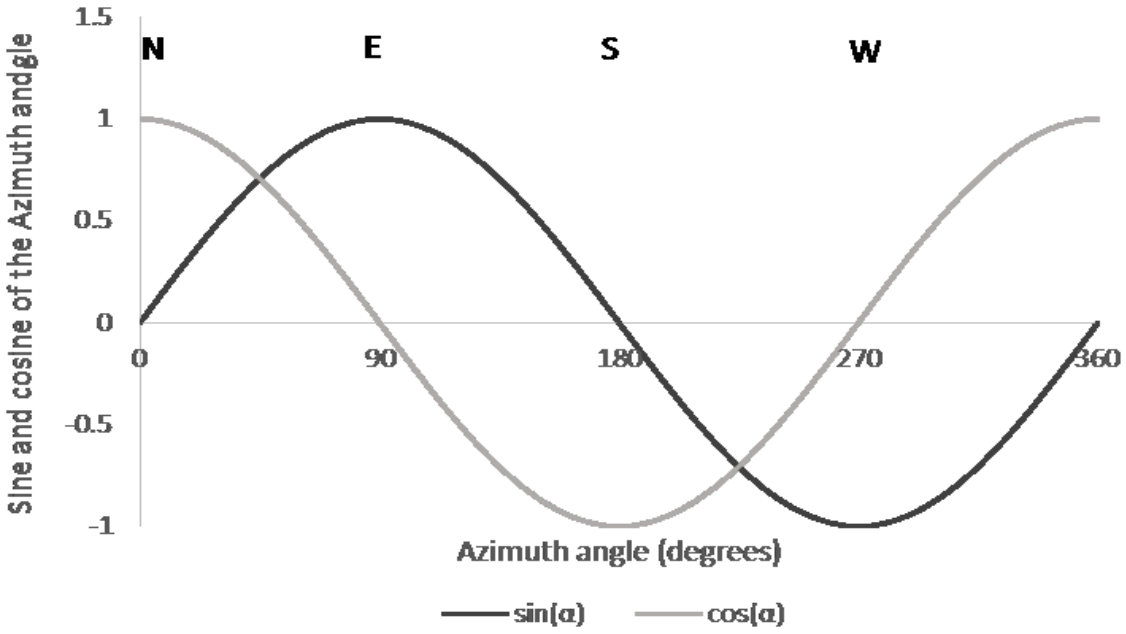

Figure 3.2 Transformation of aspect values

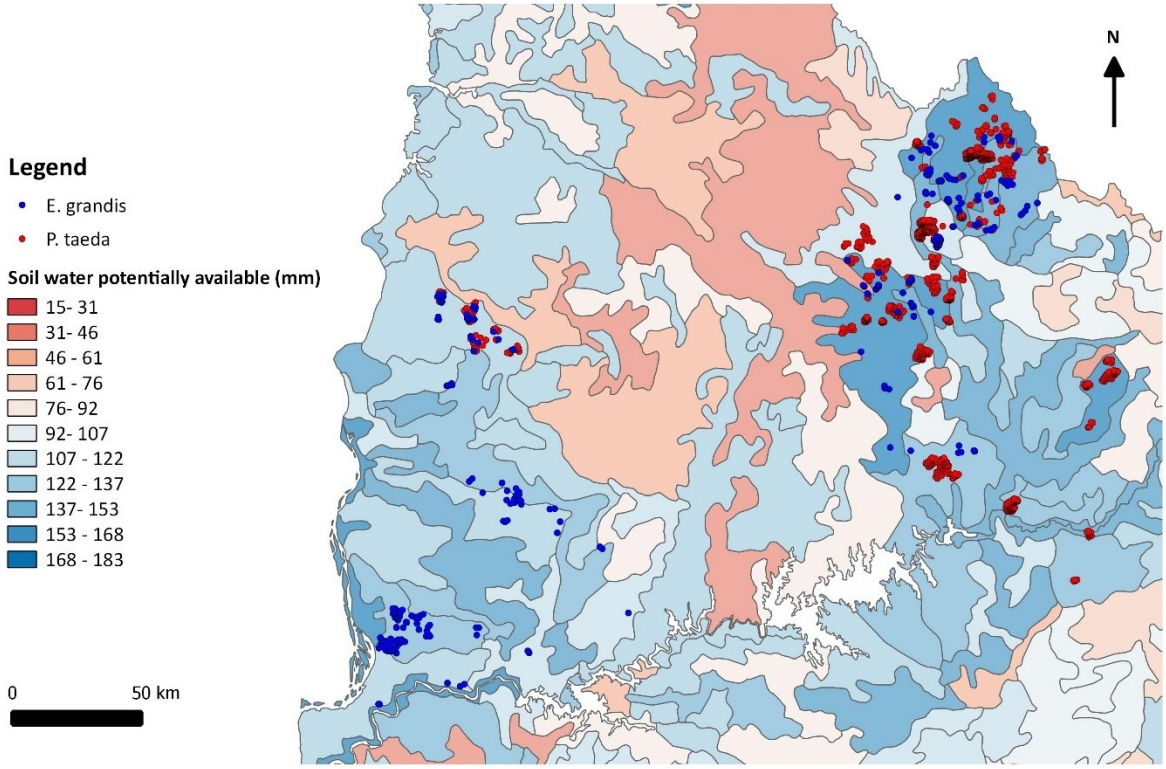

Figure 3.3 Range of water potentially available for PSPs of both species. Produced with spatial information of soil water potentially available (1:1.000.000 scale map) offered by the Ministry of Cattle, Agriculture and Fisheries (MGAP/RENARE) in http://www.cebra.com.uy/renare/mapa/cartas-tematicas/.

Datasets for both species were screened through graphic methods before and after computing the required variables to assess the relationship between variables. Suspicious values were checked in original records and corrected. All possible age intervals per plot were used.

h_{dom} was calculated as the mean total height of the 100 trees with the largest d within a hectare using Garcia's formula (García, 1998) to calculate the number of trees in each PSP equivalent to 100 trees per hectare.

70% of the plots were used for fitting while 30% were utilized for validation. A dataset was also prepared for hypothesis testing using only the longest interval of each plot of the entire dataset.

The information coverage including site variables is presented in Table 3.1.

Table 3.1 Summary of the variables used for modelling.

Variable	*P. taeda*				*E. grandis*			
	Mean	Min.	Max.	SD	Mean	Min.	Max.	SD
PSP number	-	-	727	-	-	-	315	-
Number of plot measurements	4.00	2.00	11.0	-	4.00	2.00	11.0	-
t (years)	7.13	2.00	25.9	3.20	6.95	1.18	18.7	3.47
h_{dom}(m)	10.6	2.20	27.0	4.65	21.2	4.40	46.6	7.86
d_m (cm)	17.2	2.30	41.9	7.56	17.6	3.10	45.2	7.18
d_{max} (cm)	21.1	4.00	46.7	8.71	24.3	5.00	62.6	8.77
d_{min} (cm)	12.8	0.48	36.6	6.92	10.1	0.10	41.1	6.64
SD_d (cm)	2.20	0.11	8.42	0.96	3.42	0.64	10.5	1.43
G ($m^2 \cdot ha^{-1}$)	15.6	0.10	53.6	10.9	19.2	0.78	58.1	8.95
N (stems.ha^{-1})	624	100	1667	180	886	87.0	1775	393
Plot size	338	200	500	84.0	682	400	2250	315
SWPA (mm)	148	85.1	179.6	33.8	140.5	85.1	180.6	30.0
Elev (m)	151	61.0	256	32.5	121	21	201	57.0
β (%)	5.00	0	>18	3.70	4.00	0	>18	3.33
Number of PSP in Zone 7	-	-	495	-	-	-	158	-
Number of PSP in Zone 8	-	-	90	-	-	-	6	-
Number of PSP in Zone 9	-	-	41	-	-	-	134	-
Number of plots in other zones	-	-	101	-	-	-	17	-

Growth equations

For modelling growth of h_{dom}, G, d_{max}, and SD_d, several differential equations in polymorphic and anamorphic form were tested (Tables 3.2 and 3.3). Those were fitted using non-linear least-squares as applied by Clutter (1963) using all possible intervals within PSPs. Maximum likelihood has been recommended by García (1983), but Sullivan and Clutter (1972) found that parameters estimated using non-linear least-squares and maximum likelihood, in practice, provided similar estimations. Mixed effects models are sometimes employed to account for multiple measurements within plots. In the study reported here the problems related to data serial correlation were avoided by testing the inclusion of new variables using a correlation-free dataset where only one interval per plot was included. In this way, valid hypothesis testing was undertaken.

Candidate equations were compared through the root of the mean square error (*RMSE*), as a measure of precision; the mean residual (*MR*) and mean absolute bias (*MAB*) as a measure of bias; and model efficiency (*EF*). All four prediction statistics calculated using the modelling dataset were ranked and an overall rank for each model was computed by summing the rank values for all the statistics. The best ranked model for each variable was selected. Normality was analysed graphically through histograms and Q-Q plots, whereas plots of residuals against the variables fitted and the independent variables were also assessed. After selecting the equation for each variable, the inclusion of site variables was tested using the hypothesis testing dataset. Once the variables to include were known all the equations were re-fitted using the modelling dataset.

In the case of dominant height, actual trajectories of PSP data were plotted with dominant height curves through time to assess the adequacy of the latter relative to the observations. For the validation stage, plots of residuals (observed in the validation dataset minus predicted values) versus predicted values were examined in order to detect bias. Confidence intervals for the slopes of predicted versus independent values with a level of significance of 5% were computed to compare the actual slope with the ideal slope of 1 (Goulding, 1979) .

Comparisons of approaches were done through the statistics of fit as well as statistics of prediction (using the validation dataset) for each type of equation (simple and augmented) and comparing residuals. Finally, the behaviour of models including site variables were assessed by plotting projections for contrasting growth conditions.

Table. 3.2 Polymorphic form of equations tested

Model	Expression	Number
Schumacher (1)	$Y_2 = e^{ln(Y_1)\left(\frac{t_1}{t_2}\right)+a\left(1-\frac{t_1}{t_2}\right)}$	(3.1)
Schumacher (2)	$Y_2 = e^{ln(Y_1)\left(\frac{t_1}{t_2}\right)^c+a\left[1-\left(\frac{t_1}{t_2}\right)^c\right]}$	(3.2)
Gompertz (1)	$Y_2 = e^{ln(Y_1)e^{-b(t_2-t_1)}e^{a[1-b(t_2-t_1)]}}$	(3.3)
Gompertz (2)	$Y_2 = e^{ln(Y_1)e^{-b(t_2-t_1)+c\left(t_2^2-t_1^2\right)}e^{a\left[1-e^{-b(t_2-t_1)+c\left(t_2^2-t_1^2\right)}\right]}}$	(3.4)
Weibull (1)	$Y_2 = Y_1 e^{-b\left(t_2^\gamma-t_1^\gamma\right)} + a[1-b(t_2^2-t_1^2)]$	(3.5)
Weibull (2)	$Y_2 = a - b\left(\frac{a-Y_1}{b}\right)^{\left(\frac{t_2}{t_1}\right)^\gamma}$	(3.6)
Hossfeld	$Y_2 = \frac{1}{\frac{1}{Y_1}\left(\frac{t_1}{t_2}\right)^b + a\left(1-\left(\frac{t_1}{t_2}\right)^b\right)}$	(3.7)
Von Bertalanffy-Richards (1)	$Y_2 = a\left(\frac{Y_1}{a}\right)^{\frac{ln\left[1-e^{(-bt_2)}\right]}{ln\left[1-e^{(-bt_1)}\right]}}$	(3.8)
Von Bertalanffy-Richards (2)	$Y_2 = a\left\{1-\left[1-\left(\frac{Y_1}{a}\right)^{1-v}\right]^{\frac{t_2}{t_1}}\right\}^{\frac{1}{1-v}}$	(3.9)
Von Bertalanffy-Richards (3)	$Y_2 = a\left\{1+\left[\left(\frac{a}{Y_1}\right)^v-1\right]e^{[-b(t_2-t_1)]}\right\}^{\frac{1}{v}}$	(3.10)
Levakovic	$Y_2 = \left\{{Y_1}^c\left[\left(\frac{t_1}{t_2}\right)^2+a\left(1-\left(\frac{t_1}{t_2}\right)^2\right)\right]\right\}^{\frac{1}{c}}$	(3.11)

Table 3.3 Anamorphic form of equations tested

Model	Expression	Number
Schumacher	$Y_2 = Y_1 e^{-b\left(\frac{1}{t_2}-\frac{1}{t_1}\right)}$	(3.12)
Gompertz	$Y_2 = Y_1 \frac{e^{-be^{-ct_2}}}{e^{-be^{-ct_1}}}$	(3.13)
Von Bertalanffy-Richards	$Y_2 = Y_1 \left[\frac{1-e^{-bt_2}}{1-e^{-bt_2}}\right]^c$	(3.14)
Weibull	$Y_2 = Y_1 \frac{1-e^{-bt_2{}^c}}{1-e^{-bt_2{}^c}}$	(3.15)
Hossfeld	$Y_2 = \frac{1}{\frac{1}{Y_1} + b\left(\frac{1}{t_2}\right)^c - \left(\frac{1}{t_1}\right)^c}$	(3.16)
Levakovic	$Y_2 = Y_1 \left[\left(\frac{t_2}{t_1}\right)^2 + \left(\frac{b+t_1{}^2}{b+t_2{}^2}\right)\right]^c$	(3.17)

Mortality equations

For modelling mortality, a two- step approach proposed by (Woollons, 1998) was used for both species. Firstly, a logistic equation for estimating the probability of stand death occurrence was fitted using all possible intervals of the modelling dataset. The equation is given by:

$$P = \frac{1}{1+e^{-bX}} \tag{3.18}$$

where P= probability of tree living or dying; b= vector of regression parameters and X= vector of explanatory variables

The inclusion of the site variables (previously described), population variables such as h_{dom}, G, and SD_d, as well as age, were assessed by plotting site descriptors against all the modelled variables first. The soil and physiographic descriptors were then included in the model using a backward elimination. This procedure starts with all the variables in the model, and one variable is eliminated at a time based on the higher p-value less than the α-criterion. A refit sequence is carried out until all variables are significant in the model.

Base and augmented models were compared through the Akaike Information Criterion in a second stage. Contingency tables were assessed for testing the ability to predict mortality occurrence of each model and the percentages of true answers were compared. In addition, the receiver operating characteristic (*ROC*) curve was plotted for each equation, and the area under the curve (AUC) was computed (Saveland and Neuenschwander, 1990). The *ROC* curve analysis is a distribution free method to measure the discrimination capacity of a model (Saveland and Neuenschwander, 1990). By changing the threshold value, the true positive rate (sensitivity) is plotted against the false positive rate (1-specificity). The area between the formed curve and the chance line ranges from 0.5 (where the rate of true and false positive are equally 0.5) to 1 (where the probability of true positive equals 1 and the probability of false positive equals 0). Hence, the higher AUC, the more accurately the model classifies the events.

In a second stage, an equation was selected for modelling decreasing stems per hectare by analysing several candidate equations (Table 3.4) using the same procedure and statistics as for growth and yield equations. For this stage, only intervals where mortality occurred were chosen, and within these, the longest intervals were considered for both species. This criterion was adopted in order to avoid using all possible intervals and minimize the error for long interval predictions. Because for *E. grandis* the amount of information available was scarce, the oldest interval of each plot was also included in the analysis. In this way it is also possible to capture more information about the lower asymptote, which could be difficult to identify and model.

The final number of living stems per hectare was calculated then as follows (Woollons, 1998):

$$N_{2adj} = N_1 - p(N_1 - N_2)$$

The selected two equations for each species were validated jointly using the same procedure as for validating growth equations (analysis of residuals and confidence intervals for the slopes of predicted versus independent values). Finally, to test the concordance of the system behaviour in relation with the population competition, log-log plots of stocking versus mean squared diameter calculated using the basal area equation were compared with self-thinning lines (Reineke, 1933). For this purpose, trajectories were created using 5-year and 4-year intervals for *P. taeda* and *E. grandis* respectively where the basal area equation fitted for each species was projected using only the initial real value of each plot. For this procedure all the plots were used.

Table 3.4 Mortality models tested

Model	Expression	Number
(Woollons, 1998)	$N_2 = \left\{\frac{1}{\sqrt{N_1}} + b\left[\left(\frac{t_2}{100}\right)^2 - \left(\frac{t_1}{100}\right)^2\right]\right\}^{-2}$	3.19
(Clutter et al., 1983)	$N_2 = N_1\left(\frac{T_2}{T_1}\right)^b e^{(a)(t_2-t_1)}$	3.20
(Pienaar and Shiver, 1981)	$N_2 = N_1 e^{a({t_2}^b - {t_1}^b)}$	3.21
Exponential decay anamorphic	$N_2 = N_1 e^{-b(t_2-t_1)}$	3.22

RESULTS

Growth equations

Matrices of simple linear correlations between the soil-based and physiographic variables and site index were initially assessed using the hypothesis testing dataset (Appendix I). High correlation between explanatory variables could interfere in determining the precise effect of each predictor and lead to large standard errors of the parameters. For *P. taeda* very low correlations were found between site variables; *SWPA* and *Elev*, and *Elev* and β are the most correlated with coefficients slightly over 0.3 in both cases. Moreover, none of the site variables showed high correlations with site index. Higher correlations were found in the case of the eucalypt species; the same variables *SWPA* and *Elev*, as well as *Elev* and β presented correlation coefficients of 0.84 and 0.60 respectively, whereas between *SWPA* and β the coefficient was 0.47. Additionally, it was found that those three variables were the most correlated to *SI*.

For both species the inclusion of a dummy variable (*Z7*) to distinguish growth in Zone 7 compared to the rest (Zones 9 and 8) was assessed (Methol, 2001). For the pine species, *Elev* was the site variable most correlated with the dummy (0.59), whereas correlation with *SI* was very low (0.16). For *E. grandis*, correlation was high between *Z7* and *Elev* (0.88) and *SWPA* (0.80), while the correlation with β was less evident (0.54). Therefore, it was not surprising that correlation between *SI* and *Z7* was also marked (0.72).

Dominant height

Whereas for *P.taeda* there were very modest or null improvements of the h_{dom} equations tested by adding the dummy variable, (probably because most of plots were located in Zone 7), for *E.grandis* its inclusion improved both error and bias. For the pine species the chosen model was eq. 3.8 (von Bertalanffy-Richards ploymorphic) while for *E.grandis* it was equation 3.1 with the incorporation of the dummy variable in the asymptote. This equation ranked third after equations 3.2 and 3.8, but those projected excessively high growth rate during the first two years when plotting dominant height curves against plot trajectories, hence they were discarded.

The equation for *E. grandis* was:

$$h_{dom_2} = e^{ln(H_{dom_1})\left(\frac{t_1+k}{t_2+k}\right)+(a_0+a1*Z7)\left(1-\frac{t_1+k}{t_2+k}\right)} \quad (3.1a)$$

In this equation, a constant (k) was added to t_1 and t_2 to the equation 3.1, giving the equation known as Johnson-Schumacher (Grosenbaugh, 1965). This modification greatly improved bias and precision while the equation still preserves the properties of path invariance and consistency.

When assessing the incorporation of site variables, the inclusion of *SWPA*, and *Elev* in the equations selected for *P. taeda* decreased the root mean square error modesty, whereas. β, α_s, and α_c were not significant using the correlation-free hypothesis testing dataset. However *SWPA*, α_c, and $\alpha_s$were significant for predicting *E. grandis*' h_{dom}, improving the error by 5.6 %. The augmented equations for *P. taeda* and *E. grandis* respectively were:

$$h_{dom_2} = (a_0 + a_1 SWPA + a_2 Elev)\left[\frac{h_{dom_1}}{(a_0 + a_1 SWPA + a_2 Elev)}\right]^{\frac{ln[1-e^{(-bt_2)}]}{ln[1-e^{(-bt_1)}]}} \quad (3.8a)$$

$$h_{dom_2} = e^{ln(h_{dom_1})\left(\frac{t_1+k}{t_2+k}\right)+(a_0+a_1*SWPA+a_2\alpha_c+a_3\alpha_s)\left(1-\frac{t_1+k}{t_2+k}\right)} \quad (3.2a)$$

Statistics of fit of the selected simple and augmented models are depicted in Table 3.5, while their parameters are shown in Table 3.6.

Table 3.5. Statistics of fit of the equations chosen for predicting h_{dom} through base (B) and augmented equations (A) for each species.

Species	Equation	Approach	*RMSE*	*MR*	*MAB*	*EF*	*RMSE* difference (%)
P.taeda	3.8	B	0.894	-0.007	0.686	0.95	-
	3.8a	A	0.867	-0.002	0.667	0.95	-3.0
E.grandis	3.1a	B	1.785	0.114	1.353	0.91	-
	3.2a	A	1.685	0.032	1.281	0.92	-5.6

RMSE: root mean square error; MAB: mean absolute bias; EF: efficiency

Table 3.6. Parameters of the equations selected for modelling h_{dom} in the studied species.

Species	Eq.		a /a_0	a_1	a_2	a_3	b	k
P.taeda	3.8	Estimate	30.413912	-	-	-	0.102622	-
		SE	0.323879	-	-	-	0.001877	-
		p-value	<0.001	-	-	-	<0.001	-
	3.8a	Estimate	22.265319	0.023379	0.021562	-	0.109748	-
		SE	0.441550	0.001961	0.002314	-	0.001888	-
		p-value	<0.001	<0.001	<0.001	-	<0.001	-
E. grandis	3.1a	Estimate	4.00389	0.19295	-	-	-	3.06896
		SE	0.01233	0.01010	-	-	-	0.08570
		p-value	<0.001	<0.001	-	-		<0.001
	3.2a	Estimate	3.6014737	0.0029913	0.0087987	0.0175036	-	2.4973491
		SE	0.0223338	0.0001586	0.0028142	0.0011831	-	0.0870299
		p-value	<0.001	<0.001	<0.01	<0.001	-	<0.001

Residual plots for the four models are shown in Figures 3.4 and 3.5. For both species, residuals against predicted values as well as independent variables presented minimal bias.

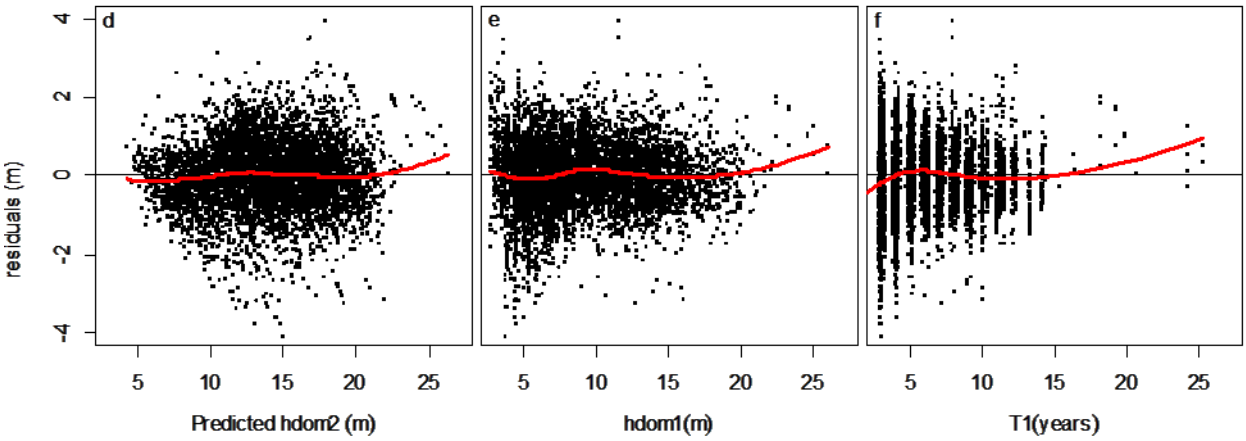

Figure 3.4. Residuals of the selected equation for modelling h_{dom} for *P. taeda* for the base (a, b, c) and augmented equation (d, e, f) including lowess line (red).

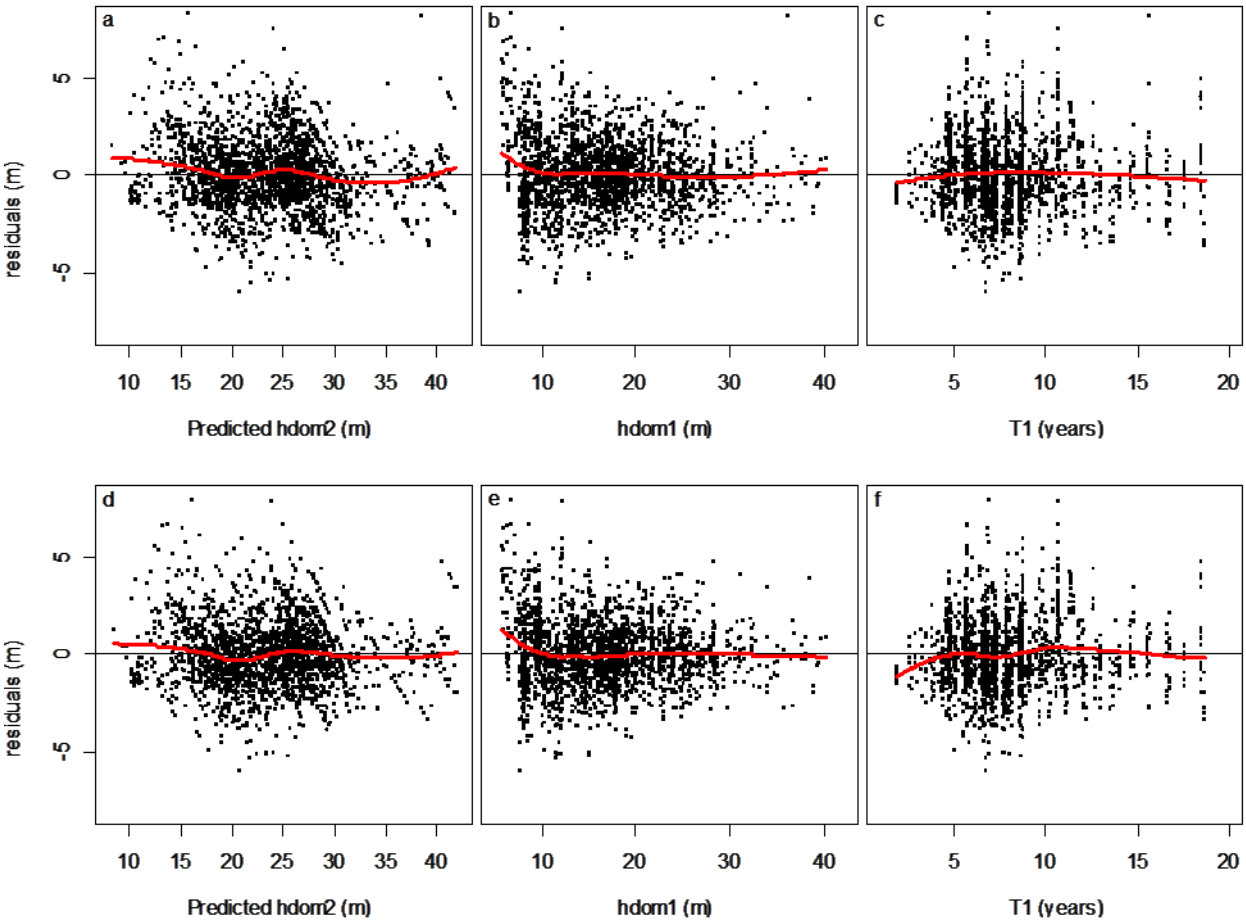

Figure 3.5. Residuals of the selected model for for modelling h_{dom} *E. grandis* for the base equation (a, b, c) and augmented equation (d, e, f) including lowess line (red).

When validating the models, residuals of both types of equations for each species using the independent dataset also showed satisfactory behaviour (Fig. 3.6). The 95% confidence interval for the slope of the relationship between observed and predicted values was 1.00-1.02 for simple and enhanced models for *P.taeda*, whereas for *E.grandis* it was 0.96-0.99 and 0.98-1.01 respectively. The *RMSE* using independent data was lower for enhanced equations with respect to the base ones but with small differences: for *P.taeda RMSE* were 0.86 and 0.85 for base and augmented equations respectively and 1.69 and 1.66 for *E.grandis*.

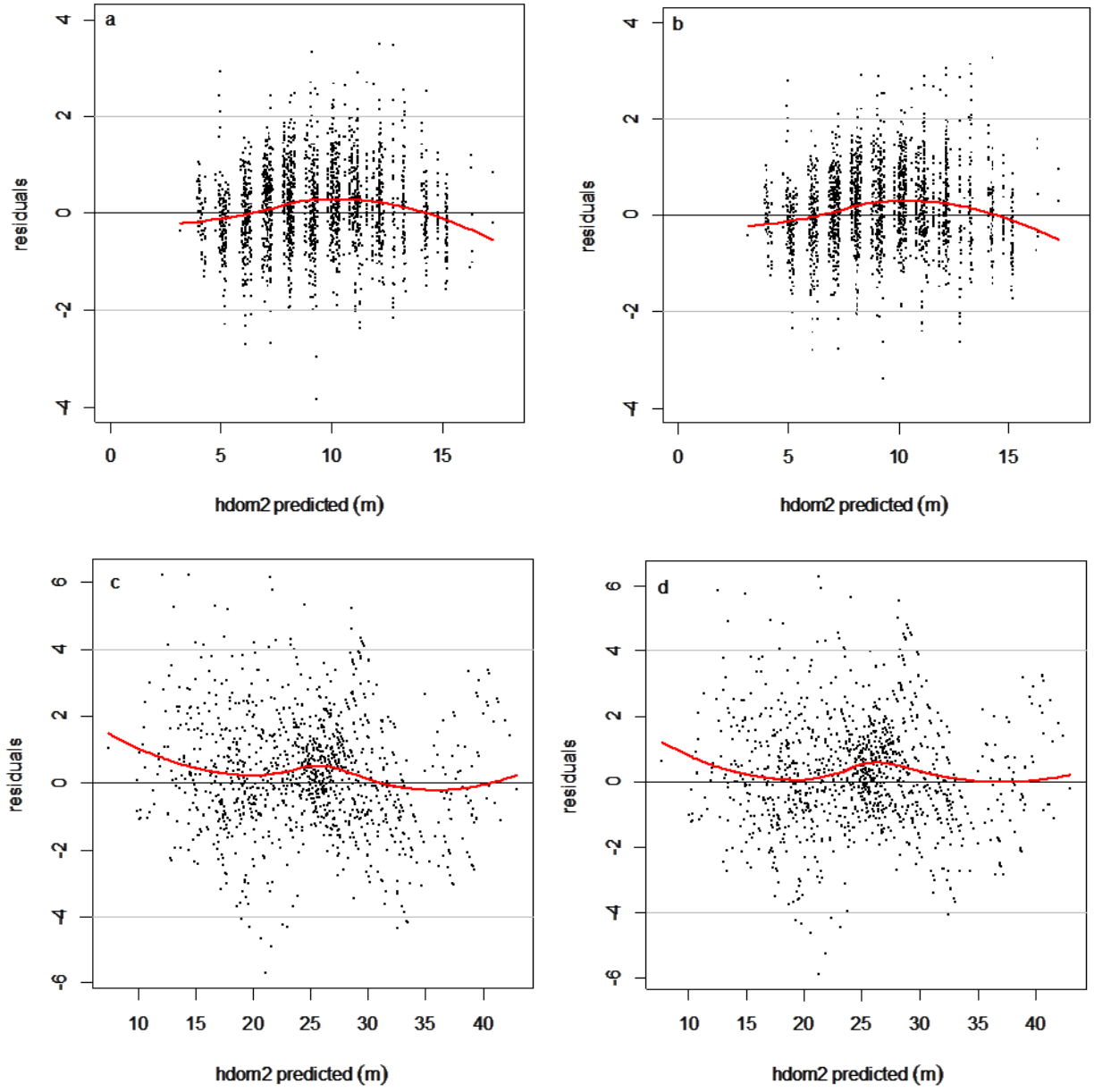

Figure 3.6 Residuals using the validation dataset for *P.taeda*'s base (a) and augmented equations (b), and for *E.grandis*' base (c), and augmented function (d) with lowess line (red).

Finally, the dominant height curves fitted showed correspondence to the trajectories of the entire dataset for each species (Fig. 3.7a and 3.8a and 3.8b). For the case of *E. grandis*, it can be noticed that plots located in the northern part of the country ($Z7$=1) reached greater dominant heights in general. This is also observed in the augmented equations curves when using the average *SWPA* and β values for each zone; similarities between curves using the dummy variable and enhanced equations using average values of the site variables *SWPA*, α_s and α_c for each zone are evident.

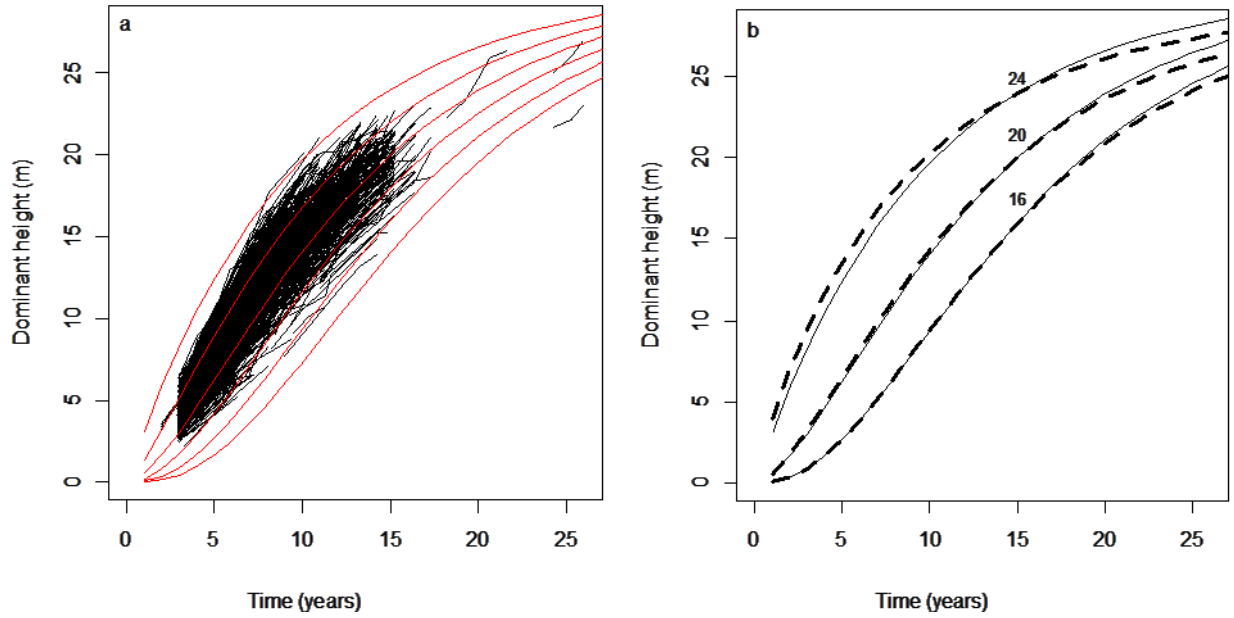

Figure 3.7 Dominant height curves (SI=14-24m) for the base equation with original plot trajectories (a) and a comparison between projections using base (continued lines) and augmented equations(dashed lines) for 3 different sites using average values of *SWPA* and elevation (b) for *P. taeda*.

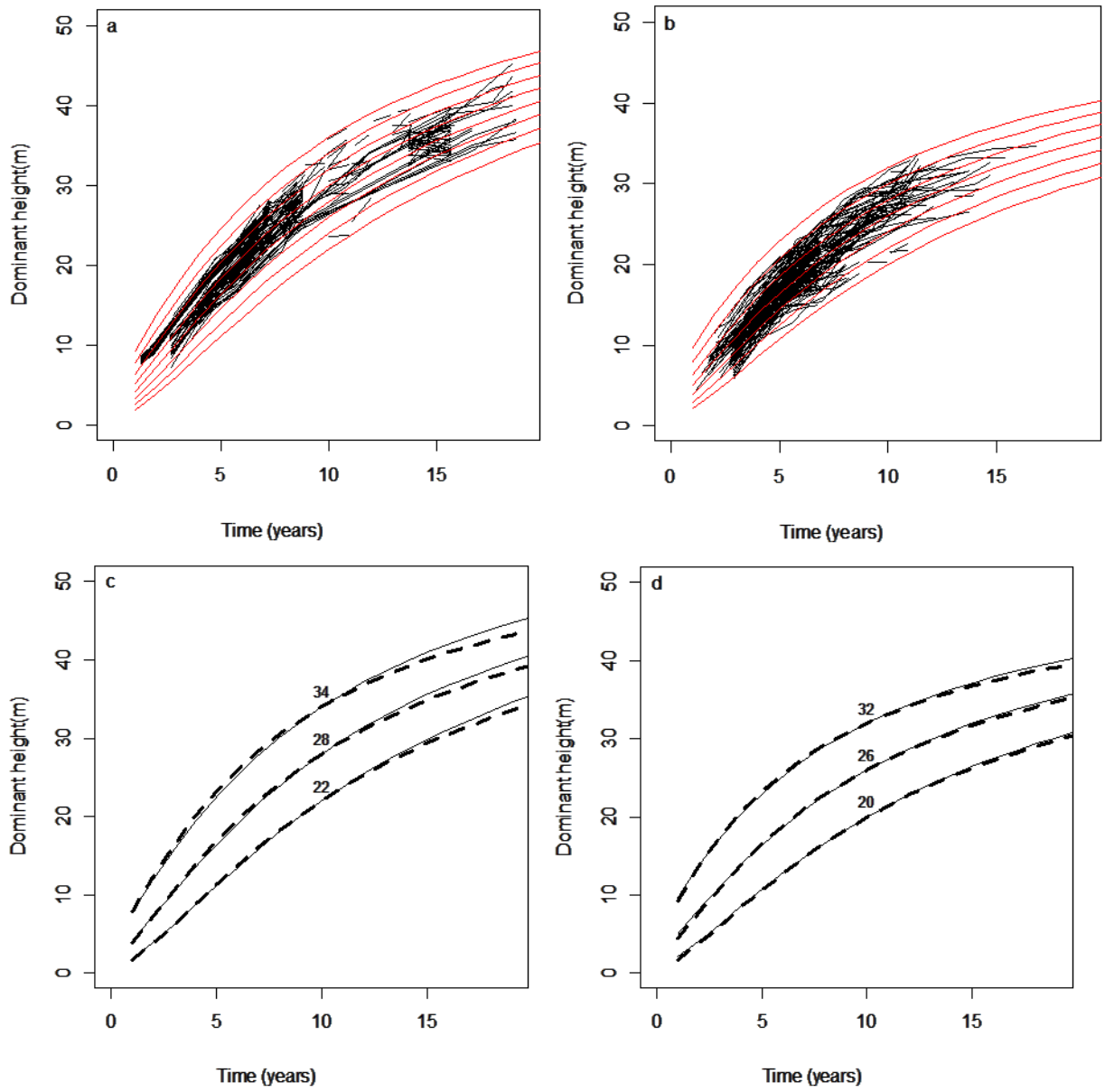

Figure 3.8 Dominant height curves for *E. grandis* using the base equations for Zone 7 (SI=22-34m) (a), and rest (SI=20-32m) (b) with observed plot trajectories, and a comparison with projections using augmented equations calculated using average values of *SWPA*, $\boldsymbol{\beta}$ and $\boldsymbol{\alpha}$ for Zone 7 (c) and rest (d).

A closer analysis of the influence of the site variables included in the equations (Figure 3.9), showed that for *P. taeda* higher growth rate was achieved in sites with higher elevation and higher *SWPA* values. For *E. grandis*, the equation projects higher growth rate for NE orientation in steeper terrains with high values of *SWPA* (Figure 3.10). In the example, for the same water availability, slopes facing NE comprised better sites than slopes facing SW, whereas flat terrains represented intermediate site quality. From a physiological point of view the model shows consistency.

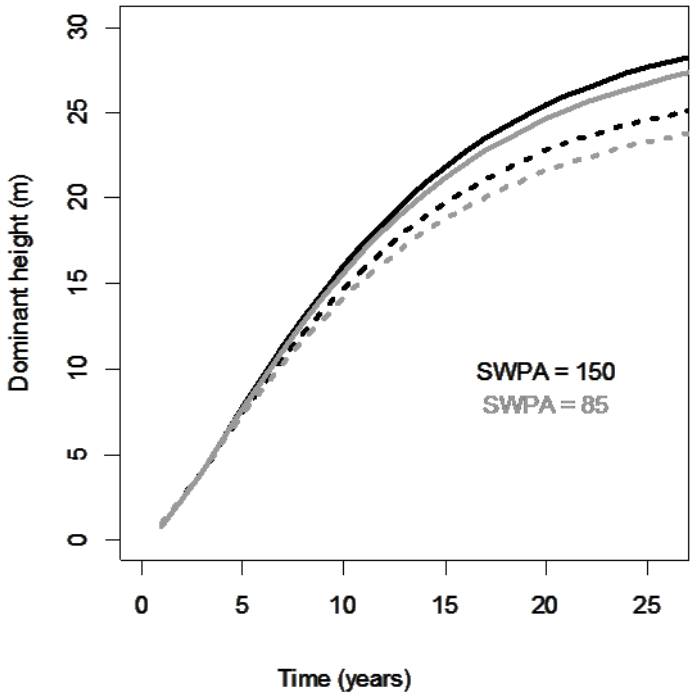

Figure 3.9 Dominant height growth curves for two levels of *SWPA* for elevation values of 230 m (continued line) and 65 m (dotted) for *P. taeda*.

The example plots also show differences in h_{dom} growth with respect to *SWPA* values changes between both species; when for *P. taeda* the increase in growth by increasing 65 mm of *SWPA* is approximately 2 m at the age 20, for *E. grandis* an increase of 53 mm represents around 5 m of height increase. This suggests that a smaller change in *SWPA,* leads to a larger increase in growth in *E. grandis* with respect to *P. taeda*.

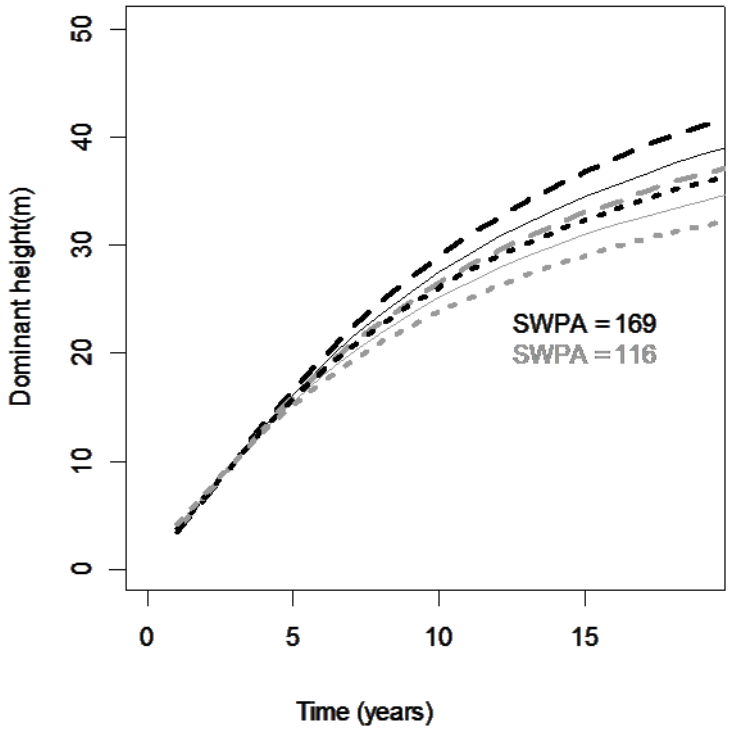

Figure 3.10 Dominant height growth curves for the average values of SWPA for zone 7 (black) and the rest (grey), for slopes of 9% facing NE (dashed) and SW (dotted), and slopes of 0% (continued).

Net Basal Area

For projecting basal area, the inclusion of a ratio of stocking per hectare after thinning and before thinning divided by the time of thinning ((Na/Nb)/tt) (Temu, 1992; Methol, 2001) was also assessed. For the pine species, this term achieved no significance in the model and was not included but for *E. grandis* the effect was significant when using the hypothesis testing dataset.

For *P. taeda* the best ranked equation was eq. 3.2 (Schumacher polymorphic 2) so it was selected. For *E.grandis*, a better distribution of residuals caused the equation 3.2 to be chosen. The thinning variable was included in the shape parameter and a dummy variable to account for zoning was added to the asymptote. The final equation for *E. grandis* was:

$$G_2 = e^{ln(G_1)\left(\frac{t_1}{t_2}\right)^{c_0+c_1\left[\frac{\left(Na/Nb\right)}{tt}\right]}+(a_0+a_1 Z7)\left\{1-\left(\frac{t_1}{t_2}\right)^{c_0+c_1\left[\frac{\left(Na/Nb\right)}{tt}\right]}\right\}} \quad (3.2b)$$

The inclusion of the site variables *SWPA*, α_c and *Elev* to the asymptote represented a significant improvement on the *RMSE* for *P. taeda* (Table 3.7). The augmented equation is given by:

$$G_2 = e^{ln(G_1)\left(\frac{t_1}{t_2}\right)^c + (a_0 + a_1 SWPA + a_2 \alpha_c + a_3 Elev)\left[1 - \left(\frac{t_1}{t_2}\right)^c\right]} \quad (3.2c)$$

For *E. grandis*, *SWPA* and *E* located in the asymptote improved the error more than 6%. The final augmented equation is as follows:

$$G_2 = e^{ln(G_1)\left(\frac{t_1}{t_2}\right)^{c_0 + c_1\left[\frac{\left(N_a/N_b\right)}{tt}\right]} + (a_0 + a_1 SWPA + a_2 Elev)\left\{1 - \left(\frac{t_1}{t_2}\right)^{c_0 + c_1\left[\frac{\left(N_a/N_b\right)}{tt}\right]}\right\}} \quad (3.2d)$$

Statistics of fit of the base and augmented models are depicted in Table 3.7 while parameters are shown in Table 3.8.

Table 3.7 Statistics of fit of the equations chosen for predicting *G* through base (B) and augmented equations (A) for each species.

Species	Equation	Approach	*RMSE*	*MR*	*MAB*	*EF*	*RMSE* difference (%)
P.taeda	3.2	B	3.151	0.014	2.246	0.90	-
	3.2c	A	2.929	0.072	2.125	0.91	-7.0
E.grandis	3.2b	B	2.847	0.051	1.998	0.82	-
	3.2d	A	2.677	0.046	1.906	0.84	-6.3

RMSE: root mean square error; MAB: mean absolute bias; EF: efficiency

Table 3.8 Parameters of the equations selected for modelling *G*.

Species	Eq.	-	a/a_0	a_1	a_2	a_3	c/c_0	c_1
P.taeda	3.2	Estimate	4.51079	-	-	-	1.013	-
		SE	0.02101	-	-	-	0.01287	-
		p-value	<0.001	-	-	-	<0.001	-
	3.2c	Estimate	3.7497295	0.0026375	0.0068628	0.0018031	1.0520980	-
		SE	0.0322047	0.0001733	0.0010891	0.0001776	0.0122932	-
		p-value	<0.001	<0.001	<0.001	<0.001	<0.001	-
E.grandis	3.2b	Estimate	3.7534	0.27345	-	-	1.07956	-0.93323
		SE	0.01995	0.01834	-	-	0.02539	0.05720
		p-value	<0.001	<0.001	-	-	<0.001	<0.001
	3.2d	Estimate	2.611299	0.0115832	-0.0033998	-	1.1164274	-1.0353749
		SE	0.0611871	0.0006817	0.0003416	-	0.0243492	0.0552464
		p-value	<0.001	<0.001	<0.001	-	<0.001	<0.001

Residual plots for the simple and augmented equations for each species are depicted in Figures 3.11 and 3.12. Only a small bias is observed for both pine equations and both eucalypt equations (with minimal bias for the ranges where most of the data is concentrated). Bias against the independent variables G_1 and t_1 is minimal for all four functions.

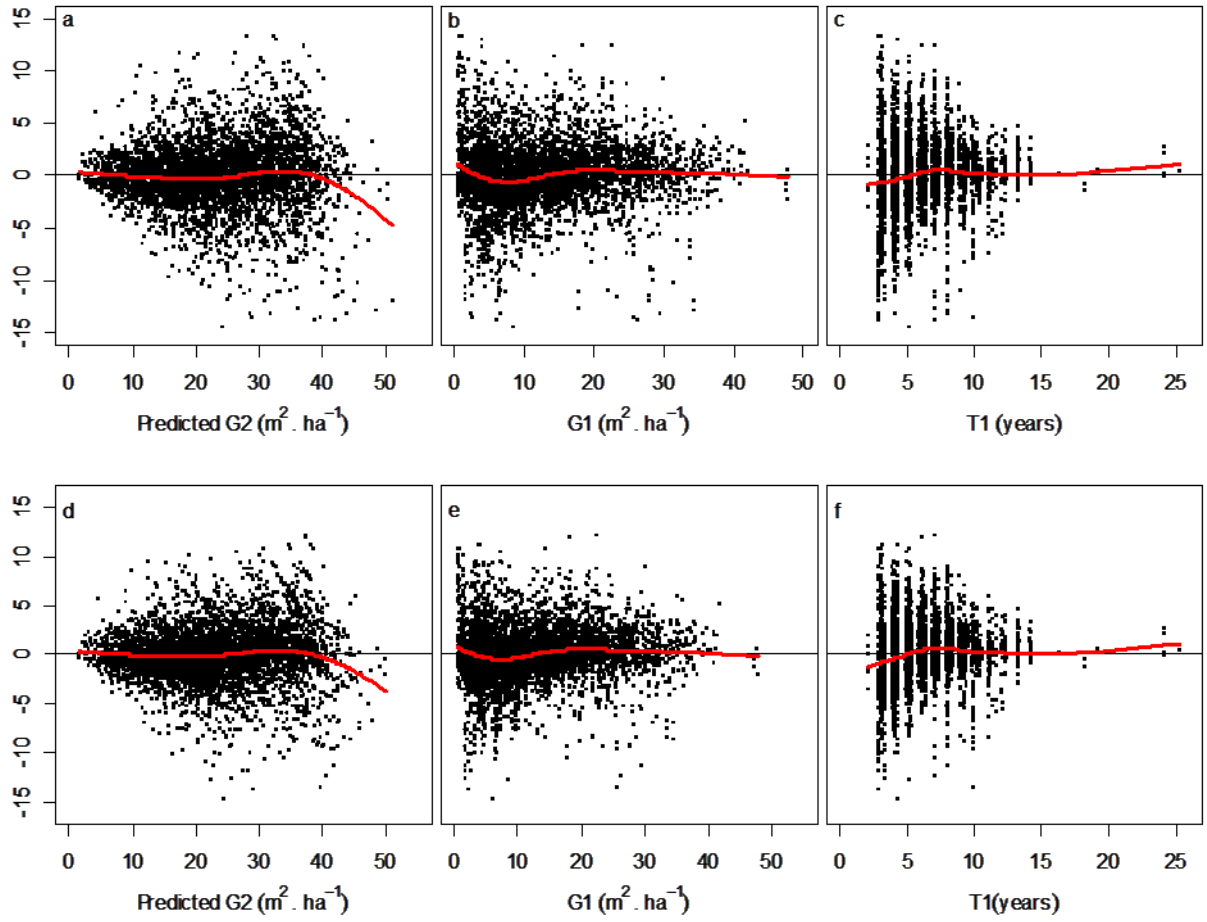

Figure 3.11. Residuals of the selected equation for modelling *G* for *P. taeda* for the base equation (a, b, c) and augmented equation (d, e, f) including lowess line (red).

A residual plot using the validation datasets did not show any strong tendency neither for simple nor for enhanced models (Figure 3.13). The 95% confident interval for the slope of predicted versus independent observed data ranged between 1.04-1.07 and 1.00-1.05 for the baseline models of *P.taeda* and *E. grandis* respectively, whereas for augmented functions the interval ranged from1.03-1.06 and 1.01-1.06 for each species. *RMSE* was 3.20 and 3.13 for *P. taeda*, and 2.76 and 2.65 for *E. grandis* for baseline and enhanced equations respectively.

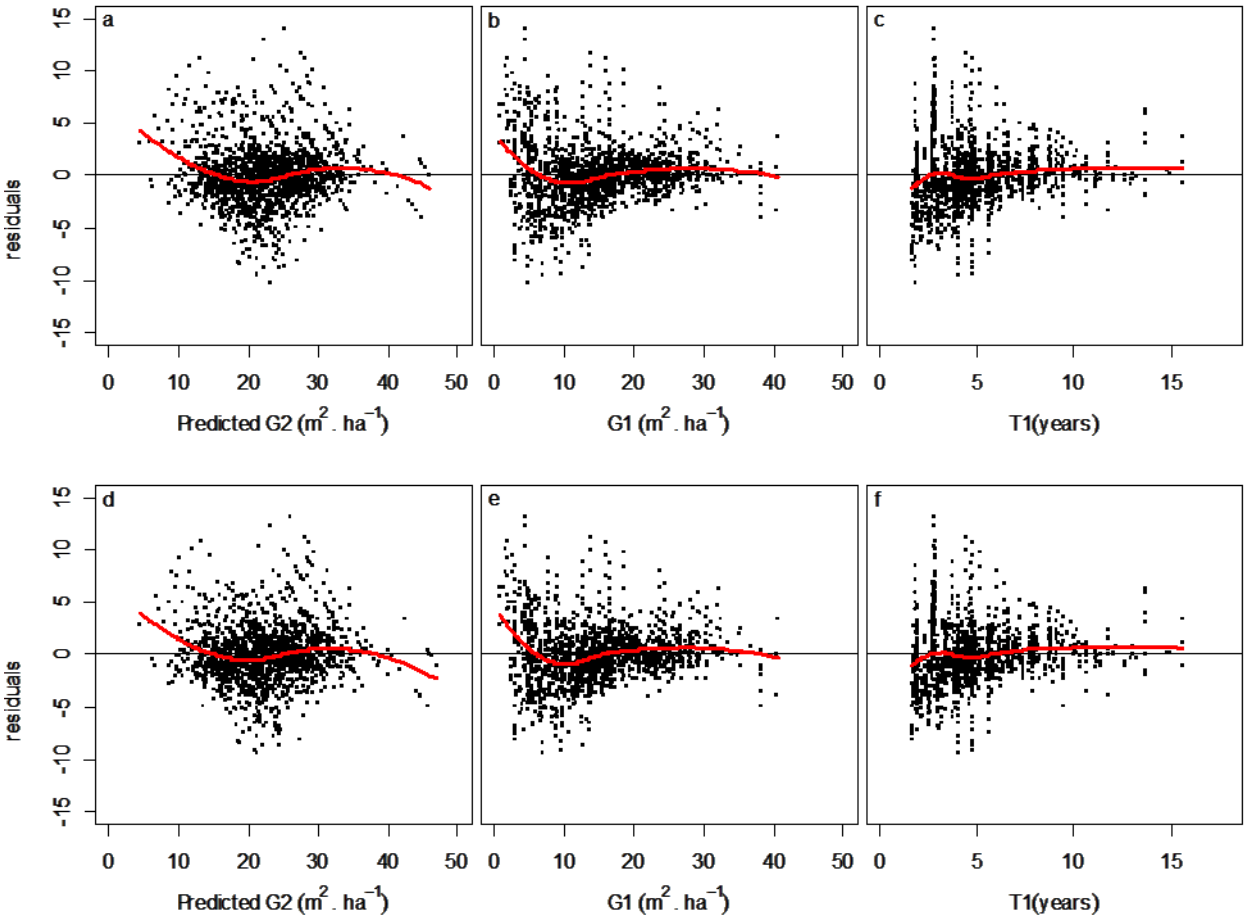

Figure 3.12 Residuals of the selected equation for modelling *G* for *E. grandis* for the base equation (a, b, c) and augmented equation (d, e, f) including lowess line (red).

The effect of the site variables over the net basal area growth curves can be observed in the example shown in Figures 3.14 and 3.15. East aspects on steeper terrains and larger water storage capacity would favour basal area growth for *P. taeda*. For *E. grandis*, the equation predicts higher basal area growth rate in sites with higher values of *SWPA* and lower *Elev*.

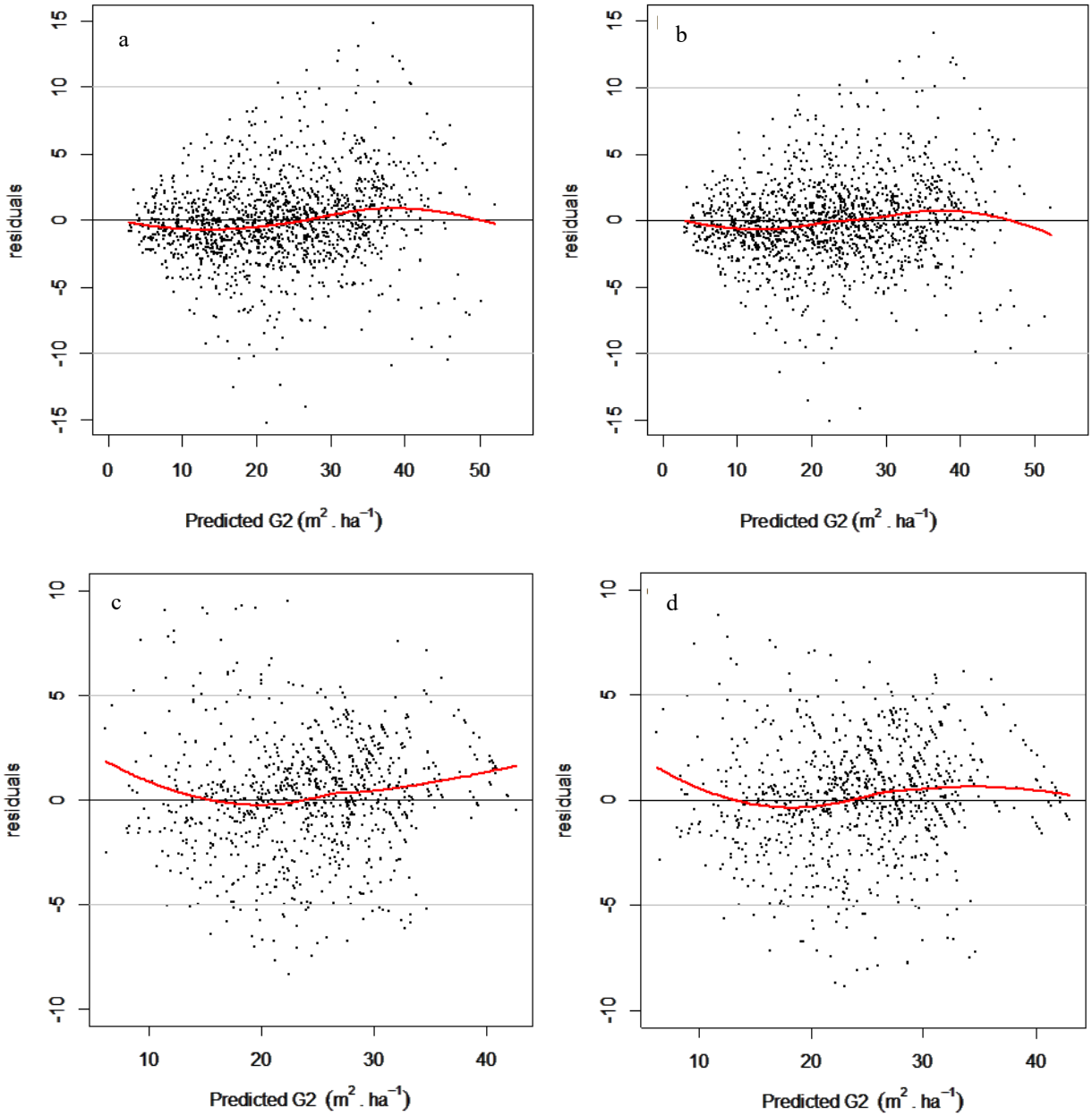

Figure 3.13 Residuals using the validation dataset for *P. taeda*'s baseline (a) and augmented equations (b), and for *E.grandis*' baseline (c), and augmented function (d) with lowess line (red).

The examples presented on Fig. 3.13 and 3.14 show that an increase in 65 mm of *SWPA* represented an increase of around 5 m^2ha^{-1} for the pine species, whereas for *E. grandis* an increase of 53 mm would increase *G* by 20 m^2ha^{-1}. As observed for dominant height, a smaller increase (with respect to the pine species) in *SWPA* presumes a larger increase in productivity for the eucalypt species.

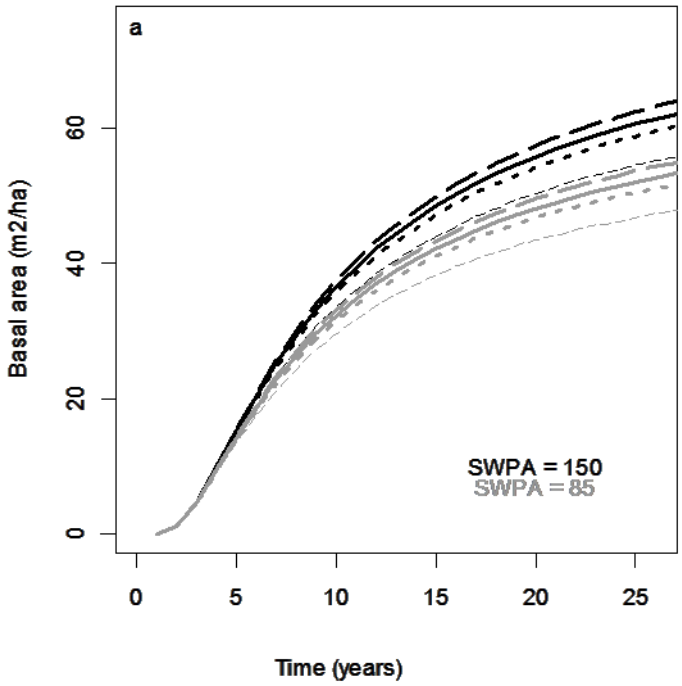

Figure 3.14 Net basal area growth curves for the two levels of *SWPA* for elevation values of 150 m (thick line) and 65 m (thin lines), 5% slopes facing E (dashed) and facing W (dotted), and 0% slopes (continued line) for *P. taeda*.

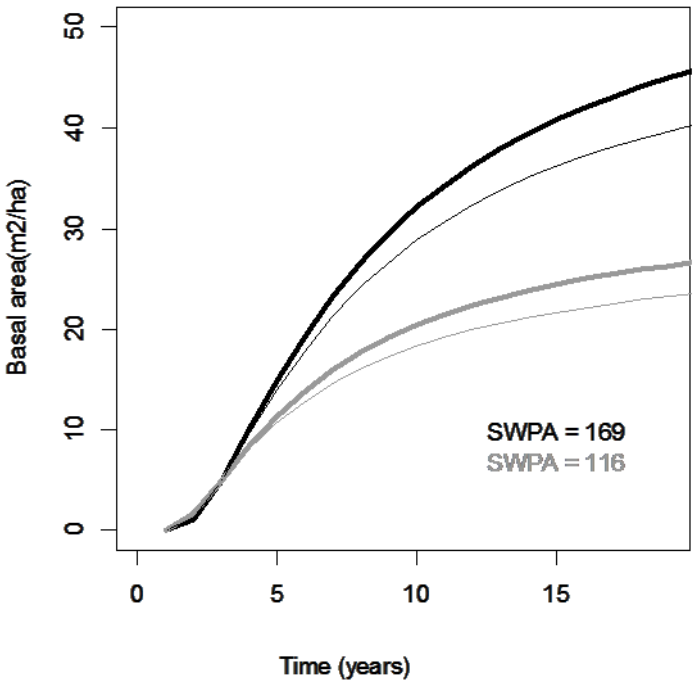

Figure 3.15 Basal area growth curves for the average values of *SWPA* for zone 7 (black) and the rest (grey) for elevation values of 130 m (thick) and 172 m (thin lines).

Maximum diameter

For *P.taeda,* although equation 3.8 showed a smaller error, equation 3.2 was chosen for presenting a better residual distribution. To correct bias, site index (*SI*) was introduced in the equation in the following way:

$$d_{max_2} = e^{ln(d_{max_1})\left(\frac{t_1}{t_2}\right)^c + (a_0 + a_1 SI)\left[1 - \left(\frac{t_1}{t_2}\right)^c\right]} \quad (3.2e)$$

Only *SWPA* placed in the asymptote was significant when testing the use of site variables through the hypothesis testing dataset, however neither the inclusion of this variable, nor the use of a dummy variable for zone improved the error, hence an augmented counterpart was not further studied. However, site variables would be indirectly introduced if *SI* was calculated using the augmented equations for h_{dom} (3.8a).

For *E.grandis*, the best equation was eq. 3.2 (Schumacher polymorphic), with the inclusion of a dummy variable for zoning in the asymptote and shape parameters as it follows:

$$d_{max_2} = e^{ln(d_{max_1})\left(\frac{t_1}{t_2}\right)^{c_0 + c_1 Z7} + (a_0 + a_1 Z7)\left[1 - \left(\frac{t_1}{t_2}\right)^{c_0 + c_1 Z7}\right]} \quad (3.2f)$$

For this species the inclusion of site variables *SWPA* and $\alpha_s$were significant and decreased the error over 10%.

The enhanced equation for *E. grandis* is as follows:

$$d_{max_2} = e^{ln(d_{max_1})\left(\frac{t_1}{t_2}\right)^{c_0 + c_1 \alpha_s} + (a_0 + a_1 SWPA + a_2 \alpha_s)\left[1 - \left(\frac{t_1}{t_2}\right)^{c_0 + c_1 \alpha_s}\right]} \quad (3.2g)$$

Statistics of fit as well as the parameters of each fitted equation are presented in Tables 3.9 and 3.10 respectively.

Table 3.9 Statistics of fit of the equations chosen for predicting d_{max} through base (B) and augmented equations (A) for each species.

Species	Equation	Approach	*RMSE*	*MR*	*MAB*	*EF*	*RMSE* difference (%)
P.taeda	3.2e	B	1.789	0.050	1.324	0.98	-
E.grandis	3.2f	B	2.179	0.100	1.610	0.91	-
	3.2g	A	1.951	0.060	1.450	0.93	-10.5

RMSE: root mean square error; MAB: mean absolute bias; EF: efficiency

Table 3.10 Parameters of the equations selected for modelling d_{max}.

Species	Eq.	-	a_0	a_1	a_2	c/c_0	c_1
P. taeda	3.2e	Estimate	6.392204	-0.100819	-	0.749582	-
		SE	0.105504	0.004479	-	0.011994	-
		p-value	<0.001	<0.001	-	<0.001	-
E. grandis	3.2f	Estimate	4.26886	1.14703	-	0.45368	-0.15881
		SE	0.07421	0.16114	-	0.02620	0.03274
		p-value	<0.001	<0.001	-	<0.001	<0.001
	3.2g	Estimate	3.4624929	0.005749	0.0714808	0.5225331	-0.0101125
		SE	0.0483201	0.0002405	0.0067483	0.0187085	0.0027341
		p-value	<0.001	<0.001	<0.001	<0.001	<0.001

Residual plots for each species showed minimal bias with respect to the predicted variable as well as the independent variables (Figures 3.16 and 3.17). For the eucalypt species, it is clear the reduction of residuals' dispersion corresponding to the augmented function.

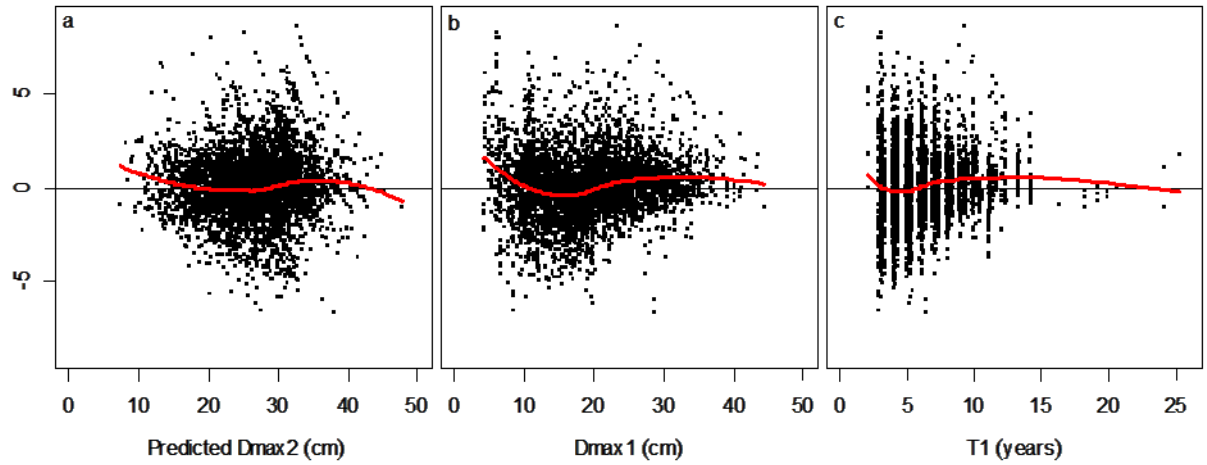

Figure 3.16 Residuals of the selected base equation for modelling d_{max} for *P. taeda* including lowess line (red).

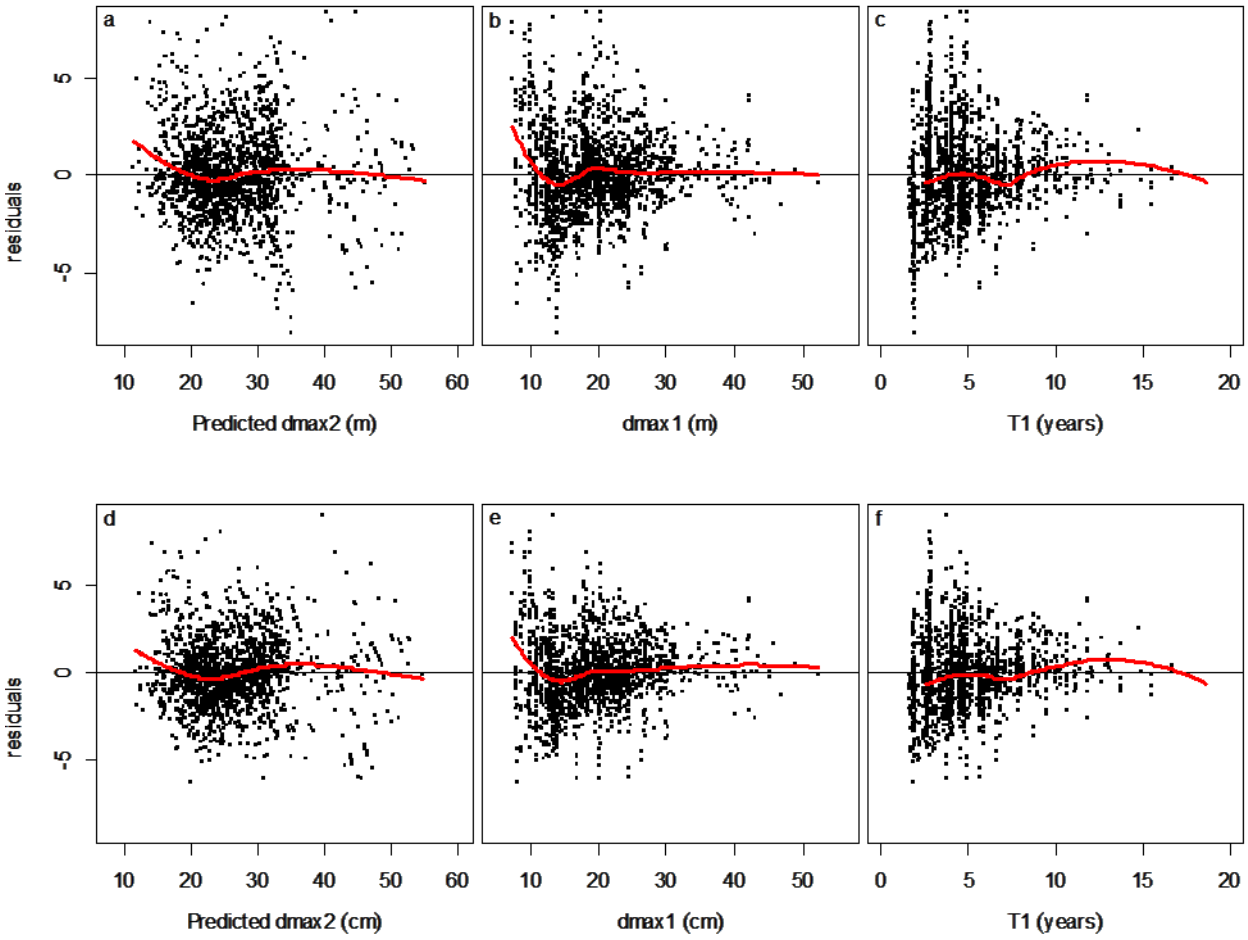

Figure 3.17 Residuals of the selected equation for modelling d_{max} for *E. grandis* for the base equation (a, b, c) and augmented equation (d, e, f) including lowess line (red).

Residual plots did not show any tendencies for either species (Figures 3.18 and 3.19). The interval with 95% of confidence for the slope of observed vs predicted values were: 1.04-1.08 for *P.taeda*, and 0.92-0.97 and 0.96-1.02 for simple and enhanced equations for *E.grandis* respectively. *RMSE* was 2.08 for the pine species, and 2.22 and 2.18 for simple and augmented eucalypt's equations.

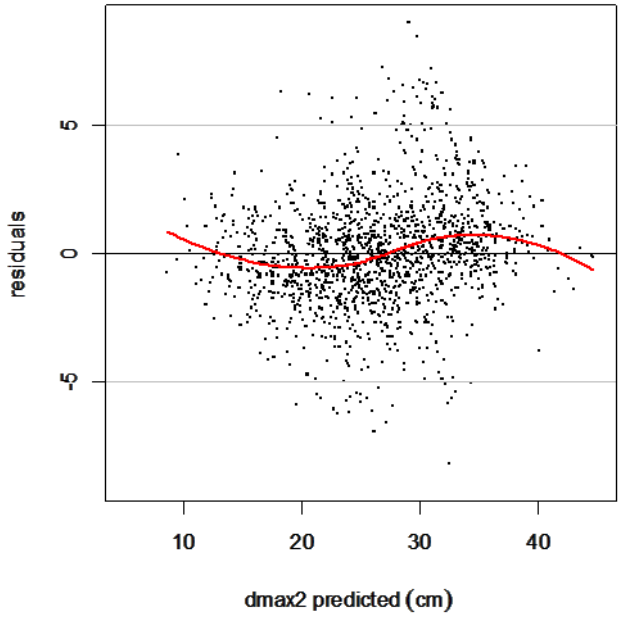

Figure 3.18 Residuals using the validation dataset for *P. taeda* simple functions with lowess line (red).

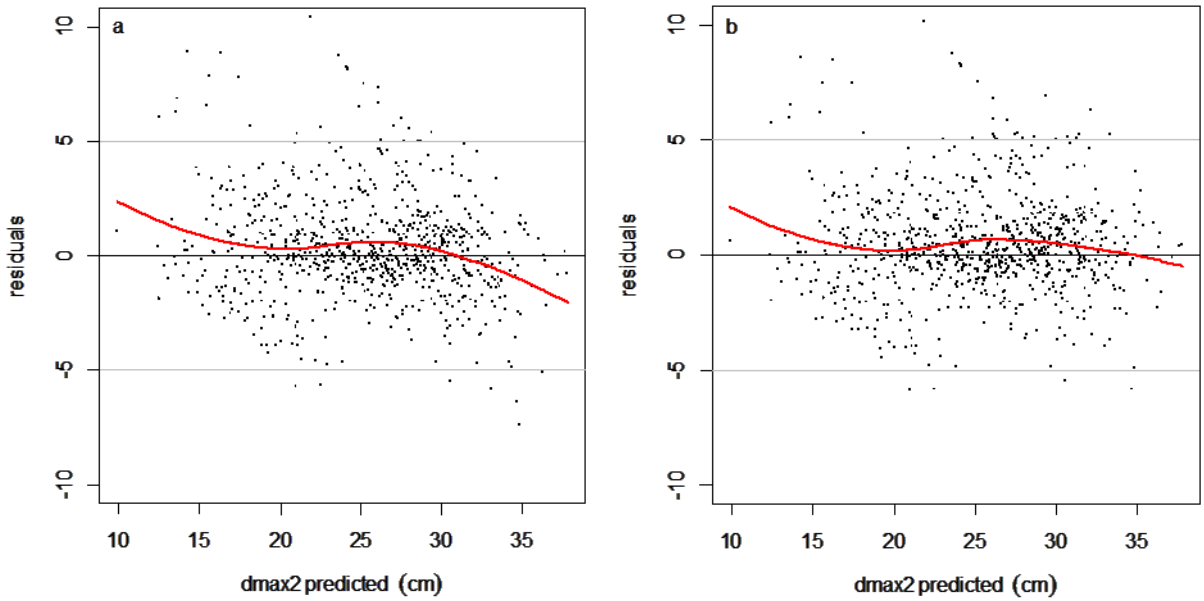

Figure 3.19 Residuals using the validation dataset for *E. grandis*' base (a), and augmented functions (b) with lowess line (red).

Site variables *SWPA* and α_s included in the *E. grandis*' equation affects d_{max} such that stands located in soils with high levels of water storage capacity and steeper terrains facing East result in larger diameters (Figure 3.20).

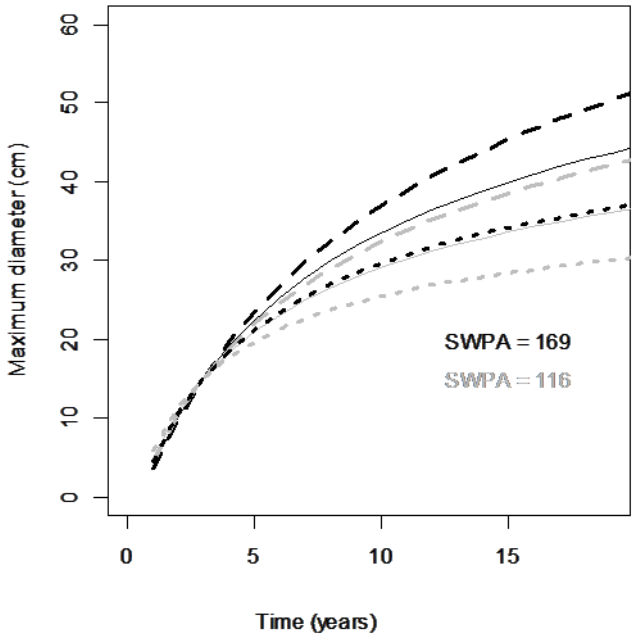

Figure 3.20 Maximum diameter growth curves for the average values of *SWPA* for zone 7 (black) and the rest (grey) for 5% slopes facing East (dashed) and West (dotted), and slope values of 0% (continued line) for *E. grandis*.

Standard deviation of diameters

For modelling SD_d for *P.taeda*, the selected equation was eq. 3.8 (Von Bertalanffy-Richards). A dummy for zoning was not significant when assessed with the hypothesis testing dataset, whereas *SWPA* and *Ele* were significant in the asymptote. However, the error was not improved, hence an augmented model was not further tested.

Equation 3.8a was the one with best fitting statistics for *E. grandis*, and the inclusion of a dummy variable in the asymptote that accounts for the differential growth rate in the zone 7 with respect to the rest of the zones was effective.

$$SD_{d_2} = (a_0 + a_1 Z7)\left(\frac{SD_{d_1}}{a_0 + a_1 Z7}\right)^{\frac{ln[1-e^{(-bt_2)}]}{ln[1-e^{(-bt_1)}]}} \quad (3.8b)$$

Testing site variables, only α_s was significant and it inclusion in the asymptote improved the error over 4%. The augmented equation is:

$$SD_{d_2} = (a_0 + a_1\alpha_s)\left[\frac{SD_{d_1}}{(a_0 + a_1\alpha_s)}\right]^{\frac{ln[1-e^{(-bt_2)}]}{ln[1-e^{(-bt_1)}]}} \quad (3.8c)$$

Statistics of fit and parameters are shown in Tables 3.11 and 3.12 respectively.

Table 3.11 Statistics of fit of the equations selected for predicting SD_d through base (B) and augmented equations (A) for each species.

Species	Equation	Approach	*RMSE*	*MR*	*MAB*	*EF*	*RMSE* difference (%)
P.taeda	3.8	B	0.484	-7.9e-5	0.335	0.72	-
E.grandis	3.8b	B	0.516	0.025	0.379	0.83	-
	3.8c	A	0.494	0.022	0.365	0.84	-4.3

RMSE: root mean square error; MAB: mean absolute bias; EF: efficiency

Table 3.12 Parameters of the equations selected to model SD_d.

Species	Eq.	-	$\boldsymbol{a}$	$\boldsymbol{a_0}$	$\boldsymbol{a_1}$	$\boldsymbol{b}$
P.taeda	3.8	Estimate	5.132918	-	-	0.070622
		SE	0.131473	-	-	0.004199
		p-value	<0.001	-	-	<0.001
E.grandis	3.8a	Estimate	-	9.230291	2.424718	0.054145
		SE	-	0.404682	0.345347	0.005234
		p-value	-	<0.001	<0.001	<0.001
	3.8b	Estimate	-	8.863645	0.450453	0.069762
		SE	-	0.305291	0.038898	0.005116
		p-value	-	<0.001	<0.001	<0.001

Residual plots of the selected equations showed only small bias for both species (Figures 3.21-3.22), whereas validation plots also indicated a good behaviour of models fitted for *P. taeda* and *E. grandis* (Fig. 3.23-3.24). It must be considered that in Figures 3.21 and 3.23 lowess lines show pessimistic estimates of bias in regions of plots where there are very few points.

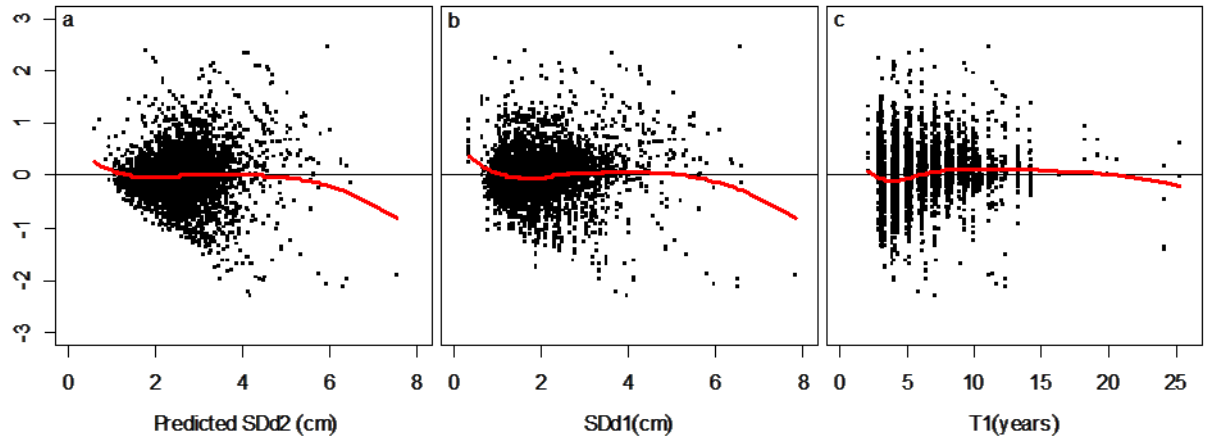

Figure 3.21. Residuals of the selected base equation for modelling SD_d for *P. taeda* including lowess line (red).

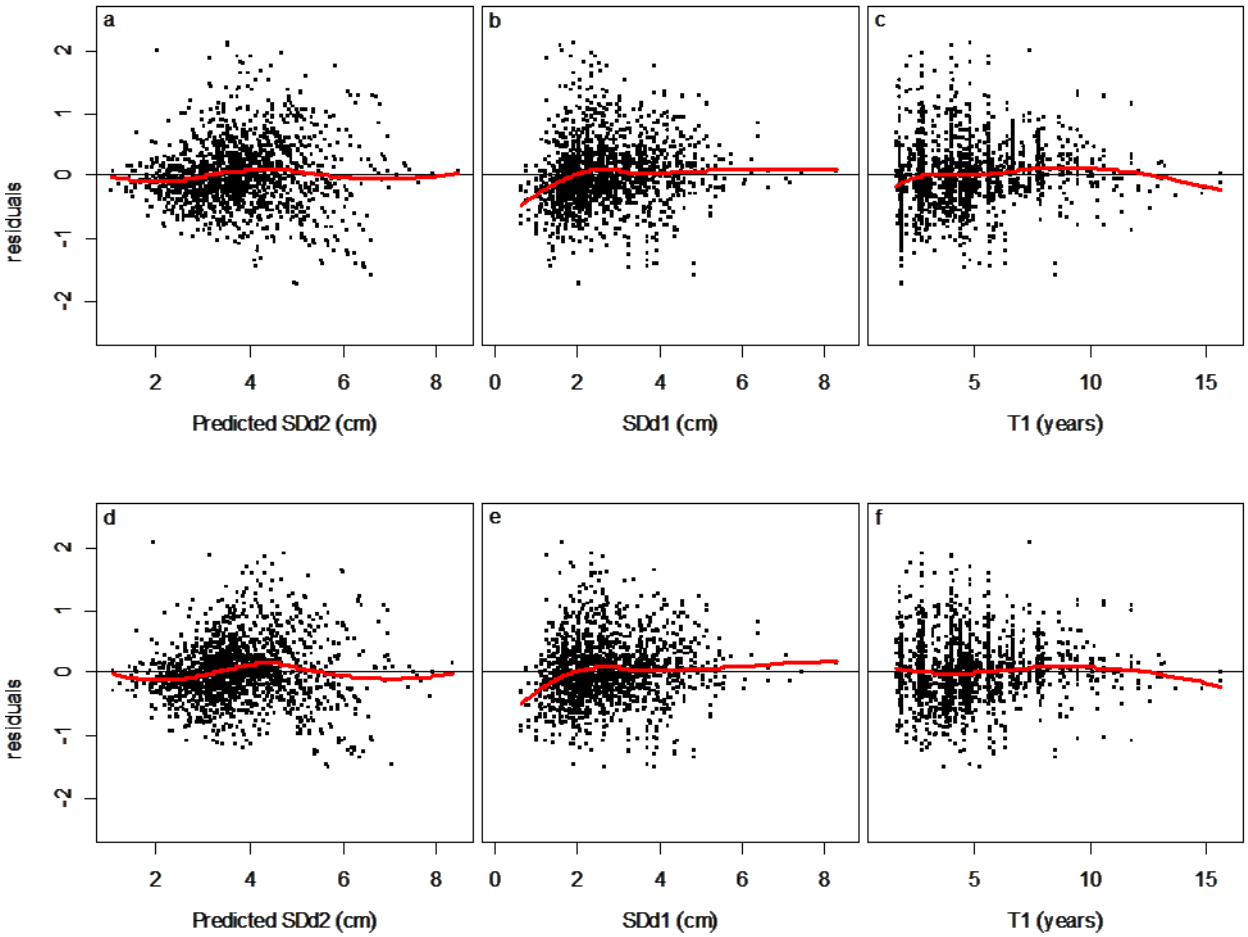

Figure 3.22. Residuals of the selected equation for modelling SD_d for *E. grandis* for the base equation (a, b, c) and augmented equation (d, e, f) including lowess line (red).

The 95% confidence intervals for the slope of predicted vs independent observed data ranged from 1.02 to 1.07 for *P. taeda*, and from 0.96 to 1.01 and from 0.94 to 0.99 for the *E. grandis* base and augmented equations. The *RMSE* calculated using the independent dataset was 0.47 for *P. taeda* whereas for *E. grandis*' baseline and augmented equations was 0.556 and 0.560 respectively. In this case, error was slightly larger for the enhanced model.

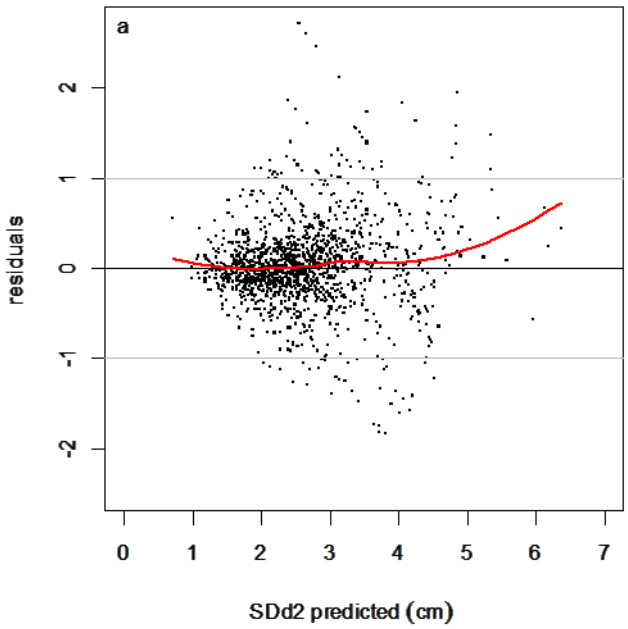

Figure 3.23 Residuals using the validation dataset for *P. taeda* base functions with lowess line (red).

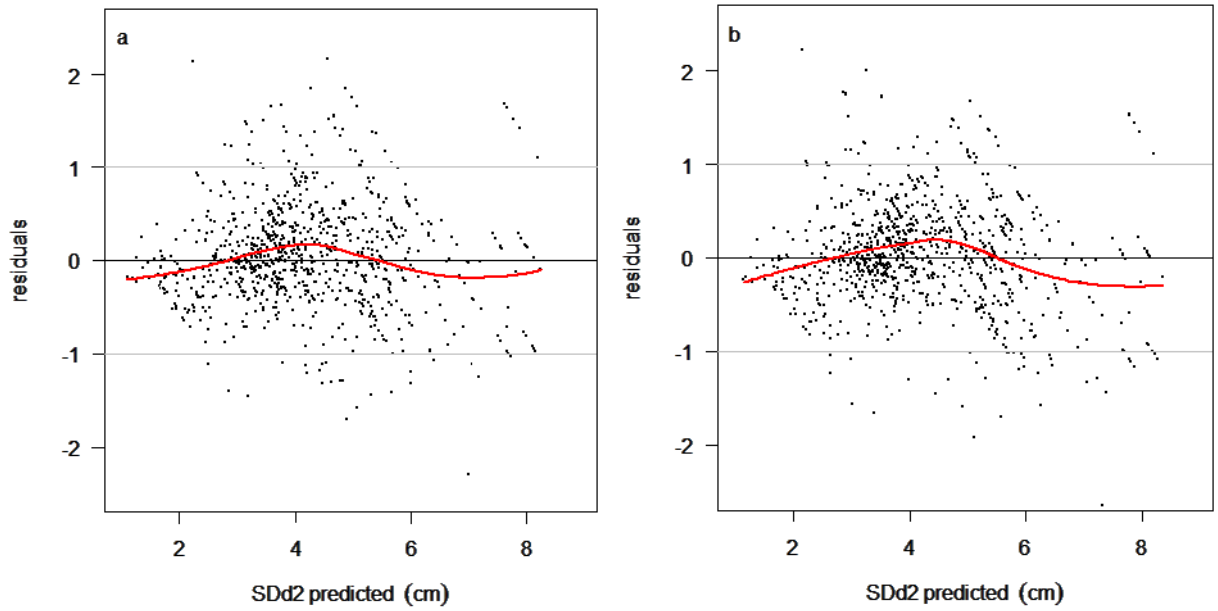

Figure 3.24 Residuals using the validation dataset for *E.grandis*' base (a), and augmented functions (b) with lowess line (red).

The site variables included in the eucalypt model modified SD_d by increasing its magnitude in sites facing East, whereas flat ground yielded higher values of SD_d than steeper sites facing West (Fig. 3.25).

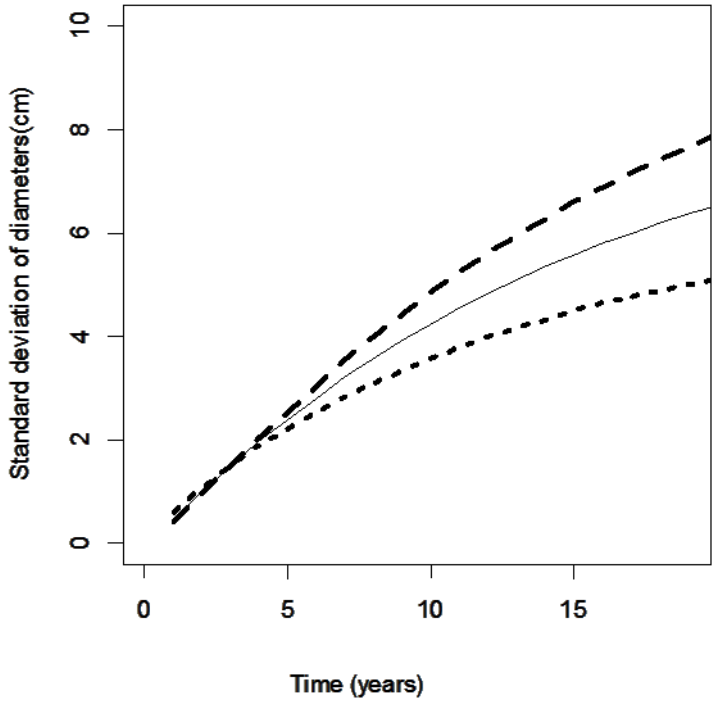

Figure 3.25 Standard deviation of diameter curves 5% slopes facing East (dashed) and West (dotted), and S values of 0% (continued line).

Mortality equations

Probability of mortality

For fitting the probability of stand death occurrence, a model using only stand variables was assessed first. For *P.taeda*, N_1, Interval *(Int)*, SDd_1, G_1, h_{dom1} and the interaction of interval and basal area (*IG*) were significant. The final equation is given by:

$$P = \frac{1}{1 + e^{-(b_0 + b_1 N_1 + b_2 Int + b_3 SD_{d_1} + b_4 G_1 + b_5 H_{d_1} + b_6 IG_1)}} \tag{3.18a}$$

When assessing the inclusion of site variables in a second stage (*SWPA*, β, α_s, α_c, and *Ele*) it was confirmed that none of them were significant for this species, hence no augmented equations were available for comparison.

The percentage of correct predictions with the fitted model was 76%, which is relatively high, whereas the area under the ROC curve (Figure 3.26), AUC value, suggests an acceptable discrimination (Hosmer *et al.*, 2013).

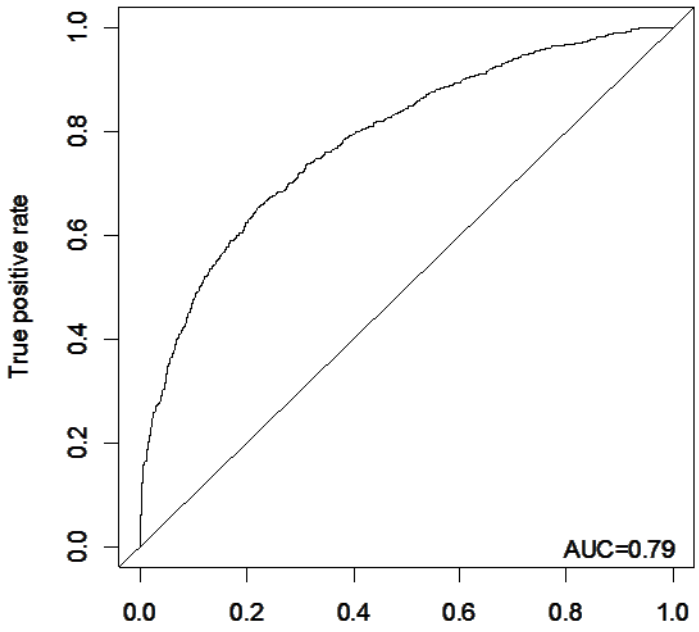

Figure 3.26 ROC curve for the probability of death equation selected for *P. taeda*.

Fitting the probability of tree survival for the *E. grandis* baseline equations, the inclusion of stand variables such as: N_1, $Z7$, SD_d, Int, and t_1 was significant, whereas G_1 and h_{dom1} were not. The equation is given by:

$$P = \frac{1}{1 + e^{-(b_0 + b_1 N_1 + b_2 Z7 + b_3 SD_{d_1} + b_4 Int + b_5 t_1)}} \tag{3.18b}$$

Testing the inclusion of site variables on equation 3.18b, $SWPA$, β, α_s, and $\alpha_c$were significant along with the mensurational. The equation is:

$$P = \frac{1}{1 + e^{-(b_0 + b_1 N_1 + b_2 SD_{d_1} + b_3 Int + b_4 SWPA + b_5 t_1 + b_6 \beta + b_7 \alpha_c + b_8 \alpha_s)}} \tag{3.18c}$$

The expression using site and stand variables had a lower AIC value and higher percentage of correct predictions (Table 3.13). ROC plots (Fig. 3.27) suggested that both offer excellent discrimination according to Hosmer *et al.*, (2013). Parameters of the equations fitted for each species are depicted in Table 3.14.

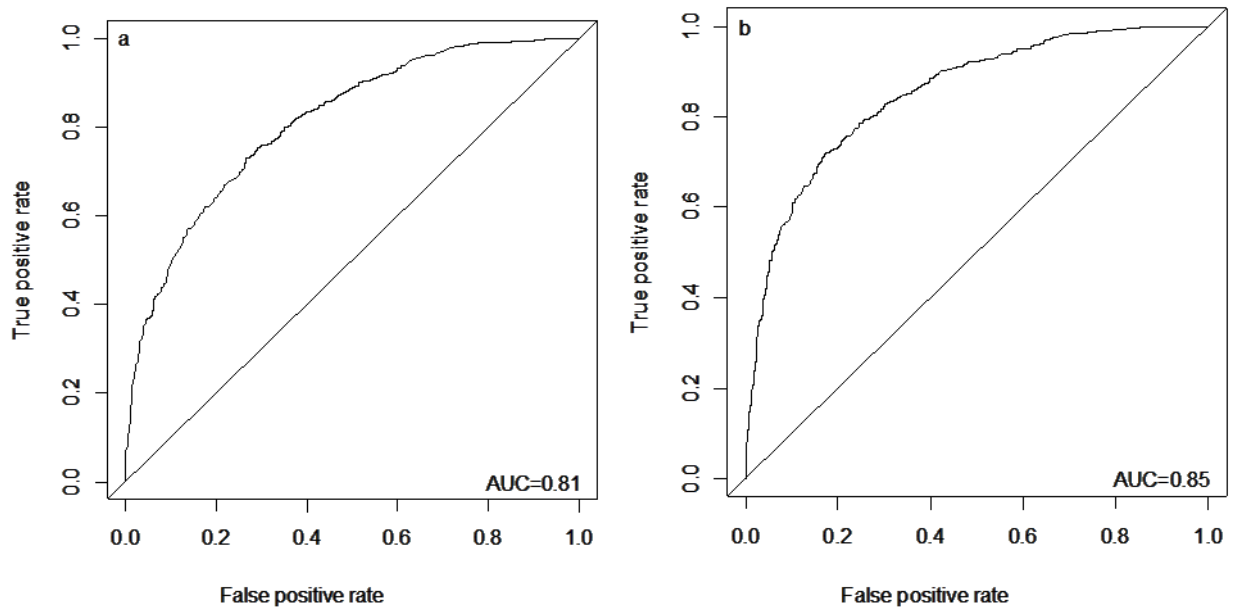

Figure 3.27 ROC curves for the probability of death equations for *E. grandis* using stand variables (baseline) (a) and stand and site variables (augmented) (b).

Table 3.13 AIC and percentage of correct predictions for the probability of death equations through base (B) and augmented equations (A) for each species.

Species	Equation	Approach	AIC	Correct predictions (%)
P.taeda	3.18a	B	-	76
E.grandis	3.18b	B	1732.1	74
	3.18c	A	1580.6	77

AIC: Akaike Information Criterion

Table 3.14 Parameters of the probability of death equations.

Species	Eq.		b_0	b_1	b_2	b_3	b_4	b_5	b_6	b_7	b_8
P.taeda	3.18a	Estimate	-4.1905612	0.0042098	0.3573926	0.5755308	0.0463895	-0.2491949	0.007767	-	-
		SE	0.3961266	0.0003453	0.0358947	0.0582761	0.0159181	0.0420398	0.0027364	-	-
		p-value	<0.001	<0.001	<0.001	<0.001	<0.01	<0.001	<0.01	-	-
E.grandis	3.18b	Estimate	-4.535313	0.002096	2.465474	0.867506	0.514887	-0.340538	-	-	-
		SE	0.442634	0.000305	0.219725	0.086757	0.043693	0.043227	-	-	-
		p-value	<0.001	<0.001	<0.001	<0.001	<0.001	<0.001	-	-	-
	3.18c	Estimate	-9.7103494	0.0026263	0.9481403	0.560091	0.0350884	-0.3628958	0.2183891	0.1242171	0.0895620
		SE	0.7565343	0.0002966	0.0937265	0.0465280	0.0038819	0.0470695	0.0397402	0.0324032	0.0243495
		p-value	<0.001	<0.001	<0.001	<0.001	<0.001	<0.001	<0.001	<0.001	<0.001

Mortality rate

In a second stage, a mortality rate was fitted. The best ranked models were the equations proposed by Woollons (1998) (3.19) and Clutter *et al.* (1983) (3.20) for *P. taeda* and *E. grandis* respectively. For the first species, *SWPA* was significant but did not improved error, hence only the base model was studied further. The fitting statistics (Table 3.15) and the residual plots (Figure 3.28) showed that the equation is satisfactory.

For *E. grandis* the baseline function was augmented with a dummy variable specific for the Zone 7 in the b parameter as it follows:

$$N_2 = N_1 \left(\frac{T_2}{T_1}\right)^b e^{(a_0 + a_1 Z7)(t_2 - t_1)} \quad (3.20a)$$

The inclusion of *SWPA*, β and α_s in the parameter b were significant, therefore the equation is given by:

$$N_2 = N_1 \left(\frac{T_2}{T_1}\right)^b e^{(a_0 + a_1 SWPA + a_2 \beta)(t_2 - t_1)} \quad (3.20b)$$

This formulation improved the error in 4% (Table 3.15). Parameters for the equations of both species are depicted in Table 3.16.

Table 3.15 Statistics of fit of the equations chosen for modelling number of dead trees through base (B) and augmented equations (A) for each species.

Species	Equation	Approach	*RMSE*	*MR*	*MAB*	*EF*	*RMSE* difference (%)
P.taeda	3.19	B	79	-7	63	0.64	-
E.grandis	3.20a	B	89	-5	62	0.93	-
	3.20b	A	86	-6	60	0.94	-3.06

RMSE: root mean square error; MAB: mean absolute bias; EF: efficiency

Table 3.16 Parameters of the equations selected for predicting number of dead trees.

Sp.	Eq.	-	a_0	a_1	a_2	b
P. taeda	3.19	Estimate	-	-	-	0.41361
		SE	-	-	-	0.01924
		p-value	-	-	-	<0.001
E. grandis	3.20a	Estimate	-0.010536	-0.012254	-	-0.089108
		SE	0.005282	0.003460	-	0.029534
		p-value	<0.05	<0.001	-	<0.01
	3.20b	Estimate	2.501e-02	-3.783e-04	2.837e-03	-7.164e-02
		SE	8.364e-03	6.956e-05	6.682e-04	2.911e-02
		p-value	<0.01	<0.001	<0.001	<0.05

Residual distributions against predicted and independent variables were satisfactory for both equations (Fig 3.28 y 3.29). An example of how site variables influence mortality are shown in Figure 3.30, which indicates that mortality increases in steeper terrains with higher water holding capacity.

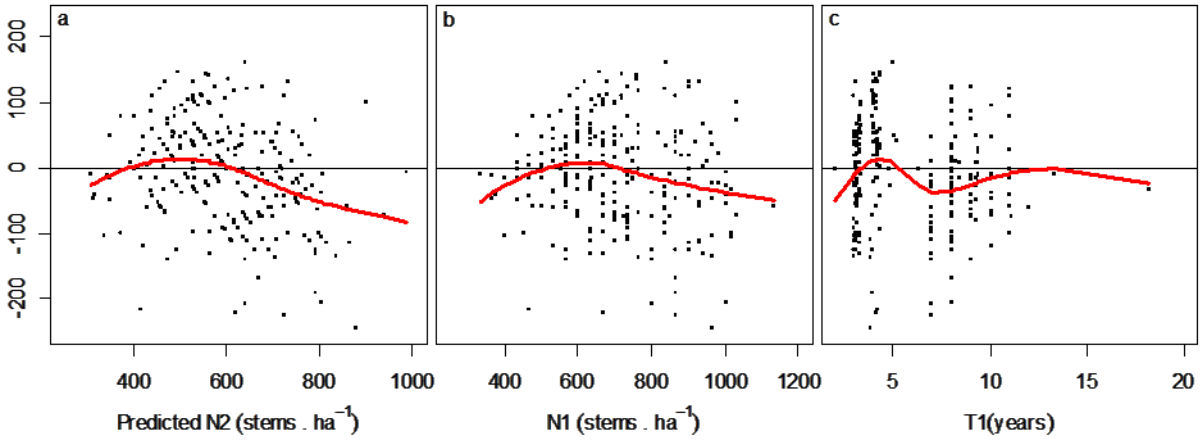

Figure 3.28 Residuals of the selected base equation for mortality rate for *P. taeda* including lowess line (red).

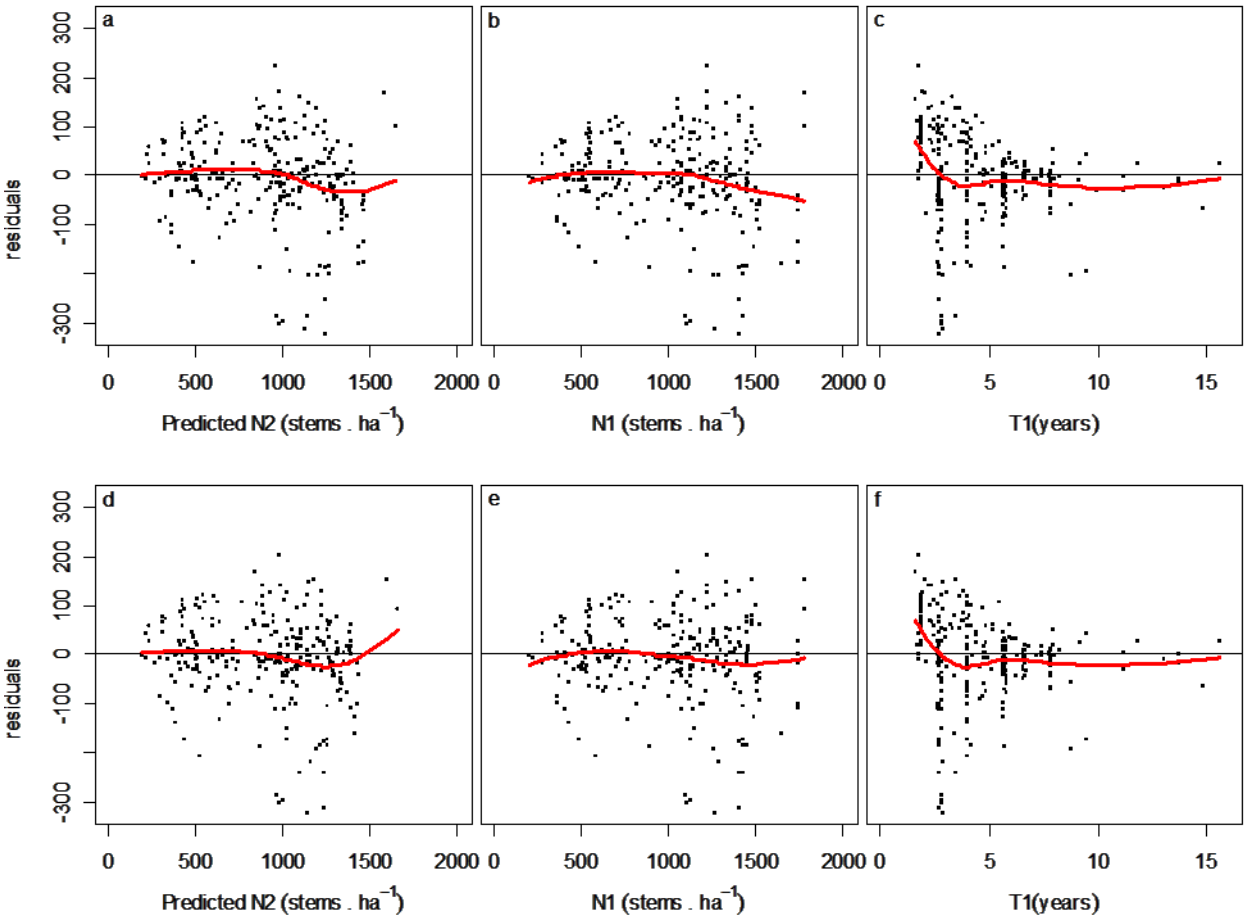

Figure 3.29 Residuals of the selected equation for *E. grandis* for mortality rate bas the base equation (a, b, c) and augmented equation (d, e, f) including lowess line (red).

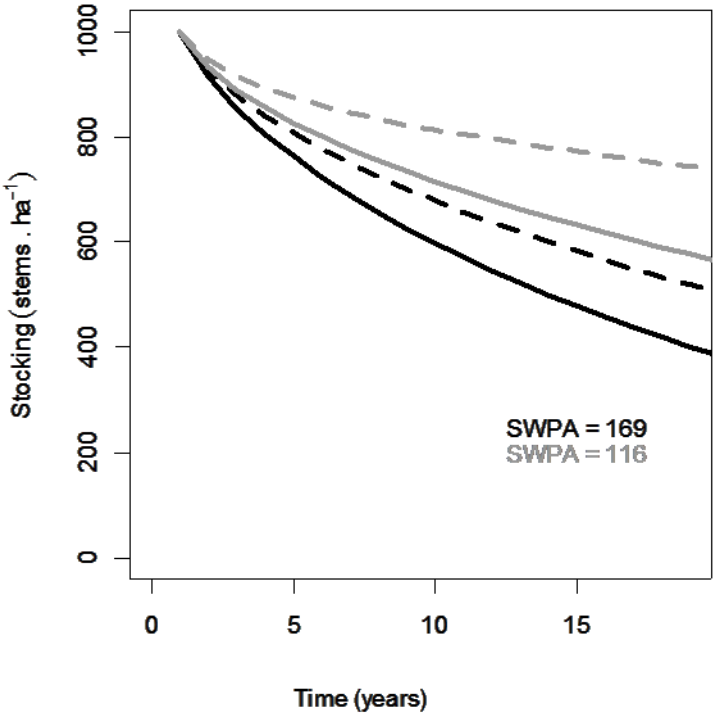

Figure 3.30 Stocking curves in sites with 5% of slope (dashed) and 0% (continued line) for two different *SWPA* values.

Validation for both species was undertaken combining the two-step procedure using the probability equation first and the mortality rate model in the second step for checking the performance of the system with independent data. For *P. taeda*, the residuals' plot showed acceptable performance of the model (Figure 3.31). Log-log plots of stocking versus mean squared diameter suggests that basal area and mortality behave well, since estimated trajectories indicated vigorous growth within the full stocking zone and mortality in the increasing competition zone just before the self- thinning line. Moreover, the behaviour shows congruence beyond the maximum age modelled (25 years). The 95% confidence interval of the slope of observed vs predicted values ranged between 0.94 and 0.97, and the *RMSE* was 46 stems.ha^{-1}.

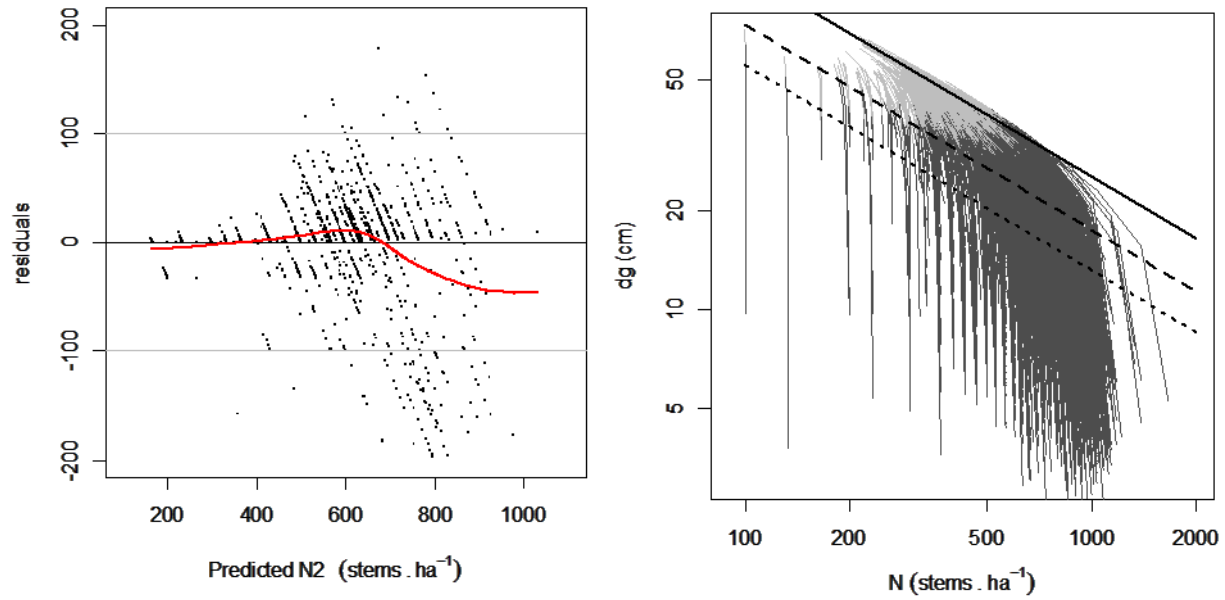

Figure 3.31 Residuals using the validation dataset for *P. taeda* with lowess line (red), and log-log plots of projected stocking vs quadratic mean diameter trajectories younger than 25 years (dark grey) and older than 25 years (light grey) including self-thinning lines. The self-thinning line has a slope of -1.605 (Reineke, 1933), whereas the increasing competition and the fully stocked lines are set to 35% (dashed) and 55% (dotted) of the maximum Stand Density Index (SDI) as a reference.

For *E. grandis* the residual plots using the independent dataset for the set of base equations and set of equations using the site variables showed small differences (Figure 3.32), with some under prediction of mortality (overestimation of stocking) for populations over 1400 stems.ha^{-1} (which represent a very extreme stocking for the Country). 95% confidence intervals of the slope of observed vs predicted ranged between 0.95 to 0.97 and 0.96 and 0.98 for base and augmented equations respectively. The log-log plots of stocking versus mean squared diameter showed that the mortality due competition is reasonable for both sets of equations, For this species the system also seems to behave well (Fig 3.33) even simulating mortality for stands older than the maximum age available for modelling (20 years). *RMSE* were 64 and 60 stems.ha^{-1} for the equation fitted using stand variables (base equations) and using a combination of stand and site variables respectively.

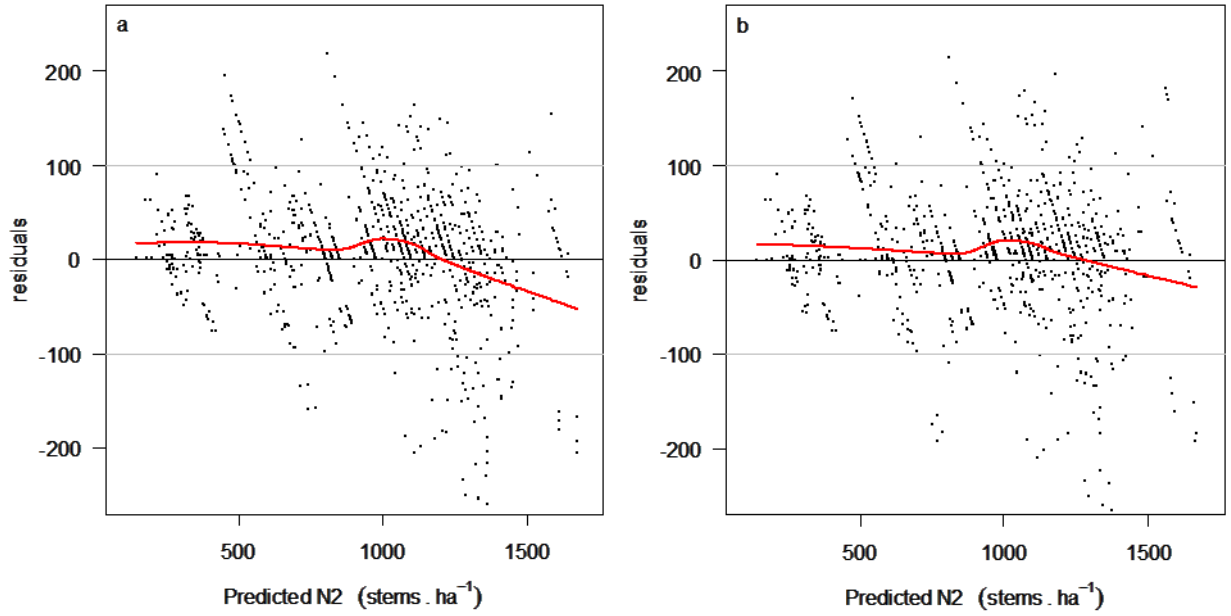

Figure 3.32 Residuals using the validation dataset for E.grandis' base (a), and augmented functions (b) with lowess line (red).

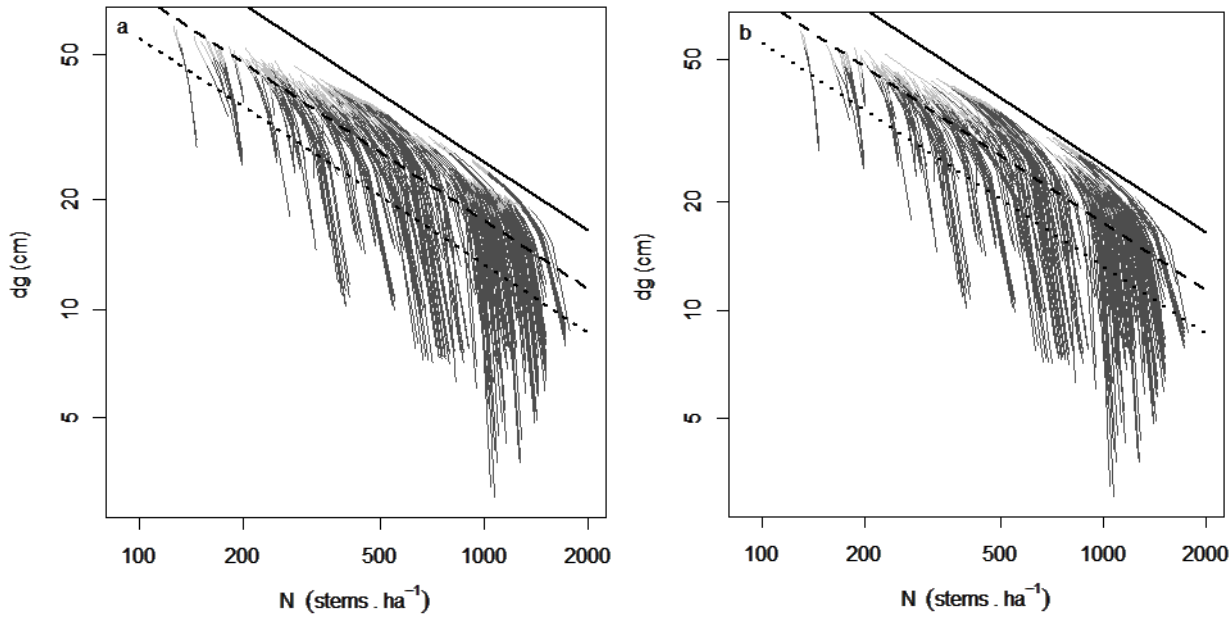

Figure 3.33 Log-log plots of projected stocking vs quadratic mean diameter trajectories younger than 20 years (dark grey) and older than 20 years (light grey) including self-thinning lines for *E. grandis*' baseline (a), and augmented set of equations (b). The self-thinning line has a slope of -1.605 (Reineke, 1933), whereas the increasing competition and the fully stocked lines are set to 35% (dashed) and 55% (dotted) of the maximum Stand Density Index (SDI) as a reference.

DISCUSSION

Traditional mensurational equations were fitted for *P. taeda* and *E. grandis* and the use of physiographic information to improve projections' quality was explored. Equations predicting h_{dom}, G, d_{max}, and SD_d were first analysed, whereas mortality equations were assessed in a second stage.

Results showed contrasting differences between the two species in the use of soil-based and physiographic information. For *E. grandis* all the variables modelled had improvement by including at least one site variable whereas for *P. taeda* only h_{dom} and G showed improvement. Despite the fact that the ranges of site characteristics were similar for plots belonging to both species, growth was better explained through the soil-based and physiographic variables studied for *E. grandis*. Moreover, when fitting base equations, localizing growth models by the use of dummy variables improved predictions only for this species. Dummy variables have been used in the country by Methol (2001) for modelling h_{dom} and G for the same eucalypt species in Uruguay, distinguishing growth curves for zones 7, 8, and 9 (see Figure1.1) . Moreover, Methol (2006) localized growth curves for h_{dom} for *Eucalyptus globulus* sp *globulus* growing in the zones 2 and 9. Because PSPs located in the zone 8 were very scarce for the eucalypt species, these were added to plots located in zone 9, spreading the information in 2 zones: 7 and rest. For the pine species, localization did not represent substantial improvement, nor the inclusion of soil-based and physiographic variables in d_{max}, SD_d or mortality equations, although stand variables did improve the latter. This difference between the species, raises the hypothesis that the range of variation between the plots for the site variables studied are not enough to influence growth, or that other factors that were not included in this study are more influential on the behaviour of d_{max}, SD_d and mortality for *P. taeda*.

In general, the explanatory variables operate reasonably in the set of equations for both species. For *E. grandis* higher levels of water potentially available increased growth of h_{dom}, d_{max}, G and SD_d , as well as the probability of mortality and the number of dead trees. The aspect modified by slope influenced all the variables but G, in a way that steep terrains facing NE (for h_{dom} and probability of death) and E (for d_{max}, SD_d and number of dead trees) increase growth and mortality. For *P. taeda*, sites with higher *SWPA* and *Elev* tended to increase growth in h_{dom} and G, while the growth in the latter also tended to be favoured in steep sites facing NE.

All the explanatory variables (site and stand variables) included in the equations were significant when tested using the autocorrelation-free hypothesis testing dataset, and their inclusion decreased the fitting error in a range from 3 to 10.5%. However, as expected, when errors were calculated with the independent dataset (prediction errors) reduction values were much lower ranging from 2 to 4%. For mortality in the eucalypt species, soil-based and physiographic variables were significant in both equations comprising the set for predicting stocking (probability of mortality and number of dead trees). However improvements were modest and were not reflected in the general prediction error. Nonetheless the behaviour of mortality tested along the prediction ability of the system of equations with respect to competition was reasonable according to Reineke's (1933) model for both studied species. Applying a boundary straight mortality line as posed by Reineke (1933) is useful as a validation method, although there is evidence that the straight line is in fact a curve concave down (Zeide, 1987).

Given that bias also improved in most of the equations and that the *SWPA* and physiographic information are readily available, from a practical point of view there are still advantages in using augmented equations especially for *E. grandis*. For this species to date in Uruguay, differential growth is distinguished by zoning (using dummy variables) as a way to characterize a set of regional attributes related mainly to geology, topography, and soils. The site variables studied, especially *SWPA*, represented differences in site quality in a more descriptive way than with the localization strategy. This is clear in Figure 3.7c and 3.7d, where h_{dom} curves using *SWPA*, α_c, and α_s, averages for both identified zones are similar to those projected by the equation using the localization dummy variable.

Physiographic and soil variables studied

Although different combinations of the site variables worked better for modelling the growth of different components in both species with diverse levels of improvement, *SWPA* was consistently significant for the majority of the models augmented with site variables in *P. taeda* and *E. grandis*. The use of a range of variables related to soil moisture, available water for stands, or rainfall has been tested before on differential equations proving to be effective (Woollons et al., 1997; Snowdon et al., 1999; Temps, 2005; Pinjuv et al., 2006) especially for improving *G* predictions. Also Ritchie and Hamann (2008) found that water holding capacity was effective for modelling height and basal area increment.

Water availability is a key element for growth. Water stress leads to stomatal closure, and a decrease in carbon fixation efficiency. This leads to a reduction in cambial activity and foliage growth, and hence a decrease in production (Landsberg and Sands, 2011). Stape *et al.* (2004) found that for *Eucalypt grandis* hybrids an increase in water availability, increases quantum efficiency and leaf area, and decreases allocation to root. They found that "capture and use-efficiency of supplies where the key components defining production, and these efficiencies were under strong water-supply influence". For *P. taeda*, Albaugh *et al.* (1998, 2004) found that stem growth efficiency (growth per LAI unit) as well as total biomass production efficiency increased by irrigation, and hypothesised that the increase occurred as a consequence of more biomass being allocated to photosynthesizing tissue.

Soil water availability maps can be developed achieving high resolution depending on base information (e.g. Schwärzel *et al*., 2009) and its importance in forest management is increasing. The variable *SWPA* used in this study is rather theoretical based on a low resolution 1:1000000 soil map, however it synthesises solidly a series of essential soils characteristics, yielding consistent results with respect to forest productivity. Furthermore, an important feature of this variable is that it represents water availability without interfering on the path invariance property of differential equations, which is a fundamental characteristic to provide robustness to mensurational models.

Slope by itself is not significant for most of the components except for mortality in *E. grandis*, very probably this is related to the fact that the average β was as low as 5% (although the range was broad). In this sense the analysis could be improved by incorporating PSPs located on steeper sites. Moreover, position on the slope could also be incorporated in future analysis as a way to complement the slope percentage value and indirectly incorporate other factors that could influence growth (i.e. soil depth and moisture).

The aspect weighted by slope (α_s and α_c) was consistent through most of *E. grandis* equations, whereas for *P. taeda* was significant only for *G*. NE and E aspect favoured growth and the effect was accented by the slope. Other studies found differences on productivity between steep and flat terrain (McArdle *et al.*, 1949) and northern and southern orientations (Coble *et al.*, 2001; Coble and Marshall, 2002). The use of sine and cosine of the azimuth angle as well as their association with slope is rarely used in differential growth equations, although, has been used for predicting site index (Trimble and Weitzman, 1956; Stage, 1976), stand volume (Stage and Salas, 2007),

probability of survival (Uzoh and Mori, 2012), and assess self-thinning lines (Weiskittel *et al.*, 2009) given its influence on radiation, temperature, and soil moisture, among other growth factors.

Elevation has no explicit effect on growth but influences key growth factors such as temperature and soil moisture at a local scale. It has been used specifically in mountainous areas for forecasting site productivity (Monserud *et al.*, 1990, Fontes *et al.*, 2003), being incorporated as an explanatory variable in growth equations for predicting h_{dom}, G, and d_{max} (Mason, 1992; Methol, 2001; Pinjuv, 2006) , N (Methol, 2001), probability of stem death, individual stem height and SD_d (Pinjuv, 2006), variance of d, and survival (Mason, 1992). It was consistently significant for *P. taeda*'s h_{dom} and G equations with a positive effect on growth. Because differences in altitude are relatively small in terms of the impact on site-specific temperature, an alternative hypothesis is that there is a negative influence of soil moisture in lower ground, since the species is occasionally planted in marginal low areas which are waterlogged for short periods. This was investigated graphically by using categorical information of drainage speed and results showed that plots located in sites classified as slow and medium drainage speed, were associated with smaller values of altitude (e. g. less than 150 m) what would confirm the first hypothesis. Although, elevation could be a surrogate of drainage for *P. taeda,* further research should be undertaken to confirm this theory as well as testing the correspondence of altitude with climate variables such as temperature.

Because *Elev* was correlated with *SWPA*, a test proposed by Cook and Weisberg (2009) was performed to investigate if the information provided by both variables is redundant. The test consists of a three-step procedure where the model excluding *Elev* was fitted first to obtain residuals 1 (Res1) in the first step; a second step fitting *Elev*= f(*SWPA*) was performed for calculating residuals 2 (Res2); and in the third step residuals of step1 are fitted as a function of residuals obtained in the step 2 (Res1=f(Res2)). A low adjusted R-squared revealed that *Elev* was able to add new information to the model, moreover the *Elev* parameter did not present a large standard error. Likewise for *P. taeda*, further analysis should be taken in order to understand which is the main growth factor being influenced by *Elev* for the eucalypt species. Furthermore, there is a possibility that confounded effects regarding variables that are not considered in the present study could be interfering with those results.

Use of the equations and constraints

Real improvements in bias and error are modest by using the augmented models, nonetheless the explanatory component adds utilities for forest management and the information needed is readily available with its quality tending to increase. However, care must be taken when using the equations when site variables border the extremes of the range of values used in this study, especially when using a combination of extreme values. Representation of all possible combinations of explanatory variables' values is a common issue in forest modelling since the set of PSPs used is restricted. To take a closer look to this potential problem, the extreme values of site variables were plotted against all the values of each of the remaining site variables used in order to search for information gaps. Results showed that PSPs combining extreme values of the site variables were scarce for the eucalypt species (i. e. extreme values of a site variable were combined with average values of the rest), however because the range of aspects in the plots presented no constraints the main relationship to investigate was *SWPA* and β extremes. In this sense PSPs located in sites with β larger than 9% are very scarce; there are no PSPs with slopes larger than 9% in sites with low *SWPA* (less than 100 mm). For *P. taeda* elevation should also be taken into consideration: extreme combinations were available in the dataset for *SWPA*, β and large values of *Elev*, whereas low values of *Elev* were strictly associated with low *SWPA* (100mm) and average β (5%).

Models for both species were adjusted using a dataset comprising a diverse genetic base, covering a large part of the variability for the country. This contributes to the generalization capacity of the models, however adaptations of certain genotypes to particular sites can occur. Interactions between genotypes and environments were not assessed and are not included in the models.

An important information gap was found for *P. taeda*'s near the harvesting age, therefore care must be taken when performing projections beyond 16 years.

CONCLUSIONS

Stand level growth equations have been developed and can be recommended to be used for managing *Pinus taeda* and *Eucalyptus grandis* growing in the Northern half of Uruguay.

Soil-based and physiographic information was significant for improving predictions of all the variables fitted for *E. grandis*: h_{dom}, G, d_{max}, SD_d, probability of mortality and number of dead trees, but were significant only for h_{dom} and G in the case of *P. taeda*. In general, the explanatory variables worked reasonably in the set of equations for both species since site characteristics that increased growth and diameter variability, also increased mortality.

SWPA was consistently significant for the models augmented with site variables in *P. taeda* and *E. grandis*, while slope by itself was not significant in general. The aspect weighted by slope (α_s and α_c) was consistent through most of *E. grandis* equations, whereas for *P. taeda* was significant only for *G*. Elevation was significant for *P. taeda*'s equations with a positive effect on h_{dom} and *G* growth, however research should be undertaken in order to understand which other factors may be represented by elevation that directly influence growth.

The use of explanatory variables (physiographic and stand variables) decreased the fitting error in a range from 3 to 10.5%, however decreases in the prediction errors calculated with the independent dataset were much lower ranging from 1.6 to 4%.

Care must be taken when using a combination of extreme values of physiographic variables since information gaps for extreme values were found in the dataset used for this study. Because information was very scarce for mature stands of *P. taeda*, precaution must be also taken when performing projections beyond 16 years.

Real improvement in bias and error are modest by using the augmented models, nonetheless the explanatory component adds options for forest management and the information needed is readily available with its quality tending to increase. Moreover the use of site variables could increase the capacity to explain the variation in diameters' distribution of stands located in different sites.

CHAPTER 4

MODELLING GROWTH USING A HYBRID APPROACH

INTRODUCTION

Hybrids of mensurational and physiological models have been conceived as alternatives that mix the best features of each approach (mensurational and physiological) while trying to avoid their shortcomings from a forest management perspective. Usually the features that are enhanced are precision, process explanation, ability to estimate wood products, and simplicity in parameters definition. Some hybridizing strategies included linking a physiological model with a mensurational model (Baldwin *et al.*, 2001; Pinkard and Battaglia, 2001;Almeida *et al.*, 2003), or linking more than two models (Peng *et al.*, 2002; Robinson and Ek, 2003).

A hybrid mensurational-physiological approach using equations based on potentially useable light sums (PULSE) was proposed by Mason et al., (2007), fundamentally combining a methodology based on light use efficiency, mostly in the way it is formulated in the 3-PG model (Landsberg and Waring, 1997), and a mensurational counterpart given by difference sigmoidal models.

The light use efficiency approach is founded in the linear relationship between absorbed photosynthetically active radiation (APAR) and dry mass production (Monteith, 1972, 1977; Landsberg, 1986) observed when production is considered at canopy level and yearly timescale. The relationship can be expressed as (Landsberg and Sands, 2011):

$$P_n = \varepsilon(\theta, F, T)APAR - Resp \qquad (4.1)$$

where P_n is net primary productivity, ε is the light use efficiency of converting absorbed photosynthetically active radiation into carbohydrates; $Resp$ is total respiration, and $\theta, F,$ and T represent soil water, nutrition, and temperature factors respectively. This principle has been very useful in forestry (as well as in other crops) because it provides a simple and yet sound framework

to study how light use efficiency ε, hence productivity, varies with site conditions (e.g. McMurtrie *et al.*, 1994; Harrington and Fownes, 1995; Coops *et al.*, 1998; Stape *et al.*, 2008; Ryan *et al.*, 2010; Binkley *et al.*, 2010). It has been adopted in the 3-PG as well as many other models (McMurtrie and Wolf, 1983; Running and Coughlan, 1988; Battaglia and Sands, 1997; Battaglia *et al.*, 2004) ,

The 3-PG (physiological principles for predicting growth) is a physiological model developed to be used academically as well as by forest managers since it incorporates several process simplifications: i) the model runs at a monthly temporal scale; ii) respiration is considered as a constant NPP/GPP ratio; iii) carbon allocation is calculated through allocation ratios driven by water and nutrient availability; and iv) it assumes a soil single layer. For those advantages and because it is free, the model has been widely studied and parameterised for several species in a variety of environments.

Based on the radiation utilization principle, 3-PG calculates net primary productivity as (Mason *et al*., 2007):

$$\mathrm{NPP} = \varepsilon \sum_{m=1}^{M} APAR_m \; min\{f_\theta f_d\} f_T f_N f_{Fr} f_s \qquad (4.2)$$

where $APAR_m$ is absorbed photosynthetically active radiation in a month; f_θ, f_d , f_T , f_N , f_{Fr} , f_s are modifiers for soil water, vapour pressure deficit, temperature, fertility, frost, and senescence respectively. Those modifiers are dimensionless ratios ranging from 0 to 1.

In 3-PG radiation (provided by the user) is firstly transformed to *APAR* through Beer's law (for which LAI is needed). The model moves through time by calculating monthly production which accumulates and generates plant growth (also root turnover and litterfall). Total biomass in each time unit is allocated into the different plant components using allocation ratios, regulated by modifiers accounting for water and nutrient availability. LAI is derived from foliar biomass in each period (and used for computing *APAR*), and an average diameter at breast height is calculated by applying allometric equations (whose parameters can be adjusted by the user).

From a mensurational perspective, growth can be modelled as a function of time using sigmoidal equations. Clutter (1963), derived a growth model from a yield form and defined it as compatible since a yield equation can be mathematically integrated to derive a growth model. Moreover,

growth equations should present a series of properties which contribute to the robustness that characterizes mensurational methods applying sigmoidal equations to model growth. Using the Bertalanffy-Richards growth equation as an example

$$y_2 = a\left(\frac{y_1}{a}\right)^{\frac{\ln(1-e^{-bt_2})}{\ln(1-e^{-bt_1})}} \tag{4.3}$$

given that y_1 and y_2 represent yield in t_1 and t_2 respectively, those properties are:

i. Consistency: t_2 should approach t_1 when y_2 approaches y_1;
ii. Path invariance: for a given value of t_1 the corresponding value of y_1 remains the same for any starting t_n, y_n pair of values;
iii. If t_2 approaches to ∞ then y_2 approaches to an upper asymptote

The PULS approach consists of the substitution of modified radiation sums for time in those compatible equations, with radiation sums restricted by adaptations of modifiers used by the 3-PG model, to model directly the descriptive variable of interest. Radiation sums can be computed as

$$R_T = \sum_{i=1}^{T} R_t \, min(f_\theta f_D) f_T \tag{4.4}$$

where R_t is the total radiation sum from month 1 to T (MJ), and f_θ, f_D, and f_T are the soil water balance, vapour pressure deficit (VPD), and temperature modifiers calculated for month t.

Nutrition is an important factor influencing net primary productivity, however the mechanisms that regulate nutrient uptake and photoassimilates dynamics are poorly understood (Landsberg and Waring, 1997). This is one of the main deficiencies in the 3-PG model (Landsberg *et al.*, 2003; Bown *et al.*, 2013) and it has also been a limitation for applying a fertility modifier in this study.

Resuming the example of the Gompertz equation for projecting dominant height, the formulation of growth vs light sums would be as it follows:

$$h_{d2} = a\left(\frac{h_{d1}}{a}\right)^{\frac{\ln(1-e^{-bR_{T2}})}{\ln(1-e^{-bR_{T1}})}} \tag{4.5}$$

The approach seeks to improve explanation of the growth process with respect to the traditional mensurational counterparts, by introducing information about key factors regulating the proportion

of radiation that could be potentially used by stands to grow. It offers the advantage of avoiding representations of processes that are poorly known, such as carbon allocation (Mason, *et al.*, 2011), while the properties of consistency and path invariance described above operate to improve robustness. Moreover, the use of LAI is avoided by employing total radiation (instead of absorbed PAR), since leaf area is rarely measured in a commercial forest. The method was firstly tested for estimating growth of ground-line diameter in a competition control experiment for Douglas fir in the United States (Mason *et al.*, 2007). At an experimental scale and under several competition situations, parameters of the equation using potentially useable light sum equations (PULSE) proved to be stable in all the cases suggesting that environmental changes were "absorbed" by the modifiers. Later, the methodology was tested for *Pinus radiata* in New Zealand at a regional scale (Mason *et al.*, 2011a) for modelling growth and yield of basal area and mean top height. Predictions using light sums were more precise than those using time for basal area and equally precise for dominant height.

In a similar approach Montes (2012) modelled increments in height and basal area, and mortality as a function of *absorbed* PAR (*APAR*) sums restricted by the same modifiers (temperature, soil water, and vapour pressure deficit), using a state space approach (García, 1984). The use of effective *APAR* as an explanatory variable required information about leaf area. Although comparisons with time-based functions were not undertaken, results showed good agreement between predicted and observed data at an experimental scale.

Results of applying potentially useable light sum equations seem promising with respect to precision and outputs for predicting height and especially basal area. Nevertheless, there is still much to explore with respect to the potential performance of this approach at a broad scale since tests of the methodology at commercial levels are rare. The main questions addressed about the methodology in this Chapter are:

1. How much would it contribute to understanding the variability in productivity of *Pinus taeda* and *Eucalyptus grandis* across regions in Uruguay?
2. Would it be suitable for modelling components of forecasting systems aimed to estimate diameter distributions (e.g. variability of diameters and maximum diameter)?
3. To what level of detail radiation should be provided?

In this chapter, potentially useable radiation sums equations (PULSE) were adjusted at a regional scale for *Pinus taeda* and *Eucalyptus grandis* to model $h_{dom,}$ G, maximum diameter (d_{max}), and standard deviation of diameters (SD_d) using different light sum alternatives. It was also tested whether detailed information of aspect and slope improve estimations in order to be considered in the hybrid formulation.

METHODS

To develop the equations, modified light sums were firstly computed, whereas in a second stage the projection equations for $h_{dom,}$ G, maximum diameter (d_{max}), and standard deviation of diameters (SD_d) were fitted directly as a function of the modified light sums. Because the methodology is being used with data currently available in Uruguay, absorbed photosynthetically active radiation is not explicitly used, as leaf area is not usually measured in standard inventories. In a sense, it is assumed that the absorbed utilized radiation is considered in the sigmoidal relationship between modified light sums and the modelled state variables.

Radiation was calculated in two ways: i) considering a tilted surface (using aspect and slope), and ii) assuming a flat surface, in order to assess whether the use of this site information improved predictions. Monthly restrictions were applied by the use of the modifiers for water balance (f_θ), and VPD (f_D), and temperature (f_T) mostly in the same way as used by the 3-PG model (Landsberg and Waring, 1997), for each permanent sample plot available in the time range of the study (1979 and 2012). Several alternatives of restriction using all possible combinations of the modifiers were tested and compared in order to understand which of these factors is more useful for each species across the regions, and which combination gives the best predictions. In this way seven alternatives of radiation sums were compared: $R_{\theta DT}$, $R_{\theta D}$, $R_{\theta T}$, R_{DT}, R_θ, R_D, R_T, representing light sums restricted by: all three modifiers (the minimum between water balance and VPD, referred here as *waterMod*, plus temperature modifier); the minimum between water balance modifier and VPD (*waterMod*); water balance and temperature modifiers; VPD and temperature modifiers; water balance modifier; VPD modifier; and temperature modifier respectively.

Data preparation

Geo-referenced permanent sample plots (PSP) measurements described in Chapter 3 were used including all possible intervals within PSPs. In this way, the same datasets used for modelling and validating time based equations were complemented with the inclusion of the modified light sums for each plot. A summary of the information used is presented in Table 4.1.

Table 4.1 Summary of the dataset used in the analysis

Variable	*P. taeda*				*E. grandis*			
	Mean	Min.	Max.	SD	Mean	Min.	Max.	SD
PSP number	-	-	727	-	-	-	315	-
Number of plot measurements	4.00	2.00	11.0	-	4.00	2.00	11.0	-
t (years)	7.13	2.00	25.9	3.20	6.95	1.18	18.7	3.47
h_{dom}(m)	10.6	2.20	27.0	4.65	21.2	4.40	46.6	7.86
d_m (cm)	17.2	2.30	41.9	7.56	17.6	3.10	45.2	7.18
d_{max} (cm)	21.1	4.00	46.7	8.71	24.3	5.00	62.6	8.77
d_{min} (cm)	12.8	0.48	36.6	6.92	10.1	0.10	41.1	6.64
SD_d (cm)	2.20	0.11	8.42	0.96	3.42	0.64	10.5	1.43
G ($m^2 \cdot ha^{-1}$)	15.6	0.10	53.6	10.9	19.2	0.78	58.1	8.95
N (stems.ha^{-1})	624	100	1667	180	886	87.0	1775	393
Plot size	338	200	500	84.0	682	400	2250	315
SWPA (mm)	148	85.1	179.6	33.8	140.5	85.1	180.6	30.0
Elev (m)	151	61.0	256	32.5	121	21	201	57.0
β (%)	5.00	0	>18	3.70	4.00	0	>18	3.33

For computing light sums and the modifiers, variables calculated on a monthly basis were: solar radiation, mean air temperature, vapour pressure deficit (VPD), rainfall, and soil water balance. Data corresponding to 28 met stations and 57 rain gauges were available for the country (Figure 4.1). Climate and soil data were provided by the National Institute of Meteorology (Instituto Nacional de Meteorología), Agroclimate and Information System Group (GRAS) of INIA Uruguay, and the Ministry of Cattle, Agriculture and Fisheries (MGAP).

Monthly average values for daily maximum and minimum temperature and sunshine duration from each met station as well as accumulated precipitation from the rain gauges were interpolated into grids of 500 x 500 m for each month corresponding to the time range of study. For rainfall the interpolation method applied was Inverse Distance Weighting, whereas Thin Plates Splines were applied for the rest of the climate variables according to studies of Hartkamp *et al.* (1999). For

maximum and minimum temperature an exploratory analysis was undertaken through the Exploratory Regression Tool (ArcGIS) to test whether those variables were influenced by latitude, longitude, elevation, and distance from the sea. It was found that none of them related to minimum temperature, whereas maximum temperature was related to latitude and distance from the sea. Because latitude and distance from the sea are highly correlated, no specific corrections for the latter were applied. Monthly averages for the period 1979-2012 were examined to check whether spatial trends of values corresponded to published information for the country. It was confirmed that on an average annual basis, rainfall increased from SW to NE, whereas the maximum temperature increased from SE to NW, and minimum temperature was registered in the centre of the Southern half of the country within published ranges (Castaño *et al.*, 2011). Distribution of average monthly rainfall, minimum, and maximum temperature for the studied period are depicted in Figures 4.2-4.4.

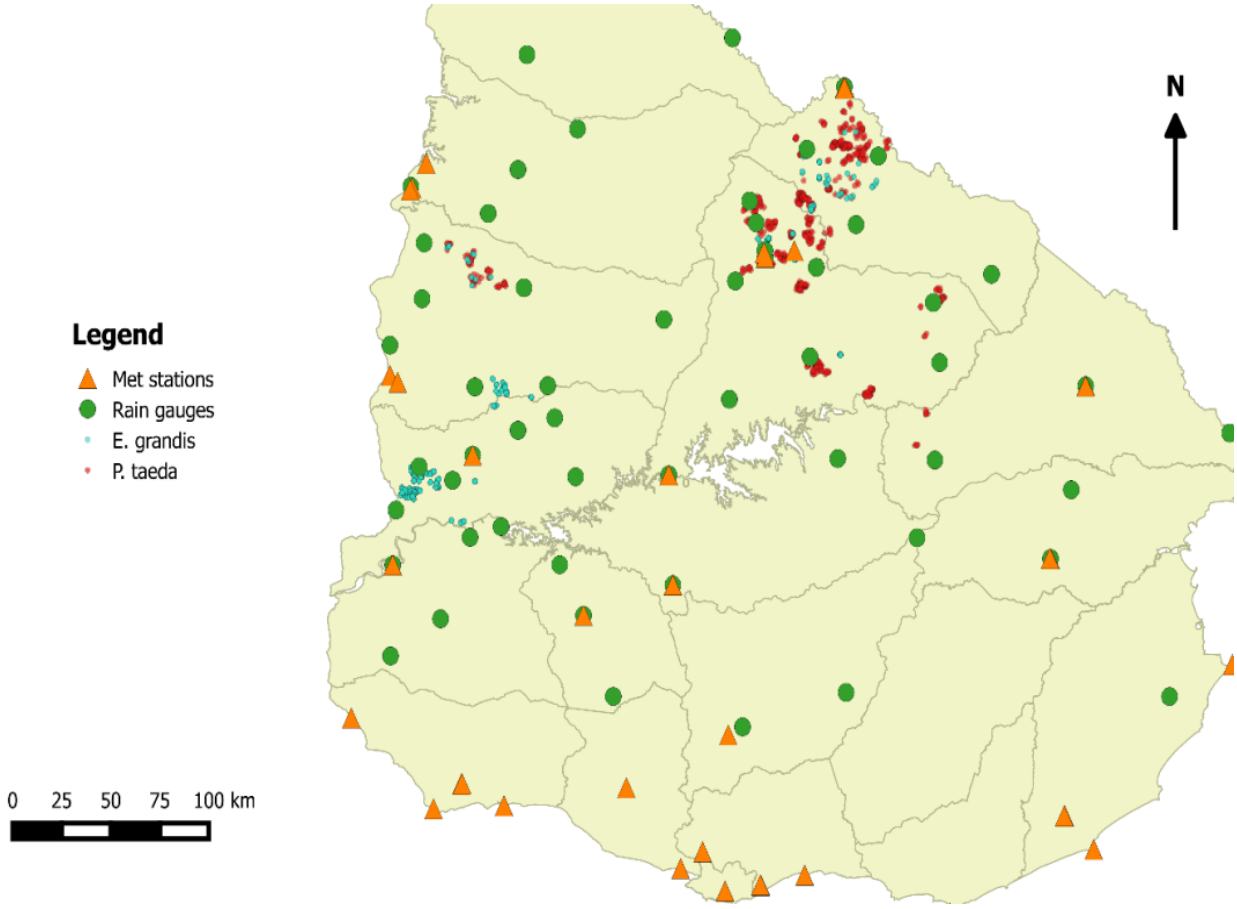

Figure 4.1 Met stations, rain gauges and plot location

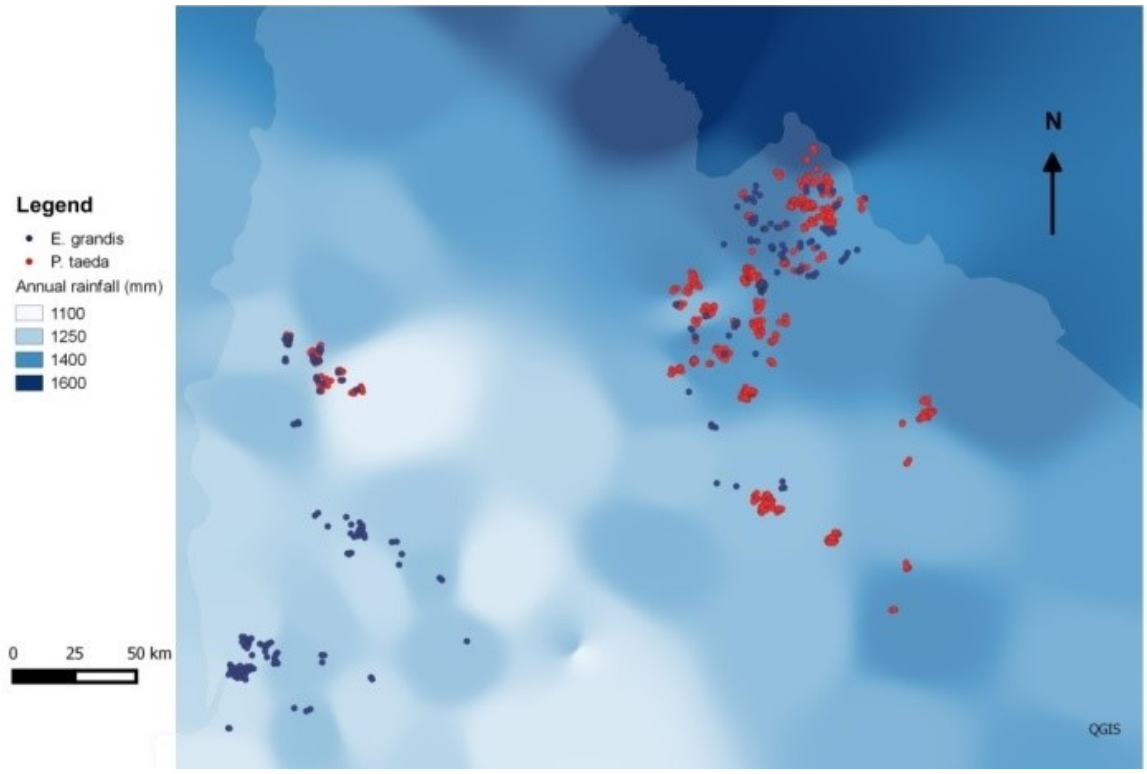

Figure 4.2 Spatial variation (average for the studied period) of accumulated annual rainfall and plot location.

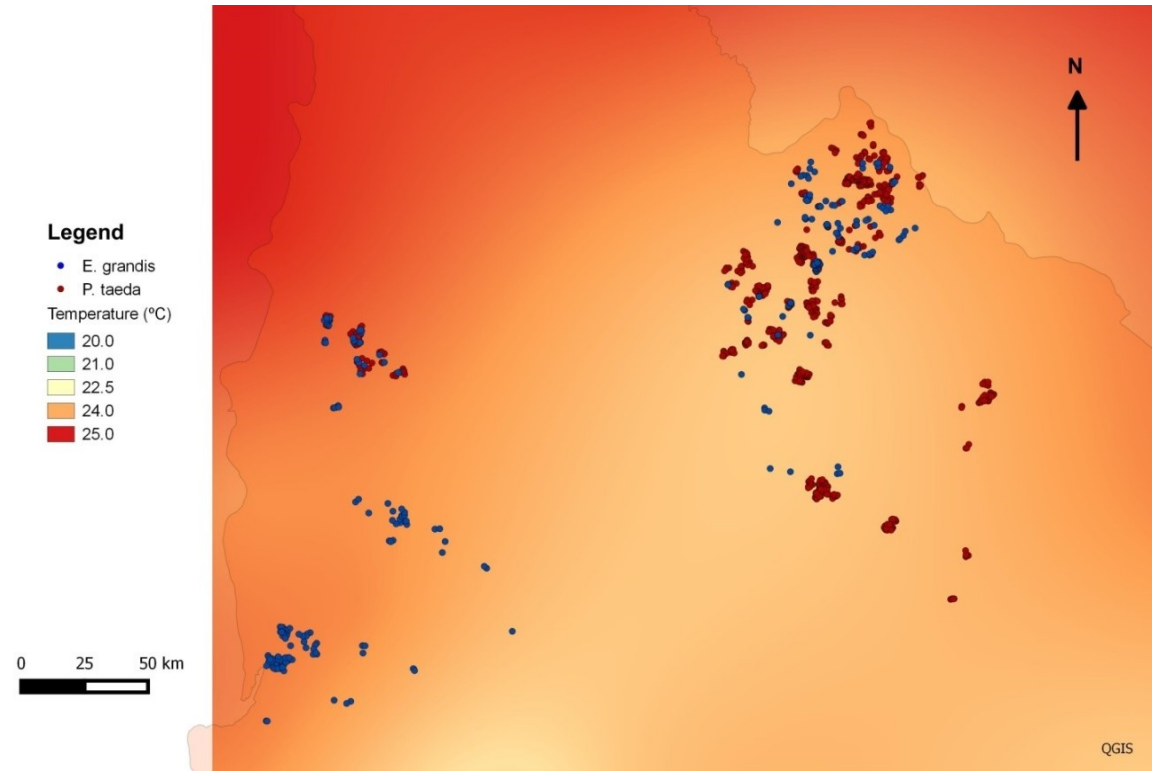

Figure 4.3 Spatial variation (average for the studied period) of maximum temperature and plot location.

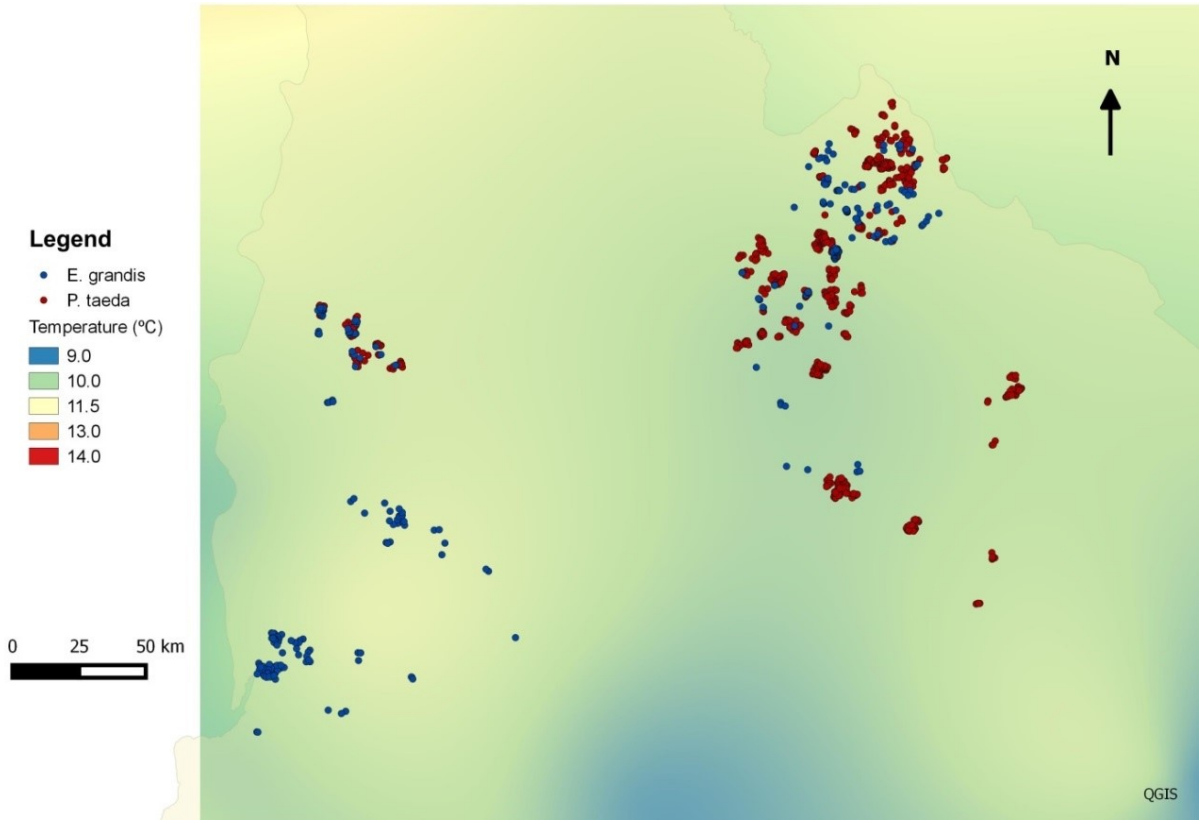

Figure 4.4 Spatial variation (average for the studied period) of minimum temperature and plot location.

The calculation of radiation and modifiers is described below. All the coefficients used for computing the different components are summarized in Table 4.2.

Radiation

Radiation was computed considering direct and diffuse radiation. Radiation measurements were not available for the study sites, so the Angstrom equation was used to calculate global horizontal radiation (MJ/m^2/day):

$$H_s = (a + b\frac{n}{N_o})H_o \qquad (4.6)$$

where n and N_o are actual and maximum sunshine duration respectively (hours), H_o extraterrestrial radiation (MJ/m2/day), a and b are parameters. This equation was adjusted for 17 meteorological stations in Uruguay by (Abal *et al.*, 2010) for developing solar maps, hence, the parameters' values were interpolated to 500 x 500 m cells using thin plates splines in order to have values for each plot location.

H_o was calculated for each day of the year as described by Landsberg and Sands (2011):

$$H_o = \frac{0.0864}{\pi} d_r \left[\frac{\pi}{24} h_d \sin(\varphi)\sin(\delta) + \cos(\varphi)\cos(\delta)\sin\left(\frac{\pi}{24} h_d\right)\right] \quad (4.7)$$

where d_r is inverse relative distance Earth-Sun, ω_s is sunrise hour angle (rad), φ is latitude (rad), δ is solar declination (rad). Those variables are calculated as follows:

$$d_r = G_{sc}\left[1 + 0.033cos\left(2\pi\frac{J}{365}\right)\right] \quad (4.8)$$

$$\delta = 0.410152374219sin(0.017202418893n_{ve}) \quad (4.9)$$

$$\omega_s = cos^{-1}\left(-tan(\varphi)tan(\delta)\right) \quad (4.10)$$

$$N = \frac{24}{\pi}\omega_s \quad (4.11)$$

Where G_{sc} the solar constant = 1367 Wm^{-2}; J the number of the day in the year between 1 and 365 or 366 (starting on January 1st); n_{ve} the number of days since vernal equinox; and h_d daylength.

In a second step, monthly average daily values of global horizontal radiation were adjusted to account for the slopes and aspects of each plot. For this purpose, the formulation proposed by Tian *et al.* (2001), based on Revfeim (1978) was used:

$$H_s^* = H_s[R_d(1 - K_r) + f_b K_r + 0.12(1 - f_b)] \quad (4.12)$$

Where H_s^* is the global radiation received on a surface with an orientation α and a slope β, f_b is a "slope reduction factor" calculated as $1 - \frac{\beta}{180}$. R_d is the direct radiation proportion of that on a flat surface given aspect and slope, which was calculated as proposed by Revfeim (1978):

$$R_d = \left[\frac{sin(\varphi)}{sin(\varphi^*)}\right]\left[\frac{d_d - sin(d)cos(e_e)cos(g)}{cos(\omega_s{}^*)}\right]\left[\frac{1}{\omega_s - tan(\omega_s)}\right] \quad (4.13)$$

Where:

$$d_d = \frac{(h_1 - h_0)}{2} \quad (4.14)$$

$$e_e = \frac{(h_1 + h_0)}{2} \quad (4.15)$$

$$g = sin^{-1}[sin(\beta)sin(\alpha)sec(\varphi^*)] \quad (4.16)$$

$$\varphi^* = sin^{-1}[sin(\varphi\,)sin(\beta) - cos(\varphi)sin(\beta)cos(\alpha)] \quad (4.17)$$

$$\omega_s{}^* = cos^{-1}[tan(\varphi^*\,)tan(\delta)] \quad (4.18)$$

Being h_1 and h_0 sunrise and sunset hour angle on an arbitrary slope.

The algorithm suggested by Erbs *et al.* (1982) was used for computing the proportion of diffuse radiation to the global horizontal radiation(K_r):

For $\omega_s \leq 1.4208$ and $0.3 \leq K_t \leq 0.8$

$$K_r = 1.391 - 3.560K_t + 4.189{K_t}^2 - 2.137{K_t}^3 \quad (4.19)$$

For $\omega_s > 1.4208$ and $0.3 \leq K_t \leq 0.8$

$$K_r = 1.311 - 3.022K_t + 3.427{K_t}^2 - 1.821{K_t}^3 \quad (4.20)$$

Being K_t the proportion of global horizontal radiation to extra-terrestrial radiation ($\frac{H_s}{H_o}$).

Calculation of modifiers

The modifier that considers vapour pressure deficit (VPD) describes a relationship where the modifier declines exponentially when VPD increases, and it is computed as (Landsberg and Waring, 1997):

$$f_D = e^{-k_g VPD} \quad (4.21)$$

where $k_g$is a coefficient based in the relationship between stomatal conductance and VPD, and VPD is calculated as it follows:

$$VPD = \frac{DT_{max} - DT_{min}}{2} \quad (4.22)$$

being DT_{max} and DT_{min} saturated vapour pressure when temperature =T_{max} or T_{min}. Those variables are calculated using minimum or maximum temperature per month (T_i) through the expression:

$$DT_i = 0.61078e^{17.269T_i/(T_i+237.3)} \quad (4.23)$$

The soil water-dependent modifier was calculated as (Landsberg and Waring, 1997):

$$f_\theta = \frac{1}{1 + [(1 - r_\theta)/c_\theta]^{n_\theta}} \quad (4.24)$$

where $c_\theta$and $n_\theta$takes different values for different soil types and $r_\theta$is moisture ratio calculated as:

$$r_\theta = \frac{\theta_T}{S\,WPA} \quad (4.25)$$

being θ_T the soil water balance, and $SWPA$ is the soil water potentially available.

Information provided by the map of $SWPA$ developed for Uruguay by (Molfino and Califra, 2001) (applied in Chapter 3) was used in order to account for the maximum available water in the root zone.

Soil water balance was estimated through the equation:

$$\theta_T = \theta_{T-1} + R - I - E - D \tag{4.26}$$

where θ_{T-1} is root zone water balance in the previous month; R is rainfall; I is canopy interception; E is evapotranspiration and D is drainage. When $\theta_{T-1} + P - I - E > SWPA$, excess water exist and it is assumed to be drained.

The 3-PG estimates evapotranspiration using the Penman-Monteith "big leaf" model:

$$\lambda E = \frac{SR_n + \lambda g_b \rho_a VPD}{S + \gamma\left(1 + \frac{g_b}{g_c}\right)} \tag{4.27}$$

Where λ is the latent heat of water vaporization (JKg); S is the slope of saturation vapour pressure curve for water (KPa^oC^{-1}); R_n is net radiation absorbed by canopy ($Jm^{-2}month^{-1}$); ρ_a is air density (Kgm^{-3}); VPD is vapour pressure deficit (mbar); γ is the psychrometric parameter (KPa^oC^{-1}); g_b is boundary layer conductance (ms^{-1}); and g_c is canopy conductance (ms^{-1}).

Boundary layer conductance depends on wind speed as well as size and shape of leaves, and density of foliage (Landsberg and Sands, 2011), however fixed values are commonly used for practical purposes and a fixed value of 0.2 ms^{-1} was assumed based on the work of Mielke *et al.* (1999). Mielke et al. (1999) observed wind speeds around 2 ms-1 leading to canopy conductance values of 0.2 ms-1for *E. grandis*. According to the National Institute of Meteorology of Uruguay (INUMET), the average wind speed is 3.5 ms-1. According to Martin *et al*. (1999), boundary layer conductance did not increase markedly when wind velocity ranged from 1 to 2 m.s-1. Therefore, it was assumed that wind speed was spatially and temporally uniform, and boundary layer conductance values assumed in this study did not seem to lead to significant error.

Canopy conductance was calculated as:

$$g_C = g_{Sx}\, min\{1, L/L_{gC}\}\, min\{f_\theta, f_D\} \tag{4.28}$$

where g_{Cx} is maximum stomatal conductance, assumed as 0.02 ms^{-1} (Almeida *et al.*, 2004; Sands, 2004), L is leaf area index, L_{gC} is leaf area index at maximum conductance, and other terms are as specified before. L_{gC} value assumed is 3.33 (Sands, 2004). Because L measurements were not available, it was assumed a relationship $L/L_{gC} = 1$ for canopy conductance.

Net radiation was estimated using a linear relationship with radiation (total shortwave radiation) as it follows:

$$R_n = q_a + q_b H_s \tag{4.29}$$

where q_a (watts/m2) and $q_b$are the intercept and the slope parameters. The values applied for *P. taeda* were the ones used in 3-PG by Sands (2004). Almeida and Landsberg (2003) registered much lower intercept values for *E. grandis* growing in Brazil, since the sensitivity of this parameter is high, it was applied for this species.

The temperature-dependent growth modifier is based in the assumption that production increases with increasing temperature and starts declining after an optimum is reached:

$$f_T(T_a) = \left(\frac{T_a - T_{min}}{T_{opt} - T_{min}}\right)\left(\frac{T_{max} - T_a}{T_{max} - T_{opt}}\right)^{(T_{max}-T_{opt})/(T_{opt}/T_{min})} \tag{4.30}$$

where T_a is mean temperature for each month, T_{min}, T_{max}, and T_{opt} are minimum, maximum, and optimum temperature required for growth respectively. In this study the mean daytime temperature was employed instead of mean temperature, as Mason *et al.* (2011) found that this modification gave better precision than daily mean temperature. As with Mason *et al.*'s study, daytime temperature was defined as:

$$mean\ daytime\ temperature =$$

$$mean\ daily\ maximum\ temperature\ 0.7575 + \ mean\ daily\ minimum\ temperature\ 0.2425$$

Table 4.2 List of parameters used for computing the potentially useable radiation sums.

Parameter	Symbol	Unit	Value	Reference
Angstrom intercept coefficient for :	a	-		(Abal *et al.*, 2010)
Salto, Paysandú,			0.23, 0.22,	
Carrasco, San José,			0.22, 0.22,	
Florida, Durazno,			0.23, 0.23,	
Rocha,Treinta y Tres,			0.25, 0.26,	
Melo, Rivera,			0.28, 0.28,	
Tacuarembó, Artigas,			0.26, 0.26,	
La Estanzuela, Salto Grande			0.21, 0.23	
Angstrom slope coefficient for:	b	-		(Abal *et al.*, 2010)
Salto, Paysandú,			0.50, 0.52,	
Carrasco, San José,			0.46, 0.50,	
Florida, Durazno,			0.47, 0.48,	
Rocha, Treinta y Tres,			0.39, 0.41,	
Melo, Rivera,			0.41, 0.45,	
Tacuarembó, Artigas,			0.46, 0.46,	
La Estanzuela, Salto Grande			0.55, 0.49	
Response of canopy to VPD	k_g	$mbar^{-1}$	0.05	(Sands, 2004)
Coefficient of soil water modifier for: clay, clay loam, sandy loam, and sandy soils	c_θ	-	0.4, 0.5, 0.6, 0.7	(Landsberg and Waring, 1997)
Power of soil water modifier for clay, clay loam, sandy loam, and sandy soils	n_θ	-	3, 5, 7, 9	(Landsberg and Waring, 1997)
Latent heat of water vaporization	λ	JKg	2460000	-
Air density	ρ_a	Kgm^{-3}	1.2	-
Slope of saturation vapour pressure curve for water at 20 °C	S	KPa^oC^{-1}	2.2	-
Psychrometric parameter	γ	KPa^oC^{-1}	0.66	-
Boundary layer conductance	g_b	ms^{-1}	0.2	(Sands, 2004, Mielke *et al.*, 1999)
Maximum stomatal conductance	g_{Sx}	ms^{-1}	0.02	(Sands, 2004)
Leaf area index at maximum conductance	L_{gC}	-	3.33	(Sands, 2004)
Intercept and slope of the relationship between R_n and H_s for:	q_a, q_b	$Wattm^{-3}$		(Landsberg and Sands, 2011)
Pinus taeda			-90, 0.8	
Eucalyptus grandis			-8.9, 0.82	(Almeida and Landsberg, 2003)
Maximum, minimum and optimum temperature for growth for :	$T_{max}, T_{min}, T_{opt}$	°C		(Landsberg and Sands, 2011)
Pinus taeda			32, 2, 20	
Eucalyptus grandis			36, 8, 25	(Almeida *et al.*, 2004)

Potentially useable light sums

Accumulated radiation for each month was multiplied by the different combination of modifiers for temperature, *waterMod*, and single modifiers for VPD and soil water. Each month was summed up from plantation to measurement date as it follows (example using the most complete light sum option):

$$R_{\theta DT} = \sum_{i=1}^{T} R_t \, min(f_\theta f_D) f_T \qquad (4.31)$$

Where R_t is the total radiation sum (MJ), and f_θ, f_D, and f_T are the soil water balance, vapour pressure deficit, and temperature modifier previously calculated for month t. Euan Mason (pers. comm.) provided R software, in the form of object oriented coding in an R workspace (R Development Core Team, 2014) that he developed for his own research that incorporated Revfeim's (1978) equations, Erbs *et al.*'s (1978) formulation of proportions of diffuse and direct radiation, the water balance model from 3-PG, and his adjustments of 3-PG's radiation sum modifiers to provide potential useable radiation estimates. Radiation flux using the Angstrom method was added in accessory code for the study reported here.

Growth equations

The methodology followed for fitting and validating growth of h_{dom}, G, d_{max}, and SD_d, as a function of radiation sums was the same described on Chapter 3. In the study reported here problems related to serial correlation were avoided by testing the inclusion of new variables using a correlation-free dataset where only one interval per plot was included.

Only the three best equations identified for each variable in the time-base study (Chapter 3) were included as candidate equations. Three differential equations were fitted for each variable of interest using seven restricted light sum alternatives (previously described), each one in two forms related to whether the net radiation was computed considering including slope and aspect or not. Each option was later compared using the methods specified in the previous chapter in order to select the best expression for modelling each variable of interest. In a second step validation was undertaken following the procedure also described in the previous chapter.

For all the statistical procedures the R software (R Development Core Team, 2014) was used.

RESULTS

Restricted light sums

Averages of radiation sums per month using the three modifiers (i. e. $R_{\theta DT}$) were categorized in three classes per species (Figure 4.5). Regional differences in the amount of light that could be utilized are suggested for both species with higher values at the very North.

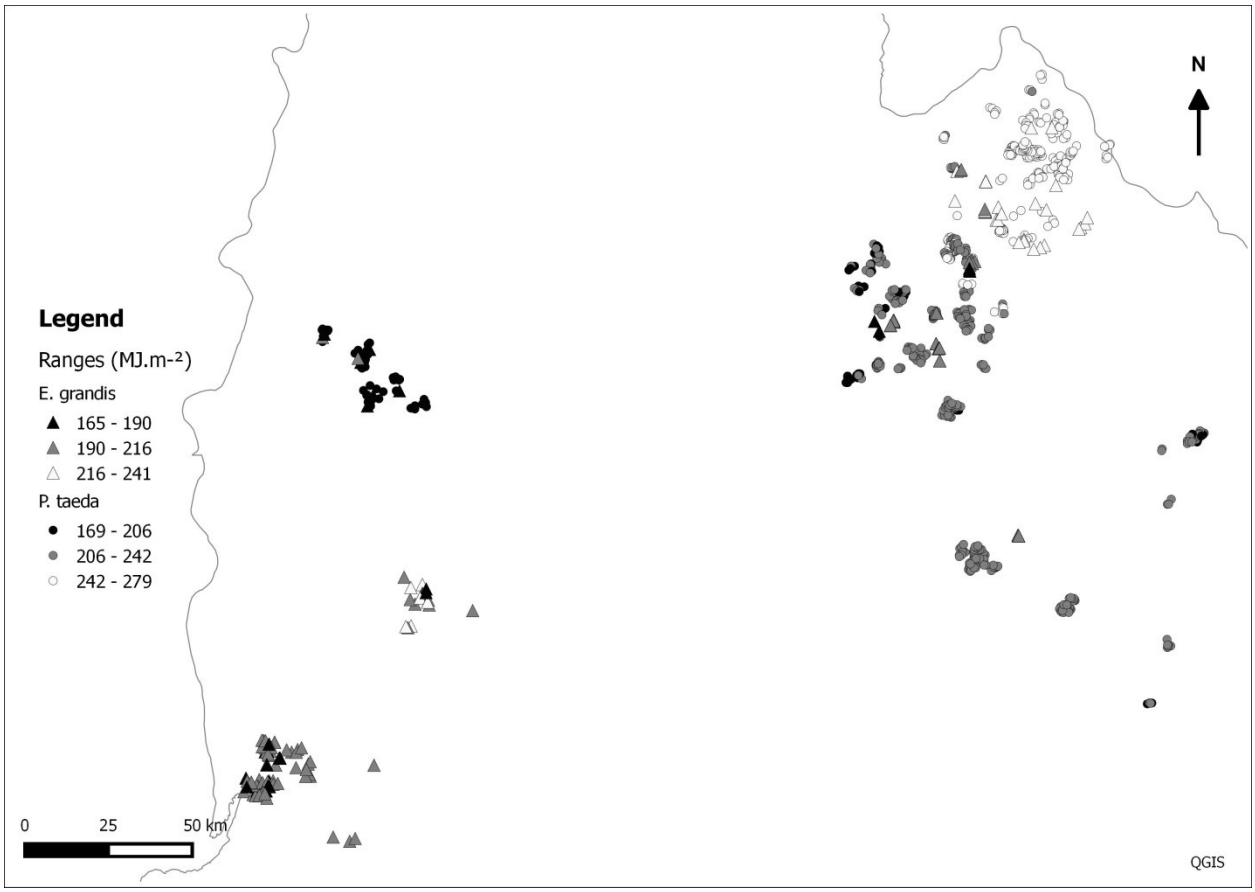

Figure 4.5 Monthly averages of accumulated potentially useable light sums for each species.

Averages of *waterMod*, temperature, VPD, and water balance used per month were computed and also divided in three categories (Fig. 4.6-4.7). It can be observed that the trends of $R_{\theta DT}$ seem to be more associated to the water-related factor, and within this, the water balance factor is the modifier presenting values with the widest range. This is consistent with the fact that for the afforested sites studied, gradient of rainfall is larger than gradient in temperature (Figures 4.2 to 4.4), plus there are also differences in soil water storage capacity (as shown in Figure 3.3) with larger capacity, in a large part of the area with heavier rainfall regimes.

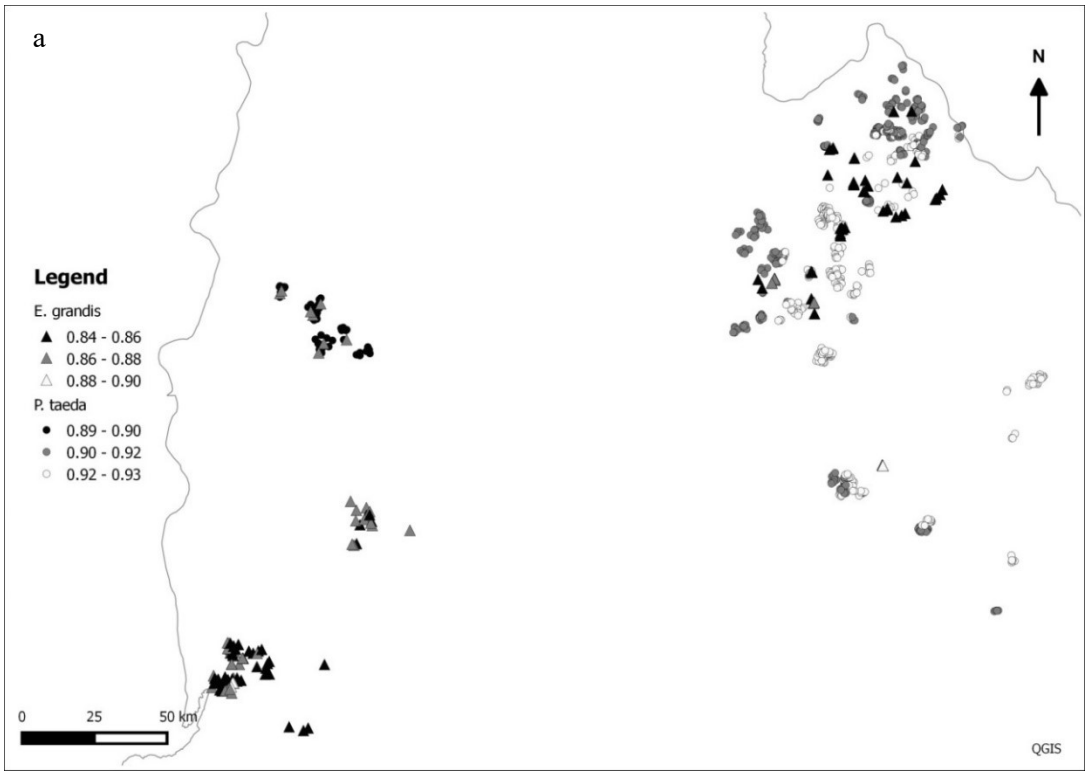

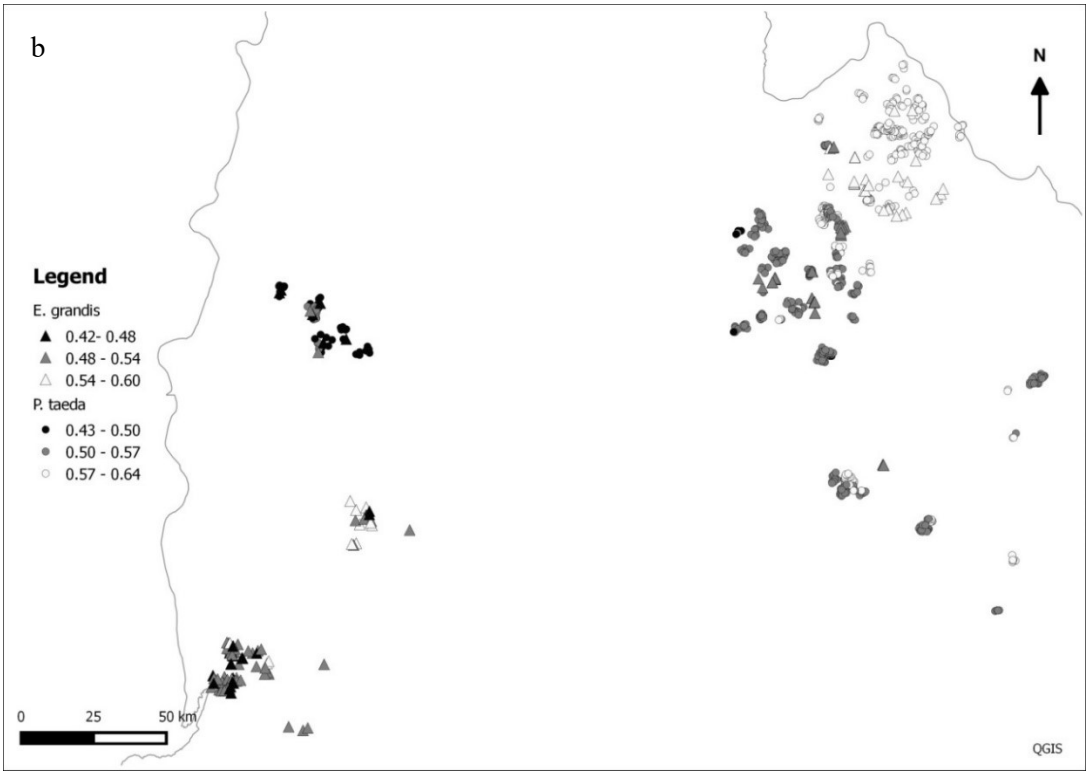

Figure 4.6 Averages of temperature (a) and *waterMod* (b) modifiers for each plot.

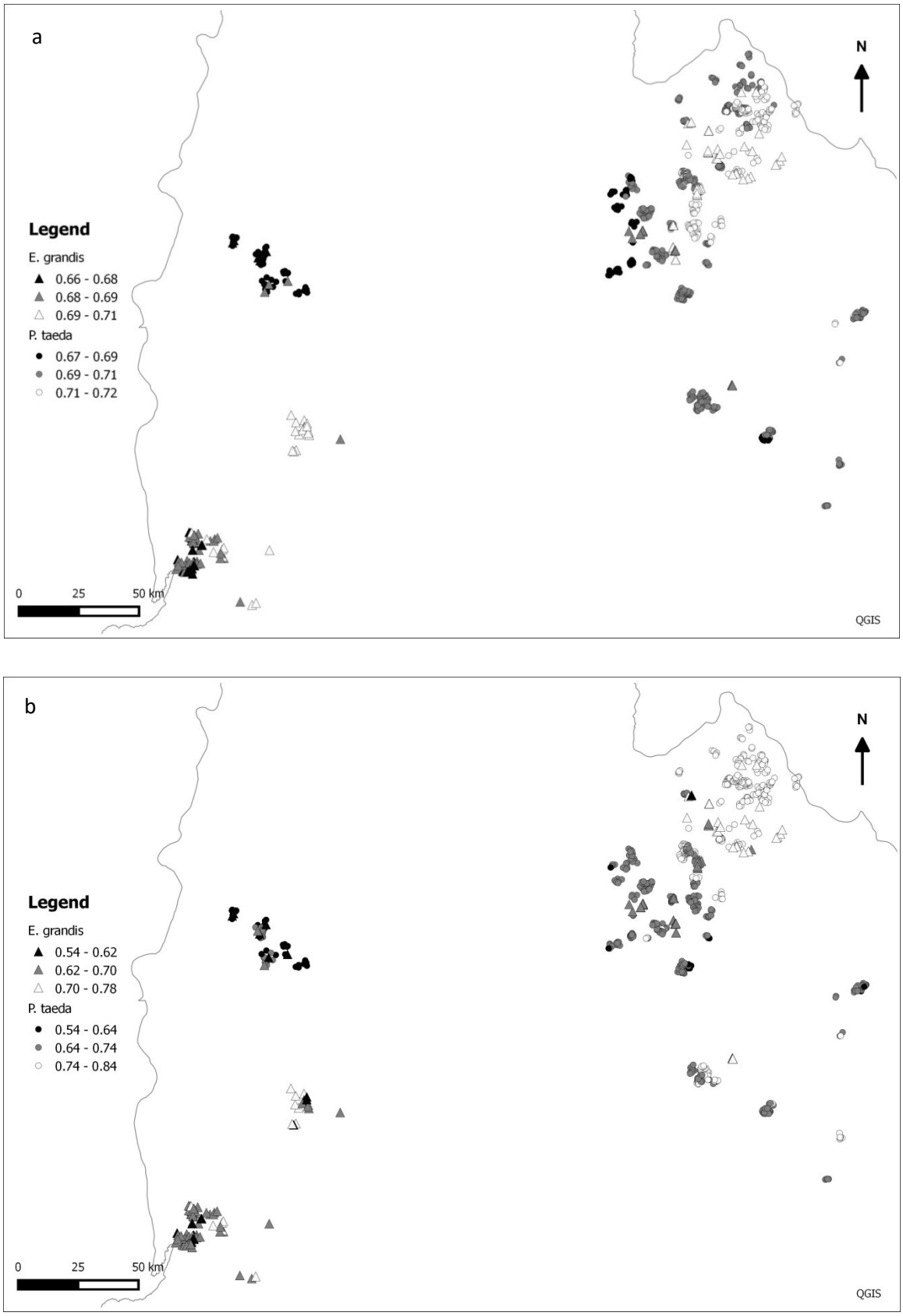

Figure 4.7 Averages of *VPD* (a) and *ASW* (b) modifiers comprising the compound water-related modifier (*waterMod*) for each plot.

Growth and yield equations

In Chapter 3, it was observed that soil water potentially available has an effect on the asymptote of most variables of both species, therefore that alternative was also assessed on light-based equations. This was made by adding a water-related index computed as a 30-year average of monthly light sums constrained by *waterMod*, $\bar{R}_{\theta D}$. When analysing the inclusion of the variable through a hypothesis testing dataset (also utilized for testing explanatory variables in augmented models in Chapter 3), it was found significant for all the components except SD_d for both species, and it was tested later using the modelling dataset. Although, for *E. grandis* the inclusion of the water related index in the asymptote presented a logical effect and a substantial improvement of the models, for *P. taeda* a clear effect was not observed and was not included, therefore all the modelled components remained with a fixed asymptote.

Results of fittings for each component as well as comparisons regarding the use of information (tilted *vs* plane surface, and several modifiers) are presented in the next section.

Dominant height

The equation with the smallest *RMSE* was Von Bertalanffy-Richards for both species, represented by equations. 4.32 and 4.33 for *Pinus taeda* and *Eucalyptus grandis* respectively. Expressions are as follows:

$$h_{dom_2} = a\left(\frac{h_{dom_1}}{a}\right)^{\frac{ln\left[1-e^{\left(-bR_{\theta DT_2}\right)}\right]}{ln\left[1-e^{\left(-bR_{\theta DT_1}\right)}\right]}} \tag{4.32}$$

and

$$h_{dom_2} = (a_0 + a_1\bar{R}_{\theta D})\left[\frac{h_{dom_1}}{(a_0 + a_1\bar{R}_{\theta D})}\right]^{\frac{ln\left[1-e^{\left(-bR_{\theta DT_2}\right)}\right]}{ln\left[1-e^{\left(-bR_{\theta DT_1}\right)}\right]}} \tag{4.33}$$

Where $R_{\theta DT_1}$ and $R_{\theta DT_2}$ are radiations modified by water balance respectively, VPD, and temperature modifiers and aggregated up to t_1 and t_2 respectively, and $\bar{R}_{\theta D}$ is a 30-year average of monthly radiation for the site modified by *waterMod*.

A comparison of errors of different alternatives regarding the use of slope and aspect for computing radiation as well as different combinations of restriction factors are depicted in Table 4.2 ordered by the error magnitude. Equations with skewed residual distributions were not considered in the rank.

In general, differences between all the alternatives were small for both species. PULS computed using the water related factor ($R_{\theta D}$) (either considering tilted or flat terrain) gave the lowest error by a small margin. *RMSE* of the options considering slope and aspect were almost identical to the *RMSE* values estimated using light sums assuming flat surfaces.

Despite not being the alternative with lowest errors, $R_{\theta DT}$ was chosen since differences with other options are small and it comprises a more complete description of growing conditions. Selected alternatives are highlighted in Table 4.3 and the parameters are presented in Table 4.4, whereas residuals of the fitting as well as residuals using the independent dataset are shown in Figures 4.8 and 4.9 respectively.

Table 4.3 Comparison of errors of the best three restricted light sums types with and without considering slope and aspect to model h_{dom}.

		Pinus taeda			***Eucalyptus grandis***			
Surface	PULS type	*RMSE* eq. 3.8	*RMSE* difference[1] (%)	*RMSE* difference[2] (%)	PULS type	*RMSE* eq. 3.8	*RMSE* difference[1] (%)	*RMSE* difference[2] (%)
Tilted	$R_{\theta D}$	0.917	0	0	$R_{\theta D}$	1.618	0	0
	$R_{\theta DT}$	**0.932**	**1.6**	**-**	**$R_{\theta DT}$**	**1.624**	**0.4**	**-**
	R_{θ}	0.956	4.1	-	R_{θ}	1.643	1.5	-
Plane	$R_{\theta D}$	0.916	0	-0.1	$R_{\theta D}$	1.620	0	0.1
	$R_{\theta DT}$	0.931	1.6	-	$R_{\theta DT}$	1.624	0.2	-
	R_{θ}	0.955	4.1	-	R_{θ}	1.645	1.5	-

RMSE: root mean square error
[1]Differences within the same group regarding the use of slope and aspect
[2]Differences between the best option per group for comparing the inclusion of slope and aspect information.

Table 4.4 Parameters of the equations selected for modelling h_{dom} using PULS approach.

Species	Eq.	-	a/a_0	a_1	b
P.taeda	4.32	Estimate	30.116567	-	0.041078
		SE	0.329911	-	0.000743
		p-value	<0.001	-	<0.001
E.grandis	4.33	Estimate	14.815317	0.140033	0.035879
		SE	1.936893	0.009702	0.001230
		p-value	<0.001	<0.001	<0.001

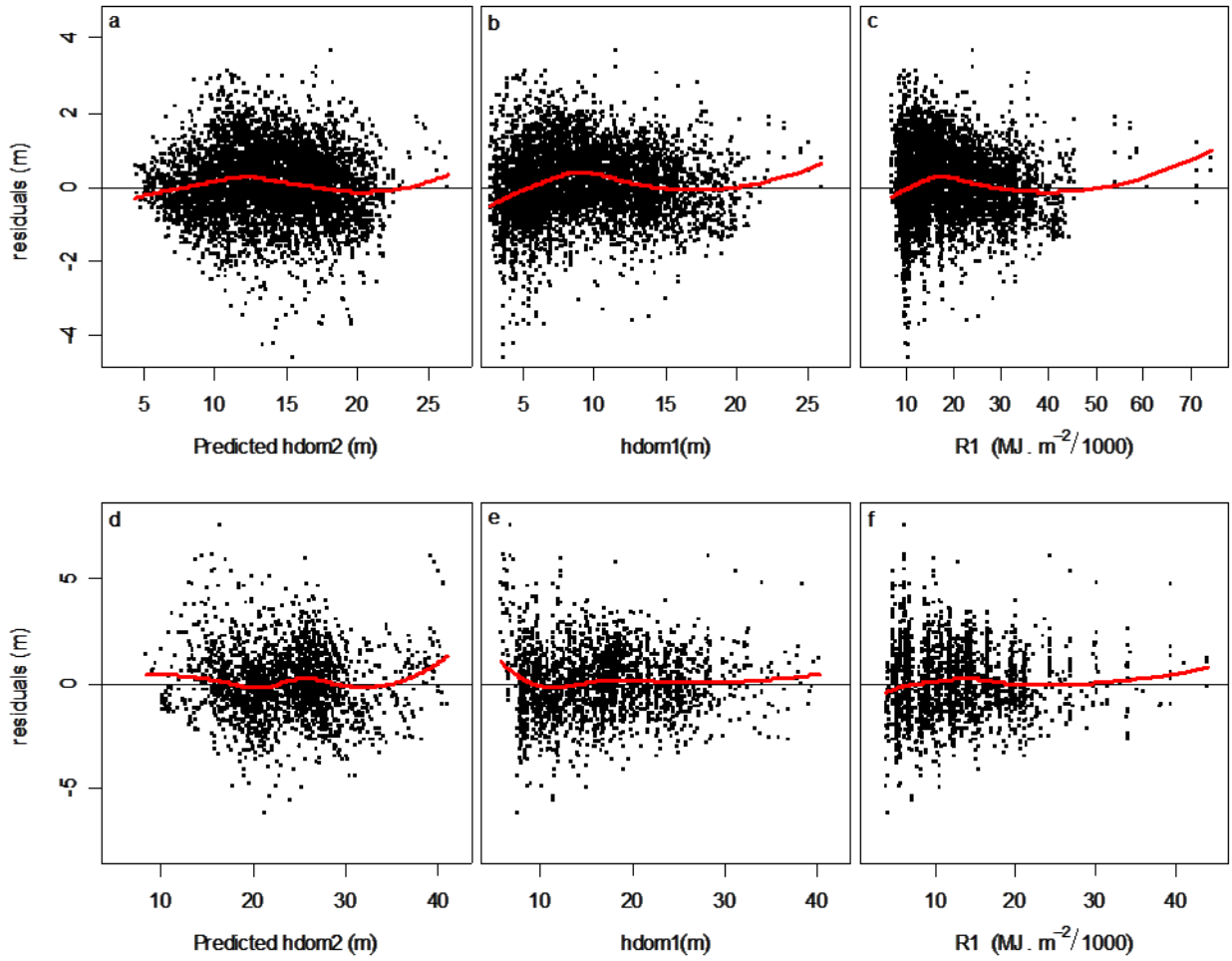

Figure 4.8 Residuals of the selected equation for modelling h_{dom} for *P. taeda* (a, b, and c) and *E. grandis* (d, e, and f).

Residuals plotted against the predicted variable as well as the independent variables showed minimal bias for both species, as also did residuals using the validation dataset. The interval with 95% of confidence for the slope of observed vs predicted values were: 0.99-1.01 for *P.taeda*, and 1.00-1.02 for *E.grandis*, whereas the *RMSEs* using the validation dataset were 0.884 and 1.518 respectively.

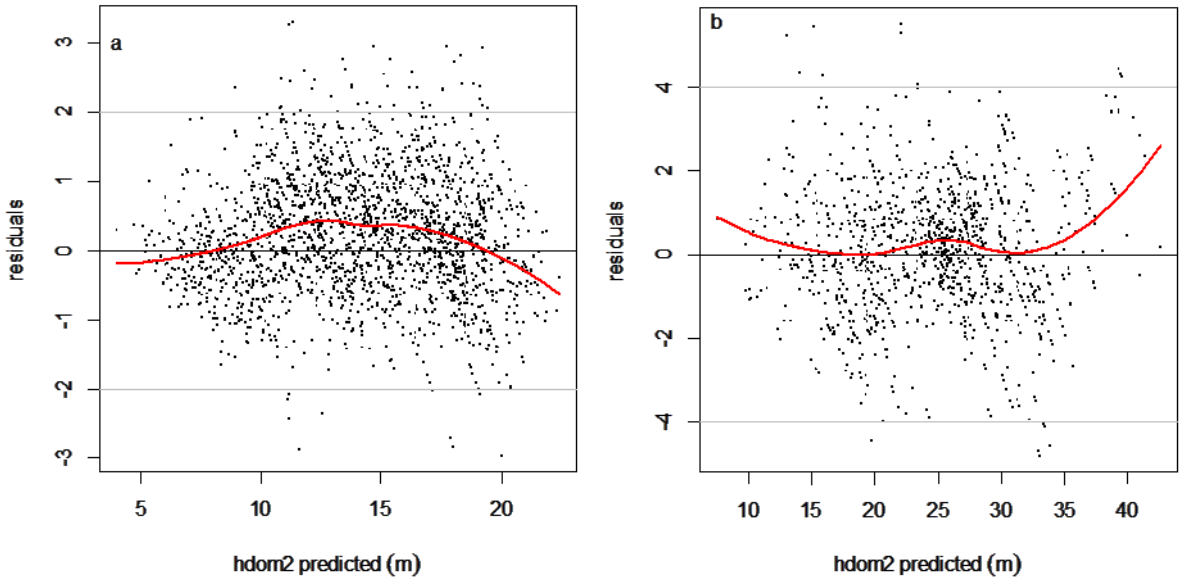

Figure 4.9 Residuals using the validation dataset for *P. taeda* (a) and *E. grandis* (b) with lowess line (red).

Net Basal Area

Different equations performed best for each studied species: equation 4.34 (Von Bertalanffy-Richards polymorphic) had the smallest errors for *P. taeda* whereas the equation 4.35 (Schumacher polymorphic with one parameter) had the smallest *RMSE* for *E. grandis*. Those equations are:

$$G_2 = a\left(\frac{G_1}{a}\right)^{\frac{ln\left[1-e^{\left(-bR_{\theta DT_2}\right)}\right]}{ln\left[1-e^{\left(-bR_{\theta DT_1}\right)}\right]}} \tag{4.34}$$

and

$$G_2 = e^{ln(G_1)\left(\frac{R_{\theta DT_1}}{R_{\theta DT_2}}\right)^c + (a_0 + a_1\bar{R}_{\theta D})\left[1-\left(\frac{R_{\theta DT_1}}{R_{\theta DT_2}}\right)^c\right]} \tag{4.35}$$

Where $R_{\theta DT_1}$ and $R_{\theta DT_2}$ are radiations modified by water balance, VPD, and temperature modifiers and aggregated up to t_1 and t_2 respectively, and $\bar{R}_{\theta D}$ is a 30-year average of monthly radiation for the site modified by water balance and VPD.

For both species differences between options using the slope and aspect information and the options that do not use this information were minimal. PULS alternatives also showed small differences, however for *E. grandis* those differences were slightly larger. For both species PULS formulation that better adjusted to the data was $R_{\theta D}$, followed by $R_{\theta DT}$, and R_{θ}. The second was the formulation selected (highlighted in Table 4.5) since differences in precision with respect to the best alternative were very small and the full formulation offers the possibility of adding temperature effect to predictions (as indicated previously). Parameters are shown in Table 4.6.

Table 4.5 Comparison of errors of the best three restricted light sums types with and without considering the slope and aspect to model *G* for each species.

	Pinus taeda				***Eucalyptus grandis***			
Surface	PULS type	*RMSE* eq. 3.8	*RMSE* difference[1] (%)	*RMSE* difference[2] (%)	PULS type	*RMSE* eq. 3.2	*RMSE* difference[1] (%)	*RMSE* difference[2] (%)
Tilted	$R_{\theta D}$	2.767	0	0	$R_{\theta D}$	2.879	0	0
	$\boldsymbol{R_{\theta DT}}$	**2.803**	**1.3**	**-**	**$\boldsymbol{R_{\theta DT}}$**	**2.926**	**1.6**	**-**
	R_{θ}	2.815	1.7	-	R_{θ}	3.005	4.2	-
Plane	$R_{\theta D}$	2.778	0	0.4	$R_{\theta D}$	2.880	-	0.03
	$R_{\theta DT}$	2.813	1.2	-	$R_{\theta DT}$	2.927	1.6	-
	R_{θ}	2.822	1.6	-	R_{θ}	3.010	4.3	-

RMSE: root mean square error.
[1]Differences within the same group regarding the use of slope and aspect
[2]Differences between the best option per group for comparing the inclusion of slope and aspect information.

Table 4.6 Parameters of the equations selected for modelling *G* using PULS approach.

Species	Eq.	-	a/a_0	a_1	b	c
P.taeda	4.34	Estimate	60.81	-	0.06975	-
		SE	92.7	-	9.491e-04	-
		p-value	<0.001	-	<0.001	-
E.grandis	4.35	Estimate	3.2921722	0.0030941	-	0.9017980
		SE	0.0942913	0.0004362	-	0.0204746
		p-value	<0.001	<0.001	-	<0.001

Residuals plots of the fitting and validation of the chosen alternatives are shown in Figures 4.10 and 4.11 respectively. No strong tendencies were found with respect to bias for any of the species. The interval with 95% of confidence for the slope of independent observations vs predicted values were: 1.00-1.04 for *P.taeda*, and 0.96-1.00 for *E.grandis*, whereas the *RMSE* using the validation dataset was 2.978 and 2.386 respectively.

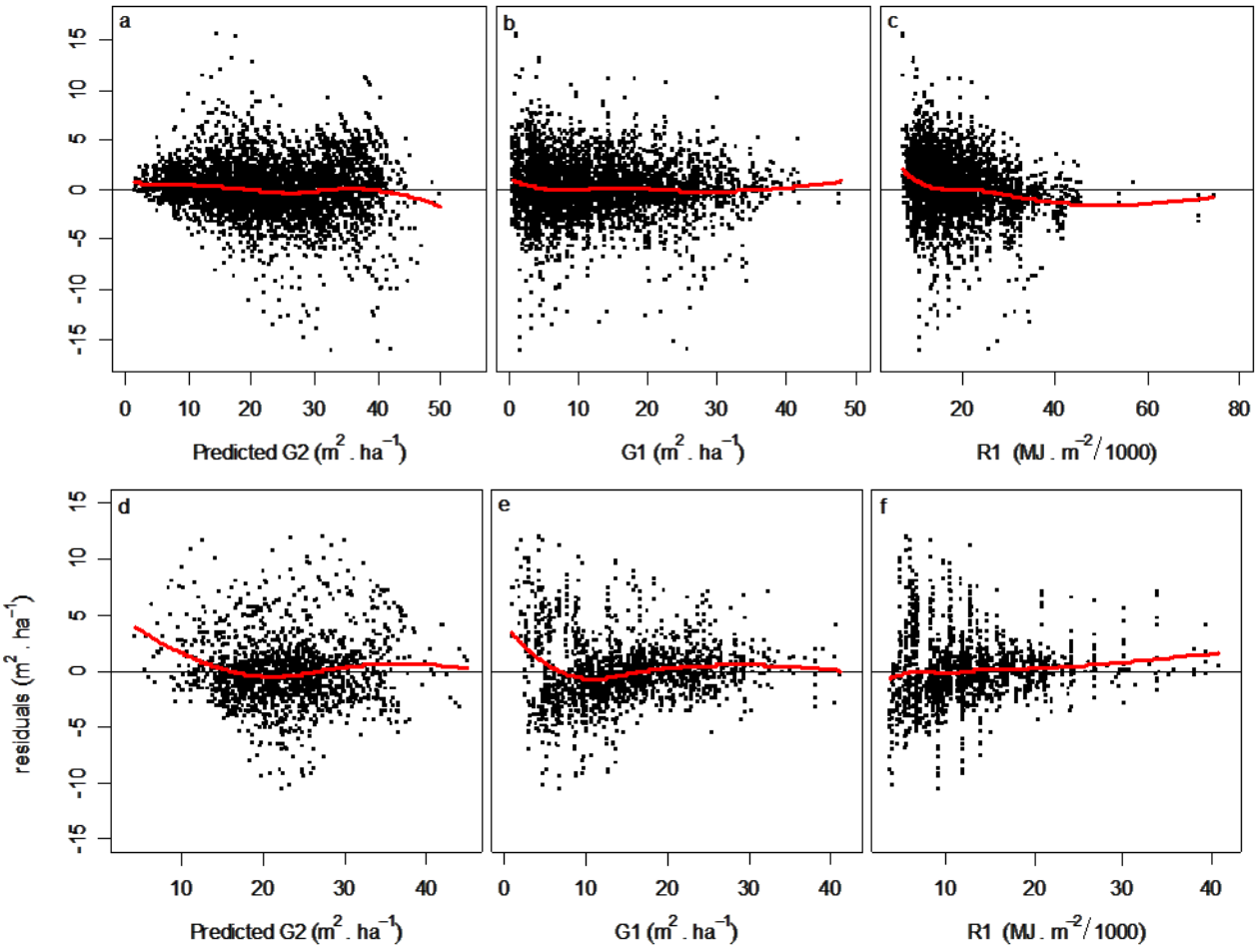

Figure 4.10 Residuals of the selected equations for modelling *G* for *P. taeda* (a, b, and c) and *E. grandis* (d, e, and f).

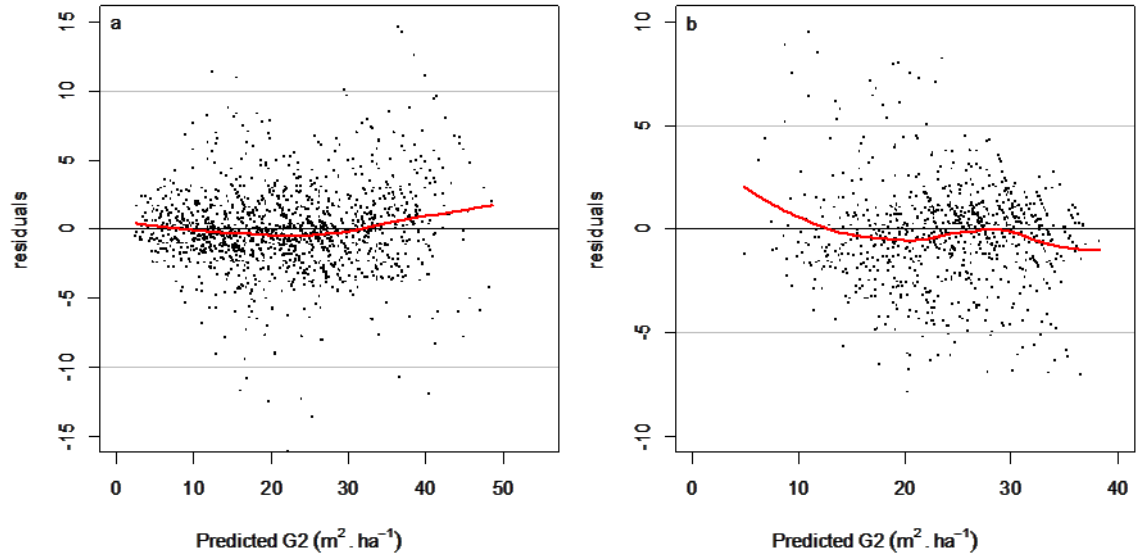

Figure 4.11 Residuals using the validation dataset for *P. taeda* (a) and *E. grandis* (b) with lowess line (red).

Maximum Diameter

For d_{max}, the equation selected was a Schumacher polymorphic with 2 parameters for both species (Eq. 4.36 and 4.37). Once again, the use of slope and aspect information had almost null influence over the standard error.

The ranks regarding PULS formulation were the same for both species, with a better fitting of the formulation using $R_{\theta D}$, however differences in *RMSE* were very small with respect to the other options. Hence the full formulation was selected (highlighted in Table 4.7). Parameters of the chosen options are depicted in Table 4.8. Selected equations for *P. taeda* and *E. grandis* respectively were:

$$D_{max_2} = e^{ln(D_{max_1})\left(\frac{R_{\theta DT_1}}{R_{\theta DT_2}}\right)^c + a\left[1-\left(\frac{R_{\theta DT_1}}{R_{\theta DT_2}}\right)^c\right]} \quad (4.36)$$

and

$$D_{max_2} = e^{ln(D_{max_1})\left(\frac{R_{\theta DT_1}}{R_{\theta DT_2}}\right)^c + (a_0 + a_1 \bar{R}_{\theta D})\left[1 - \left(\frac{R_{\theta DT_1}}{R_{\theta DT_2}}\right)^c\right]} \quad (4.37)$$

Where $R_{\theta DT_1}$ and $R_{\theta DT_2}$ are radiations modified by water balance, VPD, and temperature modifiers and aggregated up to t_1 and t_2 respectively, and $\bar{R}_{\theta D}$ is a 30-year average of monthly radiation for the site modified by water balance and VPD.

Table 4.7 Comparison of errors of the best three restricted light sums types with and without considering the slope and aspect to model d_{max} for each species.

	Pinus taeda				***Eucalyptus grandis***			
Surface	PULS type	*RMSE* eq. 3.2	*RMSE* difference[1] (%)	*RMSE* difference[2] (%)	PULS type	*RMSE* eq. 3.2	*RMSE* difference[1] (%)	*RMSE* difference[2] (%)
Tilted	$R_{\theta D}$	1.753	-	0	$\boldsymbol{R_{\theta DT}}$	**2.017**	0	0
	$\boldsymbol{R_{\theta DT}}$	**1.787**	**1.9**	**-**	R_{DT}	2.023	0.3	**-**
	R_{θ}	1.811	3.2	-	R_{θ}	2.051	1.7	-
Plane	$R_{\theta D}$	1.754	-	0.06	$R_{\theta DT}$	2.017	0	0
	$R_{\theta DT}$	1.788	1.9	-	$R_{\theta D}$	2.022	0.2	-
	R_{θ}	1.812	3.2	-	R_{θ}	2.053	1.8	-

RMSE: root mean square error.
[1]Differences within the same group regarding the use of slope and aspect
[2]Differences between the best option per group for comparing the inclusion of slope and aspect information.

Table 4.8 Parameters of the equations selected for modelling $\boldsymbol{d_{max}}$ using PULS approach.

Species	Eq.	-	$\boldsymbol{a/a_0}$	$\boldsymbol{a_1}$	$\boldsymbol{c}$
P.taeda	4.36	Estimate	4.25329	-	0.83895
		SE	0.01942	-	0.01361
		p-value	<0.001	-	<0.001
E.grandis	4.37	Estimate	2.6107845	0.0124875	0.2622174
		SE	0.1482065	0.0007718	0.0122268
		p-value	<0.001	<0.001	<0.001

Plots of residuals against modelled and independent variables did not show marked bias (Figure 4.12) and neither did residuals plotted using the independent dataset (Figure 4.13) for none of the species studied. The interval with 95% of confidence for the slope of independent observations vs predicted values were: 1.03-1.06 for *P.taeda*, and 0.88-0.93 for *E.grandis*, whereas the *RMSE* using the validation dataset was 1.886 and 2.009 respectively.

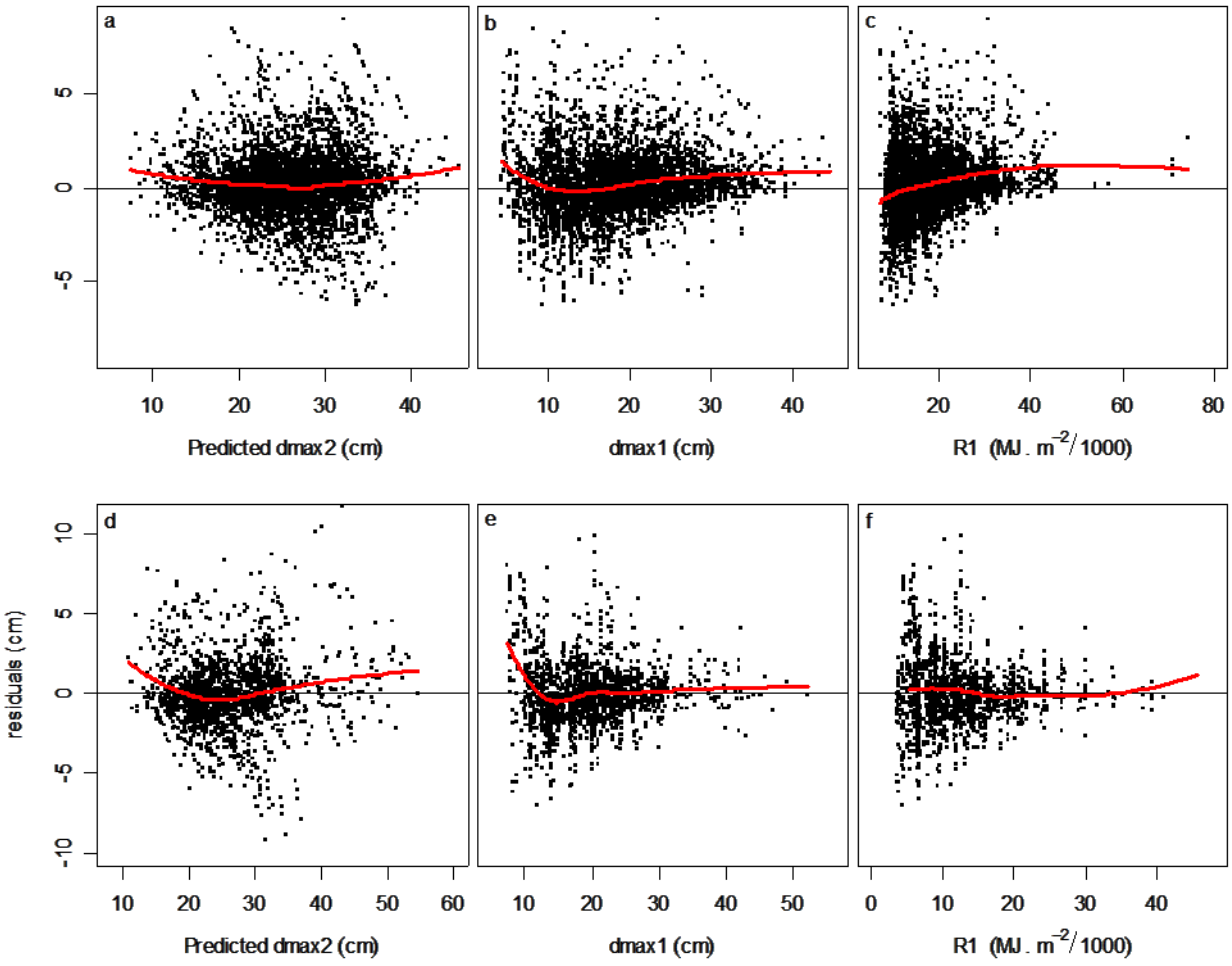

Figure 4.12 Residuals of the selected equations for modelling $\boldsymbol{d_{max}}$ for *P. taeda* (a, b, and c) and *E. grandis* (d, e, and f).

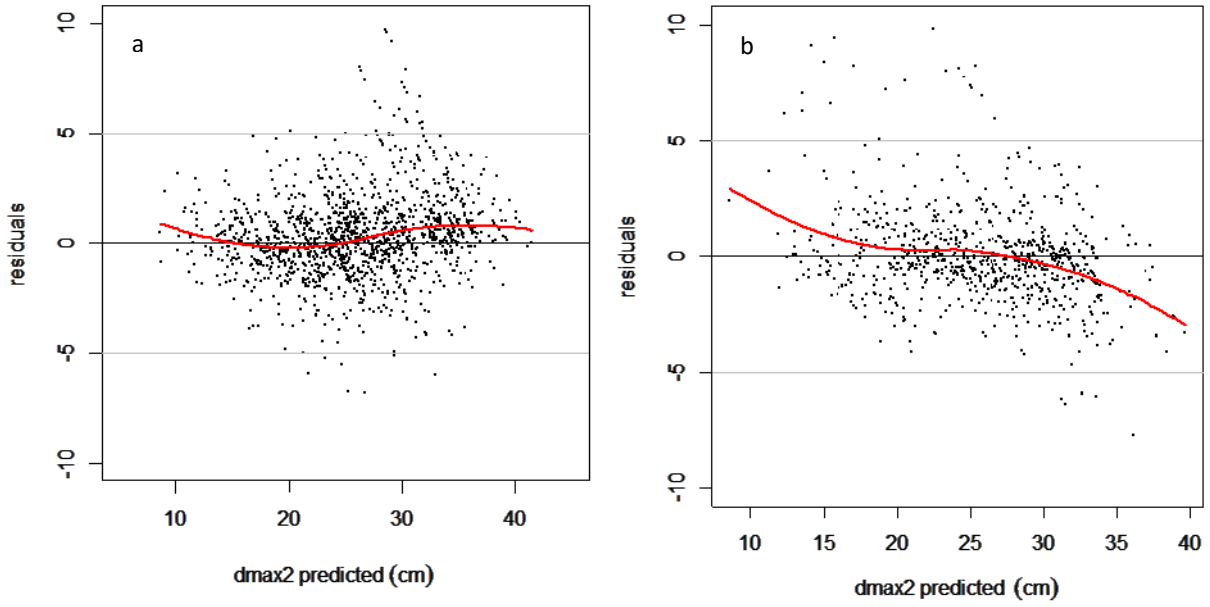

Figure 4.13 Residuals using the validation dataset for *P. taeda* (a) and *E. grandis* (b) with lowess line (red).

Standard deviation of diameters

The equation that showed a better fit for SD_d was the Von Bertalanffy-Richards (Eq. 4.38) for both species. Considering slope and aspect did not show significant improvement of the *RMSE*, whereas the differences regarding the use of PULS calculated using different combination of modifiers was almost null for both species also for this stand descriptor. The PULS option applying all three modifiers was the formulation chosen for both species (highlighted in Table 4.9). The equations for *Pinus taeda* and *Eucalyptus grandis* has the form:

$$SD_{d_2} = a\left(\frac{SD_{d_1}}{a}\right)^{\frac{ln\left[1-e^{\left(-bR_{\theta DT_2}\right)}\right]}{ln\left[1-e^{\left(-bR_{\theta DT_1}\right)}\right]}} \tag{4.38}$$

Where $R_{\theta DT_1}$ and $R_{\theta DT_2}$ are radiations modified by water balance, VPD, and temperature modifiers and aggregated up to t_1 and t_2 respectively, and $\bar{R}_{\theta D}$ is a 30-year average of monthly radiation for the site modified by water balance and VPD.

Parameters are depicted in Table 4.10.

Table 4.9 Comparison of errors of the best three restricted light sums types with and without considering the slope and aspect to model SD_d for each species.

	Pinus taeda				*Eucalyptus grandis*			
Surface	PULS type	*RMSE* eq. 3.8	*RMSE* difference [1] (%)	*RMSE* difference [2] (%)	PULS type	*RMSE* eq. 3.8	*RMSE* difference [1] (%)	*RMSE* difference [2] (%)
Tilted	$R_{\theta D}$ R_{θ}	0.482	-	0	$\boldsymbol{R_{\theta DT}}$ $R_{\theta D}$	**0.518**	**0**	**0**
	$\boldsymbol{R_{\theta DT}}$ $R_{\theta T}$	**0.483**	**0.2**	-	R_{θ}	0.520	0.4	-
	R_D	0.485	0.6		$R_{\theta T}$	0.522	0.8	-
Plane	$R_{\theta D}$ R_{θ}	0.482	-	0	$R_{\theta DT}$ $R_{\theta D}$	0.518	0	0
	$R_{\theta DT}$ $R_{\theta T}$	0.483	0.2	-	R_{θ}	0.520	0.4	-
	R_D	0.485	0.6	-	R_{θ}	0.522	0.8	-

RMSE: root mean square error.
[1]Differences within the same group regarding the use of slope and aspect
[2]Differences between the best option per group for comparing the inclusion of slope and aspect information.

Table 4.10 Parameters of the equations selected for modelling SD_d using PULS approach.

Species	Eq.	-	$\boldsymbol{a}$	$\boldsymbol{b}$
P.taeda	4.38	Estimate	4.912066	0.031274
		SE	0.120853	0.001734
		p-value	<0.001	<0.001
E.grandis	4.38	Estimate	11.517349	0.017177
		SE	0.527159	0.001575
		p-value	<0.001	<0.001

Plots showing the distribution of residuals against the modelled variables as well as the independent variables, and plots of residuals of validation are shown in Figures 4.14 and 4.15 respectively. Although, no strong patterns were found using the modelling dataset, some bias was observed for large SD_d values through the validation dataset.

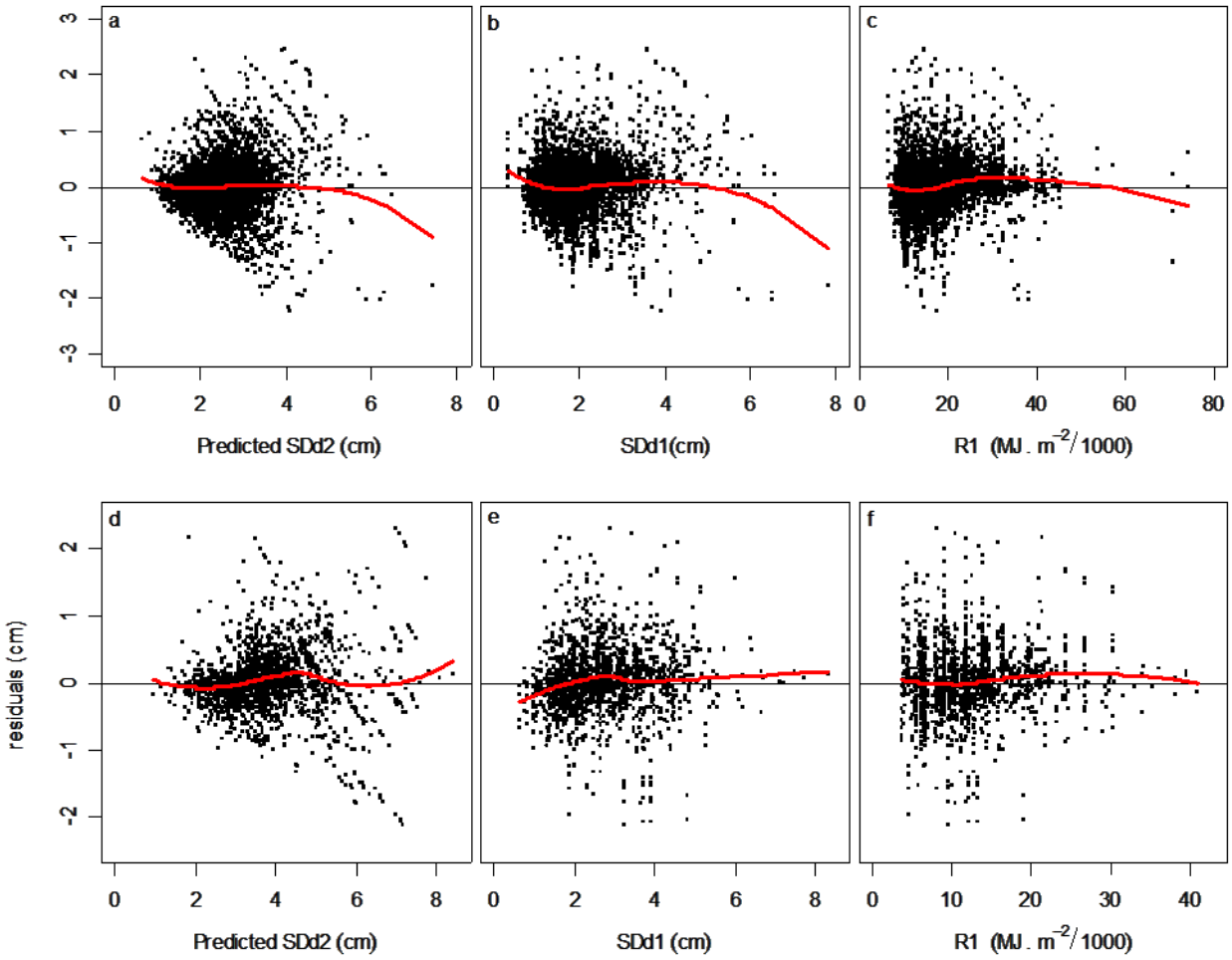

Figure 4.14 Residuals of the selected equation for modelling $\boldsymbol{SD_d}$ for *P. taeda* (a, b, and c) and *E. grandis* (d, e, and f).

The intervals with 95% of confidence for the slope of independent observations vs predicted values were: 1.01-1.07 for *P.taeda* and 1.92-1.97 for *E.grandis*, whereas the *RMSE* using the validation dataset was 0.458 and 0.510 respectively.

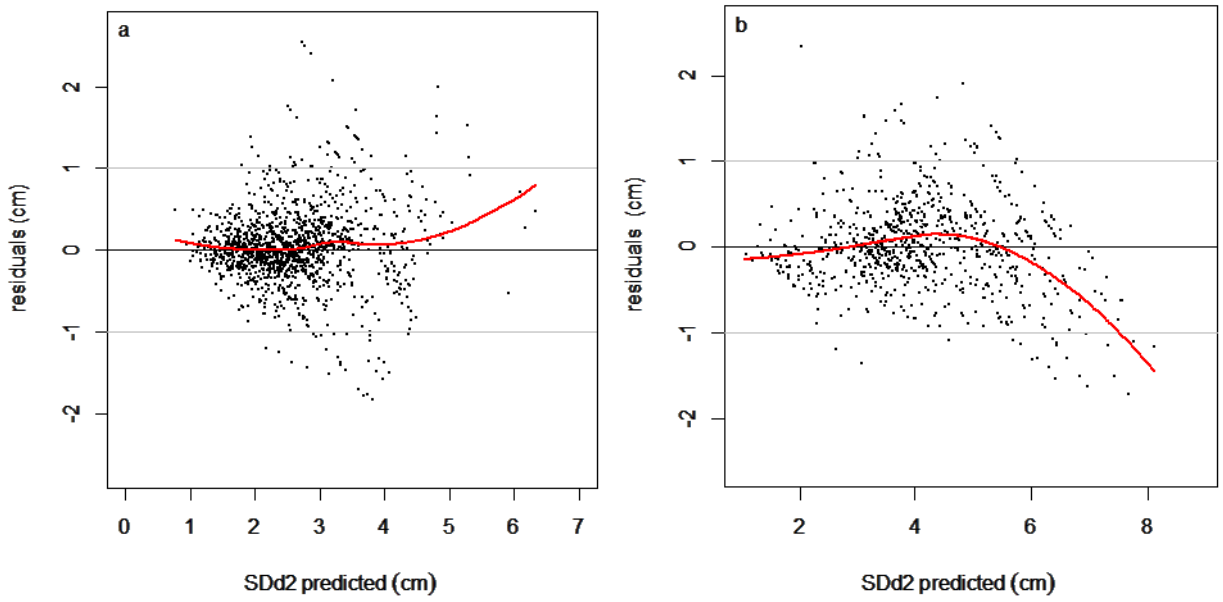

Figure 4.15 Residuals using the validation dataset for *P. taeda* (a) and *E. grandis* (b) with lowess line (red).

It must be considered that in Figures 4.14a, 4.14b and 4.15a lowess lines show pessimistic estimates of bias in regions of plots where there are very few points.

Testing the effect of changes in site conditions on growth

The behaviours of models based on modified radiation sums under different climate conditions were assessed by plotting projections for combinations of rainfall and temperature regimes. In order to compare scenarios based on realistic but contrasting conditions, data from 3 areas of the country as shown in Figure 4.16 were used given the spatial variation of minimum and maximum temperature and rainfall (see Figures 4.2-4.4). In this way, growth under historical conditions for a plot in a central location was compared to growth under increased temperature regimes from a Western location, and increased rainfall regimes from a Northern location. Monthly climate information of 17 years was applied and the series was repeated from the beginning to complete 25 years for both species.

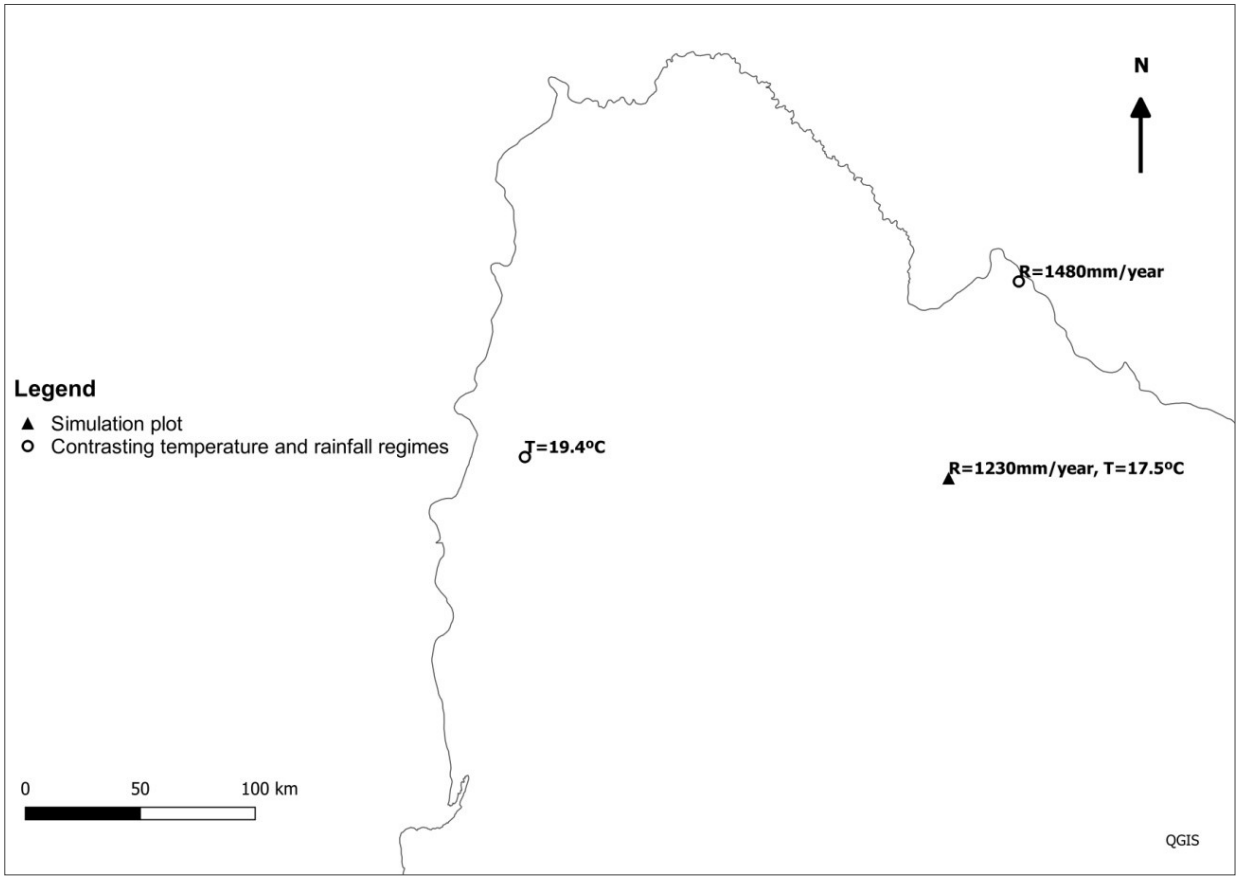

Figure 4.16 Location of plots with contrasting temperature and rainfall regimes used to assess changes in growth conditions in a simulation plot. Temperature values are averages of the studied period.

The simulation plot was located 31 º 44' 46'' latitude S and 55º 49' 06'' of longitude W, where soils have a water holding capacity of 168 mm, a slope of 2.9 degrees oriented to East, and 148 m of altitude. Temperature and rainfall combinations analyzed are depicted in Table 4.11. Simulation was initialized with real values of plots growing in the Central location for both species.

Table 4.11 Temperature and rainfall conditions assessed and 30-year monthly averages of potentially useable radiation sums modified by VPD and water balance ($\overline{\boldsymbol{R}}_{\boldsymbol{\theta D}}$) for the given condition. $\overline{\boldsymbol{R}}_{\boldsymbol{\theta D}}$ is used only for *E. grandis* (see eq. 4.33, 4.35, and 4.37).

Average monthly temperature (ºC)	Average monthly rainfall (mm)	$\overline{\boldsymbol{R}}_{\boldsymbol{\theta D}}$ ($MJm^{-2}month^{-1}$)
17.5	1230	225
17.5	1480	243
19.4	1230	213
19.4	1480	232

Time series of the modifiers (water balance, temperature, and VPD) calculated for contrasting conditions are shown in Figure 4.17 and 4.18 for *Pinus taeda* and *Eucalyptus grandis* respectively. Warmer temperatures caused a decrease in water availability and an increase in VPD restrictions. However an increase in temperature signified a more restrictive regime for the pine species and less restrictive one for the eucalypt species. Higher temperature had opposing effects on vapor pressure and water balance modifiers with respect to the temperature modifier for E. grandis compared to P. taeda.

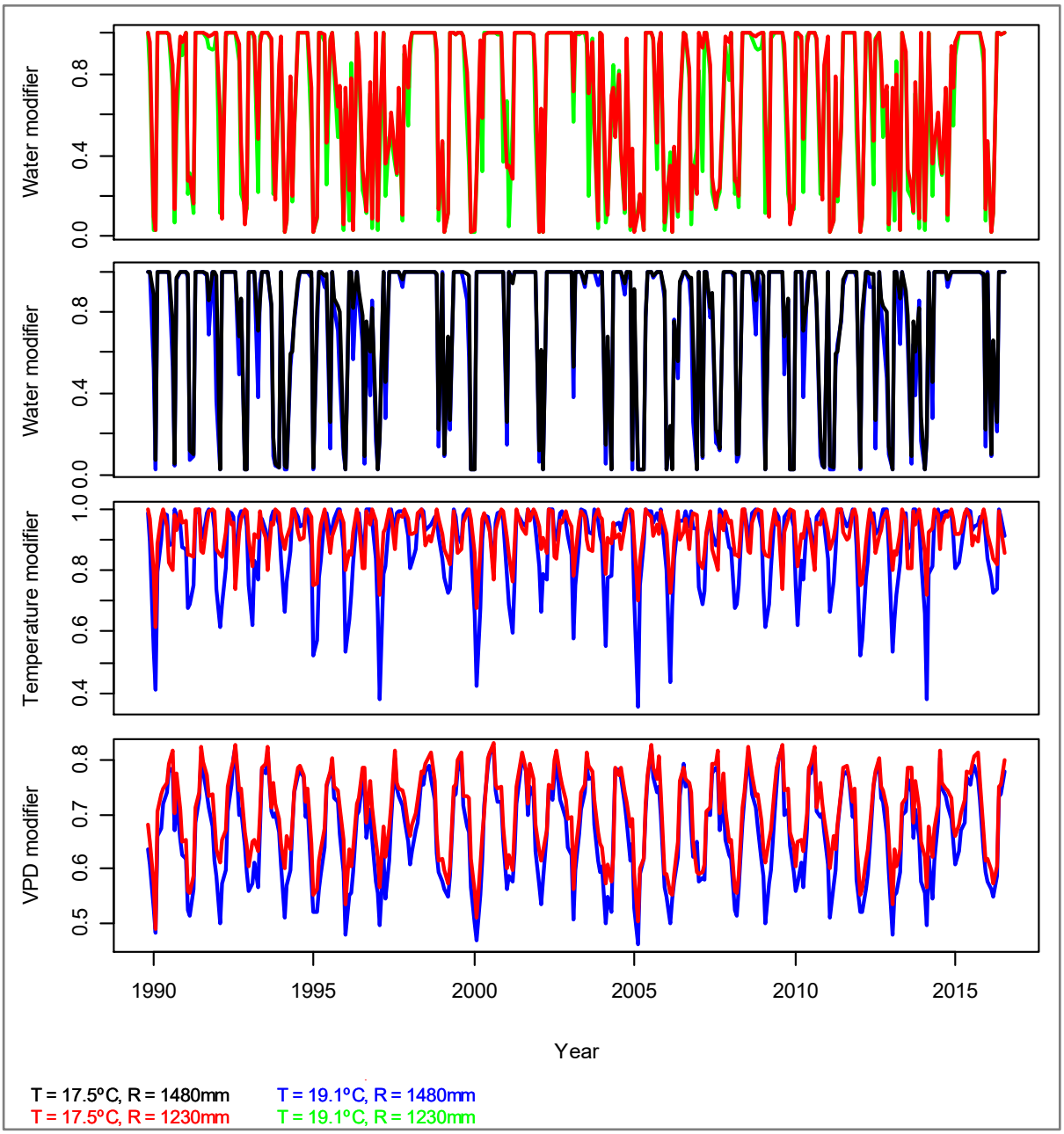

Figure 4.17. Time series of the modifiers for different temperature and rainfall regimes for *Pinus taeda*.

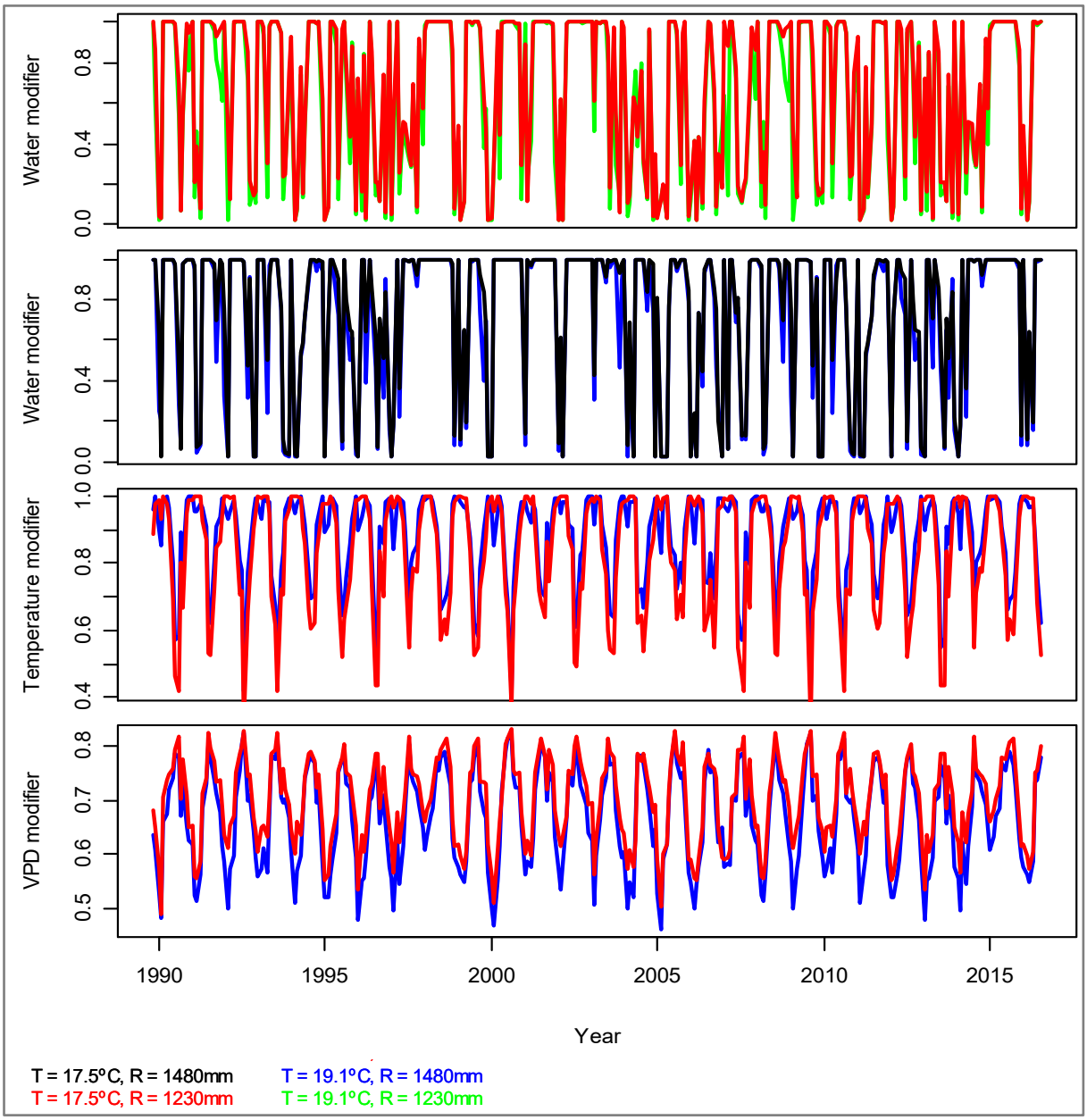

Figure 4.18 Time series of the modifiers for different temperature and rainfall regimes for *Eucalyptus grandis*.

Radiation sums for all the temperature and rainfall regime combinations are depicted per species in Figure 4.19. Light accumulation over time was higher when temperature was lower and rainfall was heavier, and lower when temperature was higher and rainfall was moderate for both species. Figures 4.20 and 4.21 show growth as a function of modified radiation sums for each state variable modelled for *Pinus taeda* and *Eucalyptus grandis* respectively.

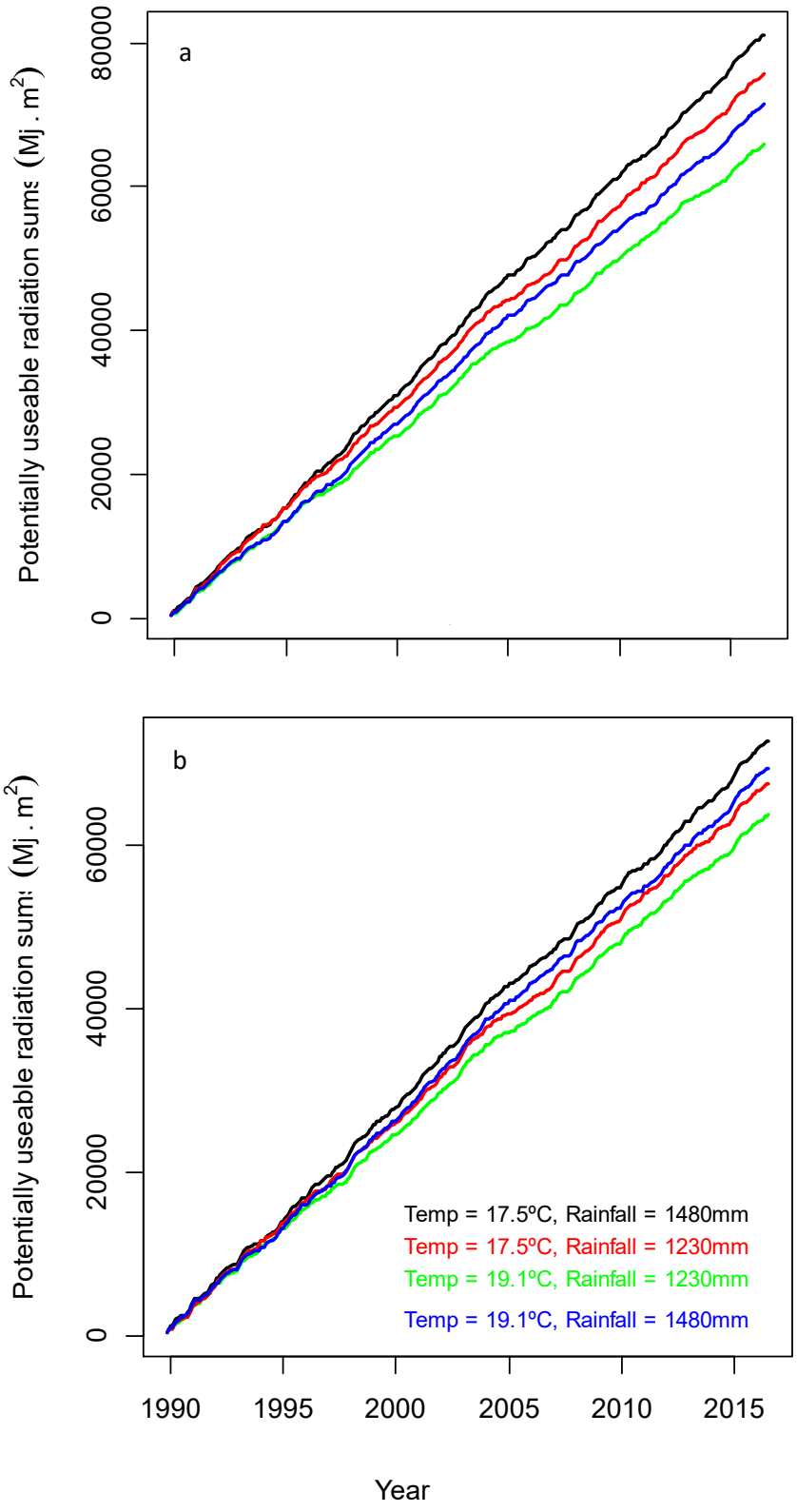

Figure 4.19. Potentially useable radiation sums for the combination of temperature and rainfall tested for (a) *Pinus taeda*, and (b) *Eucalyptus grandis*.

For both species, growth was higher for the regimes combining higher rainfall and lower temperature (1480 mm and 17.5 ºC) and lower for the combination of lower rainfall and higher temperature (1230 mm and 19.1 ºC). However, for the pine species regimes with lower temperature yielded better growth rates (Figure 4.20), whereas for *E. grandis* the regimes with higher rainfall were the ones that favoured growth the most (Figure 4.21). Moreover, differences between the less favourable regimes were not so clear for the standard deviation of diameters but conspicuous for maximum diameter of the eucalypt species. For the pine species, differences between regimes were smaller compared to the eucalypt species, and minimal for basal area when stand age approached 25 years.

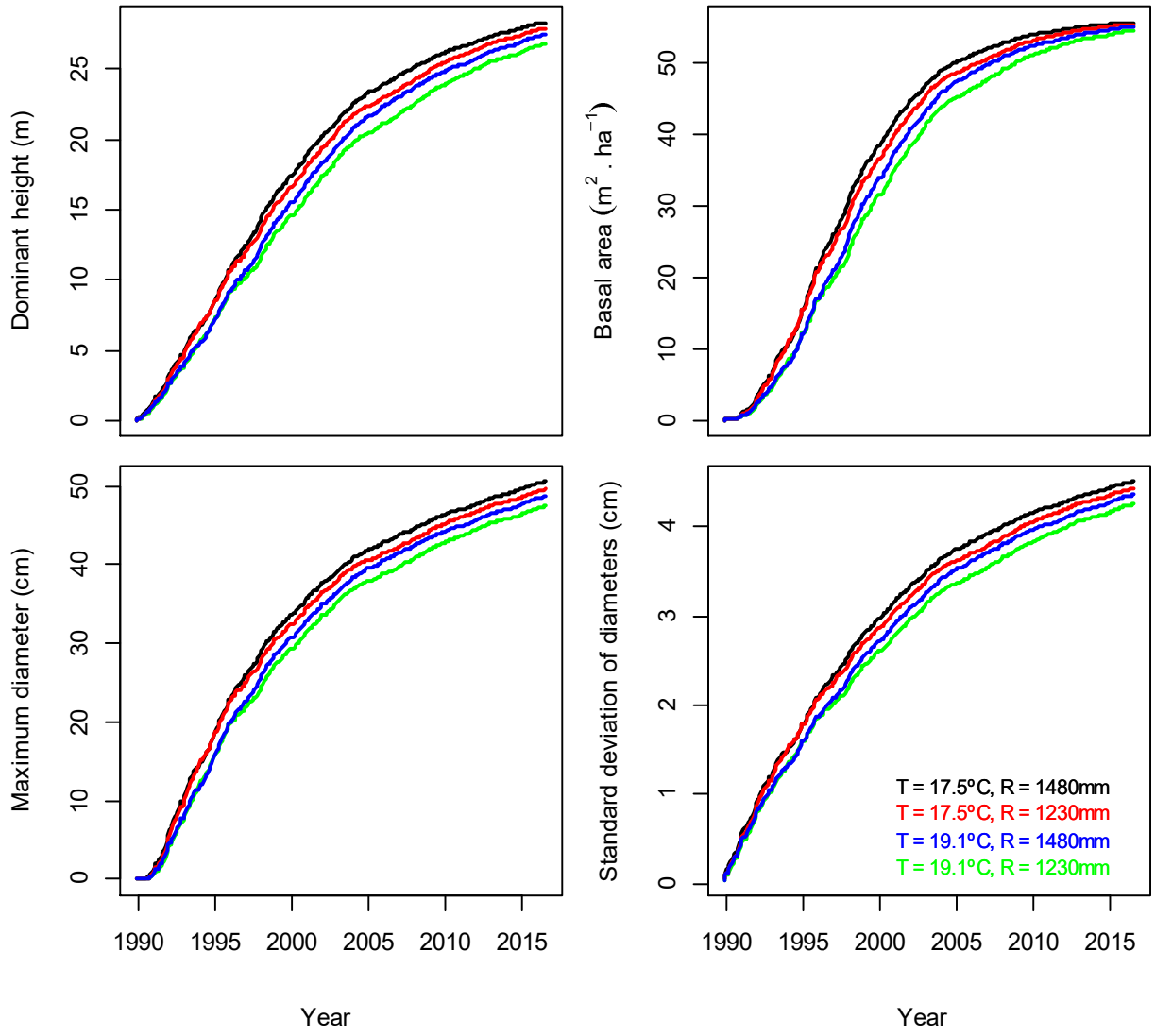

Figure 4.20 Growth curves for the modelled variables as a function of time for the radiation sums calculated for the spam of growth conditions analysed for *Pinus taeda***.**

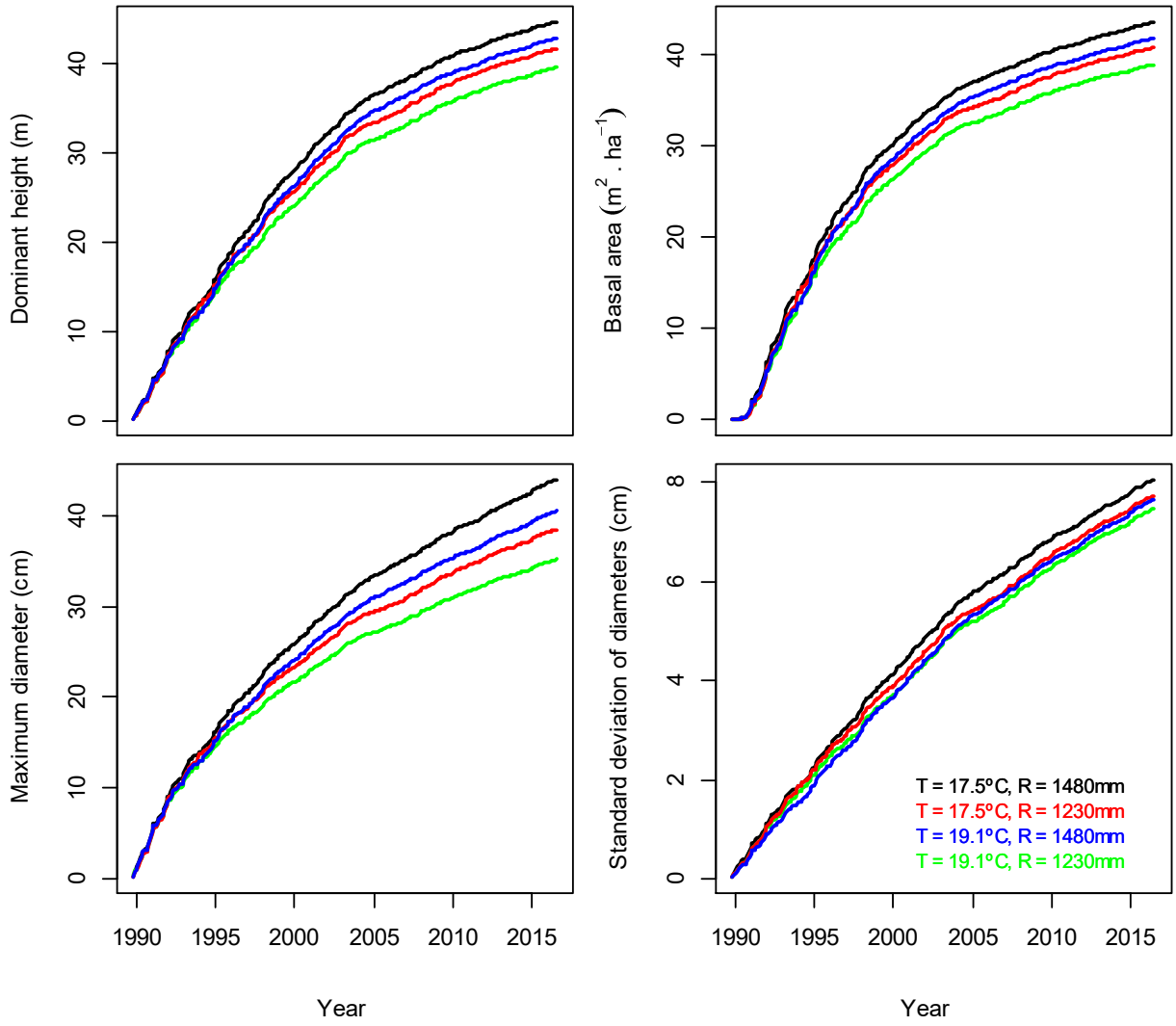

Figure 4.21 Growth curves for the modelled variables as a function of time for the radiation sums calculated for the spam of growth conditions analysed for *Eucalyptus grandis*.

DISCUSSION

This study shows that the PULS approach can be used to predict growth and stand dynamics of contrasting species at a regional scale. All four state variables for *Pinus taeda* and *Eucalyptus grandis*: dominant height, net basal area, maximum diameter breast height and standard deviation of diameters showed acceptable fitting when adjusted as functions of restricted light sums.

There are no (known) records of the use of light sums for modelling maximum diameter or standard deviation of diameters. Both variables are important for estimating diameter distributions if using the inverse Weibull, and those were successfully modelled through the light-based

approach. Using resource-driven diameter distributions would show whether or not changes in growth factors affected stand structure and how those changes influenced product volumes.

A study of different alternatives of cumulative radiation for modelling the stand descriptors provided an insight of key factors influencing growth. For the majority of the state variables, the modifiers observed to excerpt the most influence were the ones related to the water status of the stands, followed by the full formulation (using the most restrictive element between vapour pressure deficit and water balance, and temperature), and the modifier accounting for water balance alone in third place. Although differences in the standard error between the best three PULS formulations were small, those differences were larger when modelling dominant height, basal area, and maximum diameter, whereas for standard deviation of diameters error differences between the formulations were almost non-existent. For most of the variables, radiation sums restricted solely by temperature presented the poorest fittings for both species.

For both species the modifiers that had the most influence were the water balance and VPD modifiers. For *P. taeda*, water and temperature are key drivers of productivity (Teskey *et al.*, 1987), although across its natural range soil nutrient availability is suggested to be to be one of the most influencial factors (Allen and Albaugh, 1999; Jokela *et al.*, 2004; Hebert and Jack, 1998). The sensitivity of *P. taeda* to VPD, soil water content, and photosynthetically active radiation was verified by Ford *et al* (2004), the sensitivity to the first two factors was indicated by (Manogaran, 1973) and confirmed in Uruguay by Gándara *et al.*, (2014). For *E. grandis* hybrids, soil water content and atmospheric humidity was proven to be major growth modifiers in Brazil (Almeida *et al.*, 2007; Stape *et al.* , 2008, 2010). Ryan *et al.*, (2010) demonstrated that wood primary productivity increases due to increases in light interception, as well as photosynthetic efficiency, and partitioning to wood, when eucalypts are irrigated. An extensive review documenting the eco-physiology of productivity in eucalypts was presented by Whitehead and Beadle, (2004) who emphasized the enormous increase in light use efficiency that the species can achieve in well-watered soils as well as the high sensitivity of stomata in this species to vapour pressure deficit.

On the other hand, the findings from the present study contrast with the results reported by Mason *et al*. (2011), who found temperature to be the factor that most restricted light use by *Pinus radiata* in New Zealand. However, this is not surprising given that in the study region in Uruguay, in contrast to New Zealand, temperature variation is small. This is reflected in the narrow ranges and high values of the averages for this modifier showed in Figure 4.6.

Results of this study also suggest that temperature could be slightly more restrictive for eucalyptus than for the pine species, which is consistent with the fact the average annual temperature, ranging spatially from 17.7 to 19.8 ºC (Castaño *et al.*, 2011), corresponds better with the optimum growth temperature for *Pinus taeda*. For the other two modifiers, ranges between the two species were similar.

The importance of accounting for orientation and slope for computing the amount of light received by a surface in order to be used in this approach was also tested. Results showed that computing radiation considering a tilted surface did not improved the quality of the model fit. The fact that maximum slope values found in this study were 10 degrees and most of the plots were located in sites with milder slopes could have contributed to these results. Therefore it is possible that the methodology loses sensitivity in flatter terrains. However, this should be tested in sites with a wider range of slopes. Coops *et al*. (2000) showed that differences in incoming radiation between surfaces tilted to a variety of slopes and different orientations are worth considering when estimating incoming radiation for its application in forest eco-physiology. The study also showed that largest slopes presented larger estimation errors when reflected radiation was not considered. In this work, the methodology used was the one proposed by Tian *et al.* (2001), who also registered differences in estimated global radiation considering slopes and aspects at a daily timestep. Given that the digital terrain model from which slope and aspect information were extracted had a fairly fine scale (30 x 30 m), sufficient precision regarding this information would not be a main limiting factor.

When assessing the behaviour of the model for contrasting combinations of rainfall and temperature, the approach showed sensitivity to an increase of 2 oC in average temperature and 250 mm of rainfall, with a positive effect of rainfall increase and temperature decrease on growth for all response variables. The analysis showed differences between species regarding effect of climate factors on growth in the ranges studied. Because of the effect of a 30-year monthly average of radiation sums restricted by water balance or VPD on the asymptote in Eucalyptus grandis, differences between values of the variables under contrasting regimes were larger at the end of the projection period for this species. The analysis undertaken also served as an example of the possibilities of this methodology; it could be extended to test changes in water holding capacity of soils, as well the effect of droughts at different moments throughout the lifetime of the stands, or increases in temperature, for instance.

Soil information was provided by a rather coarse scale map, hence information about water holding capacity as well as soil texture would be expected to improve if finer scale maps were utilized. Further improvement with specific information about tree rooting depth in order to better estimate water holding capacity of stands would also be expected to enhance results of the tested approach in Uruguay. However, it was proved in this study that the methodology yields reasonable results using soil information that is currently available in Uruguay.

Recently, Gonzalez-Benecke *et al.* (2016) reported a new set of parameters to be used in the 3-PG model for *Pinus taeda*, and tested the model in plantations of this species in Uruguay. In their study, the authors used water holding capacity maps similar to the one used in this study as well as publicly available climate information. The model showed very good behaviour for estimating above ground biomass as well as the main mensurational variables. These are promising results which add weight to the potential application of model developed in this study since relying on stable physiological parameters is crucial for its improvement. Moreover, it also confirms that climate and soil information publicly available in Uruguay will produce acceptable results in physiological or hybrid models.

CONCLUSIONS

Results presented here suggest that PULSE can be used to predict a complete set of variables that characterize stand growth for contrasting species, as a basis for its use in forecasting systems in Uruguay.

The study of different alternatives of restricted cumulative radiation provided an insight of the factors driving growth at a regional scale. Water availability and vapour pressure deficit were the main factors (of the three studied) restricting potentially useable radiation for *Pinus taeda* and *Eucalyptus grandis*. However, the use of all three modifiers is recommended in order to make the most of the information offered by this approach.

Taking account of slope and azimuth (tilt) in computing light sums made little or no contribution to reducing fitting errors for the species and region studied.

When analysing changes in climate variables such as rainfall and temperature all the components showed consistent results with varied levels of sensitivity to changes depending on the species and the state variables assessed.

Precision of the hybrid approach presented here may tend to increase in the future with updated physiological parameters as well as increases in precision of climate and soil information. For the latter, current information publicly available is suitable for this methodology.

CHAPTER 5

MODELLING MORTALITY USING A HYBRID PHYSIOLOGICAL-MENSURATIONAL APPROACH

INTRODUCTION

Estimates of mortality are essential when modelling forest dynamics due to their influence on basal area yield and individual tree size, however the complexity of interactions among individuals as well as between individuals and environmental agents (biotics and non-biotics) make mortality forecasting difficult.

Individual mortality is a discrete event and can be modelled either through a stochastic approach, where a probability of death is used; or through a deterministic approach where a threshold level is related to individual death (Hawkes, 2000). Even-aged stand modelling usually includes the first approach using the logistic function to predict mortality (Monserud, 1976; Monserud and Sterba, 1999). For populations, the change in number of stems per hectare per time unit (stocking) is often represented by inverse sigmoidal functions (Clutter *et al.*, 1983). Either modelling mortality or stocking, the use of explanatory variables as age, size, and competition can be used to enhance predictability.

Regular (or non-catastrophic) mortality has been associated with competition, however competition is not a cause of death by itself and it is rather a factor that influences the susceptibility of trees to pests or stress (Weiskittel *et al.*, 2011). Hawkes (2000) refers to mortality as "a cumulative build-up of chronic stress rather an instantaneous response to stress". Vigour change is the key concept driving mortality since past events that reduce vigour increase susceptibility to mortality agents (Das et al. 2007), and hence the likelihood of survival (Mangel and Bonsall, 2004). Manion (1991) and Manion and Lachance (1992) proposed a model of interactions between factors that drive mortality in the form of a three-tiered spiral. In the model, the outer ring is given by predisposing site characteristics (such as moisture holding capacity, compaction, drainage, pollution), and plant characteristics (given mostly by age and genetics). The second level comprises "inciting" factors mostly related to events that can cause temporary stress such as

drought and frosts; whereas the third level is related to biotic contributing factors such as fungi, insects, nematodes, and bacterial infections. Tree vigour translates to tree growth and size, and both metrics are often used to predict mortality risk when following the aggregative approach mentioned. Pedersen (1998) found distinctive pre-mortality patterns in a large-interval scale, and that stress episodes decrease vigour increasing susceptibility to further stresses, in accordance to Manion's model. Antos *et al.*, (2008) found that basal area growth diminished considerably in a long period prior to death, whereas Das *et al.* (2007) found that along with slow diameter growth, abrupt growth decline is also associated with an increase in mortality probability. Moreover, results suggested a differential interval length of the period where growth decreases prior to dead for different species related to growth habits such as shade tolerance.

Waring (1983) pointed to the utility of a growth efficiency concept, defined as wood production per unit leaf area, as an "index of tree vigour since proportion of carbohydrates allocated to wood production decreases in parallel with a tree's resistance to insect attack and production of protective compounds". Prolonged stress lowers the photosynthetic activity of trees and their ability to accumulate reserves (Waring, 1983). Following this work, Prentice and Leemans (1990) as well as Nikolov and Fox (1994) used growth efficiency to model probability of death. Prentice and Leemans used relative growth efficiency, assumed as the ratio of realized growth efficiency and the maximum efficiency for the species, to classify vigorous (with low probability of death) and suppressed trees (with high probability of death). When efficiency is less than a minimum, a tree is assumed to be suppressed. This minimum is a "prescribed" threshold value (Prentice *et al.*, 1993; Prentice and Leemans, 1990).

Analogously, light-use efficiency (LUE) principles characterize the resources that are available for growth, maintenance and reserve, and it depends on the action of environmental factors, therefore, principles related to LUE could be as well applied to improve mortality predictions. For example, Peterman *et al.*, (2013) used the 3-PG model to assess yearly changes in gross primary productivity (GPP) associated to drought induced mortality. It is hypothesized here that the aggregated growth restrictions considered in a LUE context could represent the accumulation of stress factors that lead certain trees to death. In this sense, the approach could account for some of the pre-disposing and inciting factors posed by Manion (1991). In regimes where production is deeply related to water availability, as is the case in this study, drought periods could represent one of the main stress factors.

The physiological mechanisms leading to death caused by water stress are under discussion, with the coexistence of two main theories: i) carbon starvation and ii) hydraulic failure (Sala *et al*., 2010; McDowell *et al*., 2011) . The first mechanism predicts carbon depletion due stomatal closure to avoid water loss with a subsequent reduction of gas exchange and CO_2 assimilation, whereas the second is related to irreversible desiccation of tissues due extreme loss of water. Under a scenario of uncertainty of the physiological mechanisms associated to water-stress induced death, an "aggregate measure of fitness" (Meir *et al.*, 2015) such as net primary productivity, non-structural carbon production, growth efficiency or leaf area (McDowell *et al.*, 2011) are options often considered.

The objectives of this work were:

i) To model mortality applying a hybrid physiological-mensurational approach based on potentially useable light sums (PULS).
ii) To test whether information of historical stress conditions could be good predictors of mortality at a stand level in a hybrid approach.

METHODS

Mortality is necessarily modelled using permanent sample plot data, but coping with different measurement intervals can lead to over or underestimations of stocking depending on the occurrence of mortality in that period. To avoid this problem, Woollons (1998) proposed a two-step method where a function of probability of death occurrence is predicted first, while in a second step sigmoidal function of stocking is fitted using only the plots with death events. The approach was adopted in this study and different description levels of resource availability or stress were tested for modelling probability of mortality (step 1), whereas one formulation was tested for modelling mortality rate (step 2). Differences in growth rates were deeply related to water availability for both species, according to results described in previous chapters, hence restrictions mainly related to water were considered as following. Although frosts represent a source of stress for *E. grandis* in Uruguay, this phenomenon is rather local, and plantations are usually spatially arranged in the slopes in a way to avoid lowest temperatures in winter and subsequent damage. Therefore it was assumed in this study that frosts were not a generalized cause of stress for eucalypt plantations.

Probability of mortality

Three strategies were tested for modelling probability of mortality:

- Formulation 1: Stand + site variables
- Formulation 2: Stand variables + average of potentially useable light sums adjusted by water related modifiers (*waterMod*)
- Formulation 3: Stand variables + accumulation of long and short term water stresses

For all three formulations, time has been replaced by radiation sums modified by temperature, vapour pressure deficit, and water balance, therefore t_1 has been substituted by $R_{\theta DT_1}$ (see Chapter 4) and Interval (*Int)* is computed as the difference between $R_{\theta DT_2}$ and $R_{\theta DT_1}$.

The first formulation represents an option with the least physiological information. It is given by the model chosen to model probability of mortality (through mensurational equations) in Chapter 3 for each species with the mentioned substitutions. The second option includes a monthly 30-year average of light sums modified by water related factors only ($\bar{R}_{30}$), which represents average growth/stress conditions for each plot. This variable was tested in Chapter 4 for modifying the asymptote of growth curves and found to improve model behaviour for *E. grandis* only. The third option includes accumulation of water stress. Provided that the length and the severity of stress events are relevant, e. g. Myers and Landsberg (1989) found that the reduction in dry matter production was greater if trees were subjected to moderate water stress for a long period than to severe water stress for short period. Variables tested were: a) accumulated prolonged, moderate stress, and b) accumulated short-term, severe stress. Those variables were computed utilizing the water related modifier (*waterMod*, which is the minimum value between the vapour pressure deficit (VPD) modifier and the soil water modifier), as follows:

a. Number of consecutive months since planting where $waterMod \leq threshold\ 1$ during the growing period, given a minimum of 3 months of stress duration.
b. Number of total individual months since planting where $waterMod \leq threshold\ 2$ during the growing period.

Since $threshold\ 1$ accounts for moderate stress and $threshold\ 2$ for severe stress, then $threshold\ 1 > threshold\ 2$. Moreover, it is unknown at what level of stress mortality is most likely to be related, therefore decreasing thresholds were tested starting with the average of the minimum value of the water related modifier computed for both species (see ranges in Figure 4.6).

The growing season was considered from September to May. Long-term (moderate) and short-term (severe) water stress variables are summarized in Table 5.1.

The first and the second option are based on general growth conditions and average site water conditions on plot sites, the third option includes specific information of water stress episodes throughout the life of stands. In this sense, there is an improved mechanistic link between growth and water stress from the first to the third option.

Table 5.1 Summary of variables tested in the formulations 2 and 3.

Variable (units)	Computation	Threshold	Acronym	*Pinus taeda*			*Eucalyptus grandis*		
				Min.	Mean	Max.	Min.	Mean	Max.
Long term moderate accumulated water stress (months)	Number of consecutive months since planting (minimum 3) where $waterMod \leq threshold$	0.40	*L40*	0	5	21	0	4	34
		0.35	*L35*	0	4	20	0	3	27
		0.30	*L30*	0	3	17	0	2	24
		0.25	*L25*	0	2	15	0	2	18
Short term severe accumulated water stress (months)	Number of total individual months since planting where $waterMod \leq threshold$	0.25	*S25*	0	11	48	0	16	53
		0.20	*S20*	0	10	42	0	14	46
		0.15	*S15*	0	9	34	0	13	39
		0.10	*S10*	0	7	26	0	10	34
		0.05	*S05*	0	5	21	0	7	28
30-year monthly light sum average ($MJ.m^{-2}$)	Monthly average of 30 years of radiation sums modified by f_θ and f_D	-	$\bar{R}_{\theta D}$	207	257	288	202	225	275

For the three strategies all the stand variables used in the chosen model in Chapter 3 for each species where initially included and a backward elimination process was undertaken in order to define the final model. In this procedure, one variable is eliminated at a time based on the higher p-value less than the α-criterion, and a refit sequence is carried out until all variables are significant in the model. For the third formulation, long and short term water stress variables were tested

separately in the model and the variable of each group that provided the lowest AIC value for the model was included and the model was re-fitted and tested with both.

Mortality rate

The inclusion of variables that change for each projected interval operates against the path invariant property, hence for this step formulation 3 could not be tested. The equations used were the ones chosen in Chapter 3, for which age (t_1 and t_2) was substituted by the corresponding radiation sums modified by temperature, water balance and vapour pressure deficit ($R_{\theta DT_2}$ and $R_{\theta DT_1}$).

Data and statistical analysis

Stand information used was derived from the dataset utilized in Chapters 3 and 4; a modelling and an independent dataset were employed in the same way, and the methodology for fitting, testing variables, and validating mortality equations was as detailed in Chapter 3. A summary of the dataset is presented in Table 5.2. Likewise, significances of all variables included in the final models for each species were checked using a correlation-free hypothesis testing dataset where only one interval per plot was included, and the multi-colinearity between predictors was checked through the variance inflation factor (VIF). The potentially useable light sums computations for each plot/age applied is detailed in Chapter 4.

Table 5.2. Summary of the information used in the analysis.

Variable	*P. taeda*				*E. grandis*			
	Mean	Min.	Max.	SD	Mean	Min.	Max.	SD
PSP number	-	-	727	-	-	-	315	-
Number of plot measurements	4.00	2.00	11.0	-	4.00	2.00	11.0	-
t (years)	7.13	2.00	25.9	3.20	6.95	1.18	18.7	3.47
h_{dom}(m)	10.6	2.20	27.0	4.65	21.2	4.40	46.6	7.86
d_m (cm)	17.2	2.30	41.9	7.56	17.6	3.10	45.2	7.18
SD_d (cm)	2.20	0.11	8.42	0.96	3.42	0.64	10.5	1.43
G ($m^2 \cdot ha^{-1}$)	15.6	0.10	53.6	10.9	19.2	0.78	58.1	8.95
N (stems.ha^{-1})	624	100	1667	180	886	87.0	1775	393
Plot size	338	200	500	84.0	682	400	2250	315
SWPA (mm)	148	85.1	179.6	33.8	140.5	85.1	180.6	30.0
Elev (m)	151	61.0	256	32.5	121	21	201	57.0
β (%)	5.00	0	>18	3.70	4.00	0	>18	3.33

RESULTS

Probability of mortality

For *Pinus taeda*, the formulation applying long and short-term stress variables selected using the modelling dataset was discarded since the stress variables were not significant when tested with the hypothesis testing dataset. Therefore only the equations corresponding to Formulations 1 and 2 were further studied, which correspond to equations 5.1 and 5.2 respectively. Statistics of fit depicted in Table 5.3 show that differences between both models were small; however, equation 5.2 presented a smaller Akaike information index and was selected. The equation indicates that the probability of mortality increased with higher stocking, higher standard deviation of diameters, longer projection intervals and lower values of mean modified light sums (Table 5.4). Probability of mortality equations fitted for *P. taeda* were:

$$P = \frac{1}{1 + e^{-(b_0 + b_1 N_1 + b_2 SD_{d_1} + b_3 Int)}} \quad (5.1)$$

where N_1 and SD_{d_1} are the number of stems per hectare and the standard deviation of diameters (in cm) respectively at the beginning of the simulation interval, and Int is the simulation interval (in MJ.m^{-2}).

and

$$P = \frac{1}{1 + e^{-(b_0 + b_1 N_1 + b_2 SD_{d_1} + b_3 Int + b_4 \bar{R}_{\theta D})}} \quad (5.2)$$

where $\bar{R}_{\theta D}$ is the monthly average of 30 years of radiation sums modified by vapour pressure deficit and water modifiers (in MJ.m^{-2})., and the rest of the variables as defined before.

For the *Eucalypt* species, it was possible to model the probability of mortality using the three strategies proposed. Formulations 1 to 3 are represented by equations 5.3 to 5.5 respectively. For the approach considering the accumulation of water stress (Formulation 3), only the moderate long-term stress variable was included since the short-term water stress variable chosen was not significant when the model including both stress-related variables was tested using the hypothesis testing dataset. The adjusted equations for *E. grandis* were:

$$P = \frac{1}{1 + e^{-(b_0 + b_1 N_1 + b_2 SD_{d_1} + b_3 Int + b_4 R_{\theta DT_1} + b_5 SWPA + b_6 \beta + b_7 \alpha_c)}} \quad (5.3)$$

where $R_{\theta DT_1}$ is the radiation sums modified by vapour pressure deficit, water balance, and temperature at the beginning of the interval, $SWPA$ is soil water potentially available (mm), β is slope (percentage), and α_c is the cosine of aspect modified by slope (see Chapter 3 for the details in the calculation of the latter).

$$P = \frac{1}{1 + e^{-(b_0 + b_1 SD_{d_1} + b_2 Int + b_3 R_{\theta DT_1} + b_4 \bar{R}_{\theta D})}} \quad (5.4)$$

where all the variables are defined as before.

$$P = \frac{1}{1 + e^{-(b_0 + b_1 SD_{d_1} + b_2 Int + b_3 R_{\theta DT_1} + b_4 L_{04})}} \quad (5.5)$$

where L_{04} is the long-term moderate accumulated water stress with a threshold = 0.4 (months), and the rest of the variables as defined before.

All three equations indicate that the probability of mortality increases with standard deviation of diameters and length of projection interval and smaller initial light sums (Table 5.3). Individually, eq. 5.3 suggests that the probability of mortality increases with increasing soil water potentially available, slope and Eastern aspects; whereas eq. 5.4 and 5.5 indicate that higher mean radiation sums and more severe long-term water stress accumulation respectively would increase the probability of mortality. Statistics of fit of equation 5.3 suggested a better fit and this equation was chosen.

For both species, differences between formulations were small.

Table 5.3 AIC, AUC, and percentage of correct predictions for the probability of mortality equations.

Species	Equation	Formulation	AIC	AUC	Correct predictions (%)
P.taeda	5.1	1	4431	0.78	75
	5.2	**2**	**4419**	**0.75**	**75**
E.grandis	**5.3**	**1**	**1676**	**0.84**	**75**
	5.4	2	1817	0.81	74
	5.5	3	1794	0.81	74

AIC: Akaike Information Criterion; AUC: Area Under the ROC Curve.

Table 5.4 Parameters of the probability of mortality equations compared.

Species	Eq	-	b_0	b_1	b_2	b_3	b_4	b_5	b_6	b_7
P.taeda	5.1	Estimate	-6.0144485	0.0052454	0.3060121	0.1676708	-	-	-	-
		SE	0.2529117	0.0002849	0.0490241	0.0082107	-	-	-	-
		p-value	<0.001	<0.001	<0.001	<0.001	-	-	-	-
	5.2	Estimate	**-4.09449**	**0.005225**	**0.359153**	**0.177518**	**-0.008156**	-	-	-
		SE	0.556856	0.000285	0.050976	0.008669	0.002135	<0.001	<0.001	<0.001
		p-value	<0.001	<0.001	<0.001	<0.001	<0.001	<0.001	<0.001	<0.001
E.grandis	**5.3**	Estimate	**-9.5267038**	**0.0023578**	**0.826633**	**0.2300163**	**-0.1112372**	**0.037175**	**0.0923128**	**0.1384784**
		SE	0.7210865	0.0002832	0.0847746	0.0176437	0.0159298	0.0042472	0.0349668	0.0404837
		p-value	<0.001	<0.001	<0.001	<0.001	<0.001	<0.001	<0.01	<0.001
	5.4	Estimate	-10.5741	0.92885	0.22363	-0.15275	0.03943	-	-	-
		SE	0.8650	0.08133	0.01704	0.01465	0.00373	-	-	-
		p-value	<0.001	<0.001	<0.001	<0.001	<0.001	-	-	-
	5.5	Estimate	-2.42929	0.96153	0.22595	-0.03273	-0.23050	-	-	-
		SE	0.22526	0.08610	0.01688	0.01585	0.02050	-	-	-
		p-value	<0.001	<0.001	<0.001	<0.05	<0.001	-	-	-

ROC curves and AUC values for the chosen equations for *P. taeda* and *E. grandis* (5.2 and 5.3 respectively) are depicted in Figure 5.1. According to the discrimination rank for AUC values cited by Hosmer *et al.* (2013), the model selected for the pine species offered acceptable discrimination whereas the one chosen for the eucalypt species provided excellent discrimination.

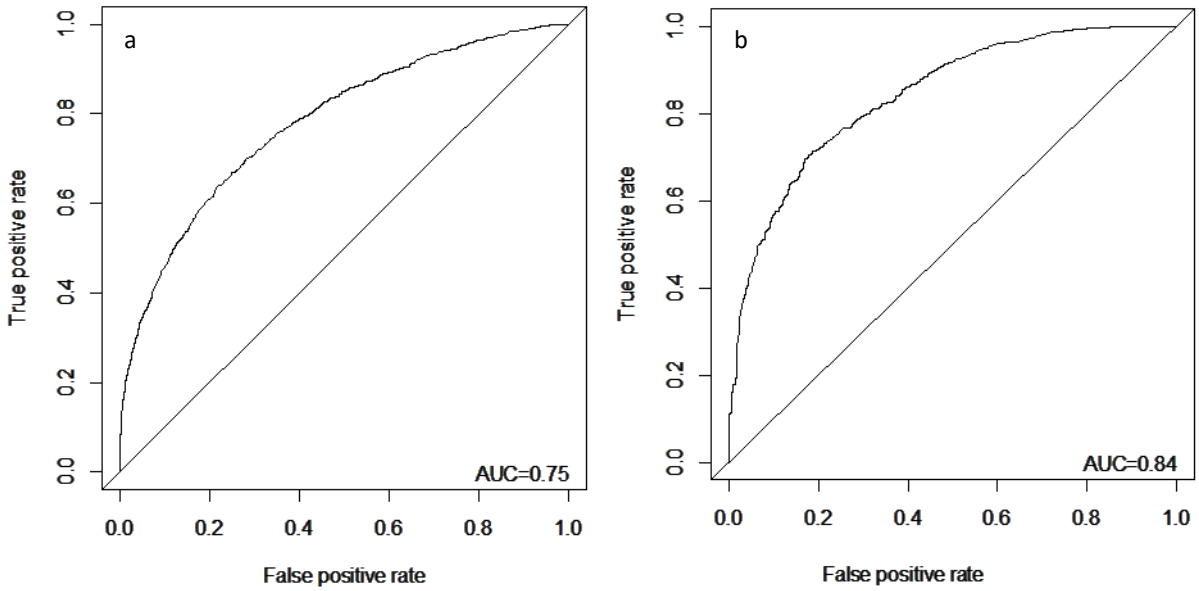

Figure 5.1 ROC curves for the probability of mortality equations chosen for (a) *P. taeda* and (b) *E. grandis*.

Mortality rate

For *Pinus taeda*, the inclusion of the 30-year monthly average term in the equation proposed by Woollons, (1998) was significant (Eq. 5.6), however the equation chosen in Chapter 3 for *Eucalyptus grandis* (Clutter *et al.*, 1983) did not show a good fit. The exponential decay anamorphic was the second best option in that study, hence it was tested showing satisfactory behaviour to be used with radiation sums. The average radiation sum term was significant when tested through the hypothesis testing dataset (Eq.5.7). The expressions for the adjusted *P. taeda* model applied was:

$$N_2 = \left\{ \frac{1}{\sqrt{N_1}} + (b_0 + b_1 \bar{R}_{\theta D}) \left[\left(\frac{R_{\theta DT_2}}{100} \right)^2 - \left(\frac{R_{\theta DT_1}}{100} \right)^2 \right] \right\}^{-2} \tag{5.6}$$

where N_1 is the number of stems per hectare at the beginning of the simulation interval, and, $\bar{R}_{\theta D}$ is the monthly average of 30 years of radiation sums modified by vapour pressure deficit and water modifiers (in MJ.m^{-2})., and $R_{\theta DT_1}$ and $R_{\theta DT_2}$ are the radiation sums modified by vapour pressure deficit, water balance, and temperature at the beginning and end of the simulation of the interval respectively.

The expressions for the adjusted *E. grandis* model applied was:

$$N_2 = N_1 e^{-(b_1 \bar{R}_{\theta D})(R_{\theta DT_2} - R_{\theta DT_1})} \tag{5.7}$$

where all the variables are as defined before.

Statistics of fit and parameters of the mortality rate equations adjusted for each species are shown in Tables 5.5 and 5.6, while the residual analysis is shown in Figure 5.2. Residual distributions against predicted and independent variables were satisfactory for both species.

Table 5.5 Statistics of fit of the equations chosen for modelling mortality rate.

Species	Equation	*RMSE*	*MR*	*MAB*	*EF*
P.taeda	5.6	92	-7	70	0.54
E.grandis	5.7	92	-9	64	0.92

RMSE: root mean square error; MAB: mean absolute bias; EF: efficiency

Table 5.6 Parameters of the equations selected for mortality rate.

Sp.	Eq.	-	$\boldsymbol{b_0}$	$\boldsymbol{b_1}$
P. taeda	5.6	Estimate	0.3673939	-0.0011964
		SE	0.0467603	0.0001774
		p-value	<0.001	<0.001
E. grandis	5.7	Estimate	-	-0.00005309
		SE	-	2.611e-06
		p-value	-	<0.001

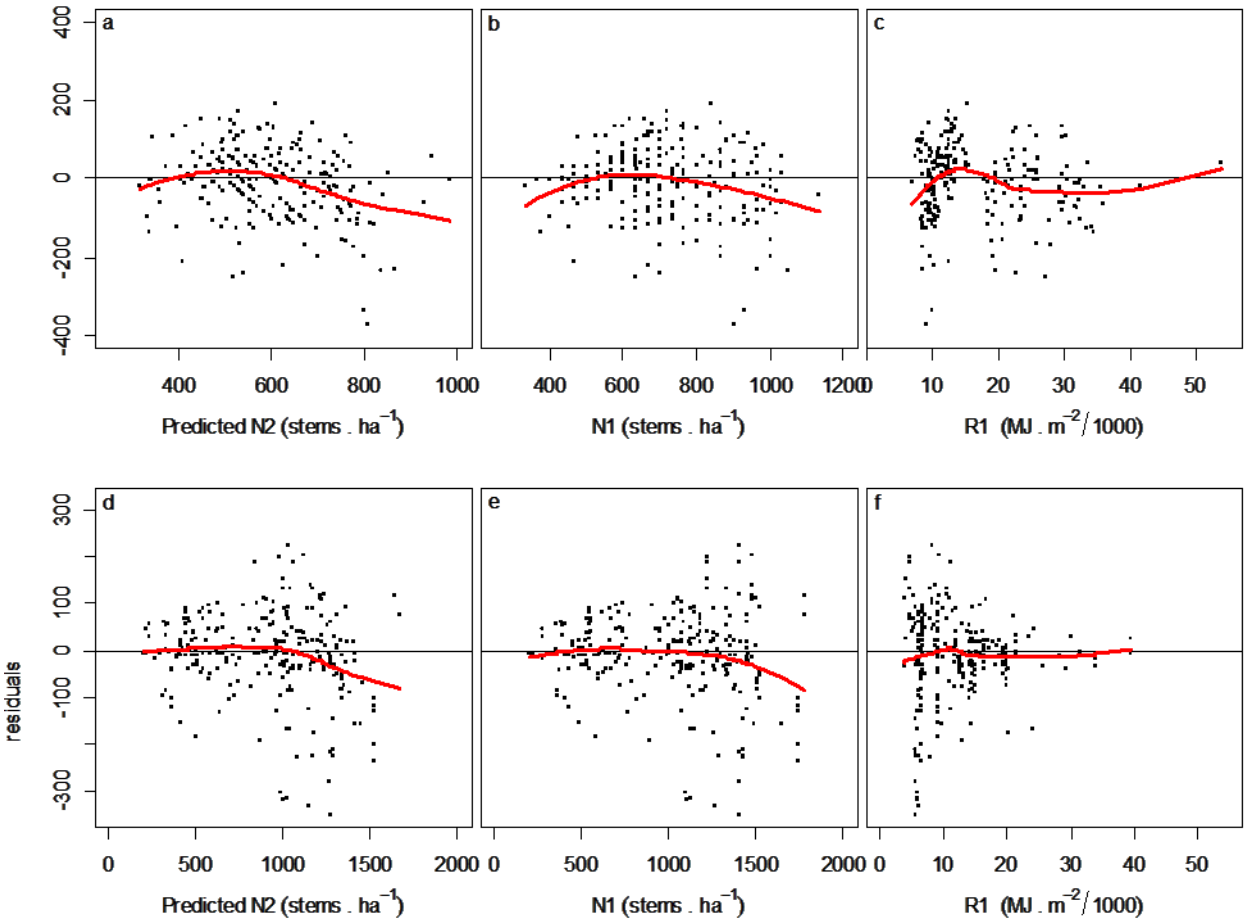

Figure 5.2 Residuals of the selected equation for *P. taeda* (a, b, and c) and *E. grandis* (d, e, and f), including lowess line (red).

Tests of the behaviour of mortality rate according to changes in $\bar{R}_{\theta D}$ showed opposing effects between species; for *Pinus taeda* higher $\bar{R}_{\theta D}$ raised the asymptote whereas for *Eucalyptus grandis* the asymptote was depressed when increasing $\bar{R}_{\theta D}$ (Figure 5.3). This means that while for the pine species the more favourable conditions the lower the mortality rate, for *E. grandis* the mortality rate increases with more favourable growth conditions.

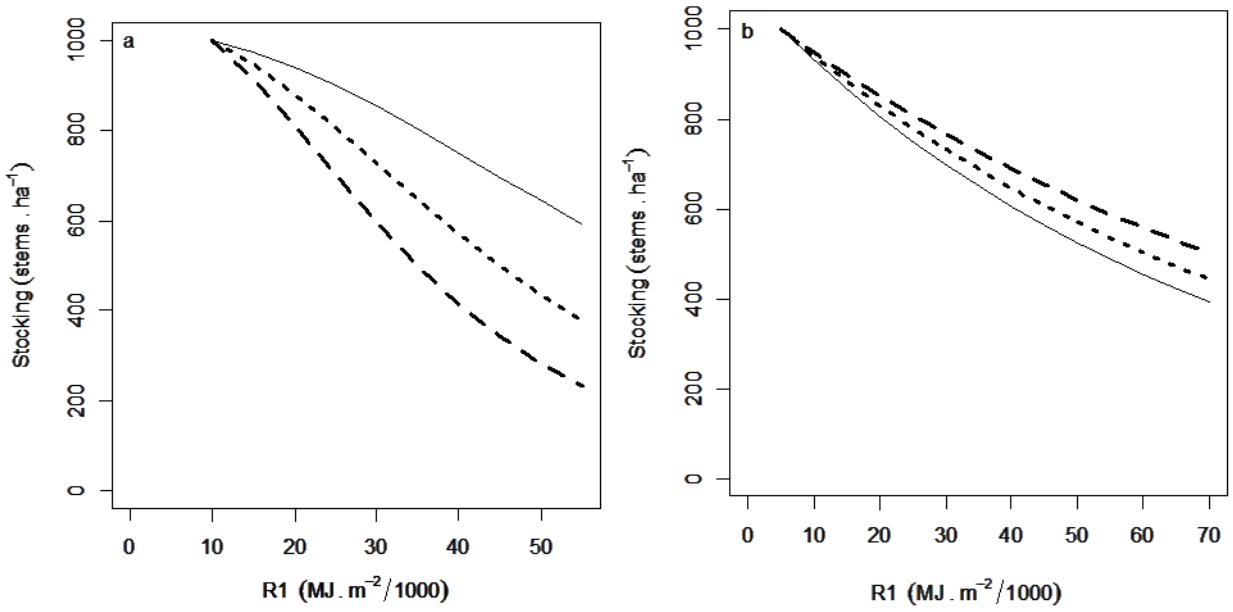

Figure 5.3 Stocking curves for *Pinus taeda* (a) and *Eucalyptus grandis* (b) applying minimum (dashed), average (dotted), and maximum (solid) values of $\bar{R}_{\theta D}$ calculated for each species. Those values for *P. taeda* are 210, 250, and 280 MJ.m^{-2}; whereas for *E. grandis*: 200, 235, and 270 MJ.m^{-2} respectively.

Validation of the selected set of equations

Validation for both species was undertaken combining the two-step procedure using the probability equation chosen for each species first and the mortality rate model in the second step for checking the performance of the system with independent data. Residuals plots showed acceptable performance of the models adjusted for predicting mortality based on radiation sums for *P. taeda* (Figure 5.4) and for *E. grandis* (Figure 5.5). Also, log-log plots of stocking versus mean squared diameter suggests that mortality models behave well and in accordance with basal area models based on radiation sums developed for each species in Chapter 4, since projected trajectories indicate vigorous growth within the full stocking zone and mortality in the increasing competition zone just before the self- thinning line. Moreover, the behaviour shows congruence beyond the maximum age modelled (25 years).

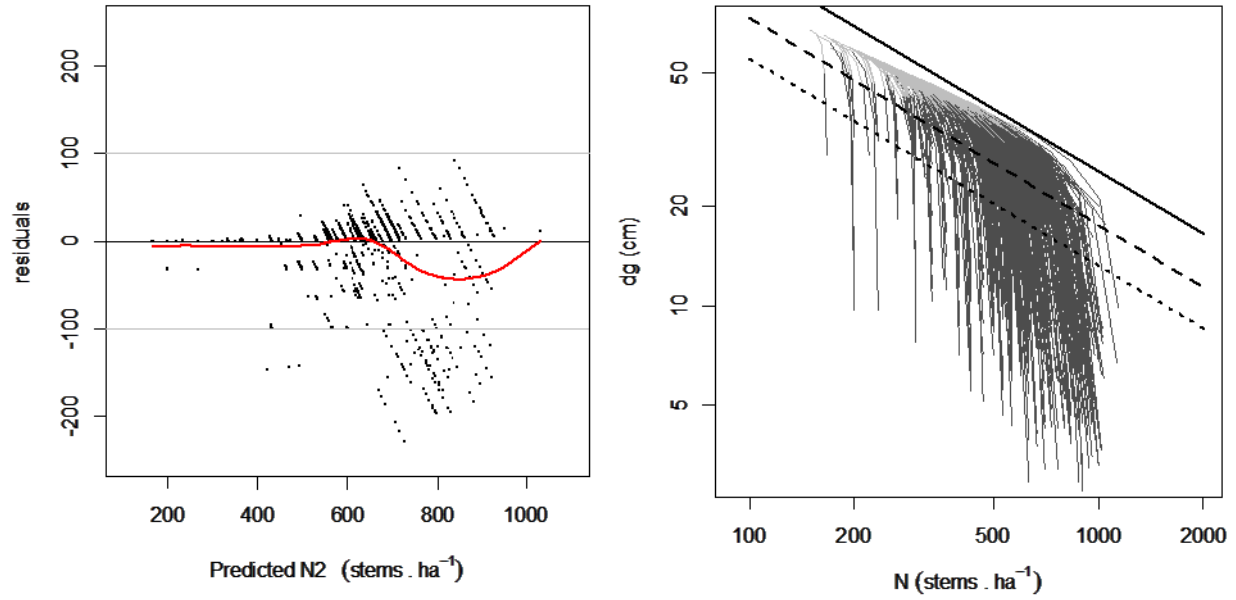

Figure 5.4 Residuals using the validation dataset for *P. taeda* with lowess line (red), and log-log plots of projected stocking vs quadratic mean diameter trajectories younger than 25 years (dark grey) and older than 25 years (light grey) including increased competition and self-thinning lines. The self-thinning line has a slope of -1.605 (Reineke, 1933), whereas the increasing competition and the fully stocked lines are set to 35% (dashed) and 55% (dotted) of the maximum Stand Density Index (SDI) as a reference.

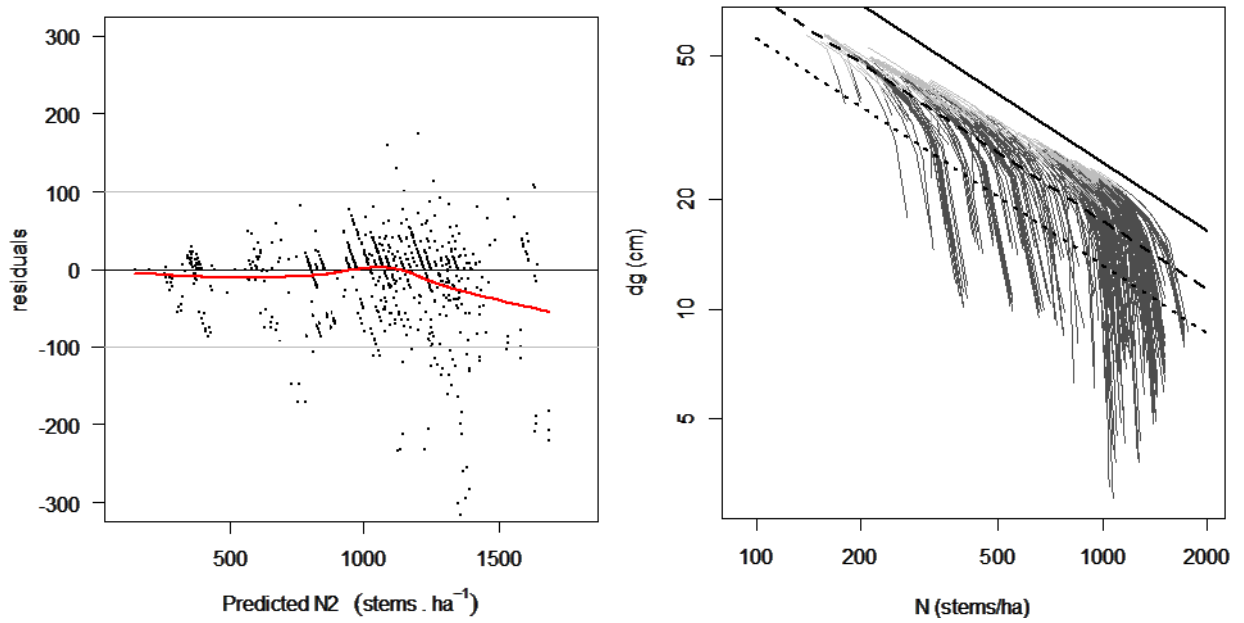

Figure 5.5 Residuals using the validation dataset for *E. grandis,* and log-log plots of projected stocking vs quadratic mean diameter trajectories younger than 20 years (dark grey) and older than 20 years (light grey) including increased competition and self-thinning lines. The self-thinning line has a slope of -1.605 (Reineke, 1933), whereas the increasing competition and the fully stocked lines are set to 35% (dashed) and 55% (dotted) of the maximum Stand Density Index (SDI) as a reference.

For *P. taeda,* the 95% confidence interval of the slope of observed vs predicted values ranged between 0.92 and 0.95, whereas the *RMSE* was 45 stems.ha^{-1}. The corresponding values for *E. grandis* were: 0.98-1.00 for the 95% confidence interval, and 57 stems.ha^{-1} for the *RMSE*.

DISCUSSION

This study was oriented towards an understanding as to whether a hybrid physiological-mensurational approach where age is replaced by light sums modified by factors representing physiological restrictions to growth (temperature, transpiration, and water available) could be applied to model mortality. Focusing on a two-step approach, the inclusion of physiological information was tested in both steps: to model the probability of mortality, and the mortality rate. Particularly, it was of interest to test whether estimations of the probability of mortality could be improved by incorporating information regarding the accumulation of water stress throughout the life of the stands.

Potentially useable radiation sums were applied with satisfactory behaviours observed with mortality equations for both species according to the validation procedure and their use can be recommended within the limits established by the modelling dataset.

Regarding the second objective of this study, results showed that increments of stress aggregation were not associated with increments of the probability of mortality for either of the species. The long term accumulated stress variable could initially be related to structural site characteristics (like shallow soils), while short term accumulated stress could be more associated with climate fluctuations and extreme drought events. Nonetheless, results showed that the incorporation of both kinds of stresses together did not predict any increase in mortality. Moreover, for *P. taeda* none of the stress-related variables were significant whereas for *E. grandis* only the long-term stress was significant and the variable using the mildest threshold provided the best fit. However, the effect of this variable on the probability of mortality was negative, showing that the longer the duration of water stress, the lower the probability of mortality (this will be discussed later). The lack of substantial association of aggregated water stress and mortality could be attributed to different causes. Initially possible issues with the formulation itself should be considered; for example regarding the use of the water modifier to be used as a stress reference. However, other studies related mortality and water stress using this relationship embedded in the 3-PG model (see Peterman *et al.*, 2013). It is also possible that the approach is sensitive to the coarse scale soil

information used in this study (i. e. a finer soil scale map would provide a better correspondence between mortality and water availability). Another issue could be that despite the fact that very low values of the soil water modifier were found in the interval used, maybe water stress episodes were not severe enough to lead to mortality, since plantations are usually located in sites where growth conditions are thought to be favourable for the species in general. This hypothesis is more suitable for *E. grandis*, than for *P. taeda* since none of the formulations that represented water limitations showed a positive relation with mortality in *E. grandis*.

The probability of mortality and mortality rate behaved logically with respect to site growth conditions for each species but were contradictory between species. For the pine species the probability of mortality tended to increase, and the asymptote of mortality rate tended to fall with poorer site conditions related to the plant water status, for the eucalypt species both mortality components showed the opposite behaviour. Moreover, all the three formulations adjusted for predicting probability of mortality for *E. grandis* showed this same tendency: characteristics stimulating growth also tended to stimulate mortality.

The fact that the models exhibited contradictory behaviours could be explained by differences with respect to water stress tolerance between species or other factors associated to competition. Because the eucalypt population comprised plots managed for pulp (with no thinnings) and managed for sawmilling (with thinnings), while the pine stands were mostly thinned, Stand Density Indices (*SDI*) were examined for each species to understand the differences in competition status of both populations. Minimum, average, and maximum SDI values were: 20, 392, and 1008 for *P. taeda*; and 35, 431, and 1107 for *E. grandis* respectively. Those values and the *SDI* distributions depicted in Figure 5.6 indicate that *E. grandis* population shows slightly higher levels of competition in general. Observing the log-log plots of projected stocking vs quadratic mean diameter trajectories (Figures 5.4 and 5.5), self-thinning in *E. grandis* starts with a smaller mean quadratic diameter compared to *P. taeda*, which indicates that the self-thinning boundary for the eucalypt could be lower than the pine and competition starts sooner. However, this should be statistically tested in order to establish more solid conclusions. The generality of the self-thinning boundary among species has been a matter of discussion. Recent evidence shows that the parameters that define this line (intercept and slope) vary from species to species, mostly due to species' particular space needs and shade tolerance (Pretzsch and Biber, 2005; Weiskittel *et al.*, 2009), where more tolerant species show steeper slope values. According to Burns and Honkala (1990) *P. taeda* is classified as intolerant to shading as an adult (but considered tolerant as a

seedling). However, Zeide (1985) remarks the difference between tolerance and self-tolerance, along with the lack of correspondence between those characteristics, and point to *P. taeda* as of intermediate self-tolerance among the Southern Pines studied. *Eucalyptus grandis* is considered very intolerant to shade and also root competition (Florence, 2004) (intolerance is very related to rapid growth and apical dominance). Eucalypts in general are also "crown-shy", being very sensitive to abrasion of buds and young leaves by other leaves and branches (Jacobs, 1955).

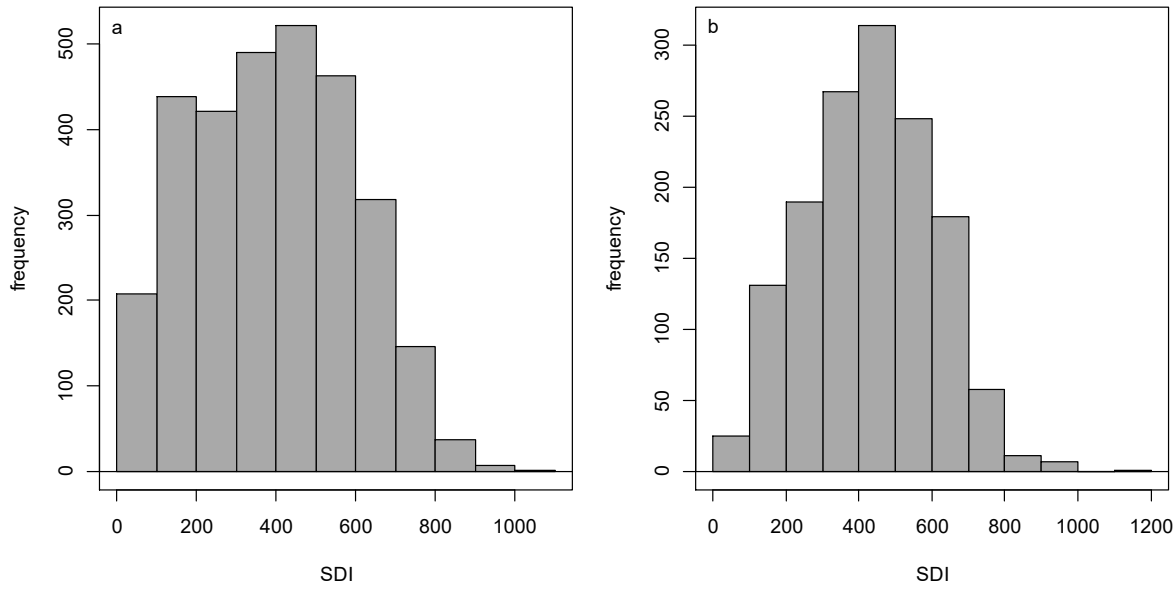

Figure 5.6 Histograms of Stand Density Index of *Pinus taeda* (a) and *Eucalyptus grandis* (b) for the two whole datasets.

Regarding water requirements, in their natural habitat both species grow under similar precipitation regimes: from 1020 to 1630 mm per year for *P. taeda* (Schultz, 1997) and 1020 to 1780 (Burns and Honkala, 1990) for *E. grandis*. Differences in tolerance between species in survival after water stress could be expected given the characteristic of eucalypts to recover from loss of functional shoots through accessory and epicormic buds, and also high growth speed in the case of *E. grandis*. Moreover, advantages of angiosperms compared to conifers regarding mechanisms to tolerate drought has been cited for Mediterranean species (Carnicer et al., 2013): for angiosperm it is expected that higher capacity to reverse embolisms, as well as maintenance of stomatal aperture during drought, and higher contents of non-structural carbohydrates (NSC), which play an important role in buffering water stress effects (see Sala *et al.*, 2012), will confer improved drought tolerance. In contrast, in a recent study, Gonzalez-Benecke *et al.* (2016) reported a new set of parameters to be used in the 3-PG model for *P. taeda*, where the adjusted value for the coefficient based in the relationship between stomatal conductance and VPD (k_g)

was 0.0408. Comparing this value with the values derived for *E. grandis* by Almeida *et al.* (2004) of 0.045 and 0.050, the eucalypt species would be slightly more sensitive to VPD, as opposed to the general tendency stated by Carnicer *et al*. (2013) for Mediterranean species. Potential differences in stomatal sensitivity to vapour pressure deficit between species were not considered in this study and the parameter k_g was kept constant for both species. This lead to a generalization of the species behaviour to changes in VPD.

Also, the powerful mechanisms of eucalypt genre to cope with water stress has been well detailed by Whitehead and Beadle, (2004). Those include: deep rooting and osmotic adjustment to maintain cell turgor, leaf structure and canopy architecture (leaves near vertical), short-lived leaves and highly dynamic leaf area index, and homeostatic manipulation according to growth conditions.

According to this evidence, sensitivity to shading and more plasticity in water stress response and resilience of *E. grandis* compared to *P. taeda* could explain the contrasting results between species observed in this study.

The approach proposed could be used to model mortality along with the growth equations developed as a function of light sums in the Chapter 4. The model provided an insight about the relationship between site characteristics and mortality for contrasting species, and could be useful to estimate mortality under a range of changing scenarios involving temperature and water availability.

CONCLUSIONS

The hybrid approach offers a valid alternative to model mortality with the advantages for forest management that the possibility of linking resource availability with competition and mortality represents.

The accumulation of water stress as formulated in this work was not found to be a factor contributing to increases in probability of mortality for managed stands of any of the species studied. However it was a factor that helped explain the probability of mortality for the eucalypt species, with a negative effect: the accumulation of mild water stress for *E. grandis* tended to decrease the probability of mortality in *E. grandis*.

For plantations in Uruguay mortality tended to increase with the lack of resources related to water in *P. taeda*, whereas for *E. grandis* mortality tended to decrease. It is hypothesized that larger resource availability increases mortality due to shading or competition factors other than water in *E. grandis*, given a potentially higher tolerance to drought episodes and resilience compared to the pine species.

CHAPTER 6

COMPARISONS OF THE MODELLING APPROACHES

INTRODUCTION

The advantages and opportunities of hybrid mensurational-physiological models for sustainable forest management have been discussed (Bartelink and Mohren, 2004; Kimmins, 1985; Landsberg, 2003; Monserud, 2003; Weiskittel *et al.*, 2011), and a variety of strategies have been used for obtaining models with desired characteristics for forest management, either by: i) aggregation of models by linking a physiological model with a mensurational model (Almeida *et al.*, 2003; Baldwin *et al.*, 2001; Pinkard and Battaglia, 2001) or linking more than two models (Peng *et al.*, 2002; Robinson and Ek, 2003); or ii) combining mensurational and physiological information in the structure of several components (Dzierzon and Mason, 2006; Henning and Burk, 2004; Mason *et al*., 2011; Montes, 2012; Snowdon *et al.*, 1999; Temps, 2005). However, very few studies compare hybrid models with other approaches at a modelling system level and a field scale. One example of this is the work presented by Pinjuv *et al.* (2006). Comparing models at this scale enables: i) better understanding of the coherence between components and consistency with co-variates; ii) comprehension of the strengths and shortcomings of models for practical uses; iii) identification of potential application risks and future improvements; iv) users to understand and choose forecasting systems according to their needs.

In previous chapters, three systems of equations for simulating stand growth and diameter distributions were developed using differential equations through three approaches:

i. Traditional time-based mensurational models that restrict independent variables to age and parameters as functions of variables for region (base approach).

ii. Augmented time based models that has parameters as linear functions of water holding capacity and physiographic variables such as elevation, aspect, and slope.
iii. Hybrid physiological-mensurational models where time was replaced by cumulative light sums since time of planting, with potential radiation use calculated by modifiers accounting for influences of temperature, vapour pressure deficit (VPD), and water balance.

The aim of this chapter is to establish a comparison between the three studied methods with respect to their suitability for predicting stand dynamics and structure, focusing on precision and bias, and the capacity to use physiographic and eco-physiological information in order to account for differences in growth rates. The analysis is oriented to understand the effectiveness of the information used by each approach as well as the utility of the information provided by models in order to manage contrasting species in Uruguay. The equations comprising each approach's set is offered in Appendix II.

METHODOLOGY

The analysis is based on five fundamental points: i) use of information; ii) assumptions and sources of error and variation; iii) precision and bias; iv) system integration, v) data requirements, difficulties for applying each methodology, and uses. Finally, a discussion of further studies is offered.

Firstly a comparison of time vs light is established, followed by a comparison between the information used by each approach for each species, and there is a discussion of the consistency of relationships between inputs and outputs across strategies.

Secondly, precision and bias of all modelled components were compared in order to understand which formulation provided the information of the highest quality. Precision was assessed through the root mean square error (*RMSE*) whereas bias was analysed through mean absolute bias (*MAB*), both statistics were calculated as shown in Chapter 2. Also, residuals against predicted variables were plotted in order to compare distributions and tendencies.

System integration analysis and comparison are used to test how well components work together but also to obtain a deeper understanding of the consequences of using constrasting approaches. These analyses were developed by assessing the competition dynamics established by each approach through log-log plots of projected stocking vs quadratic mean diameter trajectories, and

by projecting and comparing diameter distributions. For projecting diameter distributions, the reverse Weibull function was selected based on the advantages of using maximum diameter instead of minimum: it is easier to project and its predictions in managed plantations are more reliable, hence large trees of the stand are more accurately characterised (Kuru *et al.*, 1992). Moreover, maximum diameter predictions do not need to be re-adjusted after thinnings from below.

Recovering the parameters from the projected stand statistics guarantees compatibility between those and stand attributes corresponding to the distribution. In this way, the performance of the system of equations using site variables can be tested for its ability to yield accurate diameter distributions. For assessing efficacy of the system , a probability density function (pdf) that uses the simplified method of moments proposed by García, (1981) to derive the parameters for the reverse Weibull as shown by Kuru *et al.*, (1992) was analysed. The reverse Weibull computes the frequency of any diameter class as:

$$f(d) = (c/b)\left[\left(\frac{a-d}{b}\right)^{c-1}\right] e^{-\left(\frac{a-d}{b}\right)^{c}} \qquad (6.1)$$

where:

$f(d) =$ frequency of any d expected

The corresponding cumulative density function is:

$$F(d) = exp\left[-\left(\frac{a-d}{b}\right)^{c}\right] \text{ if } -\infty \leq d \leq a$$
$$F(d) = 1 \qquad \text{if } d \geq a \qquad (6.2)$$

The location, scale, and shape parameters a, b, and c respectively are given by:

$$a = d_{max} \qquad b = \frac{a-d_m}{\Gamma\left(1+\frac{1}{c}\right)} \qquad c = \frac{1}{z[1+(1-z)^2(kz_0+kz_1+kz_2+kz_3+kz_4+kz_5)]}$$

where:

$$d_m = \sqrt{{d_g}^2 - {SD_d}^2}\ , \qquad d_g = \left(\sqrt{\frac{4G}{\pi N}}\right)100\ , \qquad z = \frac{D_{de}}{(a-D_{med})}$$

The last interval measured per plot of the independent (validation) dataset was selected to project diameter distributions in order to analyse distributions near harvesting age, using diameter classes 2 cm wide. In this way, 166 and 87 plots for *P. taeda* and *E. grandis* respectively where available for validation. The number of trees per hectare in each class and the Error Index (Reynolds *et al.*, 1988) were computed for each plot using the three set of equations: with stand variables (as base models), with stand and site variables (augmented), and with potentially useable radiation sums (PULS) which represent the hybrid approach. To test for statistical differences between the groups a Kruskal-Wallis non-parametric test was conducted (Conover, 1999).

All the analyses were undertaken using the validation datasets.

RESULTS AND DISCUSSION

Use of information: differences between approaches and species

Time vs light

The substitution of time by modified radiation is the main feature of the hybrid approach assessed. As an explanatory variable, time (or age) is directly measured and can be considered free from estimation error compared to modified light sums, however it clearly provides less information. To understand the relationship between those two key variables, they were plotted as shown in Figure 6.1. For instance, for ages near reference ages of 15 and 10 for the pine and the eucalypt species respectively, radiation sums range from 39340 to 47710 MJ/m^2 for *P. taeda*, and from 19550 to 28250 MJ/m^2 for *E. grandis*. Those results show the diversity of conditions where the stands are growing, and the informative potential of the hybrid approach compared to time. It can also be observed that supressing the modifiers (regarding vapour pressure deficit, water balance, and temperature) this characteristic is almost lost. Moreover, by combining information related to growth factors, the hybrid approach allows inclusion of information that varies spatial and temporally but without interfering with the path invariance property.

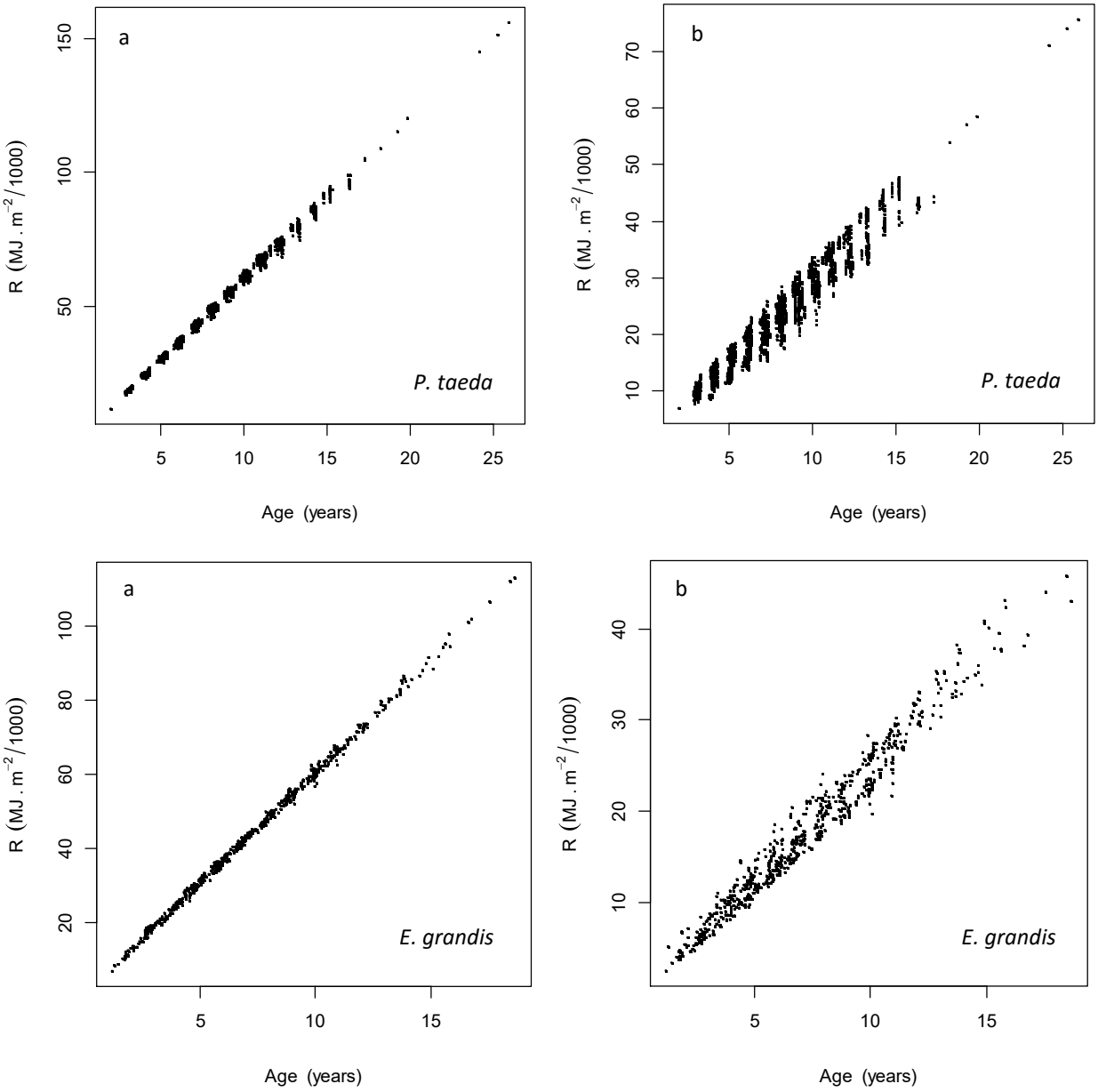

Figure 6.1 Relationship between age and accumulated light (a), and between age and accumulated light restricted by temperature, vapour pressure deficit, and water balance calculated monthly (b) for the studied species.

Information used by each modelling strategy.

A comparison of the information used in this thesis by the different components of each of the three methodologies is summarised in Table 6.1. The simplest approach uses no accessory variables (with the exception of SI for d_{max}) in the case of *P. taeda* or a dummy variable for localization in *E. grandis*. A more complex time based approach used soil and physiographic

variables such as: soil water potentially available, slope, aspect and elevation as independent variables in each component. Those variables, which are constant for a given site, are surrogates of important factors for tree growth such as available water for the roots, light, and temperature (correlations between these variables were analysed in Chapter 3).

Both the augmented and the hybrid methodology showed that water availability was a key driver for species growth in Uruguay, either by using a surrogate of water available for plants based on soil characteristics or using water balance (note that both variables are based on the same map of water holding capacity).

Slope and aspect effects usually vary among studies in the literature, since those factors operate closely related to other site characteristics such as wind and rainfall regimes, as well as soil type, fertility, latitude and elevation. The importance of aspect and slope on growth in this study was subject to species and the approach applied: for *P. taeda*, the inclusion of aspect and slope information was not significant or did not improve precision in general, whereas for *E. grandis* use of this information in the augmented formulation was more effective than accounting for aspect and slope in a light-use efficiency environment. This could be related to the fact that only the light (e.g. differences in net radiation in the several arrays of aspects and slopes of the PSP net) were considered in PULSE, whereas the use of aspect modified by slope as an explanatory variable of parameters in the augmented formulation allowed the inclusion of other effects such as temperature or soil moisture content. The hypothesis of a temperature effect would coincide with the fact that *Eucalyptus grandis* is more favoured in warmer sites (as slopes facing N and E) than the pine species, since optimum growth temperature is higher for the Eucalypt species and higher than the average temperature of the country (shown in Table 1.1). However, specific studies are needed in order to confirm whether or not there is an effect of temperature related to aspect and slope, this would need to be considered in future studies. An opposite hypothesis, is that slopes on the sample plot sites are small (0-10 degrees) and small radiation differences are not well captured by the hybrid approach. A characterization of the radiation variation as a function of slope and aspect was not undertaken in this study, but the investigation carried on by Coops *et al.* (2000) showed that variation of predicted radiation can be substantial in contrasting slopes and aspects. Coops *et al.* (2000) identified that for slopes of 15 degrees (the minimum for the study) variation in incoming solar radiation was slightly less than 100 $MJ.m^{-2}.month^{-1}$ for sites located in similar latitude of Uruguay, which gave rise to a significant variation in model outputs. However slope

average among plots used in this study was 3 degrees, therefore expected variation of solar radiation should be substantially lower.

Table 6.1 Explanatory variables used in each approach per species and component.

Component	Base		Augmented		Hybrid	
	P. taeda	*E. grandis*	*P. taeda*	*E. grandis*	*P. taeda*	*E. grandis*
h_{dom}	Age	Age, *Z7*	Age ,*SWPA, Elev*	Age, *SWPA,* α_s, α_c	R_n,θ_T, *VPD*,T_a	R_n, θ_T, *VPD*,T_a, $\bar{R}_{\theta D}$
G	Age	Age, *Z7, thinning*	Age, *SWPA, Elev,* α_c	Age, *SWPA,* β *Na/Nb)/tt*		
d_{max}	Age, *SI*	Age ,*Z7*	Age, *SWPA*	Age, *SWPA,* α_s		
SD_d	Age	Age, *Z7*	*SWPA, Elev*	Age, α_s		R_n, ,θ_T, *VPD*,T_a,
P	*N, Int,* SD_d, *G,* h_{dom}, *G.I*	Age, *Z7, N,* SD_d, *Int*	*N, Int,* SD_d, *G,* h_{dom}, *G.I*	Age, *Z7, N,* SD_d, *Int, SWPA,* β, α_s, α_c	*N, Int,* SD_d, $\bar{R}_{\theta D}$	R_n,, θ_T, *VPD*,T_a, *SWPA,* β, α_c
N_2	Age	Age, *Z7*	Age	Age, *SWPA,* β, α_s	R_n,θ_T, *VPD*,T_a, $\bar{R}_{\theta D}$	R_n, θ_T, *VPD*,T_a, $\bar{R}_{\theta D}$

Elevation was applied only in the augmented time-based equations, being significant only for dominant height and basal area for the pine species, and possible relationships of those variables with drainage rate were discussed in Chapter 3. Since elevation is not used in the radiation based approach, it will be not further discussed.

Comparisons of the use of surrogate variables vs specific variables could not be done in the present study since both groups of variables were applied to different approaches (comparison of approaches is the aim of this analysis). However, it is pointed out here that the radiation-based formulation provided more specific information of factors affecting growth than the augmented approach (e.g. water balance vs. soil water potentially available). In the latter case, the growth factor affected by the use of surrogate variables was unclear in some cases, as shown for elevation. Other studies that compared simple variables with more specific information related to eco-

physiological processes showed divergent results. Maestri (2003) found that rainfall and temperature were as good as water deficit and evapotranspiration when used as predictors of dominant height increments in *E. grandis* clones in time based formulation, whereas Snowdon *et al.* (1999) found that including photosynthesis estimations from a complex physiological model as an index in a Schumacher formulation resulted in larger error reductions than using simple rainfall information for predicting *Pinus radiata* basal area.

The species showed differences regarding the amount of information (explanatory variables) included in the components of each approach and also regarding precision gains. For *Pinus taeda*, fewer explanatory variables were significant and those were included in fewer components with smaller gains in precision for all three the approaches analyzed. This could be indicating either that other variables not tested here are more related to growth in *Pinus taeda*, or that the range of those explanatory variables are not wide enough to translate ultimately as observed differences modelled in growth rate.

Main sources of error and variation, and core assumptions

Models developed in this study were based on a PSP set comprising data from different sources and oriented mainly to wood quantification purposes, therefore information gaps were observed with respect to age coverage as well as climate, physiographic and soil variables combinations. This potential problem was studied and discussed in Chapter 3. It must also be acknowledged that the number of plots in the range of studied sites was not balanced, as usually happens with modelling datasets. Although it is important to consider these issues when applying the models, they are not major issues for comparison purposes.

In the same way, the genetic base of the stands used in this study waswide, with a fair representation of seed origins used in the country, including locally improved seeds and clonal material in the case of the eucalypt species. This contributes to the generalization capacity of the models, however adaptations of certain genotypes to particular sites can occur. Interactions between genotypes and environments were not assessed and are not contemplated in the models.

One of the main assumptions of the hybrid approach is that absorbed light is considered through a sigmoid shaped response of the state variable modelled. Although there is loss of information in light interception processes, this abstraction enables the application of a methodology that is sensitive to changes in growth conditions in cases where leaf area is not measured.

Another assumption of the hybrid methodology was that most growth differences were caused by variations in air temperature and factors related to the continuum soil-plant-atmosphere such as water balance and VPD. Other important factors such as nutrition were not studied. This was justified by our lack of understanding of the nutrient uptake process and dynamics. While nutrition is an important factor driving growth, the dominant factor in high productivity sites studied was soil water potentially available (or water holding capacity), which was linked to soil depth. For the studied areas, deepest soils are associated with higher rainfall and were also the poorest in terms of nutrients. Therefore, it is assumed that core information for differentiating growth rates at a regional level was included in the analysis.

Finally, as mentioned in Chapter 4, some climate variables were assumed to be uniform in the studied area and in the time span analysed as it was the case of wind speed. This is a common assumption considered in order to compute evapotranspiration.

Comparing precision and bias

The approaches analysed differ with respect to precision and bias and differences between species were also observed. Tables 6.2 and 6.3 show statistics of prediction (calculated using independent datasets) for both species regarding all the components required for simulating stand dynamics and diameter distributions analysed in previous chapters.

For *Pinus taeda*, the base mensurational equations in general showed the largest errors, with the exception of dominant height. For this variable the hybrid approach was less precise with a small difference (3.4%). For all the other components, the hybrid methodology was the most precise; especially for modelling net basal area and maximum diameter (precision gains were 7 and 9 % respectively). Differences in precision for predicting mortality were null between approaches (and an augmented formulation was not considered in the analysis since a physiographic variable was insignificant for the probability of mortality, and for mortality rate as described in Chapter 3). The hybrid approach was observed to provide smallest calculated bias with the exception of dominant height.

The magnitude of error improvements by modelling all the components using the hybrid approach was considerable for *Eucalyptus grandis*, and the highest improvement was over 14 % for basal area. According to the *MAB* rank, this approach was the least biased as well. For this species,

improvements of the hybrid approach with respect to the augmented were considerably larger than improvements of the augmented with respect to the base approach.

For both species and considering all the components analysed, the hybrid approach was predominantly first in the rank for precision and bias with exception of dominant height for *Pinus taeda* (rank 3).

Table 6.2 Comparisons of approaches for each component and species regarding precision. Percentage of *RMSE* gain with respect to the least precise approach is shown in brackets.

Statistic-	Component	Base		Augmented		Hybrid	
		P. taeda	*E. grandis*	*P. taeda*	*E. grandis*	*P. taeda*	*E. grandis*
RMSE	h_{dom} (m)	0.86 (2.0)	1.69 (0)	**0.85 (3.4)**	1.66 (1.8)	0.88 (0)	**1.52 (10.0)**
	G ($m^2.ha^{-1}$)	3.20 (0)	2.76 (0)	3.13 (2.5)	2.65 (4.0)	**2.98 (6.9)**	**2.38 (14.3)**
	d_{max} (cm)	2.08 (0)	2.22 (0)	2.05 (1.4)	2.18 (1.8)	**1.89 (9.1)**	**2.01 (9.5)**
	SD_d (cm)	0.47 (0)	0.56 (0)	0.46 (2.1)	0.56 (0)	**0.46 (2.1)**	**0.51 (8.9)**
	N_{2adj} ($stems.ha^{-1}$)	45 (0)	63 (0)	-	62 (1.6)	45 (0)	**57 (9.5)**
Average precision gain		0.4	0.0	1.9	1.8	**3.6**	**10.4**

Table 6.3 Comparisons of approaches for each component and species regarding *MAB*. Rank position is shown in brackets.

Stand descriptor	Base		Augmented		Hybrid	
	P. taeda	*E. grandis*	*P. taeda*	*E. grandis*	*P. taeda*	*E. grandis*
h_{dom} (m)	0.67 (2)	1.29 (3)	**0.659 (1)**	1.27 (2)	0.70 (3)	**1.17 (1)**
G ($m^2.ha^{-1}$)	2.53 (3)	2.05 (2)	2.214 (2)	2.05 (2)	**2.1 (1)**	**1.72 (1)**
d_{max} (cm)	1.52 (3)	1.58 (1)	1.49 (2)	1.55 (2)	**1.34 (1)**	**1.37 (1)**
SD_d (cm)	0.32 (2)	0.41 (2)	0.32 (2)	0.41 (3)	**0.31 (1)**	**0.38 (1)**
N_{2adj} ($stems.ha^{-1}$)	26	42 (3)	-	40 (2)	**22 (1)**	**34 (1)**

Information in Tables 6.2 and 6.3 is complemented with a comparison of residual plots with respect to the predicted variables related to growth for *Pinus taeda* (Figure 6.2) and *Eucalyptus grandis* (Figure 6.3) as well as mortality for both species (Figure 4) in order to better visualize the magnitude of differences in precision and bias between approaches.

Although, the *MAB* rank showed some differences between formulations, residual plots showed that in general, differences in bias were minimal. However, standard deviations of the diameters modelled using the hybrid approach exhibited larger bias for *E. grandis*, with a tendency to over predict large values.

In the past using hybrid approaches at the stand level produced larger gains in precision when predicting basal area than dominant height (Snowdon *et al.,* 1999; Dzierzon and Mason, 2006; Pinjuv, 2006; Mason *et al.*, 2011), and the same tendency was found in this study. However all of the known comparative studies refer to conifers, more specifically to *Pinus radiata*. In the same way it was observed that including explanatory variables has been more effective for predicting basal area than dominant height in augmented models for *Pinus radiata* (Woollons *et al.*, 1997) and *Eucalyptus grandis* (Temps, 2005). This was the case for the eucalypt species but not for *Pinus taeda*, for which the opposite tendency was observed. Nonetheless, observed differences in precision gain between basal area and dominant height with augmented models are very small.

Smaller differences in precision gain between the augmented approach and the hybrid approach are most likely related to the fact that a modifier of the asymptote was not included in *P. taeda*'s model.

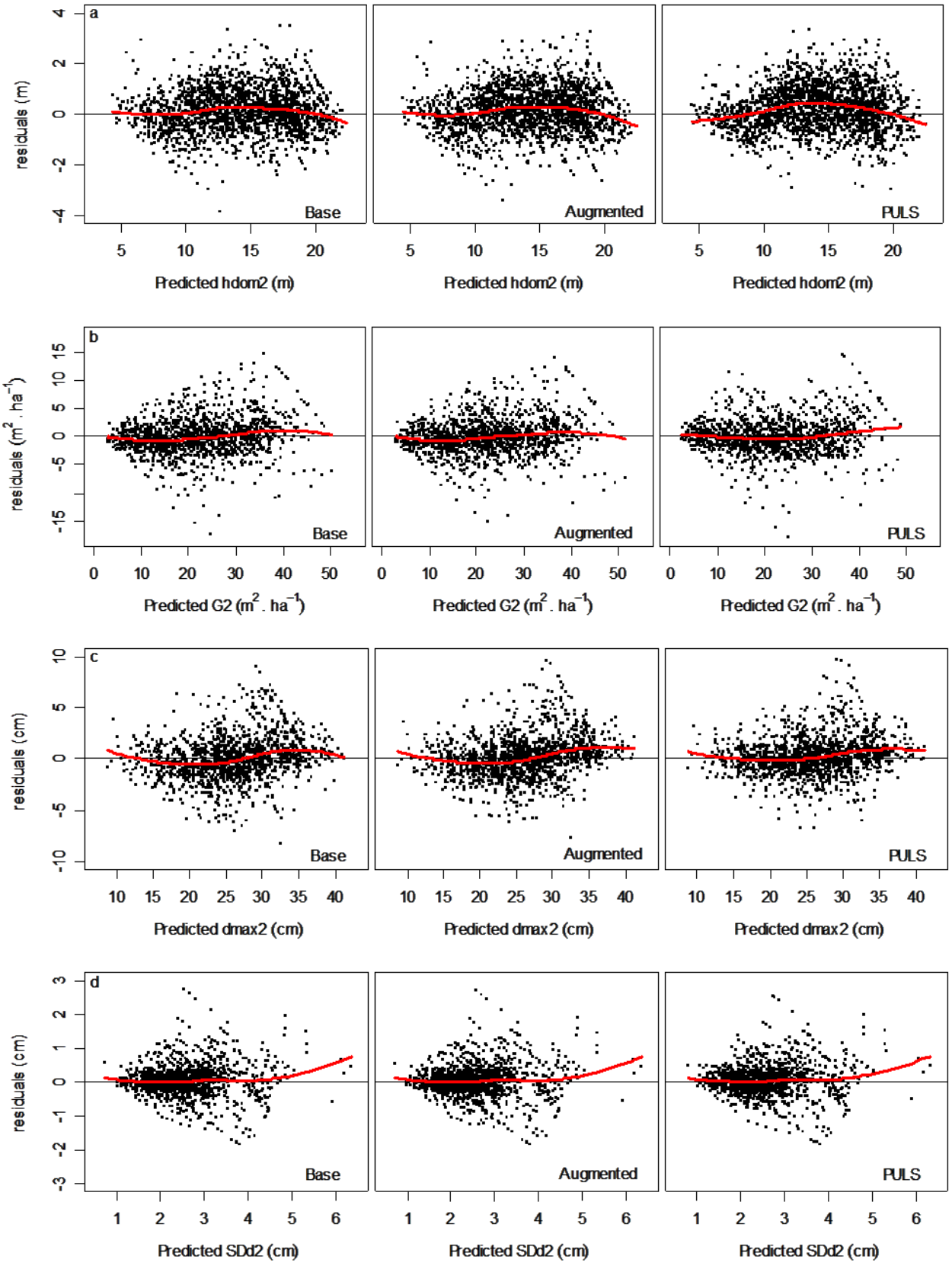

Figure 6.2 Comparison of the three approaches regarding residuals vs. predicted values for each growth component for *Pinus taeda*.

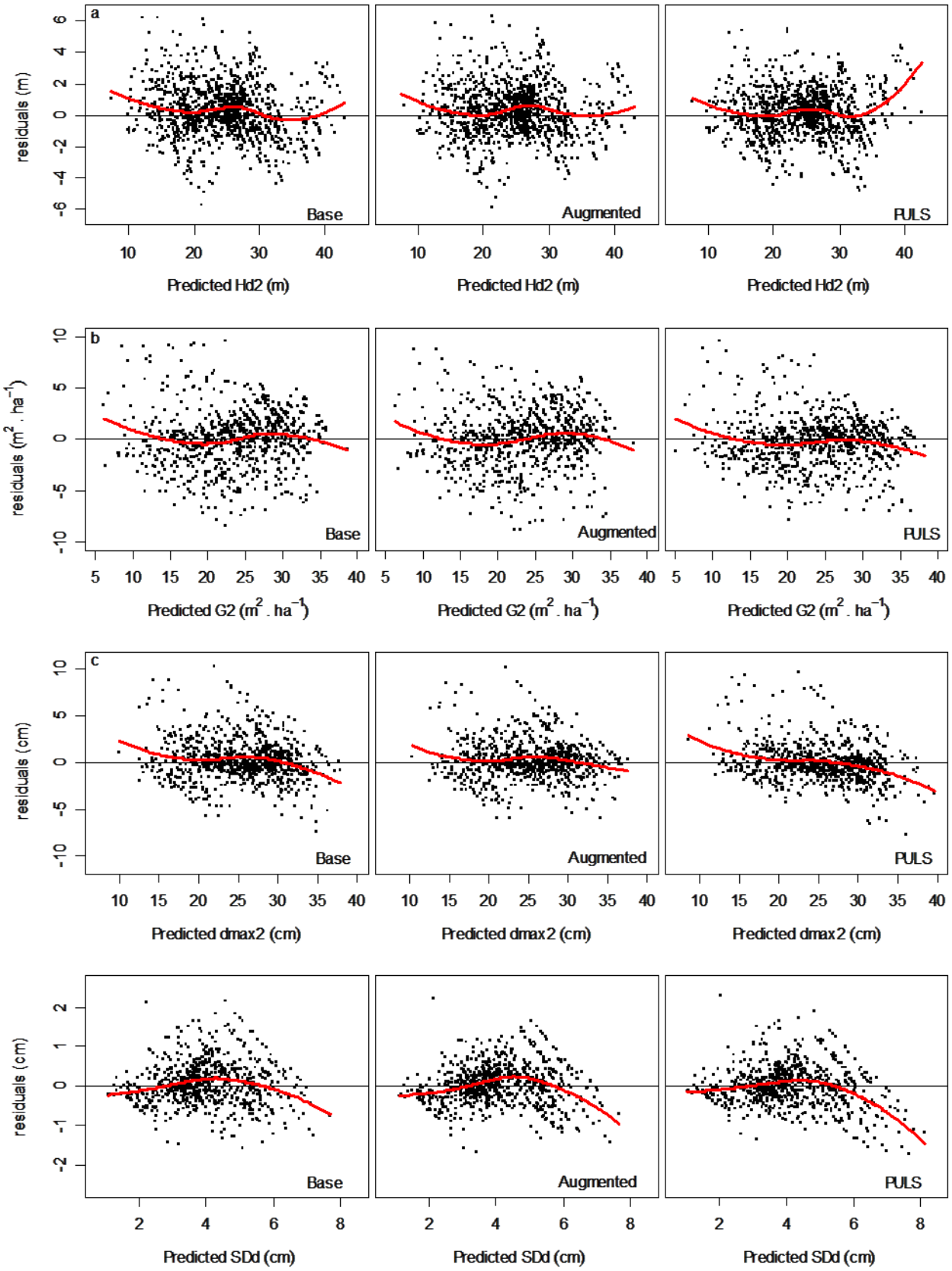

Figure 6.3 Comparison of the three approaches regarding residuals vs. predicted values for each growth component for *Eucalyptus grandis*.

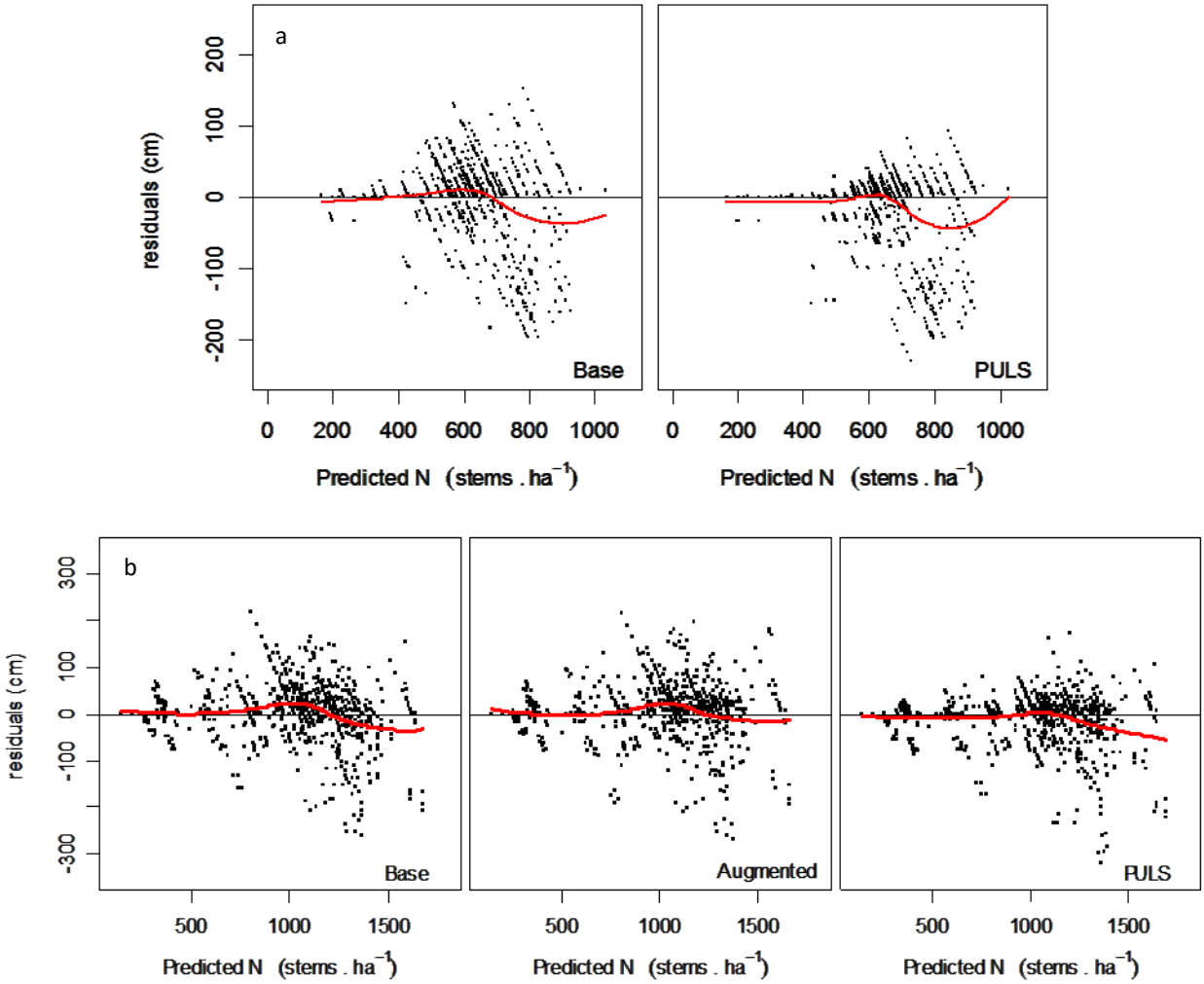

Figure 6.4 Comparison of the approaches adjusted for projecting mortality regarding residuals vs. predicted values for *P.taeda* (a) and *E.grandis* (b).

Comparisons of the behaviour of each approach with respect to prediction interval were undertaken by plotting the residuals against the interval for each variable and species for the components related to growth (Figures 6.5 and 6.6) as well as mortality (Fig.6.7). For the pine species all the components modelled using the hybrid approach showed the smallest bias with respect to interval, but underestimation would be slightly larger when predicting long intervals for base and augmented equations. It must be considered that in Figures 3.21 and 3.23 lowess lines show pessimistic estimates of bias in regions of plots where there are very few points. For *Eucalyptus grandis* results were divergent: bias of G, d_{max}, and SD_d tended to increase when projecting intervals longer than 6 years when using the hybrid equations, however not much difference was found for h_{dom}.

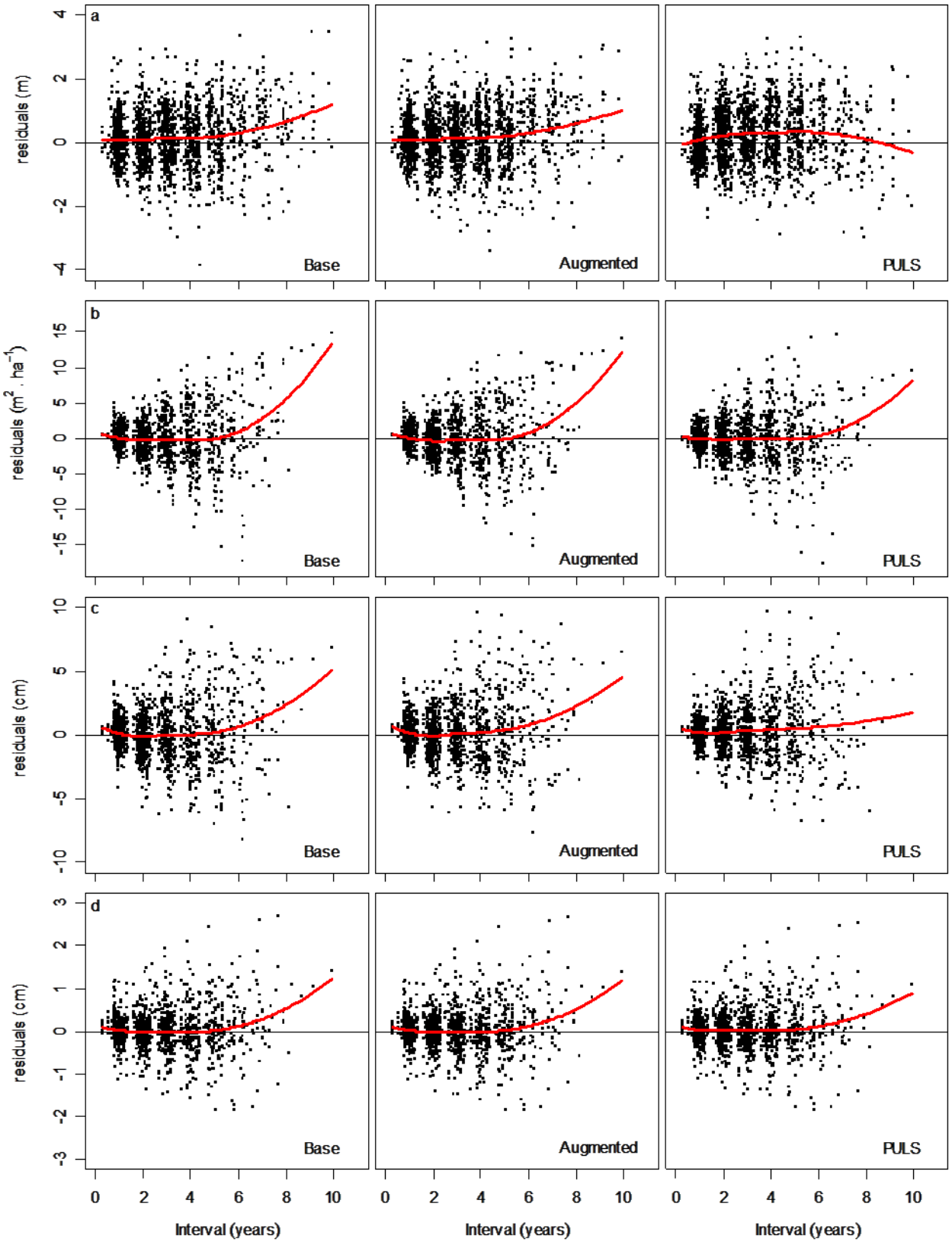

Figure 6.5 Comparison of the three approaches regarding residuals vs. projection intervals for dominant height (a), basal area (b), maximum diameter (c), and standard deviation of diameters (d) for *Pinus taeda*.

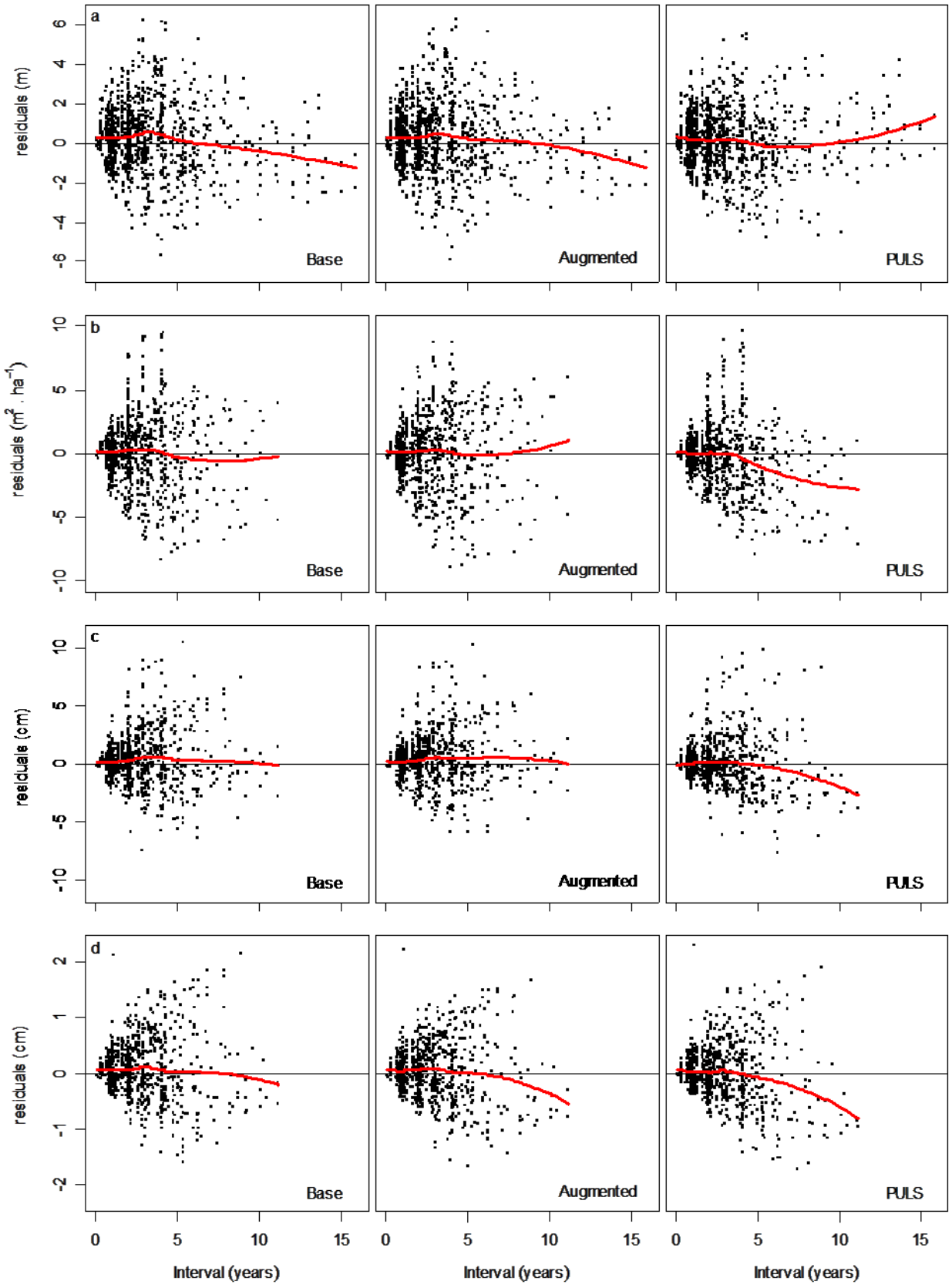

Figure 6.6 Comparison of the three approaches regarding residuals vs. projection intervals for dominant height (a), basal area (b), maximum diameter (c), and standard deviation of diameters (d) for *Eucalyptus grandis*.

For mortality, the improvement in bias when applying the hybrid approach was noticeable and consistent for both species (Fig. 6.7).

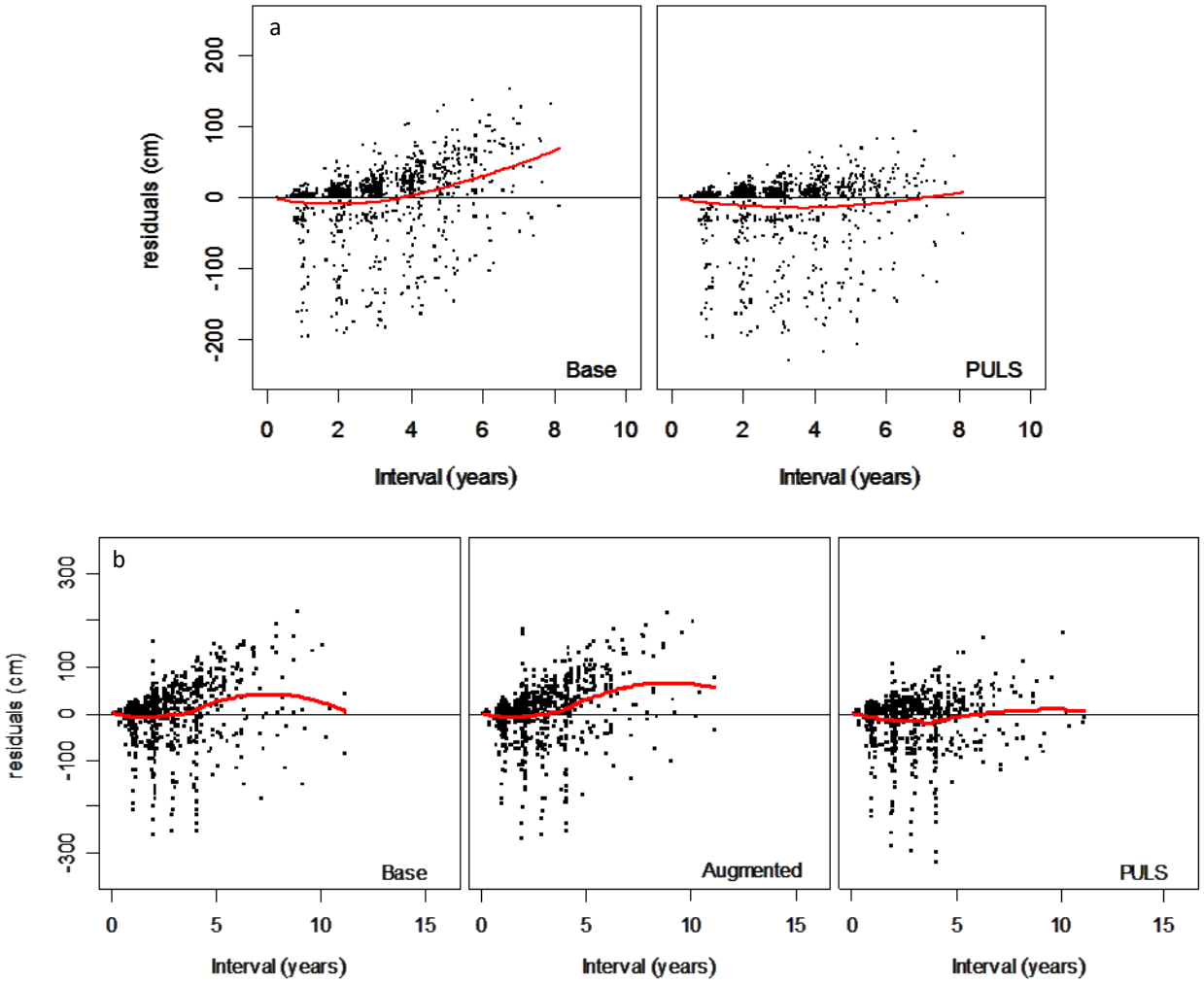

Figure 6.7 Comparison of the approaches adjusted for projecting mortality regarding residuals vs. projection intervals for *P.taeda* (a) and *E.grandis* (b).

Differences in system integration: significance on representing competition and diameter distributions

Competition dynamics

When modelling mortality, the coherence of models adjusted for projecting basal area and stocking was tested through log-log plots of projected stocking versus quadratic diameter for all the approaches analysed (see Chapter 3 and 5). Those representations show whether or not stand competition dynamics were modelled according to self-thinning relationships (Yoda *et al*., 1963). Comparisons of log-log plots of base equations vs hybrid for *P. taeda* (since an augmented option was not available), and augmented formulation and hybrid counterpart for *E. grandis* (base and augmented was very similar) are shown in Figure 6.8. The log-log plots for both species and all modelling strategies conform with the basic principles of self-thinning relationships.

As a reference, the slope of the self-thinning boundary used in this study was given by the value proposed by Reineke (1933) of -1.605 for the purposes of this study, although the line has been shown to be a curve concave down (Zeide, 2010; Charru *et al.*, 2012). Also the generality of an inter-specific self-thinning boundary line has been discussed (Weller, 1987; Zeide, 2010, 1987), and recent studies point to different values for the slope between species (Pretzsch and Biber, 2005, 2016; Weiskittel *et al*., 2009), and even within species according to stand characteristics (Weiskittel *et al.*, 2009; Zhang *et al.*, 2013). At a glance, it seems that the self-thinning line proposed by Reineke could fit *P. taeda*'s stands when base models were applied, however when using hybrid equations or for *E. grandis*, the correspondence is not so compelling. In order to count on accurate information for stand management in plantations oriented to production for sawmills, and especially for *E. grandis* growing at lower densities, self-thinning frontiers should be specifically defined for both species in Uruguay. This assessment could be done using frontier functions as shown in the studies by Bi, (2001), Weiskittel *et al.*, (2009), and Zhang *et al.* (2013).

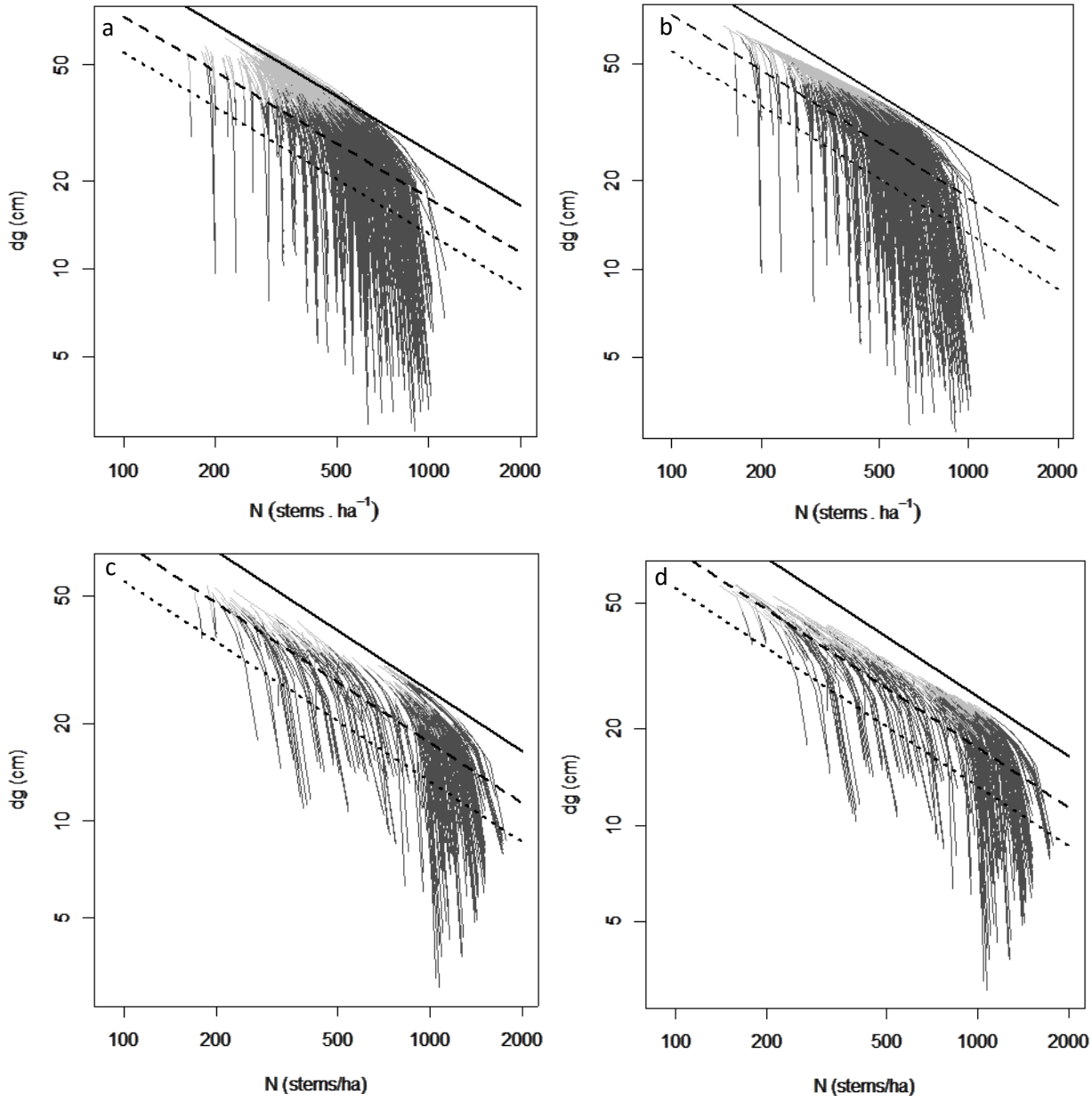

Figure 6.8 Log-log plots of projected stocking vs quadratic mean diameter trajectories for for *P. taeda*'s base (a) and hybrid (b) formulations, and *E. grandis* augmented (c), and hybrid (d) formulations. Ages younger than 20 years (dark grey) and older than 20 years (light grey) as well as self-thinning lines (solid), increasing competition (dashed), and full stocking lines (dotted) are represented. The self-thinning line has a slope of -1.605 (Reineke, 1933), whereas the increasing competition and the fully stocked lines are set to 35% (dashed) and 55% (dotted) of the maximum Stand Density Index (SDI) as a reference.

Comparing diameter distribution projections

Comparisons of diameter distributions included a projection from t_1 to t_2 or from $R_{\theta DT_1}$ to $R_{\theta DT_2}$. Therefore, diameter distributions were predicted for t_2 or $R_{\theta DT_2}$, and error indices were calculated based on the observed N_2 values. Variables projected were: h_{dom}, G, d_{max}, SD_d, P, and N_2 for *P. taeda* whereas for *E. grandis* all those variables except h_{dom} were projected. Base equations were used in the set of augmented equations when no augmented option was available, therefore, for *P. taeda* the augmented variables were h_{dom}, and G when testing the augmented approach.

Statistics of the error index (*EI*) are given in Table 6.4. Although mean values were smaller for the hybrid and base approaches for *P.taeda* and *E. grandis* respectively. A Kruskal-Wallis test revealed that there were no statistical differences between the median of the three groups analayzed (p-values were 0.9156 and 0.984 for *P.taeda* and *E.grandis* respectively).

Table 6.4 Statistics of the mean *EI* (in stems.ha^{-1}) for each approach and species.

Statistic	*P. taeda*			*E. grandis*		
	Base	Augmented	Hybrid	Base	Augmented	Hybrid
Minimum	64	66	85	93	110	78
Mean	342	337	335	327	331	330
Maximum	1026	1038	882	840	897	821
Standard deviation	174	178	158	141	140	143

A sample of diameter distributions projected in random plots suggested a reasonable representation of diameter distribution structure in the population for *P. taeda* for both short intervals (Figure 6.9) and longer intervals (Figure 6.10), applying all three methodologies. Very small differences between approaches are evident, especially in short-term projections. However, some plots have multimodal distributions, probably because of the small sizes of most of the plots, and those cannot be modelled by the inverse Weibull function, (or any other uni-modal probability density function).

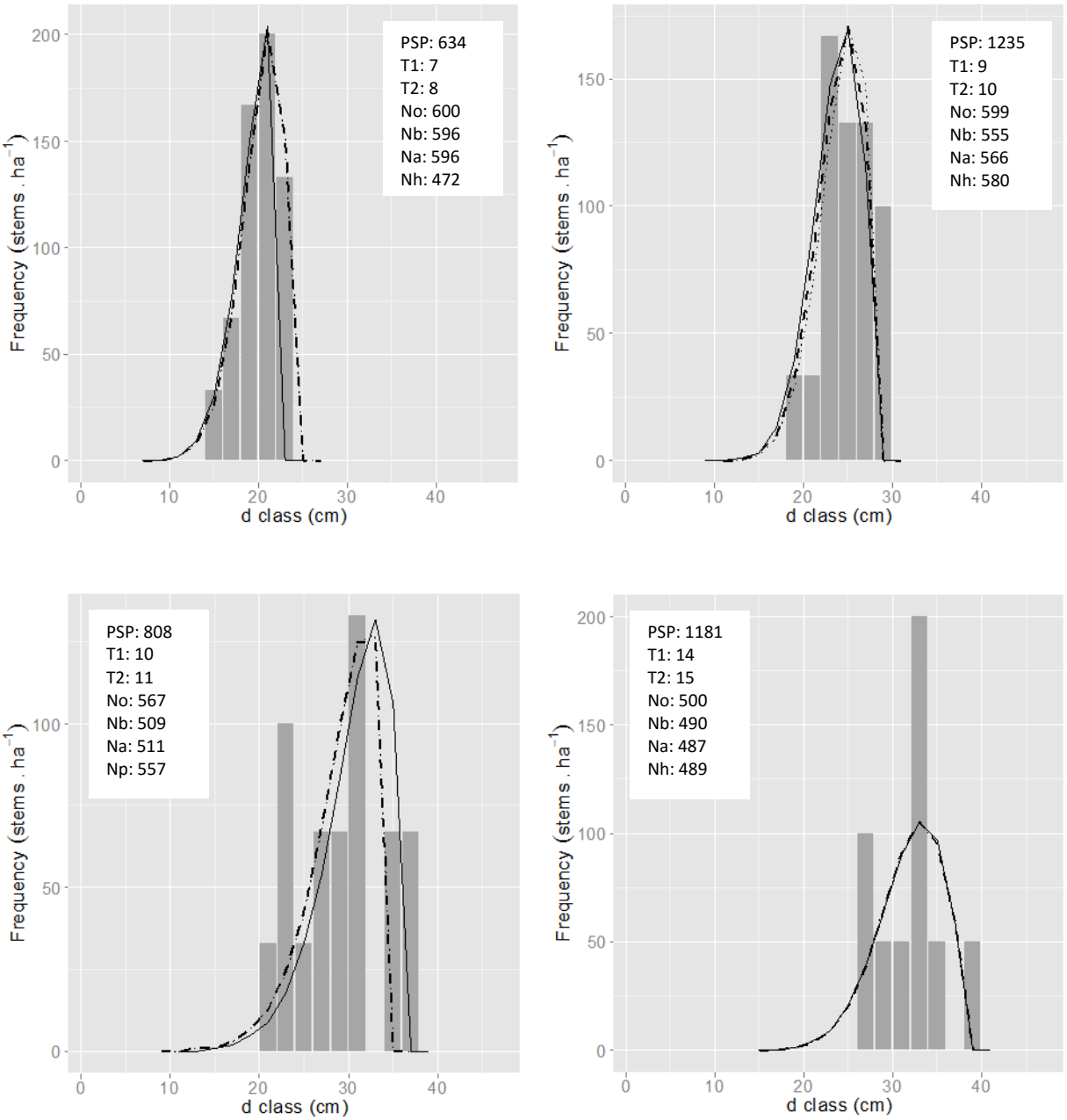

Figure 6.9 Observed (grey bars) versus projected diameter distributions using base equations (dotted), augmented (dashed), and hybrid (solid) equations applied in short intervals for *P. taeda*. Information of the total number of trees per hectare observed (No), predicted using base (Nb), augmented (Na), and hybrid equations (Nh), as well as reference values of the interval (t_1 and t_2) is included.

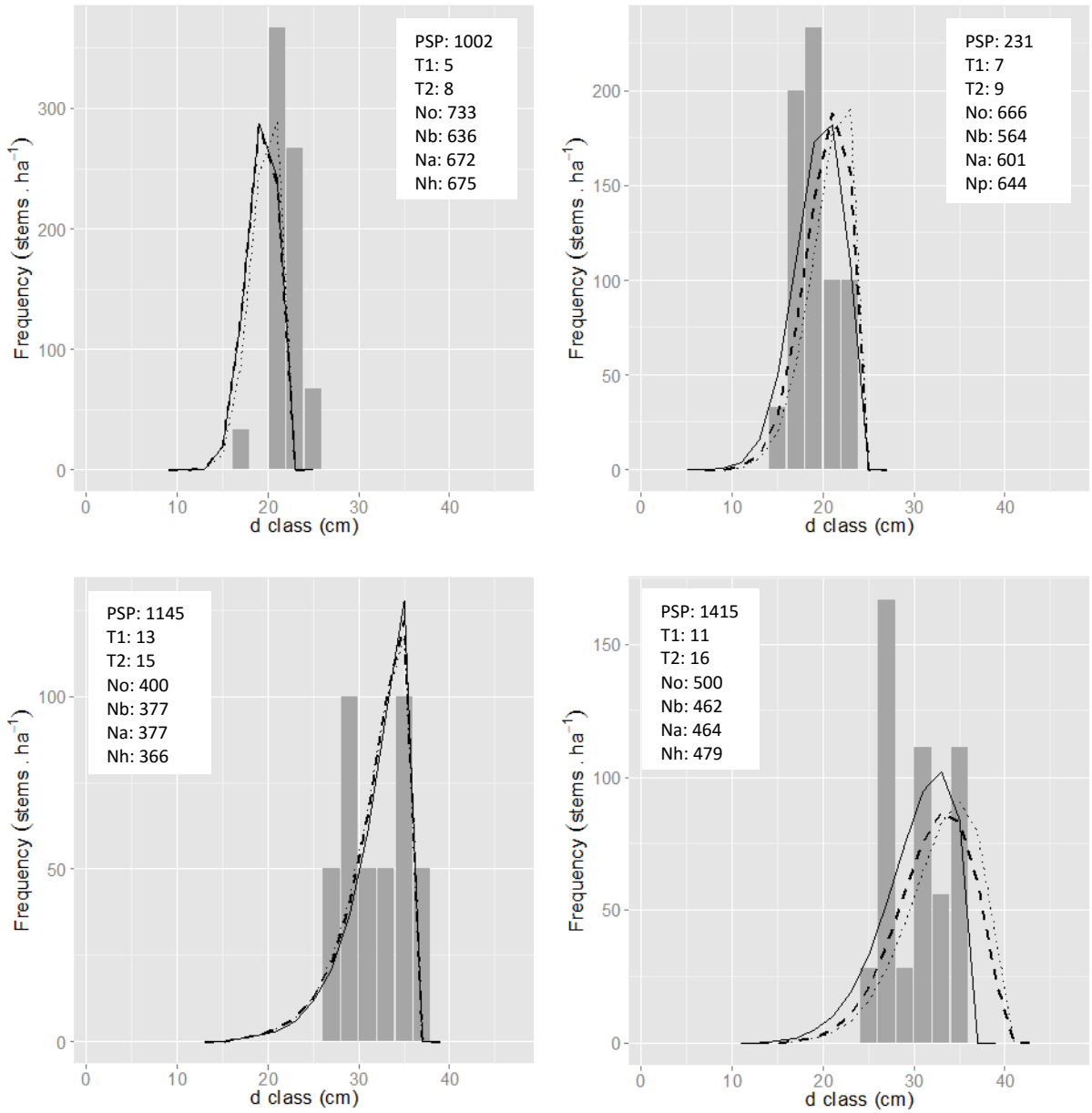

Figure 6.10 Observed (grey bars) versus projected diameter distributions using base equations (dotted), augmented (dashed), and hybrid (solid) equations applied in long intervals for *P. taeda*. Information of the total number of trees per hectare observed (No), predicted using base (Nb), augmented (Na), and hybrid equations (Nh), as well as reference values of the interval (t_1 and t_2) is included.

For *E. grandis* the projected diameter distributions also adjusted satisfactorily to observations, and differences in distributions between methodologies were also small for both short-term predictions (Fig. 6.10) and for longer intervals (Fig. 6.11).

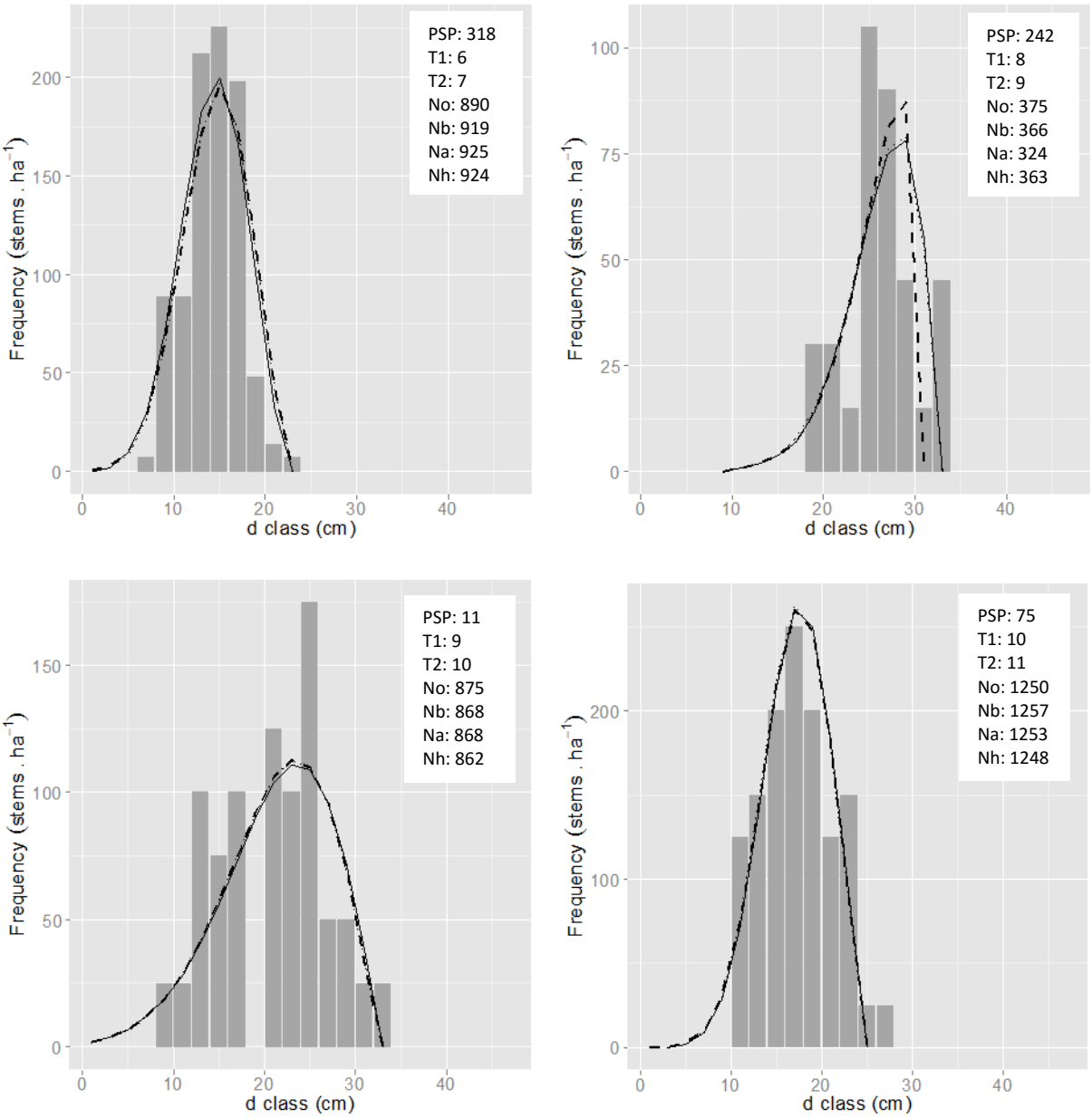

Figure 6.11 Observed (grey bars) versus projected diameter distributions using base equations (dotted), augmented (dashed), and hybrid (solid) equations applied in short intervals for *E. grandis*. Information of the total number of trees per hectare observed (No), predicted using base (Nb), augmented (Na), and hybrid equations (Nh), as well as reference values of the interval (t_1 and t_2) is included.

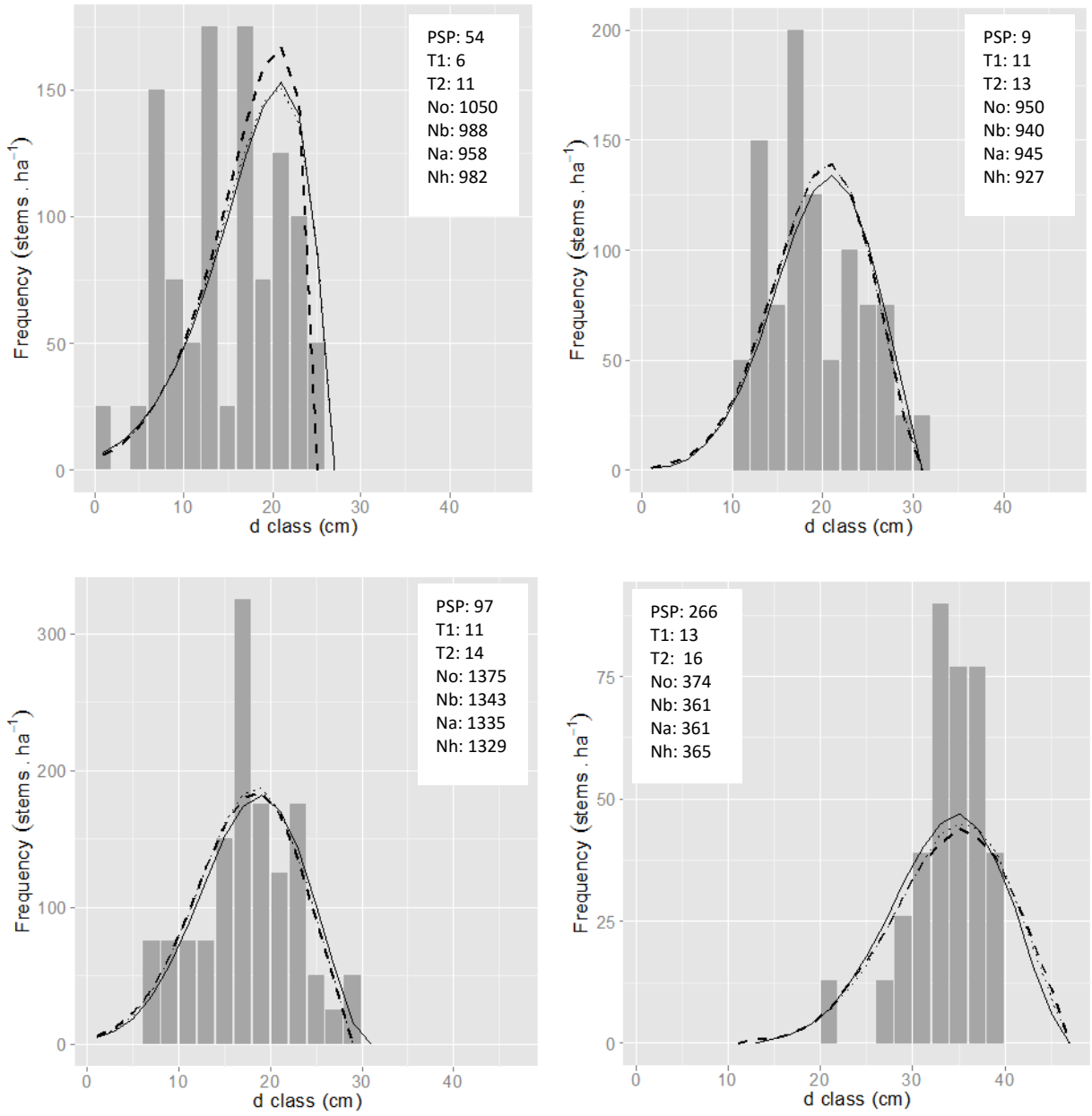

Figure 6.12 Observed (grey bars) versus projected diameter distributions using base equations (dotted), augmented (dashed), and hybrid (solid) equations applied in long intervals for *E. grandis*. Information of the total number of trees per hectare observed (No), predicted using base (Nb), augmented (Na), and hybrid equations (Nh), as well as reference values of the interval (t_1 and t_2) is included.

The fact that no differences in *EI* were detected between approaches in spite of substantial error reductions in all the variables required for projecting diameters in the hybrid approach applied to *E. grandis*, may be indicative of a large amount of error involved in projecting diameter distributions. As mentioned before, multimodal distributions could also be a source of interference for testing differences in precision for diameter distributions. For projecting distributions using the

inverse Weibull probability density function based on a parameter recovery method, the advantage of precision corresponding to the light-based models was lost.

The influence of site variables on diameter distribution accuracy has been seldom assessed, and when studied a parameter estimation method for the probability density function was utilized instead of parameter recovery. This was the case of the investigation carried on by Russell *et al*., (2012) where gains in accuracy between 1.8 to 6% in the error index were observed by including latitude and longitude information to Weibull parameter prediction for *P. taeda*. Sanquetta *et al.*, (2014) studied the correlation between the parameters (symmetry and kurtosis) of the 2-parameter Weibull distribution and climate and soil variables, finding a strong correlation between both parameters and climatic variables such as rainfall and solar radiation. The authors concluded that rainfall can be used to predict both parameters in black wattle with a positive effect of rainfall in the frequency of larger diameters.

Although there is no advantage in diameter distributions accuracy, the use of site variables can increase the capacity to explain variation in diameter distributions of stands located in diverse sites, as well as establish comparisons of sensitivity to physiographic variables between both species. Further analysis would include the testing of how diameter distributions change in contrasting environments and explore the full possibilities that this new approach can offer.

Data requirements, difficulties for applying each methodology, and uses

All the approaches studied require the same information regarding tree characteristics, however augmented and light-based methodologies need georeferenced PSP's, digital terrain models, and information about water holding capacity of soils. For PULS approach additional climate information such as radiation, rainfall, and temperature is required besides the eco-physiological parameters of the species of interest. Hence, complexity for users increases from the base approach tested here to the radiation-based formulation and this represents a disadvantage for applying the latter. However soil and physiographic information used in this analysis is free and readily available in Uruguay, so that the augmented equations could be applied fairly easily. On the other hand, historic series of climate information is not available on a public basis, which means that the use of PULS equations would pose a larger challenge with respect to the other approaches. However, real time climate variables, and water balance estimations as well as averages of historical climate data are readily available. Moreover, free access digital climate surfaces (e.g.

Bioclim) could also be utilized, but a validation of the equations applied with the use of this information should be undertaken.

Beyond potential difficulties regarding information required, the application of each methodology would depend on the goal of projections; users seeking exclusively to project diameter distributions for assessing potential products would most probably adopt the simple base approach. However, when assessing management practices or choosing plantation sites, the radiation based approach would allow testing of scenarios that are not feasible for time-based formulations. Examples of the new possibilities that those type of models allow have been presented by Mason *et al.* (2007) when testing seedling response to weed control, and also simulating growth types in response to site preparation (Mason, 2013). By introducing concepts of light use efficiency and information at a temporal scale of higher resolution than traditional inventory information, the approach offers an option to assess situations where site resources are subjected to changes through site preparation, weed control or fertilisation. In this sense, "what if" types of analyses involving temperature changes, light or water competition (including irrigation) could be performed. Moreover, light based equations offer the possibility to assess within year growth changes (Mason *et al.*, 2011).

CONCLUSIONS

Augmented and hybrid approaches showed water availability was a major factor accounting for differences in productivity for both species in Uruguay.

Slope and aspect improved predictions when applied to the augmented approach, but not for accounting for differences in radiation using the hybrid approach, which could be indicating that factors other than light are responding to slope and aspect resulting in the observed differential in growth rates.

The least precise formulation was the mensurational approach for most of the components for both species, but it was not the most biased.

The most precise approach varied slightly with species and components. For *P. taeda* the hybrid model was the most precise for basal area and maximum diameter with noticeable differences, but not for standard deviations of the diameters and mortality, and was the least precise (with a small

difference) for predicting dominant height. For *E. grandis* the hybrid approach was considerably more precise for all model components including mortality.

No substantial differences in bias with respect to predicted values between approaches were found for both species. Nonetheless, the hybrid approach showed a small tendency to over-predict basal area, maximum diameter, and standard deviation for large intervals. On the other hand, this methodology showed consistently less bias for predicting mortality over large intervals for both species.

All the modelling strategies analysed showed acceptable self-thinning relationships.

Although the methodology based on light sums was more precise in general, this improvement was not reflected in the accuracy of diameter distribution projections (not even for the eucalypt species which had important improvements for basal area and mortality). This was possibly due to the existence of multimodal plots and the high uncertainty inherent in site specific diameter distributions. Overall, all the approaches proved to have acceptable behaviour.

The three methodologies can be applied for managing stands in Uruguay, however the hybrid approach offers higher precision, especially for *E. grandis*, and utility since includes the modulation of temperature and water on growth. However, it has a cost of higher complexity.

CHAPTER 7

SYNTHESIS OF KEY FINDINGS

The goal of this study was to understand how increasing levels information incorporated into stand-level growth models can improve the outputs of forecasting systems in order to better meet forest management demands for precision, ease to use, and sensitivity to environmental factors. Increasing information levels were represented by different methodologies: simple mensurational models, mensurational models augmented with physiographic and soil water variables, and a hybrid model based on cumulative modified light sums and eco-physiological information. Those were applied to two contrasting species: *P. taeda* and *E. grandis*. It was also an aim of this work to provide updated tools for managing plantations in Uruguay. This synthesis presents the main findings, its implications on management and future research directions.

Taper and volume equations

Taper and volume equations were adjusted to accompany the growth and yield models developed in this work, or to be applied independently for plantation management. They can also be used for research, as was the case of the parameterization of the 3-PG for *P. taeda* (Gonzalez-Benecke *et al*. 2016) where results of this study were used.

Clutter *et al.* (1983) and Schumacher and Hall (1933) equations gave the best performances for predicting volume for *Pinus taeda* and *Eucalyptus grandis* respectively. For modelling taper, variable exponent equations (eq. 2.15) gave the best performance for predicting diameter at height with the lowest prediction errors, offering better estimates especially for larger trees (diameters between 35 and 50cm). Although the compatible taper equation ranked in intermediate positions, differences in bias and precision with the equation 2.15 were relatively small, therefore the compatible taper equation can be recommended for its inclusion in forecasting systems and use in inventory estimations.

Improvements of those equations would include broadening of tree size ranges, especially diameters larger than 45cm, and better descriptions of the butt log of *P.taeda* with additional measures at 0.6 to 0.7m heights (White, 1971).

Insights of growth conditions, and information to be used for modelling growth and mortality in Uruguay

The use of aspect and slope information in growth and mortality models has not been explored much so far, and the present study analysed the utility of this information in traditional mensurational models as well as in the hybrid approach.

The studied species showed differences in the number of explanatory variables included in the components of each approach and also with respect to precision gains. For the fast-growing *Eucalyptus grandis*, more explanatory variables were included and this produced larger error improvements than for *P. taeda*. For instance, soil-based and physiographic information (in augmented models) was significant for improving predictions of all the variables fitted for *E. grandis*: h_{dom}, G, d_{max}, SD_d, probability of mortality and number of dead trees, however those explanatory variables were significant only for h_{dom} and G for *P. taeda*. This could indicate either that other variables not tested here were more related to growth in the pine species, or that the range of those explanatory variables are not wide enough to translate into statistically different growth rates.

Specific information tended to be more useful than surrogate information: the augmented and hybrid approaches both indicated that water was a major factor accounting for differences in productivity for both species. For example, aspect weighted by slope (α_s and α_c) was consistent through most of *E. grandis* equations, whereas for *P. taeda* it significantly influenced only net basal area. Similarly, elevation was consistently significant for *P. taeda* with a positive effect on dominant height and net basal area growth. Research should be undertaken in order to understand the factor correlated with elevation that directly influences growth. It is hypothesized that waterlogging could be directly responsible for those differences, and those effects could be considered to improve either the hybrid or the augmented equations.

Although slopes in the PSPs were small, aspect modified by slope improved predictions when applied to the augmented approach in *E. grandis*, but did not account for differences in modified radiation sums using the hybrid approach. This could indicate that factors other than light were

influenced by those variables and caused differential growth rates, and it was hypothesized that temperature would be the main candidate. Another possible reason is that the hybrid approach methodology loses sensitivity in flatter terrains.

Accumulation of stress periods, as formulated in this study, were not related to an increase in the probability of mortality, and several possible causes related to the formulation itself, quality of soil information, as well as the severity of water stress episodes were hypothesised as reasons for this.

For *P. taeda*, resource availability increased growth of all the components and decreased mortality. For *E. grandis,* higher levels of resources increased growth of H_{dom}, d_{max}, G and SD_d , as well as the probability of mortality occurrence and the number of dead trees, whereas mild water stress (specifically defined) decreased the probability of mortality. It is hypothesized that larger resource availability increased mortality due to shading or competition factors other than water in *E. grandis*, given a potentially higher tolerance to drought episodes and resilience compared to the pine species.

The accumulation of water stress as formulated in this work was not found to be a factor increasing the probability of mortality for managed stands of any of the species studied. However it was a factor that helped explain the probability of mortality for the eucalypt species, with a negative effect: the accumulation of mild water stress tended to decrease the probability of mortality in *E. grandis*.

Adequacy of the studied approaches to model stands dynamics and structure

This study has demonstrated that forecasting systems based on potentially useable radiation sums (PULS) can be applied to project growth and mortality of contrasting species. Comparative advantages with respect to time-based systems using different levels of information were assessed.

For *E. grandis* the hybrid approach was considerably more precise for all the components including mortality, for *P. taeda* the hybrid model was the most precise for basal area and maximum diameter with noticeable differences, but produced no differences in precision for standard deviations of the diameters and mortality, and was the least precise (with a small difference) for predicting dominant height. The observed variation in model precision gain is most probably related to differences in the inclusion of explanatory variables in the asymptotes.

The least precise formulation was the mensurational approach for most of the components for both species, but it was not the most biased. This approach can be utilized either when the objective is solely to project diameter distributions, or for estimating growth and yield when information about site characteristics is limited.

No substantial differences in bias of predicted diameter distribution values between approaches were found. Nonetheless, the hybrid approach showed a small tendency to over-predict basal area, maximum diameter, and standard deviation for large intervals but showed consistently less bias for predicting mortality over large intervals for both species. Application of potentially useable radiation sums for predicting the variables needed to project diameter distributions (d_{max} and SD_d), as well as for modelling mortality had not been assessed so far.

For all the approaches, the joint dynamics of basal area and stocking showed good agreement with Reineke's (1933) self-thinning relationship, indicating the equations were sound from a stand dynamic viewpoint.

While the methodology based on light sums was more precise in general, this improvement was not reflected in the accuracy of diameter distribution projections and all three approaches proved to have acceptable behaviour. This was possibly due to the existence of diameter distributions. Because of this, no differences between models should be expected when computing individual tree volume implicitly, nonetheless, future investigations should be oriented to explore possible differences in accuracy between approaches of estimations when using explicit volume models.

The hybrid approach allows prediction of growth as a function of radiation, and specific growth modifiers such as temperature, vapour pressure deficit, and water balance. Other important factors such as nutrition were not included in the formulation due to our lack of understanding of the nutrient uptake process and dynamics. However results leaded to the conclusion that core information for differentiating growth rates at a regional level was included in the analysis since for the studied areas, deepest soils (associated with higher rainfall) are the poorest in terms of nutrients and the most productive.

PULSE enables the application of a methodology that is sensitive to changes in growth conditions, as tested through effect diagrams in a range of temperature and rainfall combinations, and applied using inventory information where leaf area is not measured. This offers new approaches to forest management with respect to mensurational models, such as:

i) Assessing the effect of factors such as climate change or irrigation on growth and mortality;
ii) Assessing the consequences of applying silvicultural treatments related to site preparation, establishment, thinning or pruning;
iii) Analyzing possible effects of changing growth factors on the structure of stands;
iv) Undertaking within year analysis and gaining temporal resolution;
v) Classification of sites according to limiting factors.

Some shortcomings of this methodology are:

i) The light based approach would rely on averages of climatic temporal series when applied by the public for projecting future scenarios, therefore validation and further testing of the model using average climate variables is prudent. However, the approach could be applied using historical climate data.
ii) Care must be taken when using a combination of extreme values of physiographic variables since information gaps for extreme values were found in the dataset used for this study. Because information was very scarce for mature stands of *P. taeda*, care must be also taken when performing projections beyond 16 years.

The hybrid equations developed in this study are based on a monthly resolution, whereas soil water availability is based on 1:1.000.000 maps and aspect and slope in 30 x 30m grids. However, the formulation could be applied to any resolution, offering great potential to assess within-stand growth variation by improving soil depth and soil water available maps, and improve precision of forest management practices.

REFERENCES

Abal, G., D'Angelo, M., Cataldo, J., Gutiérrez, A., 2010. Estimación de la irradiacioón solar global diaria promedio en el Uruguay. Presented at the VIII Encuentro de Especialistas en Energía, Potencia, Instrumentación y Medidas, Montevideo, Uruguay.

Albaugh, T. J., Allen, H. L., Dougherty, P. M., Kress, L. W., King, J.S., 1998. Leaf area and above- and belowground growth responses of *Loblolly Pine* to nutrient and water additions. Forest Science 44, 317–328.

Albaugh, T. J., Allen, H. L., Dougherty, P. M., Johnsen, K. H., 2004. Long term growth responses of loblolly pine to optimal nutrient and water resource availability. Forest Ecology and Management 192, 3–19.

Alegria, C., Tomé, M., 2011. A set of models for individual tree merchantable volume prediction for *Pinus pinaster* Aiton in central inland of Portugal. European Journal of Forest Research 130, 871–879.

Allen, H. L., Albaugh, T. J., 1999. Ecophysiological basis for plantation production: a loblolly pine case study. Bosque 20, 3–8.

Almeida, A.C., Landsberg, J. J., 2003. Evaluating methods of estimating global radiation and vapor pressure deficit using a dense network of automatic weather stations in coastal Brazil. Agricultural and Forest Meteorology 118, 237–250.

Almeida, A.C., Landsberg, J. J., Sands, P.J., 2004. Parameterisation of 3-PG model for fast-growing Eucalyptus grandis plantations. Forest Ecology and Management 193, 179–195.

Almeida, A. C., Maestri, R., Landsberg, J. J., Scolforo, J. R. S., 2003. Linking process-based and empirical forest models in Eucalyptus plantations in Brazil, in: Modelling Forest Systems. CABI Publishing, UK, pp. 401.

Almeida, A. C., Soares, J. V., Landsberg, J. J., Rezende, G. D., 2007. Growth and water balance of Eucalyptus grandis hybrid plantations in Brazil during a rotation for pulp production. Forest Ecology and Management 251, 10–21.

Amaro, A., Reed, D., Tomé, M., Themido, I., 1998. Modeling dominant height growth: Eucalyptus plantations in Portugal. Forest Science 44, 37–46.

Amateis, R.L., Burkhart, H.E., Walsh, T.A., 1989. Diameter increment and survival equations for loblollypine trees growing in thinned and unthinned plantations on cutover, site-prepared lands. Southern Journal of Applied Forestry 13, 170–174.

Antos, J. A., Parish, R., Nigh, G. D., 2008. Growth patterns prior to mortality of mature Abies lasiocarpa in old-growth subalpine forests of southern British Columbia. Forest Ecology and Management 255, 1568–1574.

Avila, O. B., Burkhart, H. E., 1992. Modeling survival of loblolly pine trees in thinned and unthinned plantations. Canadian Journal of Forest Research 22, 1878–1882.

Bailey, R. L., Borders, B. E., Ware, K. D., Jones, E. P., 1985. A compatible model relating slash pine plantation survival todensity, age, site index, and type and intensity of thinning. Forest Science 31, 180–189.

Bailey, R.L., Clutter, J.L., 1974. Base-age invariant polymorphic site curves. Forest Science 20, 155–159.

Bailey, R.L., Dell, T.R., 1973. Quantifying diameter distributions with the Weibull function. Forest Science 19, 97–104.

Baldwin, V.C., Burkhart, H.E., Westfall, J.A., Peterson, K.D., 2001. Linking growth and yield and process models to estimate impact of environmental changes on growth of loblolly pine. Forest Science 47, 77–82.

Bartelink, H.H., Mohren, G.M.J., 2004. Modelling at the interface between scientific knowledge and management issues. Towards the sustainable use of Europe's forests. Forest Ecosystem and Landscape Research: Scientific Challenges and Opportunities 49, 21–30.

Battaglia, M., Sands, P., 1997. Modelling Site Productivity of Eucalyptus globulus in Response to Climatic and Site Factors. Functional Plant Biology. 24, 831–850.

Battaglia, M., Sands, P., White, D., Mummery, D., 2004. CABALA: a linked carbon, water and nitrogen model of forest growth for silvicultural decision support. Forest Ecology and Management 193, 251–282.

Biging, G. S., 1984. Taper equations for second-growth mixed conifers of Northern California. Forest Science 30, 1103–1117.

Bi, H., 2001. The self-thinning surface. Forest Science 47, 361–370.

Bi, H., Long, Y., 2001. Flexible taper equation for site-specific management of *Pinus radiata* in New South Wales, Australia. Forest Ecology and Management 148, 79–91.

Binkley, D., Stape, J. L., Bauerle, W.L., Ryan, M. G., 2010. Explaining growth of individual trees: Light interception and efficiency of light use by Eucalyptus at four sites in Brazil. Forest Ecology and Management 259, 1704–1713.

Bown, H.E., Mason, E.G., Watt, M.S., Clinton, P.W., 2013. A potential nutritional modifier for predicting primary productivity of Pinus radiata in New Zealand using a simplified radiation-use efficiency model. Cienc. E Investig. Agrar. 40, 361–374.

Brooks, J.R., Jiang, L., Clark, A., 2007. Compatible stem taper, volume, and weight equations for young longleaf pine plantations in Southwest Georgia. Southern Journal of Applied Forestry 31, 187–191.

Brooks, J. R., Jiang, L., Ozçelik, R., 2008. Compatible stem volume and taper equations for Brutian pine, Cedar of Lebanon, and Cilicica fir in Turkey. Forest Ecology and Management 256, 147–151.

Bruce, D., Curtis, R.O., Vancoevering, C., 1968. Development of a system of taper and volume tables for Red Alder. Forest Science 14, 339–350.

Bugmann, H., Bontemps, J.-D., Tomé, M., Palahi, M., 2010. Trends in modeling to address forest management and environmental challenges in Europe. Introduction. Forest Systems 19, 3-7.

Burkhart, H.E., Tomé, M., 2012. Modeling forest trees and stands. Springer.p 457.

Burns, R.M., Honkala, B.H., 1990. Silvics of North America: 1. Conifers; 2. Hardwoods, Agriculture Handbook 654. Forest Service, Washington D. C. pp 675.

Cao, Q.V., Burkhart, H.E., Max, T.A., 1980. Evaluation of two methods for cubic-volume prediction of loblolly pine to any merchantable limit. Forest Science 26, 71–80.

Carnicer, J., Barbeta, A., Sperlich, D., Coll, M., Peñuelas, J., 2013. Contrasting trait syndromes in angiosperms and conifers are associated with different responses of tree growth to temperature on a large scale. Front Plant Sci 4. doi:10.3389/fpls.2013.00409

Castaño, J.P., Giménez, A., Ceroni, M., Furest, J., Aunchayna, 2011. Caracterización agroclimátcia del Uruguay 1980-2009 (Serie Técnica No. 193). INIA, Montevideo, Uruguay. pp 34.

Charru, M., Seynave, I., Morneau, F., Rivoire, M., Bontemps, J.-D., 2012. Significant differences and curvilinearity in the self-thinning relationships of 11 temperate tree species assessed from forest inventory data. Annals of Forest Science 69, 195–205.

Clutter, J.L., 1963. Compatible growth and yield models for loblolly pine. Forest Science 9, 354–370.

Clutter, J.L., Fortson, J.C., Pienaar, L.V., Brister, G.H., Bailey R.L., 1983. Timber management: a quantitative approach., 1st ed. John Wiley & Sons, USA. pp 333.

Coble, D., Marshall, J., 2002. Aspect differences in above- and belowground carbon allocation: a Montana case-study. Environmental Pollution 116, Supplement 1, S149–S155.

Coble, D.W., Milner, K.S., Marshall, J.D., 2001. Above- and below-ground production of trees and other vegetation on contrasting aspects in western Montana: a case study. Forest Ecology and Management 142, 231–241.

Conover, W.J., 1999. Practical nonparametric statistics, 3rd ed, Wiley series in probability and statistics. New York. pp. 584.

Cook, R.D., Weisberg, S., 2009. Appliedregression including computing and graphics. John Wiley & Sons. pp 693.

Coops, N.C., Waring, R.H., Landsberg, J.J., 1998. Assessing forest productivity in Australia and New Zealand using a physiologically-based model driven with averaged monthly weather data and satellite-derived estimates of canopy photosynthetic capacity. Forest Ecology and Management 104, 113–127.

Coops, N.C., Waring, R.H., Moncrieff, J.B., 2000. Estimating mean monthly incident solar radiation on horizontal and inclined slopes from mean monthly temperatures extremes. International Journal of Biometeorology 44, 204–211.

Crecente-Campo, F., Marshall, P., Rodríguez-Soalleiro, R., 2009. Modeling non-catastrophic individual-tree mortality for Pinus radiata plantations in northwestern Spain. Forest Ecology and Management 257, 1542–1550.

Das, A.J., Battles, J.J., Stephenson, N.L., van Mantgem, P.J., 2007. The relationship between tree growth patterns and likelihood of mortality: a study of two tree species in the Sierra Nevada. Canadian Journal of Forest Research. 37, 580–597.

Demaerschalk, J.P., 1972. Converting volume equations to compatible taper equations. Forest Science 18, 241–245.

Demaerschalk, J.P., 1971. Taper equations can be converted to volume equations and point sampling factors. The Forestry Chronicle 47, 352–354.

Diéguez-Aranda, U., González, J.G.Á., Anta, M.B., Alboreca, A.R., 2005. Site quality equations for *Pinus sylvestris* L. plantations in Galicia (northwestern Spain). Annals of Forest Science 62, 10.

Durán, A., García-Préchac, F., 2007. Suelos del Uruguay: origen, clasificación, manejo y conservación., 2nd ed. Hemisferio Sur, Montevideo, Uruguay. pp 358.

Dzierzon, H., Mason, E.G., 2006. Towards a nationwide growth and yield model for radiata pine plantations in New Zealand. Canadian Journal of Forest Research 36, 2533–2543.

Eid, T., Tuhus, E., 2001. Models for individual tree mortality in Norway. Forest Ecology and Management 154, 69–84.

Erbs, D.G., Klein, S.A., Duffie, J.A., 1982. Estimation of the diffuse radiation fraction for hourly, daily and monthly-average global radiation. Solar Energy 28, 293–302.

ESRI, 2013. ArcGis for Desktop. Environmental Systems Research Institute, Inc.

Fang, Z., Borders, B.E., Bailey, R.L., 1999. Compatible volume-taper models for loblolly and slash pine based on a system with segmented stems form factors. Forest Science 46, 1–12.

Figueiredo-Filho, A., Borders, B.E., Hitch, K.L., 1996. Taper equations for *Pinus taeda* plantations in Southern Brazil. Forest Ecology and Management 83, 39–46.

Florence, R.G., 2004. Ecology and Silviculture of Eucalypt Forests. Csiro Publishing. pp 413.

Fontes, L., Bontemps, J.-D., Bugmann, H., Van Oijen, M.A., Gracia, C., Kramer, K., Lindner, M., Rötzer, T., Skovsgaard, J.P., 2010. Models for supporting forest management in a changing environment. Forest Systems 19, 8–29.

Fontes, L., Tomé, M., Thompson, F., Yeomans, A., Luis, J.S., Savill, P., 2003. Modelling the Douglas-fir (Pseudotsuga menziesii (Mirb.) Franco) site index from site factors in Portugal. Forestry 76, 491–507.

Ford, C.R., Goranson, C.E., Mitchell, R.J., Will, R.E., Teskey, R.O., 2004. Diurnal and seasonal variability in the radial distribution of sap flow: predicting total stem flow in Pinus taeda trees. Tree Physiol. 24, 951–960.

Gándara, J., Viega, L., Ross, S., Munka, C., Bentancourt, O., 2014. Variación estacional del estado hídrico y crecimiento de *Pinus taeda* L. bajo diferente manejo silvícola en el norte de Uruguay. Agrociencia 18, 1–11.

García, O., 1998. Estimating top height with variable plot sizes. Canadian Journal of Forest Research 28, 1509–1517.

García, O., 1994. The state-space approach in growth modelling. Canadian Journal of Forest Research 24, 1894–1903.

García, O., 1984. New class of growth models for even-aged stands: Pinus radiata in golden downs forest. New Zealand Journal of Forestry Science 14, 65–88.

Garcia, O., 1983. A Stochastic Differential Equation Model for the Height Growth of Forest Stands. Biometrics 39, 1059–1072.

García, O., 1981. Simplified method-of-moments estimation for the Weibull distribution. New Zealand Journal of Forestry Science 11, 304–306.

Gonzalez-Benecke, C.A., Teskey, R.O., Martin, T.A., Jokela, E.J., Fox, T.R., Kane, M.B., Noormets, A., 2016. Regional validation and improved parameterization of the 3-PG model for Pinus taeda stands. Forest Ecology and Management 361, 237–256.

Gordon, A., 1983. Comparisosns of compatible polynomial taper equations. New Zealand Journal of Forestry Science 13, 146–155.

Goulding, C.J., 1979. Validation of growth models used in forest managament. New Zealand Journal of Forestry 24, 108–124.

Goulding, C.J., Murray, J.C., 1976. Polynomial taper equations that are compatible with tree volume equations. New Zealand Journal of Forestry Science 5, 313–322.

Groom, J.D., Hann, D.W., Temesgen, H., 2012. Evaluation of mixed-effects models for predicting Douglas-fir mortality. Forest Ecology and Management 276, 139–145.

Grosenbaugh, L.R., 1965. Generalization and reparameterization of some sigmoid and other nonlinear functions. Biometrics 21, 708–714.

Harrington, R.A., Fownes, J.H., 1995. Radiation interception and growth of planted and coppice stands of four fast-growing tropical trees. Journal of Applied Ecology 32, 1–8.

Hartkamp, A.D., De Beurs, K., Stein, A., White, J.W., 1999. Interpolation techniques for climate variables (No. 99-01), NRG-GIS Series. CIMMYT, Mexico. p 26.

Hawkes, C., 2000. Woody plant mortality algorithms: description, problems and progress. Ecological Modelling 126, 225–248.

Hebert, M.T., Jack, S.B., 1998. Leaf area index and site water balance of loblolly pine (Pinus taeda L.) across a precipitation gradient in East Texas. Forest Ecology and Management 105, 273–282.

Henning, J.G., Burk, T.E., 2004. Improving Growth and Yield Estimates with a Process Model Derived Growth Index. Canadian Journal of Forest Research 34, 1274–1282.

Honer, T.G., 1967. Standard volume tables and merchantable conversion factors for the commercial tree species of central and eastern Canada. (No. FMR-X-5). For Manage Res and Serv Inst, Ottawa. pp. 264.

Hosmer, D.W., Lemeshow, S., Sturdivant, R., 2013. Applied logistic regression, 3rd ed, Wiley Series in Probability and Statistics. Wiley, New Jersey. pp. 510.

Jack, S.B., Long, J.N., 1996. Linkages between silviculture and ecology: an analysis of density management diagrams. Forest Ecology and Management 86, 205–220.

Jacobs, M.R., 1955. Growth Habits of the Eucalypts. Forestry and Timber Bureau, Department of the Interior. pp. 262.

Jiang, L., Brooks, J.R., Wang, J., 2005. Compatible taper and volume equations for yellow-poplar in West Virginia. Forest Ecology and Management 213, 399–409.

Jokela, E.J., Dougherty, P.M., Martin, T.A., 2004. Production dynamics of intensively managed loblolly pine stands in the southern United States: a synthesis of seven long-term experiments. Forest Ecology and Management 192, 117–130.

Jordan, L., Berenhaut, K., Souter, R., Daniels, R.F., 2005. Parsimonious and completely compatible taper, total, and merchantable volume models. Forest Science 51, 578–584.

Kimmins, J.P., 2008. From science to stewardship: Harnessing forest ecology in the service of society. Forest Ecology and Management 256, 1625–1635.

Kimmins, J.P., 1985. Future shock in forest yield forecasting: the need for a new approach. The Forestry Chronicle 61, 503–512.

Kimmins, J.P., Blanco, J.A., Seely, B., Welham, C., Scoullar, K., 2008. Complexity in modelling forest ecosystems: How much is enough? Forest Ecology and Management, 6th North American Forest Ecology Workshop: From science to sustainability 256, 1646–1658.

Korzukhin, M.D., Ter-Mikaelian, M.T., Wagner, R.G., 1996. Process versus empirical models: which approach for forest ecosystem management? Canadian Journal of Forest Research 26, 879–887.

Koskela, L., Nummi, T., Wenzel, S., Kivinen, V.-P., 2006. On the analysis of cubic smoothing spline-based stem curve prediction for forest harvesters. Canadian Journal of Forest Research 36, 2909–2919.

Kozak, A., 2004. My last words on taper equations. The Forestry Chronicle 80, 507–515.

Kozak, A., 1988. A variable-exponent taper equation. Journal of Forest Research 18, 1363–1368.

Kozak, A., Munro, D.D., Smith, J.H.G., 1969. Taper functions and their application in forestry inventory. The Forestry Chronicle 45, 278–283.

Kuru, G.A., Whyte, A.G.D., Woollons, R.C., 1992. Utility of reverse Weibull and extreme value density functions to refine diameter distribution growth estimates. Forest Ecology and Management 48, 165–174.

Landsberg, J., 2003. Modelling forest ecosystems: state of the art, challenges, and future directions. Canadian Journal of Forest Research 33, 385–397.

Landsberg, J., 1986. Physiological ecology of forest production. Academic Press, New York. pp. 165.

Landsberg, J.J., Waring, R.H., 1997. A generalised model of forest productivity using simplified concepts of radiation-use efficiency, carbon balance and partitioning. Forest Ecology and Management 95, 209–228.

Landsberg, J., Sands, P., 2011. Physiological ecology of forest production, 1st ed, Terrestrial Ecology Series. Elsevier, USA. pp. 198.

Leites, L.P., Robinson, A.P., 2004. Improving taper equations of loblolly pine with crown dimensions in a mixed-effect modeling framework. Forest Science 50, 204–212.

Liu, C.J., 1980. Log volume estimation with spline approximation. Forest Science 26, 361–369.

Maestri, R., 2003. Modelo de crescimento e produção para povoamentos clonais de Eucalyptus grandis cosniderando variáveis ambientais. Universidade Federal do Paraná, Curitiba. pp 143.

Mäkelä, A., Landsberg, J., J., Alan, R. EK, Burk, T. E., Ter-Mikaelian, M., Agren, G.I., Oliver, C. D., Puttonen, P., 2000. Process-based models for forest ecosystem management: current statae fo the art and challenges for pratical implementation. Tree Physiology 20, 289–298.

Mangel, M., Bonsall, M.B., 2004. The shape of things to come: using models with physiological structure to predict mortality trajectories. Theoretical population biology, demography in the 21st Century 65, 353–359.

Manion, P., 1991. Tree disease conscepts, 2nd Edition. ed. Prentice Hall, New Jersey. pp. 402.

Manion, P., Lachance, D., 1992. Forest decline concepts. APS press, Minnesota. pp. 249.

Manogaran, C., 1973. Economic feasibility of irrigating southern pines. Water Resource Research 9, 1485–1496.

Martin, T.A., Hinckley, T.M., Meinzer, F.C., Sprugel, D.G., 1999. Boundary layer conductance, leaf temperature and transpiration of Abies amabilis branches. Tree Physiology. 19, 435–443.

Mason, E., 1992. Decision-support systems for establishing radiata pine plantations in the central North Island of New Zealand. University of Canterbury, Christchurch, New Zealand. pp. 251.

Mason, E.G., 2013. Linking hybrid mensurational/eco-physiological growth and yield models with crop establishment: a replacement for time gain analysis. New Forests 44, 951–959.

Mason, E.G., Methol, R., Cochrane, H., 2011. Hybrid mensurational and physiological modelling of growth and yield of *Pinus radiata* D. Don usin potentially useable radiation sums. Forestry 84, 99–108.

Mason, E.G., Rose, R.W., Rosner, L.S., 2007. Time vs. light: a potentially useable light sum hybrid model to represent the juvenile growth of Douglas-fir subject to varying levels of competition. Canadian Journal of Forest Research 37, 795–805.

Max, T., Burkhart, H., 1976. Segmented polynomial regression applied to taper equations. Forest Science 22, 283–289.

McArdle, R., Meyer, W., Bruce, D., 1949. The yield of Douglas Fir in the Pacific Northwest (Technical Bulletin No. 201). United States Department of Agriculture, Washington, D.C. pp. 75.

McDill, M.E., Amateis, R.L., 1992. Measuring forest site quality using the parameters of a dimensionally compatible height growth function. Forest Science 38, 409–429.

McDowell, N.G., Beerling, D.J., Breshears, D.D., Fisher, R.A., Raffa, K.F., Stitt, M., 2011. The interdependence of mechanisms underlying climate-driven vegetation mortality. Trends in Ecology & Evolution 26, 523–532.

McMurtrie, R.E., Gholz, H.L., Linder, S., Gower, S.T., 1994. Climatic Factors Controlling the Productivity of Pine Stands: A Model-Based Analysis. Ecological Bulletins 173–188.

McMurtrie, R., Wolf, L., 1983. Above- and Below-ground Growth of Forest Stands: a Carbon Budget Model. Annals of Botany 52, 437–448.

Meir, P., Mencuccini, M., Dewar, R.C., 2015. Drought-related tree mortality: addressing the gaps in understanding and prediction. New Phytologist 207, 28–33.

Methol, R., 2006. SAG globulus: Sistema de apoyo a la gestion de plantacions de Eucalyptus globulus. (Serie Técnica 158 No. 158). INIA, Montevideo, Uruguay. pp 34.

Methol, R., 2001. Comparisons of approaches to modelling tree taper, stand structure and stand dynamics in forest plantations. University of Canterbury, Christchurch, New Zealand. pp 298.

MGAP/DS, 1976. Carta de reconocimiento de suelos del Uruguay Escala 1:1.000.000.

MGAP/RENARE, 1994. Indices de propductividad de suelos grupos CONEAT.

MGAP/RENARE, n.d.a Cartas Temáticas › RENARE [WWW Document]. URL http://www.cebra.com.uy/renare/mapa/cartas-tematicas/ (accessed 2.23.16a).

MGAP/RENARE, n.d.b Modelo Digital de Terreno › RENARE [WWW Document]. URL http://www.cebra.com.uy/renare/mapa/modelo-digital-de-terreno/ (accessed 2.23.16b).

Mielke, M.S., Oliva, M.A., Barros, N.F. de, Penchel, R.M., Martinez, C.A., Almeida, A.C. de, 1999. Stomatal control of transpiration in the canopy of a clonal *Eucalyptus grandis* plantation. Trees 13, 152–160.

Molfino, J.. H., Califra, A., 2001. Agua disponible de las tierras del Uruguay. Segunda aproximación. URL http://www.cebra.com.uy/renare/wp-content/files_mf/1395761584AguadisponibleenSuelosdelUruguayversioncorr.pdf/ accessed (accessed 2.24.16)

Monserud, R.A., 2003. Evaluating forest models in a sustainable forest management context. Forest Biometry, Modelling and Information Science 1, 35–47.

Monserud, R.A., 1976. Simulation of forest tree mortality. Forest Science 22, 438–444.

Monserud, R.A., Moody, U., Breuer, D.W., 1990. A soil-site study for inland Douglas-fir. Can. J. For. Res. 20, 686–695.

Monserud, R.A., Sterba, H., 1999. Modeling individual tree mortality for Austrian forest species. Forest Ecology and Management 113, 109–123.

Monteith, J.L., 1977. Climate and the efficiency of crop production in Britain. Philosophical transactions of the Royal Society of London 281, 277–294.

Monteith, J.L., 1972. Solar Radiation and Productivity in Tropical Ecosystems. Journal of Applied Ecology 9, 747–766.

Montes, C.R., 2012. A resource driven growth and yield model for loblolly pine plantations. North Carolina State University, Raleigh, North Carolina. pp. 77.

Moras, G., 2010. Tablas de volumen de Eucalyptus globulus ssp globulus al sur del Rio Negro. Universidad de la República, Montevideo, Uruguay. pp. 103.

Muhairwe, C.K., 1999. Taper equations for Eucalyptus pilularis and Eucalyptus grandis for the north coast in New South Wales, Australia. Forest Ecology and Management 113, 251–269.

Munro, D.D., 1974. Forest growth models - a prognosis, in: Proceedings of IUFRO Meeting S4.01.4, Research Research Note. Presented at the Growth models of tree and stand simulations, Royal College of Forestry, Stockholm, pp. 7–21.

Myers, B.J., Landsberg, J.J., 1989. Water stress and seedling growth of two eucalypt species from contrasting habitats. Tree Physiol 5, 207–218.

Nikolov, N.T., Fox, D.G., 1994. A coupled carbon-water-energy-vegetation model to assess responses of temperate forest ecosystems to changes in climate and atmospheric CO2. Part I. Model concept. Environmental Pollution 83, 251–262.

Ormerod, D.W., 1973. A simple bole model. The Forestry Chronicle 49, 136–138.

Palahí, M., Tomé, M., Pukkala, T., Trasobares, A., Montero, G., 2004. Site index model for Pinus sylvestris in north-east Spain. Forest Ecology and Management 187, 35–47.

Pedersen, B.S., 1998. The role of stress in the mortality of Midwestern oaks as indicated by growth prior to death. Ecology 79, 79–93.

Peng, C., Liu, J., Dang, Q., Apps, M.J., Jiang, H., 2002. TRIPLEX: a generic hybrid model for predicting forest growth and carbon and nitrogen dynamics. Ecological Modelling 153, 109–130.

Peterman, W., Waring, R.H., Seager, T., Pollock, W.L., 2013. Soil properties affect pinyon pine – juniper response to drought. Ecohydrol. 6, 455–463.

Pienaar, L.V., Shiver, B.D., 1981. Survival functions for site-prepared slash pine plantations in the flatwoods of Georgia and Northern Florida. Southern Journal of Applied Forestry 5, 59–62.

Pinjuv, G.L., 2006. Hybrid forest modelling of *Pinus radiata* D. Don in canterbury, New Zealand. University of Canterbury, Christchurch, New Zealand.

Pinjuv, G., Mason, E.G., Watt, M., 2006. Quantitative validation and comparison of a range of forest growth model types. Forest Ecology and Management 236, 37–46.

Pinkard, E.A., Battaglia, M., 2001. Using hybrid models to develop silvicultural prescriptions for Eucalyptus nitens. Forest Ecology and Management 154, 337–345.

Porté, A., Bartelink, H.H., 2002. Modelling mixed forest growth: a review of models for forest management. Ecological Modelling 150, 141–188.

Prentice, I. c., Leemans, R., 1990. Pattern and process and the dynamics of forest structure: a simulation approach. Journal of Ecology 78, 340.

Prentice, I.C., Sykes, M.T., Cramer, W., 1993. A simulation model for the transient effects of climate change on forest landscapes. Ecological Modelling 65, 51–70.

Pretzsch, H., Biber, P., 2016. Tree species mixing can increase maximum stand density. Canadian Journal of Forest Resesearch (in press).

Pretzsch, H., Biber, P., 2005. A Re-Evaluation of Reineke's Rule and Stand Density Index. Forest Science 51, 304–320.

QGIS Development Team, 2015. QGIS Geographic Information System. Open Source Geospatial Foundation Project.

R Development Core Team, 2014. R: A Language and Environment for Statistical Computing. R Foundation for Statistical Computing, Vienna, Austria.

Reineke, L.H., 1933a. Perfecting a stand-density index for even-aged forests. Journal of Agricultural Research 46, 627–638.

Revfeim, K.J.A., 1978. A Simple Procedure for Estimating Global Daily Radiation on Any Surface. J. Appl. Meteor. 17, 1126–1131.

Reynolds, M.R., Burk, T.E., Huang, W.-C., 1988. Goodness-of-Fit Tests and Model Selection Procedures for Diameter Distribution Models. Forest Science 34, 373–399.

Ritchie, M.W., Hamann, J.D., 2008. Individual-tree height-, diameter- and crown-width increment equations for young Douglas-fir plantations. New Forests 35, 173–186.

Robinson, A.P., Ek, A.R., 2003. Description and validation of a hybrid model of forest growth and stand dynamics for the Great Lakes region. Ecological Modelling 170, 73–104.

Robinson, A.P., Monserud, R.A., 2003. Criteria for comparing the adaptability of forest growth models. Forest Ecology and Management 172, 53–67.

Rojo, A., Perales, X., Sánchez-Rodríguez, F., Álvarez-González, J.G., Gadow, K. von, 2005. Stem taper functions for maritime pine (*Pinus pinaster* Ait.) in Galicia (Northwestern Spain). European Journal of Forest Research 124, 177–186.

Roux, X.L., Lacointe, A., Escobar-Gutiérrez, A., Dizès, S.L., 2001. Carbon-based models of individual tree growth: A critical appraisal. Annals of Forest Science 58, 38.

Running, S.W., Coughlan, J.C., 1988. A general model of forest ecosystem processes for regional applications I. Hydrologic balance, canopy gas exchange and primary production processes. Ecological Modelling 42, 125–154.

Russell, M.B., Burkhart, H.E., Amateis, R.L., Prisley, S.P., 2012. Regional locale and its influence on the prediction of loblolly pine diameter distributions. Southern Journal of Applied Forestry 36, 198–203.

Ryan, M.G., Stape, J.L., Binkley, D., Fonseca, S., Loos, R.A., Takahashi, E.N., Silva, C.R., Silva, S.R., Hakamada, R.E., Ferreira, J.M., Lima, A.M.N., Gava, J.L., Leite, F.P., Andrade, H.B., Alves, J.M., Silva, G.G.C., 2010. Factors controlling Eucalyptus productivity: how water availability and stand structure alter production and carbon allocation. Forest Ecology and Management, Productivity in Tropical Plantations 259, 1695–1703.

Sala, A., Piper, F., Hoch, G., 2010. Physiological mechanisms of drought-induced tree mortality are far from being resolved. The New Phytologist 186, 274–281.

Sala, A., Woodruff, D.R., Meinzer, F.C., 2012. Carbon dynamics in trees: feast or famine? Tree Physiol 32, 764–775.

Sands, P., 2004. Adaptation of 3-PG to novel species: guidelines for data collection and parameter assignment (Technical Report No. 141). Cooperative Research Centre for Susutainable Production Forestry. pp. 35.

Sanquetta, C.R., Behling, A., Dalla Corte, A.P., Péllico Netto, S., Rodrigues, A.L., Simon, A.A., 2014. A model based on environmental factors for diameter distribution in black wattle in Brazil. PLoS ONE 9, e100093. doi:10.1371/journal.pone.0100093

Saveland, J.M., Neuenschwander, L.F., 1990. A signal detection framework to evaluate models of tree mortality following fire damage. Forest Science 36, 66–76.

Schultz, R.P., 1997. Loblolly pine: the ecology and culture of loblolly pine (*Pinus taeda* L.), Agriculture Handbook. Forest Service, Washington D. C. pp 493.

Schumacher, F., Hall, F., 1933. Logaritmic expression of timber-tree volume. Journal of Agricultural Research 47, 719–734.

Schwärzel, K., Feger, K.-H., Häntzschel, J., Menzer, A., Spank, U., Clausnitzer, F., Köstner, B., Bernhofer, C., 2009. A novel approach in model-based mapping of soil water conditions at forest sites. Forest Ecology and Management, Forest Soil Science: Celebrating 50 Years of Research on Properties, Processes and Management of Forest Soils, Virginia, USA 258, 2163–2174.

Snowdon, P., Jovanovic, T., Booth, T.H., 1999. Incorporation of indices of annual climatic variation into growth models for Pinus radiata. Forest Ecology and Management 117, 187–197.

Souza, C.A.M. de, Silva, G.F. da, Xavier, A.C., Chichorro, J.F., Soares, C.P.B., Souza, A.L. de, 2008. Evaluation of segemented taper models in the estimation of height and merchantable volume of Eucalyptus sp. bole. Revista Árvore 32, 453–463.

Spurr, S.H., 1954. Simplified computation of volume and growth. Journal of Forestry 52, 914–922.

Stage, A.R., 1976. Notes: An expression for the effect of aspect, slope, and habitat type on tree growth. Forest Science 22, 457–460.

Stage, A.R., Salas, C., 2007. Interactions of elevation, aspect, and slope in models of forest species composition and productivity. Forest Science 53, 486–492.

Stape, J.L., Binkley, D., Ryan, M.G., 2008a. Production and carbon allocation in a clonal Eucalyptus plantation with water and nutrient manipulations. Forest Ecology and Management 255, 920–930.

Stape, J.L., Binkley, D., Ryan, M.G., 2004. Eucalyptus production and the supply, use and efficiency of use of water, light and nitrogen across a geographic gradient in Brazil. Forest Ecology and Management, Synthesis of the physiological, environmental, genetic and silvicultural determinants of the growth and productivity of eucalypts in plantations. 193, 17–31.

Stape, J.L., Binkley, D., Ryan, M.G., Fonseca, S., Loos, R.A., Takahashi, E.N., Silva, C.R., Silva, S.R., Hakamada, R.E., Ferreira, J.M. de A., Lima, A.M.N., Gava, J.L., Leite, F.P., Andrade, H.B., Alves, J.M., Silva, G.G.C., Azevedo, M.R., 2010. The Brazil Eucalyptus Potential Productivity Project: influence of water, nutrients and stand uniformity on wood

production. Forest Ecology and Management, Productivity in Tropical Plantations 259, 1684–1694.

Sullivan, A.D., Clutter, J.L., 1972. A Simultaneous growth and yield model for loblolly pine. Forest Science 18, 76–86.

Temps, M, 2005. Adição da precipitação pluviométrica na modelagem do crescimento e da produção florestal em povoamentos não desbastados de *Pinus taeda*. Universidade Federal do Paraná. pp. 113.

Temu, M.J., 1992. Forecasting yield of Douglas Fir in the South Island of New Zealand. University of Canterbury, Christchurch, New Zealand. pp. 249.

Teskey, R.O., Bongarten, B.C., Cregg, B.M., Dougherty, P.M., Hennessey, T.C., 1987. Physiology and genetics of tree growth response to moisture and temperature stress: an examination of the characteristics of loblolly pine (*Pinus taeda* L.). Tree Physiology 3, 41–61.

Thomas, C.E., Parresol, B.R., 1991. Simple, flexible, trigonometric taper equations. Canadian Journal of Forest Research 21, 1132–1137.

Tian, Y.Q., Davies-Colley, R.J., Gong, P., Thorrold, B.W., 2001. Estimating solar radiation on slopes of arbitrary aspect. Agricultural and Forest Meteorology 109, 67–74.

Trimble, G.R., Weitzman, S., 1956. Site Index studies of upland Oaks in the Northern Appalachians. Forest Science 2, 162–173.

Uzoh, F.C.C., Mori, S.R., 2012. Applying survival analysis to managed even-aged stands of ponderosa pine for assessment of tree mortality in the western United States. Forest Ecology and Management 285, 101–122.

Valentine, H.T., Gregoire, T.G., 2001. A switching model of bole taper. Canadian Journal of Forest Research 31, 1400–1409.

Von Teuffel, K., Hein, S., Kotar, M., Pinto Preuhsler, E., Puumalainen, J., Weinfurter, P., 2006. End user needs and requirements, in: Sustainable Forest Management: Growth Models for Europe. Springer Berlin Heidelberg, Germany.

Waring, R.H., 1983. Estimating forest growth and efficiency in relation to canopy leaf area. Advances in Ecological Research 13, 327–354.

Weiskittel, A., Gould, P., Temesgen, H., 2009a. Sources of variation in the self-thinning boundary line for three species with varying levels of shade tolerance. Forest Science 55, 84–93.

Weiskittel, A.R., Hann, D.W., Kershaw, J.A., Vanclay, J.K., 2011. Forest growth and yield modeling. John Wiley & Sons, Hoboken, NJ. pp. 415.

Weller, D.E., 1987. A reevaluation of the -3/2 power rule of plant self-thinning. Ecological Monographs 57, 23–43.

Westfall, J.A., Scott, C.T., 2010. Taper models for commercial tree species in the Northeastern United States. Forest Science 56, 515–528.

Whyte, A.G.D., 1971. Sectional measurement of trees: a rationalised method. New Zealand Journal of Forest Science 1, 74–79.

Whitehead, D., Beadle, C.L., 2004. Physiological regulation of productivity and water use in Eucalyptus: a review. Forest Ecology and Management 193, 113–140.

Woollons, R.C., 1998. Even-aged stand mortality estimation through a two-step regression process. Forest Ecology and Management 105, 189–195.

Woollons, R.C., Snowdon, P., Mitchell, N.D., 1997. Augmenting empirical stand projection equations with edaphic and climatic variables. Forest Ecology and Management 98, 267–275.

Yoda, K., Kira, T., Ogawa, H., Hozumi, K., 1963. Self-thinning in overcrowded pure stands under cultivated and natural conditions. Journal of Biology of Osaka City University 14, 107–129.

Zeide, B., 2010. Comparison of self-thinning models: an exercise in reasoning. Trees 24, 1117–1126.

Zeide, B., 2002. Density and the growth of even-aged stands. Forest Science 48, 743–754.

Zeide, B., 1993. Analysis of growth equations. Forest Science 39, 594–616.

Zeide, B., 1987. Analysis of the 3/2 power law of self-thinning. Forest Science 33, 517–537.

Zeide, B., 1985. Tolerance and self-tolerance of trees. Forest Ecology and Management 13, 149–166.

Zhang, J., Oliver, W.W., Powers, R.F., 2013. Reevaluating the self-thinning boundary line for ponderosa pine (*Pinus ponderosa*) forests. Can. J. For. Res. 43, 963–971.

APPENDICES

APPENDIX I: Correlation matrices of physiographic variables, *SI*, and *Z7*

P. taeda

	SWPA	***Ele***	$\boldsymbol{\beta}$	$\boldsymbol{\alpha_s}$	$\boldsymbol{\alpha_c}$	***SI***	***Z7***
SWPA	1.00	0.31	-0.12	0.08	-0.02	-0.14	0.25
Ele	0.31	1.00	0.33	0.04	0.01	0.18	0.59
$\boldsymbol{\beta}$	-0.12	0.33	1.00	0.10	-0.09	0.17	0.22
$\boldsymbol{\alpha_s}$	0.08	0.04	0.10	1.00	0.09	0.04	0.08
$\boldsymbol{\alpha_c}$	-0.02	0.01	-0.09	0.09	1.00	-0.04	0.06
SI	-0.14	0.18	0.17	0.04	-0.04	1.00	0.16
Z7	0.25	0.59	0.22	0.08	0.06	0.16	1.00

E. grandis

	SWPA	***Ele***	$\boldsymbol{\beta}$	$\boldsymbol{\alpha_s}$	$\boldsymbol{\alpha_c}$	***SI***	***Z7***
SWPA	1.00	0.84	0.47	-0.19	-0.02	0.63	0.80
Ele	0.84	1.00	0.60	-0.16	-0.01	0.68	0.88
$\boldsymbol{\beta}$	0.47	0.60	1.00	0.06	0.09	0.42	0.54
$\boldsymbol{\alpha_s}$	-0.19	-0.16	0.06	1.00	0.16	-0.12	0.04
$\boldsymbol{\alpha_c}$	-0.02	0.01	0.09	0.16	1.00	0.05	0.10
SI	0.63	0.68	0.42	-0.12	0.05	1.00	0.72
Z7	0.80	0.88	0.54	0.04	0.10	0.72	1.00

APPENDIX II: Sets of equations selected for each analysed approach

BASE FORMULATION

Pinus taeda

$$h_{dom_2} = 30.413912\left(\frac{H_{dom_1}}{30.413912}\right)^{\frac{ln\left[1-e^{(-0.102622t_2)}\right]}{ln\left[1-e^{(-0.102622t_1)}\right]}}$$

$$\mathrm{G_2} = \mathrm{e}^{\ln(\mathrm{G_1})\left(\frac{\mathrm{t_1}}{\mathrm{t_2}}\right)^{1.013}+(4.51079)\left\{1-\left(\frac{\mathrm{t_1}}{\mathrm{t_2}}\right)^{1.013}\right\}}$$

$$d_{max_2} = e^{ln(d_{max_1})\left(\frac{t_1}{t_2}\right)^{0.749582}+(6.392204-0.100819SI)\left[1-\left(\frac{t_1}{t_2}\right)^{0.749582}\right]}$$

$$SD_{d_2} = (5.132918)\left(\frac{SD_{d_1}}{5.132918}\right)^{\frac{ln\left[1-e^{(-0.070622t_2)}\right]}{ln\left[1-e^{(-0.070622t_1)}\right]}}$$

$$P = \frac{1}{1+e^{-(-4.1905612+0.0042098N_1+0.3573926Int+0.5755308\ SD_{d_1}+0.0463895G_1-0.2491949\ H_{d_1}+0.007767IG_1)}}$$

$$N_2 = \left\{\frac{1}{\sqrt{N_1}} + 0.41361\left[\left(\frac{t_2}{100}\right)^2 - \left(\frac{t_1}{100}\right)^2\right]\right\}^{-2}$$

Eucalyptus grandis

$$h_{dom_2} = e^{ln(H_{dom_1})\left(\frac{t_1+3.06896}{t_2+3.06896}\right)+(4.00389+0.19295Z7)\left(1-\frac{t_1+3.06896}{t_2+3.06896}\right)}$$

$$G_2 = e^{ln(G_1)\left(\frac{t_1}{t_2}\right)^{1.07956-0.93323\left[\frac{\left(N_a/N_b\right)}{tt}\right]}+(3.7534+0.27345Z7)\left\{1-\left(\frac{t_1}{t_2}\right)^{1.07956-0.93323\left[\frac{\left(N_a/N_b\right)}{tt}\right]}\right\}}$$

$$d_{max_2} = e^{ln(d_{max_1})\left(\frac{t_1}{t_2}\right)^{0.45368-0.15881Z7}+(4.26886+1.14703Z7)\left[1-\left(\frac{t_1}{t_2}\right)^{0.45368-0.15881Z7}\right]}$$

$$SD_{d_2} = (9.230291 + 2.424718Z7)\left(\frac{SD_{d_1}}{a_0 + a_1 Z7}\right)^{\frac{ln\left[1-e^{(-0.054145t_2)}\right]}{ln\left[1-e^{(-0.054145bt_1)}\right]}}$$

$$P = \frac{1}{1 + e^{-(-4.535313\ \ +0.002096\ \ N_1+2.465474\ \ Z7+0.867506\ \ SD_{d_1}+0.514887\ \ Int-0.340538\ \ t_1)}}$$

$$N_2 = N_1\left(\frac{T_2}{T_1}\right)^{-0.089108} e^{(-0.010536-0.012254\,Z7)(t_2-t_1)}$$

AUGMENTED FORMULATION

Pinus taeda

$$h_{dom_2} = (22.265319 + 0.023379SWPA + 0.021562Elev)\left[\frac{h_{dom_1}}{(22.265319 + 0.023379SWPA + 0.021562Elev)}\right]^{\frac{ln\left[1-e^{(-0.109748t_2)}\right]}{ln\left[1-e^{(-0.109748t_1)}\right]}}$$

$$G_2 = e^{ln(G_1)\left(\frac{t_1}{t_2}\right)^{1.0520980} + (3.7497295 + 0.0026375SWPA + 0.0068628\alpha_c + 0.0018031Elev)\left[1-\left(\frac{t_1}{t_2}\right)^{1.0520980}\right]}$$

$$d_{max_2} = e^{ln\left(d_{max_1}\right)\left(\frac{t_1}{t_2}\right)^{0.749582} + (6.392204 - 0.100819SI)\left[1-\left(\frac{t_1}{t_2}\right)^{0.749582}\right]}$$

$$SD_{d_2} = (5.132918)\left(\frac{SD_{d_1}}{5.132918}\right)^{\frac{ln\left[1-e^{(-0.070622t_2)}\right]}{ln\left[1-e^{(-0.070622t_1)}\right]}}$$

$$P = \frac{1}{1 + e^{-(-4.1905612 + 0.0042098N_1 + 0.3573926Int + 0.5755308SD_{d_1} + 0.0463895G_1 - 0.2491949H_{d_1} + 0.007767IG_1)}}$$

$$N_2 = \left\{\frac{1}{\sqrt{N_1}} + 0.41361\left[\left(\frac{t_2}{100}\right)^2 - \left(\frac{t_1}{100}\right)^2\right]\right\}^{-2}$$

Eucalyptus grandis

$$h_{dom_2} = e^{ln(h_{dom_1})\left(\frac{t_1+2.4973491}{t_2+2.4973491}\right)+(3.6014737+0.0029913*SWPA+0.0087987\alpha_c+0.0175036\alpha_s)\left(1-\frac{t_1+2.4973491}{t_2+2.4973491}\right)}$$

$$G_2 = e^{ln(G_1)\left(\frac{t_1}{t_2}\right)^{1.1164274-1.0353749\left[\frac{\left(N_a/N_b\right)}{tt}\right]}+(2.611299+0.0115832SWPA-0.0033998Elev)\left\{1-\left(\frac{t_1}{t_2}\right)^{1.1164274-1.0353749\left[\frac{\left(N_a/N_b\right)}{tt}\right]}\right\}}$$

$$d_{max_2} = e^{ln(d_{max_1})\left(\frac{t_1}{t_2}\right)^{0.5225331-0.0101125\alpha_S}+(3.4624929+0.005749\,SWPA+0.0714808\alpha_S)\left[1-\left(\frac{t_1}{t_2}\right)^{0.5225331-0.0101125\alpha_S}\right]}$$

$$SD_{d_2} = (8.863645 + 0.450453\alpha_s)\left[\frac{SD_{d_1}}{(8.863645 + 0.450453\alpha_s)}\right]^{\frac{ln\left[1-e^{(-0.069762t_2)}\right]}{ln\left[1-e^{(-0.069762t_1)}\right]}}$$

$$P = \frac{1}{1 + e^{-(-9.710349+0.0026263N_1+0.9481403SD_{d_1}+0.560091Int+0.0350884SWPA-0.3628958t_1+0.2183891\beta\,+0.1242171\alpha_c+0.0895620\ \alpha_s)}}$$

$$N_2 = N_1\left(\frac{T_2}{T_1}\right)^{-7.164e-02} e^{(0.02501-0.0003.783SWPA+0.002837\beta\,)(t_2-t_1)}$$

HYBRID FORMULATION

Pinus taeda

$$h_{dom_2} = 30.116567\left(\frac{h_{dom_1}}{30.116567}\right)^{\frac{ln\left[1-e^{\left(-0.041078R_{\theta DT_2}\right)}\right]}{ln\left[1-e^{\left(-0.041078R_{\theta DT_1}\right)}\right]}}$$

$$G_2 = 60.81\left(\frac{G_1}{60.81}\right)^{\frac{ln\left[1-e^{\left(-0.06975R_{\theta DT_2}\right)}\right]}{ln\left[1-e^{\left(-0.06975R_{\theta DT_1}\right)}\right]}}$$

$$D_{max_2} = e^{ln\left(D_{max_1}\right)\left(\frac{R_{\theta DT_1}}{R_{\theta DT_2}}\right)^{0.83895}+4.25329\left[1-\left(\frac{R_{\theta DT_1}}{R_{\theta DT_2}}\right)^{0.83895}\right]}$$

$$SD_{d_2} = 4.912066\left(\frac{SD_{d_1}}{4.912066}\right)^{\frac{ln\left[1-e^{\left(-0.031274R_{\theta DT_2}\right)}\right]}{ln\left[1-e^{\left(-0.031274R_{\theta DT_1}\right)}\right]}}$$

$$P = \frac{1}{1+e^{-(-4.09449\ +0.005225\ N_1+0.359153\ SD_{d_1}+0.177518\ Int-0.008156\ \bar{R}_{\theta D})}}$$

$$N_2 = \left\{\frac{1}{\sqrt{N_1}} + (0.3673939 - 0.0011964\bar{R}_{\theta D})\left[\left(\frac{R_{\theta DT_2}}{100}\right)^2 - \left(\frac{R_{\theta DT_1}}{100}\right)^2\right]\right\}^{-2}$$

Eucalyptus grandis

$$h_{dom_2} = (14.815317 + 0.140033\bar{R}_{\theta D})\left[\frac{h_{dom_1}}{(14.815317 + 0.140033\bar{R}_{\theta D})}\right]^{\frac{ln\left[1-e^{\left(-0.035879R_{\theta DT_2}\right)}\right]}{ln\left[1-e^{\left(-0.035879R_{\theta DT_1}\right)}\right]}}$$

$$G_2 = e^{ln(G_1)\left(\frac{R_{\theta DT_1}}{R_{\theta DT_2}}\right)^{0.9017980} + (3.2921722 + 0.0030941\bar{R}_{\theta D})\left[1-\left(\frac{R_{\theta DT_1}}{R_{\theta DT_2}}\right)^{0.9017980}\right]}$$

$$D_{max_2} = e^{ln\left(D_{max_1}\right)\left(\frac{R_{\theta DT_1}}{R_{\theta DT_2}}\right)^{0.2622174} + (2.6107845 + 0.0124875\bar{R}_{\theta D})\left[1-\left(\frac{R_{\theta DT_1}}{R_{\theta DT_2}}\right)^{0.2622174}\right]}$$

$$SD_{d_2} = a\left(\frac{SD_{d_1}}{a}\right)^{\frac{ln\left[1-e^{\left(-bR_{\theta DT_2}\right)}\right]}{ln\left[1-e^{\left(-bR_{\theta DT_1}\right)}\right]}}$$

$$P = \frac{1}{1 + e^{-(-9.5267038 + 0.0023578N_1 + 0.826633\ SD_{d_1} + 0.2300163Int - 0.1112372R_{\theta DT_1} + 0.037175SWPA + 0.0923128\beta + 0.1384784\alpha_c)}}$$

$$N_2 = N_1 e^{-(-0.00005309\bar{R}_{\theta D})(R_{\theta DT_2} - R_{\theta DT_1})}$$